The University of
Nottingham

UNITED KINGDOM · CHINA · MALAYSIA

CHARACTERISATION OF DEGRADED SOLVENTS FROM THE AMINE SCRUBBING PROCESS

RACHEL VICTORIA LEWIS, MChem.

Thesis submitted to the University of Nottingham

for the Degree of Doctor of Engineering

April 2017

Abstract

Whilst there have been a number of studies into amine degradation at laboratory scale few have investigated this phenomenon at pilot plant scale. The aims of this thesis were to use a variety of analytical techniques to analyse both primary and blended amine solvents from pilot plants in the UK and North West Europe. The results from the analyses were correlated in an effort to present a comprehensive overview of solvent behaviour at this scale.

The analytical methods used were Gas Chromatography Mass Spectroscopy (GC-MS), Gas Chromatography Flame Ionisation Detection (GC-FID), Inductively Coupled Plasma Mass Spectroscopy (ICPMS), Ion Chromatography (IC), and ^{13}C Nuclear Magnetic Resonance (NMR) spectroscopy. The corrosive effects of the solvents were investigated using electrochemical testing.

The data from GC-MS and GC-FID was correlated in order to quantify the major degradation products found in amine solvents. ICPMS was used to quantify the metals in the solvents and was correlated with IC data. The use of ^{13}C NMR spectroscopy had previously been used to monitor the speciation of amines in solvent systems, but had not been correlated to any other data. This work used ^{13}C NMR spectroscopy to quantify the amine species in the solvent and correlated this data to GC-MS results. From the electrochemical testing it was shown that corrosion only increases when oxygen is present in the system but is negligible at low temperatures (40°C). The use of continuous cationic exchange resins to remove metals was shown to be an effective method of mitigating degradation in primary amine solvents. It was also shown that ^{13}C NMR spectroscopy can be used for the rapid analysis of the extent of degradation and can be used in conjunction with other analytical methods to monitor amine degradation.

Acknowledgements

Firstly, I would like to express my sincere gratitude to my supervisor Prof. Colin Snape whose immense knowledge and thoughtful insight have helped guide this project from beginning to end. Equal credit must also be given to both my former and current industrial supervisors at E.ON/ Uniper, Dr. Chris Satterley and Dr. Robin Irons. The financial contributions made by the EPSRC and Uniper are also gratefully acknowledged. Thanks are also due to my secondary supervisor, Prof. Peter Licence, as well as Dr. David Fitzgerald from Doosan Babcock.

I would also like to thank Dr. Will Meredith for his assistance with the GC-MS and GC-FID instruments at the University of Nottingham. Thanks are also due to Mr. Colin Davis at Uniper whose assistance with the electrochemical corrosion testing equipment was invaluable. Collaborations with other departments at the University of Nottingham have made this project possible and as such, thanks are due to Mr. Shazad Aslam in the School of Chemistry for the ^{13}C NMR analysis, and Dr. Scott Young and Dr. Saul Vazquez-Reina in the School of Biosciences for the ICPMS analysis.

Thanks are due to all those within the EFET EngD centre, especially those in this cohort. Special thanks go to Shamal and Ben, for helping to keep things in perspective.

Finally, for their constant support and encouragement, I would like to thank my friends and family, particularly Dr. Antonia Benton and my late Grandma, Mrs. Veronica Coulson, who was the strongest and most determined person I have ever known. I am forever indebted to Dr. Sam D. Bailey, for always being there for me. I would never have been able to finish without his support. Finally, special thanks are due to my father, Dr. Kevin Lewis for always believing in me and giving me the confidence to manage and follow through whatever I decide to do. Without him, none of this would have been possible.

Contents

Table of Figures

Nomenclature

AEHEIA	N-(2-aminoethyl)-N'-(2-hydroxyethyl)imidazolidin-2-one
AMP	2-amino-2-methyl-1-propanol
BHEEDA	N,N'-bis(2-hydroxyethyl)ethylenediamine
BHEI	N,N'-bis(2-hydroxyethyl)imidazolidin-2-one
BHEOX	N,N'bis(2-hydroxyethyl) oxalamide
B_o	External magnetic field
CCS	Carbon capture & storage
$CDCl_3$	Deuterated chloroform
CO	Carbon monoxide
CO_2	Carbon dioxide
CO_3^{2-}	Bicarbonate
DEA	Diethanolamine
DMAE	2-dimethylamino ethanol
DMP	N,N'-dimethylpiperazine
DNPZ	Di-nitrosopiperazine
E	Energy
EDA	Ethylenediamine
EI	Electron Ionisation
E_{oc}	Open circuit potential
EOR	Enhance Oil Recovery
E_{pp}	Passivation Potential
E_{ref}	Reference Potential
eV	electron volts
FGD	Flue Gas Desulphurisation
FPZ	N-formylpiperazine
ɣ	Gyromagnetic ratio
GC-FID	Gas chromatography flame ionisation detection
GC-MS	Gas chromatography mass spectrometry
GHG	Greenhouse gas
Gt	Gigatonnes
H_2	Hydrogen
H	Plancks constant, 6.26e10-34 Js
ħ	Reduced Plancks constant, = h/2pi
HCO^{3-}	Carbonate
HEA	N-(2-hydroxyethyl) acetamide
HEEDA	N-(2-hydroxyethyl) ethylenediamine
HEF	N-(2-hydroxyethyl) formamide
HeGly	N-(2-hydroxyethyl) glycine
HHEA	2-Hydroxy-N-(2-hydroxyethyl)acetamide
HEHEAA	N-(2-hydroxyethyl)-2-(2-hydroxyethylamino) acetamide
HEI	N-(2-hydroxyethyl) imidazole
HEIA	N-(2-hydroxyethyl) imidazolidin-2-one
HEP	N-(2-hydroxyethyl) piperazine
HEPO	N-(2-hydroxyethyl) piperazin-3-one
HSS	Heat stable salt

I	Angular momemtum quantum number
IC	Ion Chromatography
I_{corr}	Corrosion current
ICPMS	Inductively coupled plasma mass spectrometry
MAE	Methylaminoethanol
MEA	Monoethanolamine
MDEA	Methyldiethanolamine
µ	Magnetic moment
m	mass of nucleus
m/z	mass to charge ratio
MNPZ	Mono-nitrosopiperazine
$M\Omega\ cm^{-1}$	Mega Ohms per cm
MPZ	Methylpiperazine
mV	millivolts
Mw	molecular weight
NaOH	Sodium hydroxide
NMR	Nuclear magnetic resonance
NOE	Nuclear Overhauser Effect
OZD	2-oxazolidone
P	Intrinsic angular momentum, spin
$pg\ C\ s^{-1}$	picograms of carbon per second
ppb	parts per billion
ppm	parts per million
PZ	Piperazine
psi	pounds per square inch
THEED	N,N,N'-tris(2-hydroxyethyl) ethylenediamine
TIC	Total Ion Current
µS	microSiemens
V	Volts
Wm^{-2}	Watts per meter squared
wt %	weight per cent

Chapter 1: Background

1.1 Introduction

This chapter provides an overview of the role of carbon dioxide (CO_2) on climate change and the proposed reduction targets which are in place. Various methods of CO_2 removal are discussed with a focus on amine absorption/ stripping and solvent degradation. Lastly, the scope of this work and the research objectives are discussed.

1.2 Carbon Dioxide Emissions and the Environment

Over the past 200 years the atmospheric concentration of CO_2 has increased dramatically. Since the beginning of the industrial age (circa 1750) around 5 % of the world's available fossil fuel resources have been combusted, releasing an estimated 280 gigatonnes (Gt) of CO_2 back into the atmosphere.[1] In this period the atmospheric concentration of CO_2 has increased from 280 parts per million (ppm) to approximately 398 ppm in 2014, an increase of 42 %.[1-4] The rise in CO_2 concentration affects the incoming and outgoing energy balance of the earth-atmosphere system. In order to reach an appropriate energy balance the amount of energy from the Sun which is absorbed by the Earth's surface must equal the amount emitted from the Earth back into space as long wave radiation- approximately 240 Watts per square meter ($W\ m^{-2}$).[5] For this to be possible the average surface temperature of the Earth would need to be around -19 °C making life unsustainable. The actual average temperature of the Earth's surface is 14 °C which is due to the naturally occurring greenhouse effect. The most important greenhouse gases (GHGs) are water vapour and CO_2 which allow ultraviolet and visible wavelengths to reach the Earth's surface but absorb the infrared radiation it emits. The average surface temperature increases because the GHGs re-emit the energy they have absorbed in all directions and reflect some of the outgoing energy. According to the Intergovernmental Panel on Climate Change (IPCC) the average global temperature has increased by 0.74 ± 0.18 °C, over the 20th century and this is *"very likely due to the observed increase in anthropogenic GHG concentrations"*.[5] Currently, fossil fuels are accountable for 86 % of world energy use and it is widely acknowledged that without mitigation of emissions the atmospheric concentration of CO_2 will continue to rise, further increasing the average surface temperature as well as having other effects such as causing sea levels to rise.[2] The longest running study of atmospheric CO_2 concentrations, measured at the Mauna Loa Observatory (MLO) in Hawaii since 1958, shows that CO_2 concentrations have increased by 26 % over the last 55 years.[4, 6] Figure 1.1 below shows the most recent measurements from the National Oceanic and Atmospheric Administration Earth System Research Laboratory at the MLO. The red line represents the monthly mean values and the black line represents those values after correction for the average seasonal cycles. In 2014, the average annual atmospheric CO_2 concentration was 398.55 ppm, with an average annual increase of 2.1 ppm per year over the preceding decade (2005-2014). This value is greater than the average annual increase for the previous decade (1995-2004) which was 1.9 ppm per year.

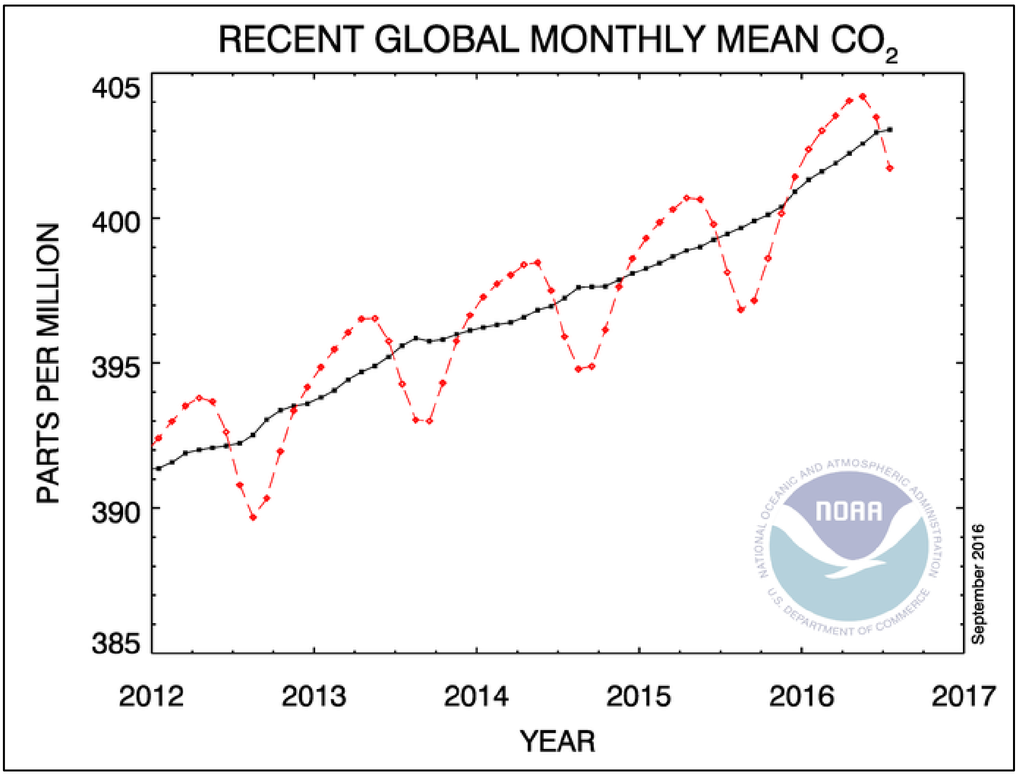

Figure 1.1: Monthly mean CO_2 concentrations from the MLO, Hawaii[4]

Climate change is increasingly becoming a political issue as evidenced by the Kyoto Protocol which came into effect on February 16th 2005 and required at least a 5 % reduction in CO_2 emissions by 2012, compared to 1990 levels. In 2012 the Doha Amendment was made to the Kyoto Protocol which established a second period of commitment from 2013 – 2020 in which CO_2 emissions are to be cut by an average of 18 % from 1990 levels. At the Paris climate conference (COP21) in December 2015, the first universal and legally binding global climate deal was reached between 195 countries.[7] A long-term goal of limiting the increase in the global average temperature to well below 2 °C above pre-industrial levels was agreed upon, with the aim of keeping the increase at 1.5 °C. This agreement is due to come into effect in 2020. However, even if the concentration of CO_2 is stabilised by 2100 the warming effects will continue for centuries due to the long time- scales on which climate processes operate.[1] In order to mitigate climate change, various measures to reduce emissions are under development ranging from renewable and low- or zero- carbon technologies to the use of carbon capture and storage (CCS) techniques. CCS will play an important role during the transition to low- or zero- carbon technologies.[8]

1.3 Carbon Dioxide Capture and Storage

When considering how best to capture CO_2 from power plants there are three alternatives: oxyfuel combustion, pre-combustion carbon capture and post-combustion carbon capture. The following section will give a brief summary of the three technologies.

1.3.1 Oxyfuel Combustion

In oxyfuel combustion nitrogen is eliminated from the flue gases by burning the fuel in a mixture of oxygen and recycled flue gas (which is predominantly CO_2 and water vapour), the ash, particulate matter, water and sulphur having been removed. An air separation unit is needed for the production of pure oxygen and this is the main operating cost of the system. The flue gas is cooled to condense the water vapour leaving a pure stream of CO_2 which can be compressed, dried and further purified before being transported for storage. Advantages of oxyfuel combustion are that it uses common technologies and processes, very little modification of the power plant is required and little space is needed for additional equipment. In addition to this there is no requirement for solvents. Despite the advantages of oxyfuel combustion it is an energy intensive process in terms of separating air into pure oxygen, and a relatively low CO_2 purity is achieved due to the energy cost of producing a purer stream. Operational flexibility is also limited.[9]

1.3.2 Pre-Combustion Carbon Capture

Pre-combustion carbon capture involves partially combusting fuel with pure oxygen or air (and sometimes steam) to produce a syngas consisting mainly of carbon monoxide (CO) and hydrogen (H_2). The CO is then converted to produce CO_2 and more H_2 by the water-gas shift reaction (Equation 1.1). The H_2 can then be used to drive a gas turbine or collected to be used in other applications such as transport. The CO_2 is separated by using physical solvents which work well at the high CO_2 concentrations and high pressures involved.

$$CO + H_2O \rightleftarrows CO_2 + H_2 \qquad \textbf{Equation 1.1}$$

Due to the higher pressure of the process and the higher partial pressure of CO_2, its removal from the CO_2-H_2 mixture is easier than capture from the flue gas after combustion. Pre-combustion capture has low overall emissions and low fresh-water consumption. However, the equipment is complex and has many individual processes. The technology cannot be retro-fitted and there are only limited similarities with existing plants. The operational flexibility is limited by the highly complex systems involved and it is only possible to improve thermal efficiency by increasing plant complexity which, in turn, limits both the availability and especially the flexibility of the plant.[10]

1.3.3 Post-Combustion Carbon Capture

Post-combustion carbon capture involves capturing the CO_2 from the flue gas after the fuel has been burned. There are several methods by which to capture and separate the CO_2 from the flue gas, the most common of which is using chemical solvents such as alkanolamines in a process known as amine scrubbing. The ability to retro-fit the equipment required to existing plants reduces the capital cost of implementing the technology, therefore making it a more attractive option in the short term. This form of capture is by far the most developed in terms of industrial deployment and is utilised in the world's largest operational CCS plant on coal at Boundary Dam (Saskatchewan, Canada) and at Sleipner West (Norway).[11, 12] This project will focus on the use of amine scrubbing technology as there are immediate chemical challenges which need to be addressed if this technology is to become commercially attractive in the near future. Other less developed methods of post-combustion carbon capture include the use of solid adsorbents, membranes and cryogenic separation techniques.

Post-combustion carbon capture is similar to wet flue gas desulphurisation and gas purification processes and removes CO_2 from the flue gas after combustion has occurred. Flue gases typically contain 5 - 15 % CO_2 depending on the fuel being used. Amine scrubbing systems use a chemical solvent to absorb CO_2 at low temperatures and near atmospheric pressures. The CO_2 is separated in a stripping process which occurs at high temperatures and higher pressures. Stripping with steam in a second column recovers the chemical solvent which can then be re-used in the absorption process. Figure 1.2 shows the post-combustion CO_2 capture process using amine scrubbing technology.

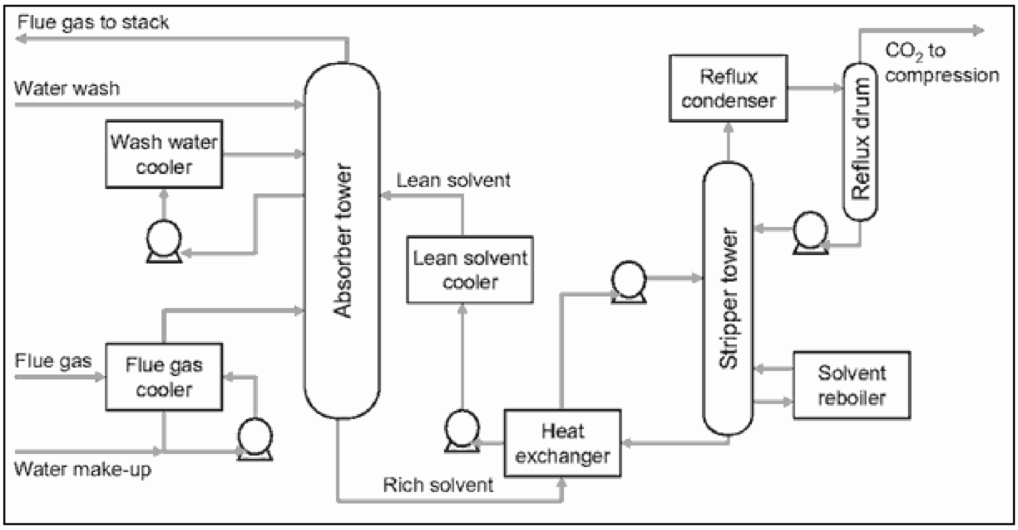

Figure 1.2: Post-combustion capture process using amine scrubbing[1]

1.4 Carbon Capture by Amine Scrubbing

Amine scrubbing has been used to separate CO_2 from natural gas and hydrogen since 1930. The basic process was patented in the same year.[13] In the 1970's CO_2 removal by amine solvents was used in Enhanced Oil Recovery (EOR), mainly in the US.[3] The first commercial CO_2 capture facility, Sleipner West, began operation in 1996 in Norway and is operated by Statoil. It was developed in response to the introduction of a carbon tax in 1991 and captures one million tonnes of CO_2 every year using an amine scrubbing process.[3,12] Amine scrubbing using chemical solvents is currently the most widely used technology for post-combustion carbon capture due to its effectiveness in removing CO_2 and the low cost when compared to other post-combustion capture techniques.[2]

The most common solvent used in amine scrubbing is monoethanolamine (MEA).[1, 2, 14-19] Amine scrubbing is an absorption process which occurs in a large packed column which can be made containing different packings and can vary in height depending on the CO_2 concentration in the flue gas, the concentration of the solvent, the pressure and temperature, and the required percentage of CO_2 recovery.[2] The flue gas is cooled to around 40 °C and then enters the absorber (or "scrubber") column where the CO_2 reacts with an aqueous amine solution (usually 15 - 30 wt %) in an exothermic process. The absorption occurs at the amine site which is weakly basic; CO_2 is a weak acid, so the two react to produce a carbamate ion (Equation 1.2), while in the presence of water a bicarbonate ion forms (Equation 1.3).

$$CO_2 + 2RNH_2 \rightleftharpoons RNHCOO^- + RNH_3^+ \quad FAST$$ **Equation 1.2**

$$CO_2 + 2RNH_2 + H_2O \rightleftharpoons HCO_3^- + RNH_3^+ \quad SLOW$$ **Equation 1.3**

This process can remove 90 - 95 % of the CO_2 from the flue gas. The solvent is now 'CO_2-rich' as it exits the bottom of the scrubber. The rich solvent is pumped into the top of an amine stripper column via a heat exchanger, which heats the rich solvent using heat from the regenerated 'CO_2- lean' solvent cycling back to the absorber. The CO_2-rich solvent is heated to around 120 - 140 °C using steam diverted from a low-pressure turbine within the plant, resulting in reduced electricity generation and an overall efficiency loss of around 30 % (including the compression of CO_2). The CO_2 is removed as the solvent flows down the stripper column by the break-down of the carbamate formed during the absorption process. This regenerates the solvent and produces a concentrated stream of CO_2. Steam and CO_2 leave the top of the stripper column at around 80 °C and the mixture is then cooled so that the water condenses to leave a pure CO_2 stream, which can then be compressed for transportation and storage. In order to remove HSSs the solvent is passed through a thermal reclaimer at the bottom of the stripper column. This removes the irreversibly formed HSSs by distillation. The regenerated amine solvent is then cycled back through the absorber column via the heat exchanger.

Alkanolamines are used in the scrubbing process because they contain at least one amine group and one hydroxyl group. The amine group, as previously mentioned, is a weak base and is the reactive site for CO_2 absorption. The hydroxyl group reduces the vapour pressure and increases water solubility. Primary amines, such as MEA, are favoured over more hindered or tertiary amines because the rate of reaction is fast. Using primary amines, two moles of amine are needed to absorb one mole of CO_2 (Equation 1.2 and Equation 1.3). Hindered and tertiary amines react to form bicarbonate ions (Equation 1.4) due to lack of a hydrogen atom attached to the nitrogen atom. For this reason, hindered and tertiary amines are able to absorb one mole of CO_2 using one mole of amine. However, the stoichiometric advantage this gives is offset by the slow reaction rate.

$$CO_2 + R_1R_2R_3N + H_2O \rightleftharpoons (R_1R_2R_3NH^+)(HCO_3^-) \quad SLOW \qquad \textbf{Equation 1.4}$$

Prior to the amine absorption process, the flue gas must be treated to remove SO_x and NO_x as these can react with the amine to give non-recoverable heat stable salts. For this reason, the need for Flue Gas Desulphurisation (FGD) and $DeNO_x$ systems is greatly increased in plants where amine capture technology is implemented.

1.4.1 Degradation and Corrosion

A major disadvantage of using amine solvents is their tendency to degrade. Degradation causes several problems, such as adding to the operational costs of the plant due to solvent make up needs, corrosion of the plant equipment and potential impacts on the environment of any degradation products which may be released due to amine slip. The two main types of degradation observed are thermal and oxidative, both with and without CO_2. Thermal degradation only occurs at temperatures above 200 °C so should therefore not be a problem in flue gas systems, although there is some evidence of thermal degradation in stripper columns.[17] Oxidative degradation occurs at lower temperatures and when there is O_2 present and causes fragmentation of the amine solvent. This is a process unique to the application of amines in flue gas scrubbing as it does not occur in the oxygen-free acid gas treating processes for which amine solvents were originally used. Oxidative degradation occurs mainly in the absorber region of the amine plant. Degradation products include amines, carboxylic acids, amides, and trace amounts of nitrosamines. Degradation is discussed further in Sections 2.3 and 2.4.

Corrosion of process equipment used in amine scrubbing systems is a major economic issue. The presence of dissolved metal ions in the aqueous amine solution is thought to contribute to amine degradation by catalysis.[17] When the amine solvents absorb CO_2 they become corrosive and therefore are a source of the metals ions in solution. In order to control levels of corrosion the concentration of amine solvent used is usually kept between 15 and 30 wt % and the plant is constructed from stainless steel in order to minimise the corrosive effects, despite the added capital cost. To minimise this cost, it is also possible to use concrete to construct the absorber column, as has been done at Boundary Dam, Canada. Corrosion is discussed further in Section 2.5.

1.4.2. Cost of Carbon Capture by Amine Scrubbing

One of the prohibitive factors in the large-scale deployment of amine scrubbing technology is the cost. A technoeconomic assessment of the Duke Energy Gibson 3 plant in Indiana, USA, estimated the capital costs involved in operating this plant at a

90% capture rate, capturing 0.91 million tonnes CO_2 per year. These costs are shown in Table 1-I.[20]

Table 1-I: Estimated capital costs for the Duke Energy Gibson 3 plant, Indiana, USA

Cost Parameter	30 % MEA	Mixed Amines: 30 %	Mixed Amines: 35 %
Total fixed capital, US$ million	134.4	135.8	128.9
Annual Operating Cost (Inc. capital), US$ million	59.0	57.4	54.6
Cost of CO_2 capture and compression, US$/ tonne CO_2	64.4	62.8	59.8
Estimated impact on power generation costs, US$/ MWh	68.7	66.0	61.8

It was estimated that the use of mixed amine solvents could result in an operating cost which was up to 10 % less than the cost of using 30 % MEA, due to the reduced degradation of mixed amine solvents therefore reducing the solvent make up costs. The operating costs for the Duke Energy Gibson 3 plant are shown in Table 1-II.[20]

Table 1-II: Estimated operating costs for the Duke Energy Gibson 3 plant, Indiana, USA

Operating Costs, US $million/ year (unless otherwise stated)	30 % MEA	Mixed Amines: 30 %	Mixed Amines: 35 %
Variable Costs			
Material consumed and waste disposal	5.8	4.3	4.3
Total variable	23.5	21.60	20.7
Total operating costs	59.0	57.4	54.6
Additional cost of CO_2 captured per MWh generated, US$/ MWh	68.7	66.0	61.8
Reduction in cost compared to 30 % MEA	-	4 %	10 %

1.5 Scope of this Work and Research Objectives

The study of solvent degradation during amine scrubbing operations is of the utmost importance in terms of plant efficiency and running costs. The objective of this work is to analyse single and blended amine solvents from pilot plants in the UK and North West Europe using a range of analytical techniques. Given the variety of degradation products formed during amine scrubbing processes it is necessary to identify simple, rapid analytical methods which can be used to monitor the formation and accumulation of oxidative degradation products. By using several methods of analysis and correlating the data from each it is possible to establish which methods of analysis are most suitable in providing a comprehensive overview of the amine scrubbing process in terms of the extent of degradation and identification of products. This will enable the proactive management of solvent degradation at pilot, demonstration and commercial scales.

The specific goals of this research are as follows:

- Analyse pilot scale degraded amines using Gas Chromatography-Mass Spectroscopy, Gas Chromatography-Flame Ionization Detection, Ion Chromatography, Inductively Coupled Plasma Mass Spectroscopy and ^{13}C NMR spectroscopy.
- Correlate the data from each technique to establish rapid measurement of the extent of amine degradation.
- Evaluate the contribution of each analytical technique.
- Evaluate the use of cationic ion exchange resins as a method of preventing degradation and corrosion.
- Establish a link between amine degradation and corrosion of plant equipment using electrochemical techniques.

Chapter 2: Literature Review

2.1 Introduction

The main focus of this chapter is to review the current literature on amine degradation with particular focus on oxidative degradation. First, some of the amines which are commonly used in post-combustion carbon capture are reviewed, followed by an examination of the proposed mechanisms and likely degradation products. The role of carboxylic acids and metals in the degradation process is discussed, before a brief review of thermal degradation. The role of corrosion in the system is also investigated as well as proposed technologies to mitigate this process. Finally, the analytical techniques used to study amine degradation are discussed. The aim of this chapter is to find the gaps in current literature and to establish how this work will contribute to current research.

2.2 Amines for Carbon Capture

Alkanolamines are the most studied solvents used for carbon capture by amine scrubbing. The benchmark amine is monoethanolamine (MEA), with others such as methyldiethanolamine (MDEA), piperazine (PZ) and 2-amino-2-methyl-1-propanol (AMP) also being studied in detail. Each of these amines is discussed below along with a discussion on how blends of these amines can be used in the amine scrubbing process.

2.2.1 MEA

MEA (Figure 2.1) is a primary amine and is the benchmark solvent used in industry as it is relatively cheap and is an effective absorber of CO_2.[21] Primary amines are favoured over more hindered or tertiary amines because the rate of reaction is fast (for MEA this is 6 m^3/ mol/ sec).[22] Primary amines have a high heat of absorption for CO_2

and a low CO_2 absorption capacity- two moles of amine are needed to absorb one mole of CO_2 (see Equation 1.2).

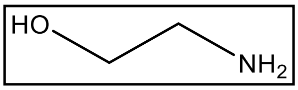

Figure 2.1: Structure of monoethanolamine (MEA)

2.2.2 MDEA

MDEA (Figure 2.2) is a tertiary amine and was first used for natural gas desulphurisation. Tertiary amines react to form bicarbonate ions (Equation 1.4) due to the absence of a hydrogen atom on the nitrogen atom. For this reason, tertiary amines are able to absorb one mole of CO_2 using one mole of amine. Tertiary amines also have a lower heat of absorption than primary amines (1.1 MJ/ kg CO_2 for MDEA compared to 1.9 MJ/ kg CO_2 for MEA).[22] However, the stoichiometric advantage this gives is offset by the slow reaction rate (e.g. for the tertiary amine MDEA the reaction rate is 5×10^{-3} m^3/ mol/ sec).[22]

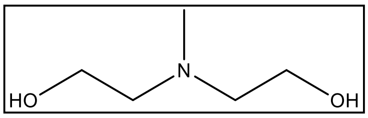

Figure 2.2: Structure of methyldiethanolamine (MDEA)

It has been shown that a major thermal degradation product of MDEA is diethanolamine (DEA), formed by the methylation of one molecule of MDEA and demethylation of another.[23] Oxidative degradation products observed are similar to those formed in MEA degradation (see Section 2.3).

2.2.3 Other Amines

Several other amines are also used in amine scrubbing, such as piperazine (PZ, Figure 2.3) or 2-amino-2-methyl-1-propanol (AMP, Figure 2.4). PZ is mainly used as a promoter to increase the rate of CO_2 absorption so there are few studies which use PZ as an individual solvent. The Rochelle group at the University of Texas at Austin have done substantial research on PZ as a carbon capture amine. Work by Nielsen *et al.*

showed that concentrated aqueous PZ had greater CO_2 absorption rate, capacity and thermal stability than MEA.[24] It was shown by Closmann that both oxidative and thermal degradation are negligible, but Freeman worked to identify some of these products.[25, 26] Thermal degradation products identified included, among others, formic, acetic, oxalic and glycolic acids, N-methylpiperazine (MPZ), N,N'-dimethylpiperazine (DMP) and N-(2-hydroxyethyl)piperazine (HEP). Oxidative degradation products identified included formic, acetic, glycolic, oxalic, nitric and nitrous acids, ethylenediamine (EDA) and N-formylpiperazine (FPZ).[26]

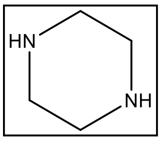

Figure 2.3: Structure of piperazine (PZ)

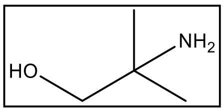

Figure 2.4: Structure of 2-amino-2-methyl-1-propanol (AMP)

2.2.4 Blended Amines

In order to overcome some of the problems associated with an individual amine, blends of two or more amines are sometimes used. For example, adding PZ to a solvent can increase the rate of reaction. PZ is a cyclic secondary amine which has exposed nitrogen groups which results in a very fast reaction with CO_2 (70 m^3/ mol/ sec).[22] The ring structure also provides increased resistance against thermal degradation so the stripping process is able to be carried out at higher temperatures. AMP is a hindered amine which has similar absorption capacity and heat of absorption to MDEA but has a much faster reaction rate (0.58 m^3/ mol/ sec).[22] By blending amines it is possible to produce a solvent which has a better CO_2 absorption rate and a higher CO_2 absorption capacity than a single amine solvent does.

2.2.4.1 MDEA/ MEA Blends

The oxidative and thermal degradation of MDEA/ MEA blended amine solvent in the ratio of 1:4 has been studied by a research group at the University of Regina, Canada.[27, 28] They found that as the ratio of MEA and MDEA concentration was varied then the degradation products also varied. At increased temperature and CO_2 loading there were more degradation products observed. It was also noted that despite MDEA being more resistant to degradation as an individual solvent compared to MEA, in the blend MDEA degraded preferentially in order to protect MEA. The major degradation products identified were 2-(methylamino)ethanol, 1-amino-2-propanol, 1,3-propanediamine and 1,2-propanediamine. Minor degradation products included 3-methylpyridine and N,N-dimethylurea. There was no quantification of degradation products and as noted by the Commonwealth Scientific and Industrial Research Organisation (CSIRO), in Australia, the strongest limitation of these studies is that no degradation experiments at typical absorber conditions (usually 40-70 °C) were performed.[22] Also, the impact of SO_X and NO_X on degradation has not been reported, despite Pedersen *et al*. reporting the formation of nitrosodiethanolamine (NDELA) in the presence of NO_X.[29]

2.2.4.2 AMP/ PZ Blends

Blends of AMP/ PZ have been studied by Wang *et al*..[30] They found that the loss rate of AMP in the blend was close to that of individual AMP but the loss rate of PZ in the blend was higher than individual PZ. It was proposed that the increased loss of PZ in the blend was likely to be due to reactions between PZ and degradation products of AMP, such as formic acid.[30]

It was also found by both Freeman and Jackson that in the presence of $NO_{X,}$ PZ may produce mono-nitrosopiperazine (MNPZ, Figure 2.5) and other nitroso compounds such as di-nitrosopiperazine (DNPZ, Figure 2.5), which are both potentially carcinogenic.[26, 31]

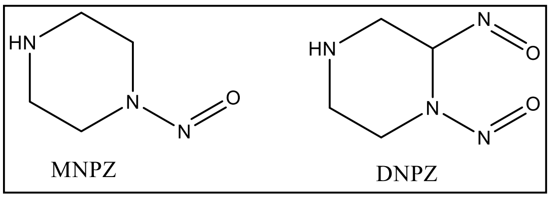

Figure 2.5: Structure of mono-nitrosopiperazine (MNPZ) and di-nitorospiperazine (DNPZ)

2.2.4.3 MDEA/PZ Blends

The oxidative and thermal degradation of MDEA/ PZ blends using 7 M MDEA and 2 M PZ has been studied previously.[25] It was found that oxidative degradation at 55 °C produced mostly formates and at 70 °C formyl amides and bicine were also observed. The largest degradation products in terms of overall molal quantity were observed to be the secondary amines DEA and methyl aminoethanol (MAE). It was suggested that PZ degrades faster when blended with MDEA despite its higher resistance to oxidative degradation compared to MDEA.[25] It was also shown that MDEA/ PZ blends are stable up to 150°C in the absence of CO_2 loading. Thermal degradation products identified include 2-dimethylamino ethanol (DMAE), N-(2-hydroxyethyl)-N-methyl formamide, DEA and bicine among others (Figure 2.6).

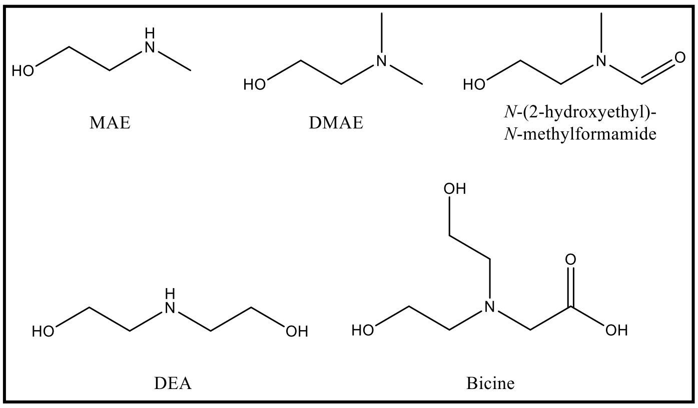

Figure 2.6: Structures of thermal degradation products from MDEA/ PZ blends; methyl amineethanol (MAE), 2-dimethylamino ethanol (DMAE), N-(2-hydroxyethyl)-N-methyl formamide, diethanolamine (DEA) and bicine

2.3 Oxidative degradation

Oxidative degradation is mainly described at absorber conditions where the solutions are loaded with CO_2 and some of the degradation products are similar to those from thermal degradation both at lab scale and at pilot scale. There are only a few studies which report oxidative degradation when CO_2 is not present.[32] Gouedard *et al*. distinguishes the most likely oxidative degradation products as those which have been reported by two or more research groups and which have had realistic mechanisms of formation proposed.[23] The most likely products from primary alkanolamines are listed in Table 2-I in order of increasing molecular weight (nominal mass). The main reactions which give these products are dealkylation, addition and piperazinone formation.[32] In addition to the most likely degradation products there are also a number of degradation products whose formation is proven or very likely to occur but for which there have been no explained mechanisms. These are listed in Table 2-II. It is possible that these products are formed in the analysis of the sample and are therefore not a true representation of the degradation products within the sample.

Table 2-I: MEA oxidative degradation products [23]

Chemical structure	Name (abbreviation)	M_w (g/mol)	References
NH_3	Ammonia	17	19, 32-35
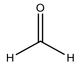	Formaldehyde	30	33, 34
$H_3C—NH_2$	Methylamine	31	19, 34
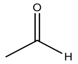	Acetaldehyde	44	18, 19, 34, 35
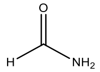	Formamide	45	18 [34]
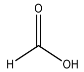	Formic acid	46	18, 19, 34
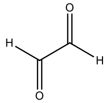	Glyoxal	58	34
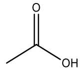	Acetic acid	60	18, 19, 34
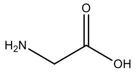	Glycine	75	36
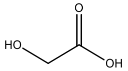	Glycolic acid	76	32, 34, 37
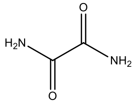	Oxalamide, oxamide	88	37
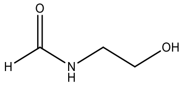	N-(2-hydroxyethyl)formamide (HEF)	89	18, 19, 32, 37

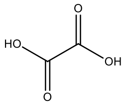	Oxalic acid	90	34, 37, 38
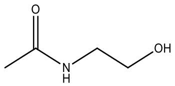	N-(2-hydroxyethyl)acetamide (HEA)	103	18, 19, 32, 35, 37
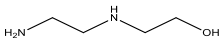	N-(2-hydroxyethyl)ethylenediamine (HEEDA)	104	16, 18, 32, 35
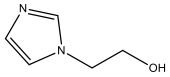	N-(2-hydroxyethyl)imidazole (HEI)	112	18, 34
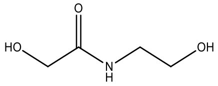	2-Hydroxy-N-(2-hydroxyethyl)acetamide (HHEA)	119	18, 37
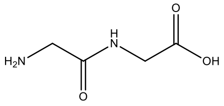	N-glycylglycine	132	35, 39
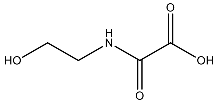	N-(2-hydroxyethyl)oxamic acid	133	32, 37
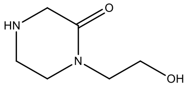	N-(2-hydroxyethyl)piperazin-2-one	144	18, 19, 32
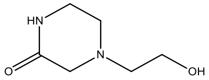	N-(2-hydroxyethyl)piperazin-3-one (HEPO)	144	18, 19, 32
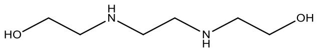	N,N’-bis(2-hydroxyethyl)ethylenediamine (BHEEDA)	148	23
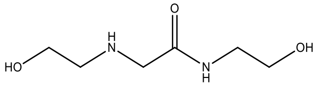	N-(2-hydroxyethyl)-2-(2-hydroxyethylamino)acetamide (HEHEAA)	162	18, 19

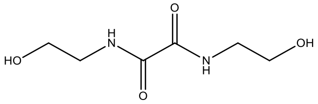	N,N'-bis(2-hydroxyethyl)oxalamide (BHEOX)	176	37, 18

Table 2-II; MEA oxidative degradation products without mechanisms [23]

Chemical structure	Name (abbreviation)	M_w (g/mol)	References
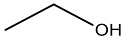	Ethanol	46	35
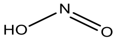	Nitrous acid	47	38, 39
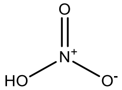	Nitric acid	63	16, 38, 39
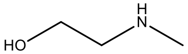	2-(methylamino)ethanol (MAE)	75	16, 33
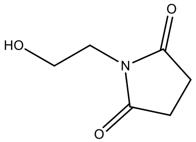	N-(2-hydroxyethyl)-succinimide	143	32, 37
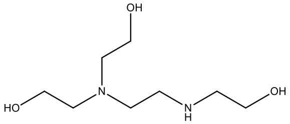	N,N,N'-tris(2-hydroxyethyl)ethylenediamine (THEED)	192	32

Goff and Rochelle examined oxidative degradation mechanisms of MEA and showed that the degradation *"can be controlled by the rate of mass transfer of O_2 into the amine solution, rather than the kinetics of the degradation reactions."*[17] The mechanism of oxidative degradation of MEA is not clear. There are two proposed mechanisms which give the same degradation products. The first is electron abstraction from a lone pair of the nitrogen and the second is hydrogen abstraction from the nitrogen, α-carbon or β-carbon.

2.3.1 Electron Abstraction

The electron abstraction theory is based largely on studies performed at Edgewood Arsenal by the U.S. Army Chemical Research and Development Laboratories.[17, 40] The studies were mainly focussed on tertiary amines and concluded that the rate-limiting step is electron abstraction rather than the second proposed mechanism of oxidative degradation, hydrogen abstraction. Papers from Lindsay Smith *et al*. have calculated the rate of reaction for the oxidation of tertiary amines by hexacyanoferrate ($Fe(CN)_6^{3-}$).[41] The proposed reaction mechanism for MEA is shown in Figure 2.7 and involves the removal of an electron from the nitrogen of the amine group by a free radical such as Fe^{3+} to form an amine radical which is then deprotonated to form an imine radical. The studies showed that the imine radical reacts with a second free radical to form an imine which then reacts with water to form an aldehyde and ammonia.[17] It was proposed by Chi and Rochelle that the imine radical could also react with oxygen to form a peroxide radical (Figure 2.8) which leads to the formation of hydrogen peroxide and an imine.[40] Hydrolysis of the imine results in formation of hydroxyacetaldehyde and ammonia. The Fe^{3+} ion can be regenerated by reaction of Fe^{2+} with O_2 or another free radical.[17] Electron abstraction has only been proven for tertiary amines.[42-45]

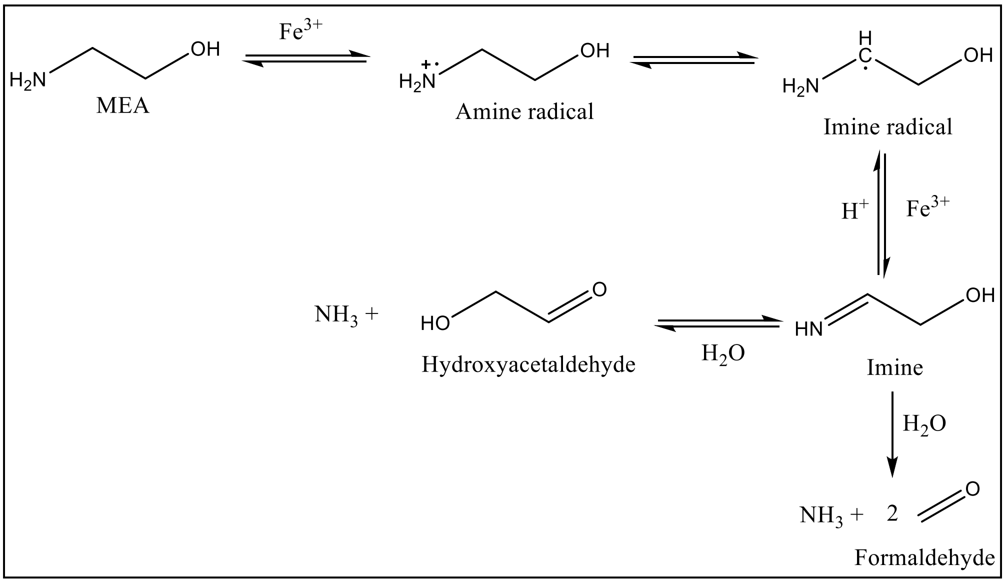

Figure 2.7: Proposed electron abstraction mechanism for oxidative degradation of MEA[17]

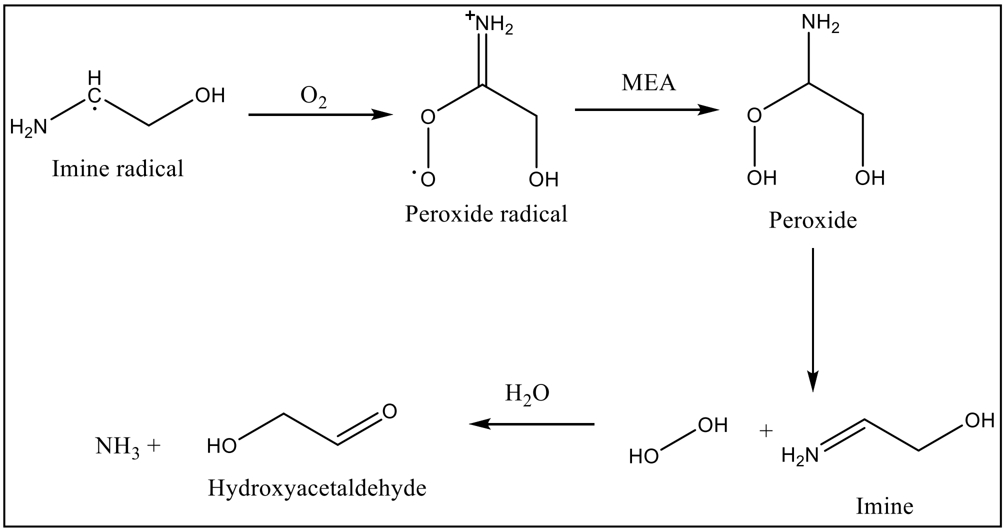

Figure 2.8: Proposed electron abstraction mechanism for oxidative degradation of MEA[40]

2.3.2 Hydrogen Abstraction

As previously stated, the studies carried out at Edgewood Arsenal used mainly tertiary amines for which electron abstraction was the dominant mechanism. However, for the single primary amine which was tested, benzylamine, the dominant mechanism was found to be hydrogen abstraction from the α-carbon.[17, 43] In another study Goff and Rochelle also report that MEA degrades by hydrogen abstraction.[17] They report that in this study *"aqueous solutions of alkanolamines were degraded by using ionization radiation as the initiation step"* to form radicals such as $H^{\cdot}$, $OH^{\cdot}$, e^{-}_{aq}, H_2 and H_2O_2. The proposed mechanism (Figure 2.9) proceeds through a five-membered cyclic hydrogen-bonded conformation of MEA at pH > 6. Free radicals abstract a hydrogen atom from the nitrogen, α-carbon or β-carbon. The amine radical which has been formed then transfers the radical internally through the ring structure resulting in the cleavage of the N-C bond. The degradation products are an amine and an aldehyde or aldehyde radical.

Bedell proposed another radical pathway based on hydrogen abstraction to explain the formation of glycine.[36, 46] As glycine is a noted oxidative degradation product of MEA it would be expected that glycolamide would be formed from the radical formation on the carbon adjacent to the nitrogen, but this is not a reported product.[47] Bedell proposes that glycolamide hydrolyses to form glycolic acid and ammonia, which are both noted MEA oxidation products.[36] It has been proposed that two molecules of glycine can react together to form N-glycylglycine although no mechanistic details were given.[35, 39]

According to Goff and Rochelle it is likely that the mechanism of MEA degradation is via hydrogen abstraction from one of the carbon atoms, rather than from the nitrogen atom.[17]

Studies on pilot plant samples have shown that oxidative degradation is the dominant mechanism at this scale.[15, 18] Major degradation products were identified as HEPO and N-(2-hydroxyethyl)glycine (HeGly), with high concentrations of HEA, HEI and HEF also present.[15] A mechanism for the formation of HeGly has not yet been proposed.[48]

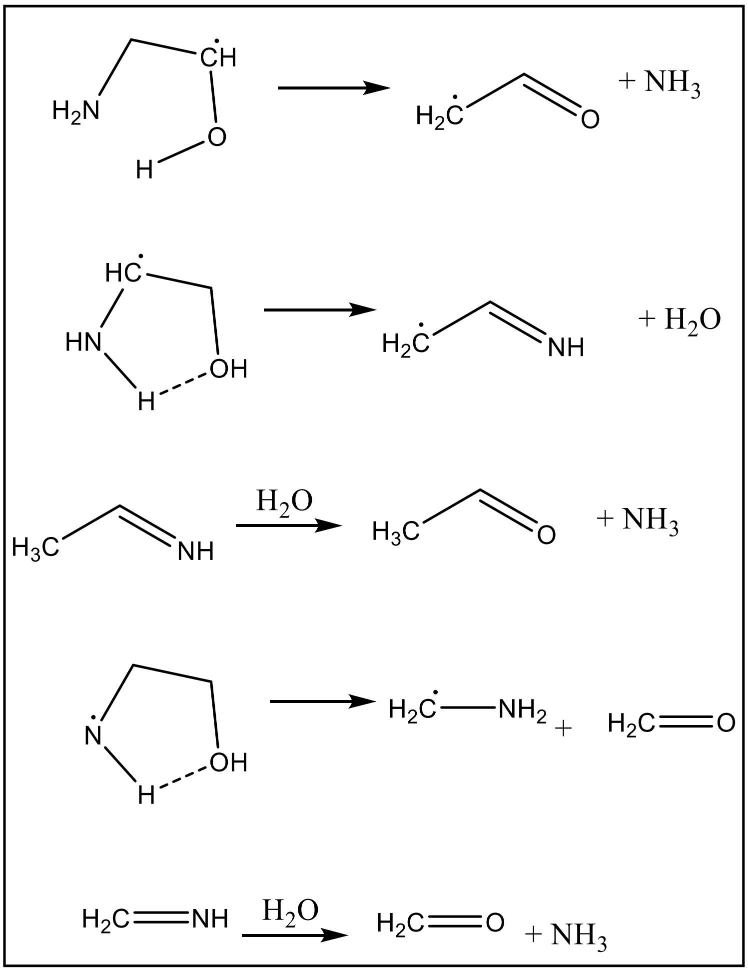

Figure 2.9: Proposed hydrogen abstraction mechanism for oxidative degradation of MEA[17]

2.3.3 Carboxylic Acid Formation

The formation of carboxylic acids has been described by Rooney *et al*. and Lepaumier *et al*..[47,32] In both studies volatile amines such as ammonia or methylamine are formed, as well as aldehydes which are acid precursors. Rooney *et al*. quantified the rate of alkanolamine degradation in the presence of oxygen both with and without CO_2 to form heat stable salts (HSSs) such as acetates, formates, glycolates and oxalates.[47] Their results provided evidence that O_2 plays a crucial role in the formation of HSSs. Initial work on the oxidative degradation of alkanolamines was focussed on MEA and was driven by the U.S. Navy's efforts to clean up CO_2-contaminated air in nuclear powered submarines.[47] It was shown by Kindrick *et al*. that when a 50:50 gaseous mixture of CO_2 and O_2 was contacted with various amine solutions, MDEA had the best resistance to O_2 and DEA had the least resistance.[49] In 1956 it was shown that MEA undergoes deamination to give formic acid, ammonia, substituted amides and high molecular weight polymers.[47] A U.S. Naval Research Report showed that the oxidative degradation of MEA gave glycine, glycolic acid and oxalic acid and the mechanism, attributed to Jefferson Chemical, is shown in Figure 2.10.[50] The CO_2 absorption capacity of MEA solutions is decreased by the presence of these acids as they form non-regenerative salts. The results of Rooney *et al*. showed that after seven days of subjecting a 20 % MEA solution to oxidative degradation conditions in the absence of CO_2 acetate, glycolate and formate all formed, as well as some unknown anions.[47] When the 20 % MEA solution was loaded with 0.25 M/ M CO_2, results showed that formate was detected from seven days and acetate from 14 days, and glycolate was not detected at all. When CO_2 is present in the solution the total number of mmoles of anions is much less than when no CO_2 is present. This may be due to a lowering of the oxygen solubility when CO_2 is added which results in less mmoles of acetate, formate and glycolate forming.[51]

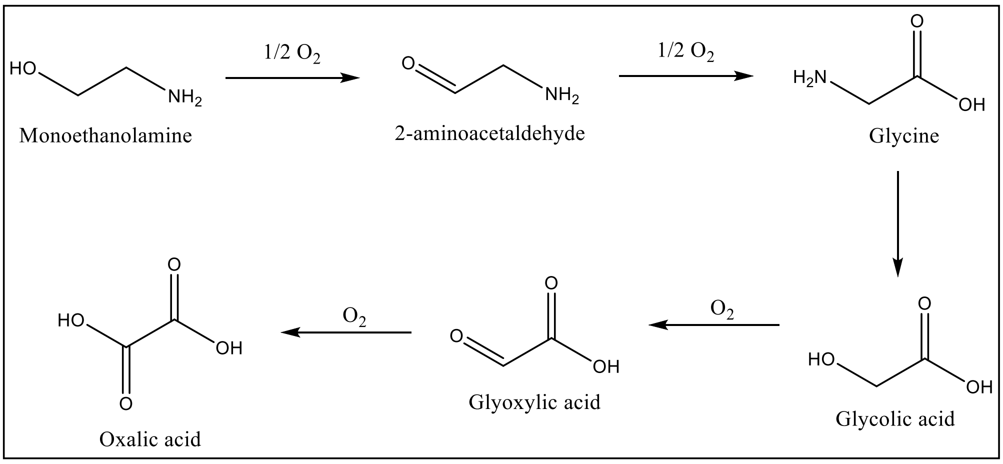

Figure 2.10: Proposed oxidative degradation mechanism of MEA attributed to Jefferson Chemical [47, 50]

Figure 2.10 shows a proposed mechanism for the formation of the acid forms of glycolate, glyoxalate and oxalate from the oxidative degradation of MEA, but it does not show how acetate or formate may be formed. Rooney *et al*. proposed a mechanism to account for the formation of acetate and formate as well as those presented above in Figure 2.10.[47] The mechanism was proposed after it was shown by others that aldehydes were formed during degradation. Rooney's mechanism is shown in Figure 2.11 and although it presents the acid form of acetic, formic, glycolic, glyoxalic and oxalic acids, these anions are almost completely ionised to the amine HSS form when in strong salt basic solutions.[47]

The work by Lepaumier *et al*. reports that the main oxidative degradation products are volatile compounds, amines, aldehydes and carboxylic acids.[32] The group found that for secondary and tertiary amines the main reactions in degradation were demethylation, methylation, dealkylation, addition, ring closure and replacement of the hydroxyethyl chain by a methyl group. Bicine was also identified from MDEA and DEA. As noted previously, for primary amines such as MEA the main degradation reactions were found to be dealkylation, addition and piperazinone formation.

The dealkylation of MEA is proposed to result in the formation of ammonia and ethylene oxide. Ethylene oxide can be hydrolysed into ethylene glycol which oxidises on contact with air to give carboxylic acids.[32] Aldehydes are well known to rapidly oxidise to acids and it is the same in this case. Ethylene oxide formed from dealkylation of MEA can also react with HEEDA to give BHEEDA as shown in Figure 2.12.[32]

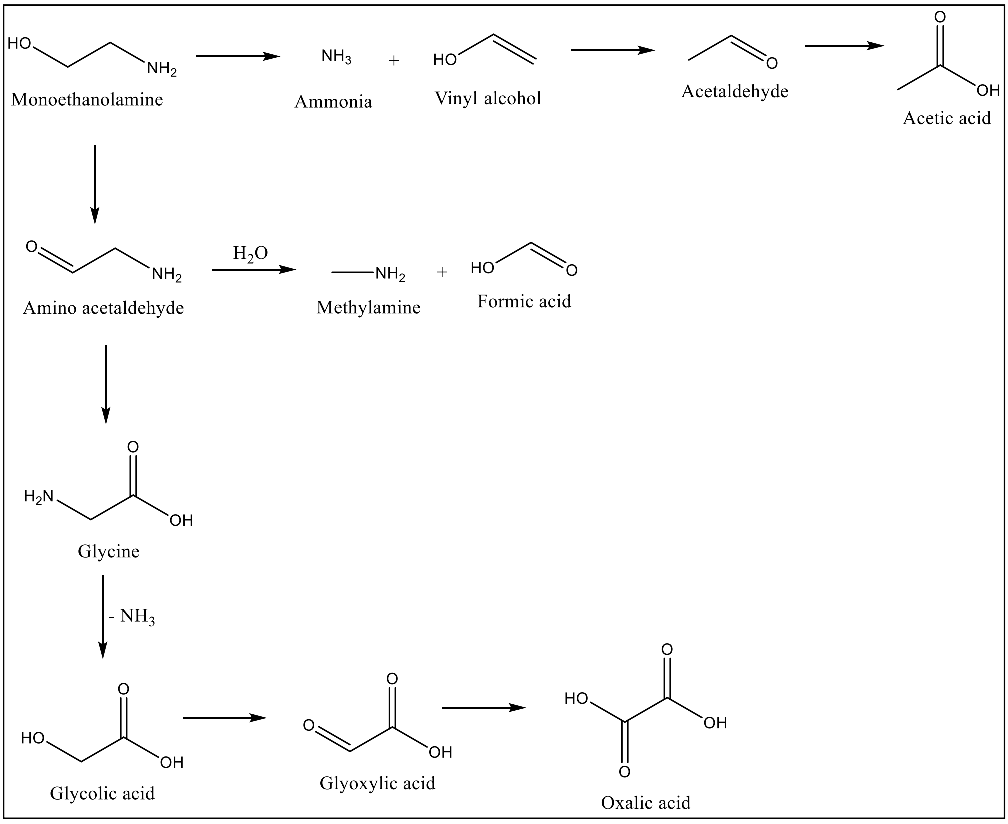

Figure 2.11: Proposed oxidative degradation mechanism of MEA [47]

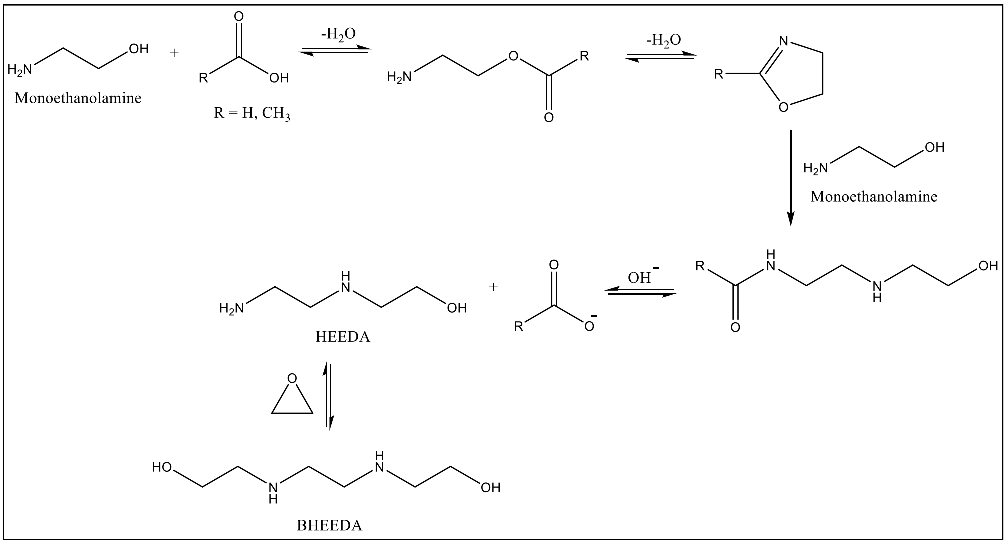

Figure 2.12: HEEDA and BHEEDA formation [32]

Carboxylic acids are known to cause corrosion and fouling in pilot plants and they increase the degradation ratio due to their reaction with amines to form HSSs.[37] Supap acknowledges the mechanism proposed by Chi and Rochelle in which a radical-induced oxidation of MEA to give formate and acetate proceeds via a peroxide radical to give hydrogen peroxide (see Figure 2.8) which decomposes to form formic and acetic acids, but points out that despite the detailed proposed mechanistic works the existence of such radicals is yet to be verified.

The study by Supap *et al*. investigated the roles which carboxylic acids (formic, acetic, glycolic, oxalic and succinic acids) play in the oxidation process once they have been formed and the role of MEA-HSSs in further degradation processes was also investigated.[37] It was found that both formic and acetic acids exist in two forms in equilibrium- as formate and acetate HSSs of MEA and as HEF and HEA respectively. Glycolic acid was found to favour HSS formation with MEA over the reaction with MEA to form N-(2-hydroxyethyl) glycolamide which was found to be unstable and observed to hydrolyse back into glycolate and MEA. Oxalic acid was found to be a reactive intermediate which decomposed to give formic acid which then produced the stable HEF. The formation of N-(2-hydroxyethyl) oxamide was less observed. Stable N-(2-hydroxyethyl) succinimide was formed from succinic acid via a N-(2-hydroxyethyl) succinamide intermediate.

HSSs are non-regenerable in stripper conditions because carboxylic acids are more acidic than carbonic acid (H_2CO_3).[52, 53] Carboxylic acids have a lower pKa value than carbonic acid. In an aqueous solution, as in amine scrubbing, carbonic acid exists in equilibrium with CO_2 and the concentration of H_2CO_3 is much lower than the concentration of CO_2. Therefore, the pKa of aqueous carbonic acid is around 6.35 whereas the pKa of carboxylic acids is typically around 4. This means that HSSs are non-regenerable in stripper conditions as the pKa values are much lower than those of the commonly used MEA and MDEA (~9.45 and ~8.52 respectively).

2.3.4 Metal Catalysed Reactions

Several studies have shown that oxidative degradation is catalysed by dissolved metals including iron, copper and vanadium.[17, 40, 54-58] In the absence of dissolved metals no significant degradation is observed. Blachly *et al*. noted that as little as 10 ppm of dissolved copper was enough to cause serious degradation of the amine solution and also that copper catalysed degradation rates were much higher than iron catalysed degradation rates when the same concentration of metal was present.[58] This is also shown in work by Goff, Rochelle and Sexton.[33,17,59,57] Goff and Rochelle measured degradation in terms of ammonia evolution and showed that the degradation rate increased with iron concentration, but the rate was much less than first order in iron.[17] Solutions which were lean-loaded (0.15 mol CO_2/ mol MEA) were observed to degrade 1.5 – 2 times faster than the rich-loaded solutions (0.40 mol CO_2/ mol MEA). In order to double the degradation rate the iron concentration must be increased by a factor of 100, regardless of the solution loading. This weak dependence on catalyst concentration indicates a mass transfer limitation. In solutions where both copper and iron are present, in comparison to iron alone, the rate of degradation is faster. Goff and Rochelle explain this by proposing that copper changes the stoichiometry of the degradation reactions- copper could either change the rate limiting step in the reaction or change the selectivity of the formation of degradation products, resulting in a change in the oxygen stoichiometry. Solutions which contained both iron and copper showed a weaker effect of iron on the degradation rates but the lean-loaded solutions still degraded much faster than the rich-loaded solutions. Previous studies on MEA degradation were interpreted as being kinetically controlled but Goff and Rochelle suggest that the MEA degradation process is mass transfer controlled instead.[54, 55,17]

Oxidative degradation is significant in flue gases which typically contain around 5 % oxygen. It is known that dissolved iron catalyses the oxidation of amines. Sexton and Rochelle found that HEF and HEI are important products of MEA oxidation when Fe^{2+} is present.[59,34] Sexton suggests that the formation of HEF occurs by the reaction of MEA with formaldehyde followed by oxidation to the amide. Sexton and Rochelle carried out experiments at low-gas flow rate in which solutions were degraded with 100 mL/ min of 98 % O_2/ 2 % CO_2 and mass transfer was achieved by vortexing.[58] They also carried out high-gas flow rate experiments using 7.5 L/ min of 15 % O_2/ 2 % CO_2 sparged through the solution with additional mass transfer achieved by vortexing. From the low-gas flow rate experiments it was found that the production rate of HEF was almost one order of magnitude higher in the presence of Fe^{2+} and Cu^{2+} than when Fe^{2+} alone was present, whereas the production rate of HEI increased by a factor of three. The result of such degradation is that the MEA loss rate is more than double that of when copper is not present in the solution. Adding copper to an oxidised MEA solution seems to increase the mass transfer characteristics of the solution- oxygen is consumed at a much higher rate than in other catalysed systems. It was also observed that chromium and nickel (present in stainless steel alloys) catalyse MEA degradation as well, resulting in MEA losses which are 55 % greater than iron catalysed degradation. Putting the metals in order of highest to lowest oxidation potential for aqueous MEA solutions gives Fe^{2+}/ Cu^{2+} > Cr^{3+}/ Ni^{2+} > Fe^{2+} > V^{5+}. The high-gas flow rate experiments performed by Sexton and Rochelle showed that the main difference between solutions containing both iron and copper and those containing only iron is the increase in production of formate and HEF when copper is present. There is an increase of a factor of two in production of HEF in the presence of copper. HEI is only detected when both metals are in solution and is at a much lower concentration than at the low-gas flow rate. The amount of gas-phase aldehydes (formaldehyde and acetaldehyde) present in the degraded MEA solution decreases in the presence of iron and copper. Sexton and Rochelle propose that the reason for this is that the aldehydes react faster in the presence of the two metals therefore leaving a lower concentration in solution. The formation rates of all other degradation products were observed to be similar between the two systems (Fe^{2+}/ Cu^{2+} vs. Fe^{2+}) which contradicts Goff who observed that copper and iron individually produce different steady-state ammonia formation rates for MEA.[33]

The presence of metals in the amine solvent system is also thought to promote the formation of nitrosamines which are potential carcinogens. It was found by Wang and Mitch that the presence of dissolved copper promoted the formation of N-nitrosamine in the absorber unit and that the effect was increased at higher oxygen concentrations.[60]

2.3.5. Environmental Effects

In addition to the degradation of the solvents and the high capital and operating costs, as discussed in section 1.4.2, the issue of emissions from the amine scrubbing plant are to be considered when selecting a solvent and designing the plant. Emissions may originate from either the flue gas outlet or the reclaimer.[61] One of the major classes of emissions which must be controlled is nitrosamines and nitramines. As discussed above, these are carcinogenic compounds which can contaminate air and drinking water supplies if released in to the atmosphere. These compounds can also be formed from the photooxidation of secondary and tertiary amines released to the atmosphere.[62] It is therefore important to minimise amine emissions in the carbon capture process.

2.4 Thermal Degradation

In the literature, thermal degradation is reported mainly at stripper conditions between 120 – 140 °C. Most studies suggest that the degradation is due to the high temperatures in the presence of CO_2. The high partial pressure of CO_2 and the high temperatures involved in thermal degradation mean that successive degradation compounds form when MEA degrades. The main degradation compounds (Table 2-III) are well established and mechanisms have been proposed (Figure 2.13 to Figure 2.15).

Table 2-III: Thermal degradation products

Chemical structure	Name (abbreviation)	M_w (g/mol)	References
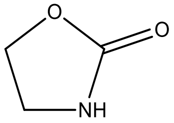	2-oxazolidone (OZD)	87	18, 19, 39, 63
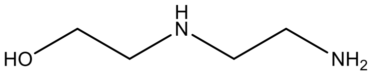	N-(2-hydroxyethyl)ethylenediamine (HEEDA)	104	16, 18, 35, 63
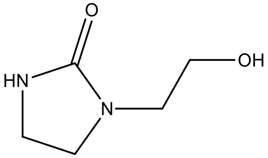	N-(2-hydroxyethyl)imidazolidin-2-one (HEIA)	130	18, 34, 35, 38, 39, 63
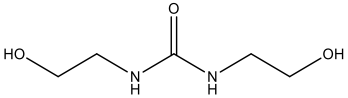	N,N'-bis-(2-hydroxyethyl)urea	148	16, 18

OZD is formed by the reaction of MEA with CO_2 to form a carbamate which undergoes cyclisation to form 2-oxazolidone (Figure 2.13).[63]

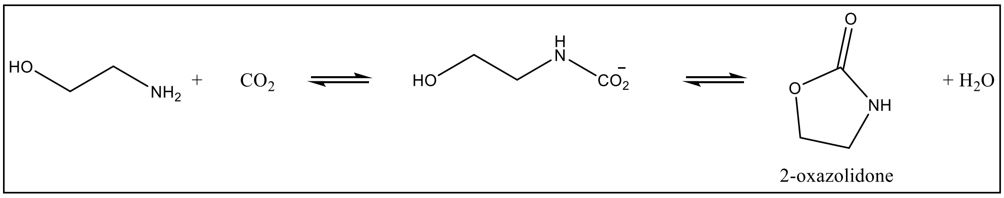

Figure 2.13: Formation of 2-oxazolidinone[63]

It was also reported by Yazvikova *et al*. (cited by Davis and Rochelle) that the MEA carbamate can react with another molecule of MEA to irreversibly form N,N'-di(2-hydroxyethyl) urea (MEA urea) (Figure 2.14).[16]

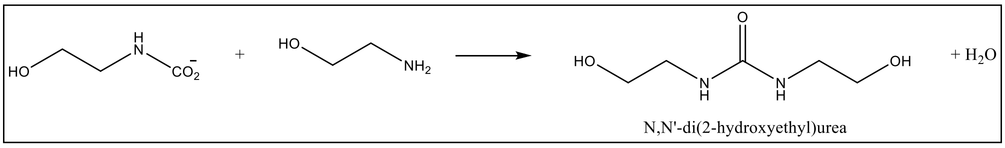

Figure 2.14: Formation of N,N'-di(2-hydroxyethyl) urea[16]

2-Oxazolidone can react with another molecule of MEA to form HEIA which can then be hydrolysed to form HEEDA (Figure 2.15). HEEDA can degrade further to give secondary degradation products, listed in Table 2-IV.

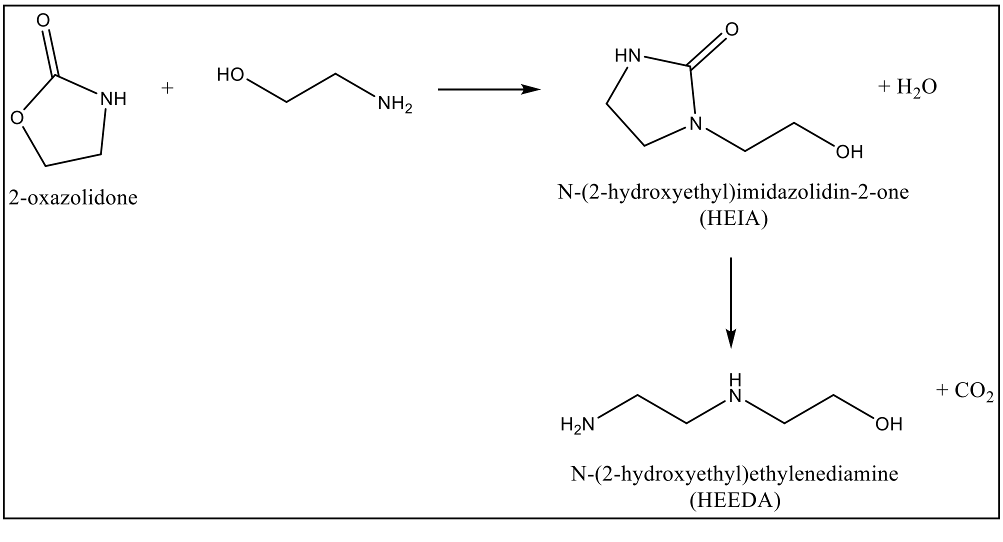

Figure 2.15: Proposed mechanism of formation of HEIA and HEEDA

As shown in Figure 2.14 ureas can be formed by the reaction of carbamates with amines. However, this is a less favourable reaction than the cyclisation to OZD (Figure 2.13) so ureas are minor degradation products.

Lepaumier *et al*. observed that the amounts of HEIA and AEHEIA increased over time suggesting that they are relatively stable products. The amounts of OZD and HEEDA are constant which suggests that they are intermediates which undergo further reactions.[18]

The mechanism of thermal degradation is the subject of some debate. It is generally accepted that the first step is the formation of 2-oxazolidone by ring-closure of the MEA carbamate, but then the order in which HEEDA and HEIA form is debated. It was previously reported by Polderman (cited by Gouedard *et al.*) that HEIA was the precursor to HEEDA but the use of HPLC analysis by Davis and Rochelle and Lepaumier *et al*. showed that it is the opposite (Figure 2.16).[23,16,18]

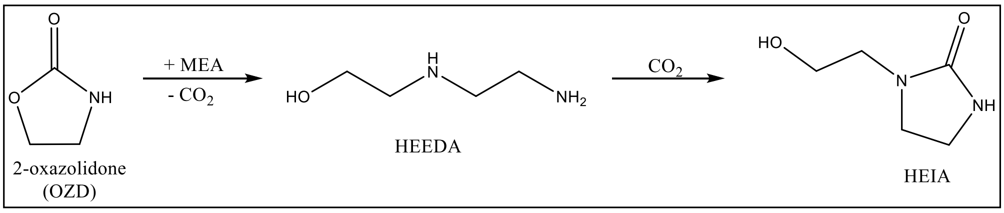

Figure 2.16: Formation of HEIA from HEEDA

Davis and Rochelle found that HEIA appeared to be a stable product and carried out experiments to show that HEEDA was the precursor to HEIA. They found that HEEDA converted to HEIA in stoichiometric quantities to the CO_2 concentration very quickly, but HEIA did not convert to HEEDA until very long hold times. This supports the theory that HEEDA is a precursor to HEIA.[16] The results are supported by the report by Fazio in which the synthesis of diamines from oxazolidone starting materials is described.[64] The formation of AEHEIA could be explained in the same manner; HEEDA reacts with

2-oxazolidone to give a trimer which, in the presence of CO_2 can give AEHEIA (Figure 2.17).

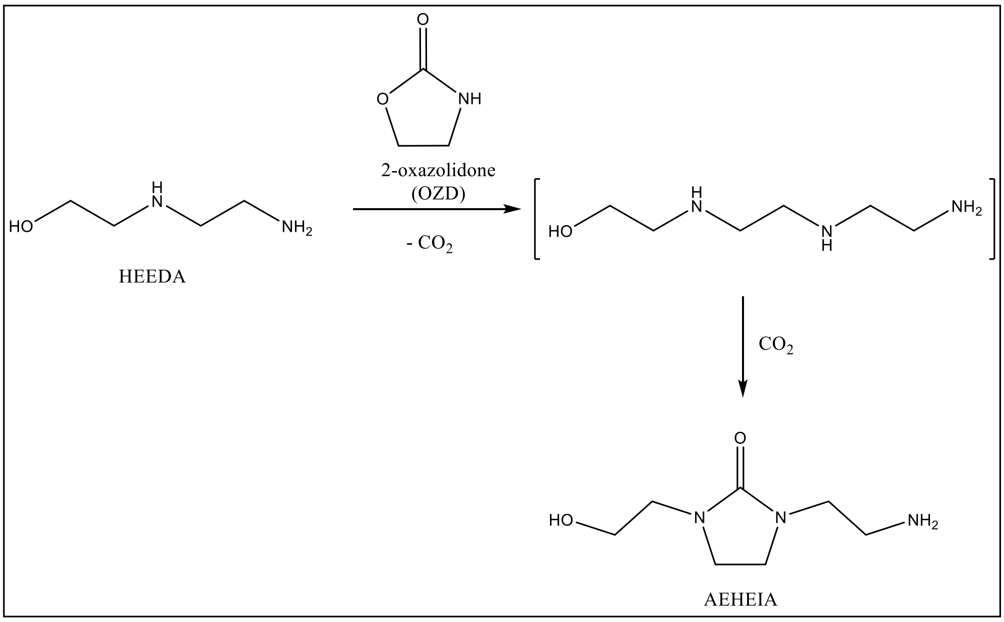

Figure 2.17: Formation of AEHEIA

Lepaumier *et al*. compared the results of their laboratory degradation studies to results from the MEA campaign carried out at the Esbjerg pilot plant in Denmark.[18] It was found that there were more degradation products present in the real samples than in the laboratory samples, a finding also observed by Strazisar when analysing samples from the IMC Chemicals facility in Trona, California.[19] The contribution of thermal degradation in the pilot plant samples was found to be quite limited. There was no detection of HEEDA in the sample and HEIA was only detected in a very small quantity.

Table 2-IV: Thermal degradation products from HEEDA

Chemical structure	Name (abbreviation)	M_w (g/mol)	References
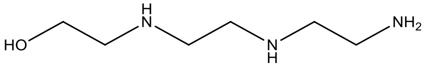	N-(2-hydroxyethyl)-diethylenetriamine	147	38
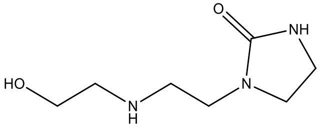	N-(2-hydroxyethylamino)-ethyl-imidazolidin-2-one	173	38
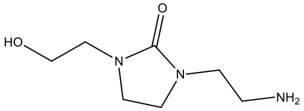	N-(2-aminoethyl)-N'-(2-hydroxyethyl)imidazolidin-2-one (AEHEIA)	173	18
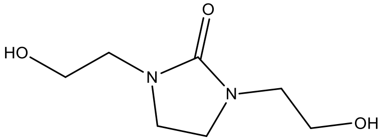	N,N'-bis(2-hydroxyethyl)imidazolidin-2-one (BHEI)	174	63
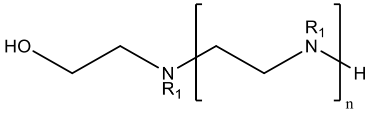	-	-	38

2.5 Corrosion

Corrosion of process equipment used in amine scrubbing systems for CO_2 capture is a major economic issue. As previously discussed the presence of dissolved metal ions in the aqueous amine solution enhances amine degradation. When the amine solvents absorb CO_2 they become corrosive and therefore are one of the causes of the metal ions in the solution.

Corrosion in amine systems begins with the acid gases (H_2S and CO_2) and is enhanced by various physical and chemical factors.[65] In very simple terms the corrosion rate in an amine system is dependent on four factors: corrosive acid concentration, temperature, fluid velocity and HSS concentration.[66, 67] The degradation products of amines have been shown to promote corrosion by complexing iron in the same manner as HSSs.[68, 69] In order to justify the dependence of rate on the four factors listed above it is necessary to relate these variables to the fundamental building blocks of the physical corrosion process.[67] These fundamental building blocks are the oxidation of iron and the interaction between the corrosion products and the corrosive environment. The corrosive agent is typically a form of an acid gas in solution, either H_2S or CO_2. The forms of CO_2 are carbonic acid (H_2CO_3), bicarbonate (HCO_3^-) and carbonate (CO_3^{2-}). The primary corrosion product referred to by Cummings *et al*. is iron sulphide which is insoluble in aqueous solutions and has a tendency to attach uniformly over the area where the oxidation of iron has occurred.[67] This provides a barrier to additional corrosion by blocking access to the free metal. Iron carbonate is also fairly insoluble but it does not form as steadfast a layer over the surface of the free metal.

The formation of HSSs in amine solutions leads to corrosion of the plant equipment. As acid gas loading increases the pH of the solution decreases. When the temperature of the system is increased in the stripper column to regenerate the solvent the weaker and more volatile acids (such as formic and acetic acids) become less strongly bound to the amine. In a hot aqueous environment, the temporarily un-neutralised acids result in very corrosive conditions. High corrosion rates have been reported in the regenerator bottom section, the reboiler and the hot lean inlet of lean/ rich heat exchanger.[53]

As discussed earlier, the degradation of MEA proceeds through the formation of a carbamate ion. Primary amines can also form bicarbonate ions and the relationship between carbamate and bicarbonate concentration is a key parameter which influences corrosion.[53] Selectivity to the carbamate formation is influenced by increasing the amine concentration or the pH of the solution. Bicarbonate reacts very easily with iron to form $FeCO_3$ which provides a protective barrier to further corrosion. However, with primary amines the protective layer is not uniform and the selectivity towards carbamate increases in this case. When this occurs the most probable product is $Fe_2(OH)_2CO_3$. As selectivity for carbamate increases a rapid increase in corrosion rate is seen.[53] To minimise corrosion by carbamate the concentration must be kept very low. With primary amines CO_2 can also induce stress corrosion cracking. This is reported to be induced by carbamate formation in the metal with MEA restricting the pH to values where intergranular cracking occurs.[53]

The degradation products of amines are known to form complexes with iron. Amino acids, formamides and diamines have all been shown to contribute to corrosion in amine solutions. The amino acid bicine has been found in several gas treating plant amine systems along with hydroxyethyl sarcosine.[67, 70] The majority of authors have shown that bicine contributes to corrosion in amine systems. However, it was suggested by Bosen and Bedell that bicine is not involved in corrosion and that the complexing of iron by bicine can be reduced by adding potassium or sodium hydroxide.[70] Cummings *et al*. worked through the same theory as Bosen and Bedell and found some differences.[67] Cummings found that in the presence of bicine the solubility of iron sulphide increased by a factor of 443- this solubility was not measured by Bosen and Bedell. The effect of ‘neutralising’ the bicine by adding sodium hydroxide was tested and in both reports it was found that the solubility of iron sulphide decreased.[67, 70] However, the decrease in solubility is of little importance when the result is compared to a case where there is no bicine present.[67] Therefore, as stated by Cummings *et al*., there is little benefit to 'neutralising' the bicine by adding sodium or potassium hydroxide- it is much more favourable to remove bicine from the system or to prevent its formation altogether. It is recommended to keep levels of amino acids such as bicine at a low concentration, with recommendations varying from 2000 ppm to >250 ppm. The removal has been achieved by ion exchange but this is only economical if operated skilfully.

The model used by Bosen and Bedell was extended by Cummings *et al*. to include the chelation of iron in systems containing CO_2 but no H_2S.[70,67] The insolubility of iron carbonate was observed in both rich and lean amine solutions (0.30 mol CO_2/ mol of amine and 0.01 mol CO_2/ mol of amine, respectively). The solubility increased by a factor of almost 200,000 when bicine was added to the system in both rich and lean cases. As Cummings *et al*. noted, this indicates a potential for increased corrosion due to increased iron solubility. Also, the results showed that iron carbonate was much more soluble in lean solution than in rich solution so the presence of bicine caused solubility to increase in the lean side of the amine system. This is problematic as the iron carbonate will precipitate out in the rich-side of the system leaving the bicine free to chelate more iron in the lean side of the system. If this cycle repeats itself several times then severe corrosion could be observed on the lean side of the system.

Diamines can also be strong chelators of iron and can therefore facilitate corrosion. Diamines result from the degradation of primary and secondary amines and the only way to eliminate diamine formation is to use a tertiary amine. In most systems the amount of diamines present does not reach a significant level as they are result of side reactions with CO_2. Systems which slowly accumulate diamines also typically run with high HSS content. Heat stable salts in amine systems can be removed by ion exchange, distillation or hydrolysis.

2.6 Analytical Techniques

Several analytical techniques have previously been used for the analysis of degraded amine solvents. These include Gas Chromatography Mass Spectroscopy (GC-MS), Ion Chromatography (IC), ^{13}C NMR Spectroscopy, Inductively Coupled Plasma Mass Spectroscopy (ICPMS) and Gas Chromatography Flame Ionisation Detection (GC-FID).

2.6.1 Gas Chromatography Mass Spectroscopy

Gas Chromatography Mass Spectroscopy (GC-MS) is the most widely used technique for analysing degraded amines. The main purpose of using GC-MS for amine analysis is to identify the degradation products in the solvent. Further details on the analytical technique and the experimental method used in this work are given in Chapter 3.

Lepaumier *et al*. used gas chromatography to quantify the remaining starting amine and the identified degradation products.[15, 18, 32, 63, 71] Thermal degradation products HEIA and AEHEIA were observed to increase over time indicating their relative stability, whereas OZD and HEEDA remained constant suggesting that they were intermediate compounds which underwent further reactions.

GC-MS was also used by Supap *et al*. to identify formic and acetic acids, imidazole and HEA.[35]

2.6.2 Ion Chromatography

Ion Chromatography (IC) is a form of liquid chromatography which uses ion-exchange resins to separate atomic or molecular ions based on their interaction with the resin within the analytical column. It is used to quantify the levels of amines and

HSSs in solvents. Further details on the analytical technique and the experimental method used in this work are given in Chapter 3.

Davis and Rochelle used cation IC to measure the disappearance of MEA and the appearance of ionic degradation products such as HEEDA. It was also used to identify unknowns using known addition spiking.[38]

Sexton and Rochelle used anion IC to identify anionic species from oxidative degradation and cation IC to identify cationic species.[34] The quantification of amides was achieved by adding 1 mL of 5 M NaOH to 1 mL of sample and allowing 24 hours for hydrolysis of any amides. Detection of carboxylic acid released by hydrolysis was done by running the samples using the method for anionic species. Non-ionic species were not retained on the columns and were not measured by the ionic conductivity detector. Products identified by anion IC are reported as being: formate, formamide, nitrite, nitrate, oxamide, oxalate, glycolate and acetate.[34]

Zhou *et al*. used both anion and cation IC to identify thermal degradation products. Products identified were OZD, HEIA, AEHEIA, HEEDA and ammonium in the cation method, and formate in the anion method.[72]

2.6.3 ^{13}C NMR Spectroscopy

Nuclear magnetic resonance (NMR) spectroscopy is a non-destructive analytical technique which uses the magnetic properties of atomic nuclei to determine the physical and chemical properties of atoms or the molecules in which they are contained. It has been used in only a few studies to investigate the speciation of amines and has not been correlated with any other analytical techniques. Further details on the analytical technique and the experimental method used in this work are given in Chapter 3.

The first quantitative ^{13}C NMR experiments on amine-CO_2-H_2O solutions date back to 1984 by Barth *et al*..[73] According to Perinu *et al*. most papers on ^{13}C NMR of amine-CO_2-H_2O systems focus on quantitative NMR spectroscopy with only a few reporting qualitative data.[74-76] Quantitative NMR spectroscopic studies have been used for determining the distribution of species in solutions of CO_2 in aqueous amines. The use of ^{1}H and ^{13}C NMR allows quantitative information to be gathered on the following species: amine, carbonate, bicarbonate and CO_2. Some evidence for the detection and quantification of OZD has also been reported.[77]

It is not possible to distinguish between amine and protonated amine (amine/ amineH^+) or between carbonate and bicarbonate (HCO_3^-/ CO_3^{2-}) because in these systems species which have exchanging protons have a common peak, due to the proton transfer occurring at a faster rate than the NMR time-scale. For this reason only the sum of their concentrations can be obtained.[73] In 1998 a method was developed to calculate concentrations of carbonate and bicarbonate within a single peak.[73]

In online NMR spectroscopic measurements the experimental set-up is directly coupled to the NMR probe. This allows a non-invasive direct measurement at experimental conditions regarding temperature, pressure and composition and is therefore a valuable technique in the study of amine degradation products.[77] It is noted however that there seems to be no application of NMR spectroscopy to the degraded amine samples which form in the thermal reclaimer where larger, more viscous degradation products may occur.

2.6.4 Inductively Coupled Plasma Mass Spectroscopy

Inductively Coupled Plasma Mass Spectroscopy (ICPMS) is a powerful analytical technique used to determine the levels of trace metals in a sample. A wide range of elements can be detected and quantified using ICPMS, but this technique has not been widely used in the analysis of degraded amine solvents. Further details on the analytical technique and the experimental method used in this work are given in Chapter 3.

2.6.5 Gas Chromatography Flame Ionisation Detector

The use of flame ionisation detection (FID) with GC provides an accurate, mass sensitive response which is proportional to the mass of carbon passing through the detector. It is used to quantify compounds, but has not been widely used in amine solvent analysis. Further details on the analytical technique and the experimental method used in this work are given in Chapter 3.

2.6.6 Summary of Analytical Techniques

As discussed above, several analytical techniques have been applied to the characterisation of degraded amines but there has been little work on using multiple analytical methods. By correlating the results from complementary techniques it is possible to understand the solvent behaviour at pilot scale. The use of ^{13}C NMR spectroscopy is limited and has not been carried out on any solvents from pilot plant applications. ^{13}C NMR spectroscopy has the potential to be used as a rapid measure of the extent of degradation as this work will show.

2.7 Summary and Conclusions

This chapter has reviewed the current literature on amine degradation, discussing the commonly used amine solvents, the mechanisms of degradation and proposed degradation products. The use of several analytical techniques has been briefly discussed. The main points from this literature review are:

- Amine degradation and corrosion of the plant equipment are major problems in amine scrubbing systems. Several studies have been carried out into degradation mechanisms but most of these have been done at laboratory scale. Only a limited number of studies have researched degradation at pilot plant scale. The need to further investigate pilot plant samples of degraded amine solvents has been highlighted by these few studies. There have been several differences between lab scale and pilot scale samples such as different amounts of degradation products and different mechanisms of degradation, but there is little understanding of the reasons for these differences. This emphasises the need for further study.

- It is widely acknowledged that there are two types of degradation possible in amine systems- oxidative degradation and thermal degradation. Oxidative degradation is believed to occur mainly at absorber conditions with CO_2-loaded amine solvent, primarily by hydrogen abstraction. Thermal degradation is thought to occur in the stripper unit at higher temperatures. However, one study which compared lab scale and pilot scale degradation samples found that thermal degradation plays a minor role at pilot scale. Further investigation into this is required in order to establish why this is so.
- Several factors affect the oxidative degradation process. These include the formation of heat stable salts (HSSs) from the initial aldehyde degradation products and the effect of dissolved metal ions which have been shown to catalyse the degradation of the solvent. Extensive investigation of these factors has been carried out by several authors, but most of these were done at laboratory scale. The need to investigate pilot scale samples is evident as there may be differences in the effects of various factors when the process is scaled up.
- Corrosion of plant equipment should also be taken into consideration in amine scrubbing systems. Corrosion is enhanced by the formation of HSSs and the complexation of iron by degradation products such as amino acids, for example bicine. The recommendation is to remove amino acids by ion exchange or prevent their formation altogether, rather than to neutralise them using sodium hydroxide which has been shown to be ineffective.

- A variety of analytical techniques have been used to characterise amine degradation products. The most widely used technique is GC-MS as this provides the most useful information, along with IC. The use of other analytical techniques such as ^{13}C NMR spectroscopy has the potential to be used as a rapid measure of the extent of degradation.
- There has been little work on correlating data from different analytical techniques and as such, this work focuses on filling this gap in the current literature. The correlation between GC-MS and GC-FID will allow greater accuracy in determining the quantity of degradation products, while the use of ^{13}C NMR spectroscopy with GC-MS will provide a rapid analysis of the extent of amine degradation.

Chapter 3: Analytical Methods and Experimental Apparatus

3.1 Introduction

The first part of this chapter provides details of the chemicals used and samples which have been analysed in this work. This is followed by details about the experimental techniques that were used along with the methods employed to perform the analyses. Information on equipment specifications and operating procedures are presented in great detail.

3.2 Materials

3.2.1 Degraded amines

Table 3-I and Table 3-II detail the samples tested in this work. The blended amine solvents were received from a UK pilot plant that had been operated under purposefully severe conditions in order to investigate how the solvent would behave at extreme operating conditions. This was a proprietary blend, the composition of which cannot be disclosed. The single amine solvent samples were all from a pilot plant in North West Europe and had been operated both with and without ion exchange. A second batch of the same single amine solvent (W1- 17) had been operated with continuous ion exchange in an attempt to mitigate degradation. All solvent samples were from the lean side of the amine system. Due to commercial sensitivity, the composition of the primary amine solvent cannot be disclosed.

Table 3-I: Blended amine samples analysed

Sample ID	Total hours	Cumulative solvent operational hours	Condition	Total hours operating at this condition	Loading
B1.1	192	35	Solvent performance testing	35	Rich: 0.40
B1	1176	195	Solvent performance testing	160	Rich: 0.37
B2	2160	367	Solvent performance testing	81	Rich: 0.37
			Plant dynamic performance testing	82	
			Solvent performance testing	9	
B3	2688	499	Solvent performance testing	68	Rich: 0.37 Lean: 0.12
			High SO_2 testing (70 ppm)	64	
B3.1	2712	508	High O_2 testing (Case 1)	9	Rich: 0.36 Lean: 0.11
B3.2	2952	529	High O_2 testing (Case 2)	30	Rich: 0.38 Lean: 0.12
B3.3	3312	561	High O_2 testing (Case 3)	62	Rich: 0.37 Lean: 0.15
B3.4	3336	570	High regeneration temperature	9	Rich: 0.36 Lean: 0.08
B3.5	3384	587	High regeneration temperature	26	Rich: 0.37 Lean: 0.05
B3.6	3456	595	High regeneration temperature	34	Rich: 0.37 Lean: 0.05
B4	3792	659	Solvent performance testing	64	Rich: 0.40 Lean: 0.11
B5	3888	682	HCl testing	23	Rich: 0.41 Lean: 0.17

Table 3-II: Single amine samples analysed

Sample ID	Operating hours	Date sampled	Comments	Wt % amine	Loading
Before IX 1	4425	05.06.14	Before ion exchange	19.5	0.3
Before IX 2	4425	05.06.14	Before ion exchange	19.5	0.3
After IX	4425	05.06.14	After ion exchange	19.5	0.3
W 1	0	05.02.15	-	98.7	n/a
W 2	20	10.02.15	-	32.9	0.18
W 3	54	12.02.15	-	35.1	0.17
W 4	170	17.02.15	-	32.2	0.15
W 5	218	19.02.15	-	34.3	0.16
W 6	241	25.02.15	-	34.6	0.16
W 7	363	05.03.15	-	34.6	0.16
W 8	432	18.03.15	-	33.1	0.16
W 9	478	20.03.15	-	36.0	0.17
W 10	550	25.03.15	-	34.5	0.17
W 11	637	08.04.15	Reclaimer A Phase 1 operational between 08.04.15-27.04.15	33.2	0.16
W 12	707	15.04.15		31.6	0.16
W 13	738	20.04.15		31.5	0.16
W 14	847	27.04.15		32.5	0.16
W 15	892	29.04.15	-	32.2	0.16
W 16	2155	11.11.15	Reclaimer B operational between 30.06.15- 05.10.15	34.9	0.17
W 17	2179	12.11.15	Reclaimer A Phase 2 operational between 19.10.15-04.11.15	37.5	0.16

3.2.2 Standards

Table 3-III lists the reagents used to make up the standards used in analyses. All reagents were supplied by Sigma-Aldrich.

Table 3-III: Chemicals used for standard preparation

Reagent	CAS #	Molecular weight (g/mol)	Assay (%)
Acetic acid	64-19-7	60.05	≥ 99.7
Formic acid (88 wt. % in water)	64-18-6	46.03	88.0-91.0
Glycolic acid (70 wt.% in water)	79-14-1	76.05	70.0
Oxalic acid dihydrate	144-62-7	126.07	≥ 99.0
Sodium nitrate	7631-99-4	84.99	≥ 99.0
Sodium nitrite	7632-00-0	69.00	≥ 97.0
HEEDA	111-41-1	104.15	99.0
OZD	497-25-6	87.08	98.0
HEA	142-26-7	103.12	Technical grade
HEIA (75 % in H_2O)	3699-54-5	130.15	75.0
HEI	1615-14-1	112.13	97.0
Bicine	150-25-4	163.17	≥ 99.0
N-(2-hydroxyethyl) succinimide	18190-44-8	143.14	95.0
Succinic anhydride	108-30-5	100.07	≥ 99.0
Sodium Hydroxide (50 % in H_2O)	1310-73-2	40.00	50.0
Multi Cation Standard 2 for IC	n/a	n/a	≤ 0.1 % in nitric acid
1,4-dioxane	123-91-1	88.11	100.0
$CDCl_3$	865-49-6	120.38	99.8

3.3 Gas Chromatography Mass Spectroscopy

The combined use of Gas Chromatography (GC) with Mass Spectroscopy (MS) allows the separation and identification of individual components in a mixture in a single process. It is a semi-quantitative process, where the total ion current (TIC) is used as a proxy of the concentration of each species. To make GC-MS a quantitative analytical technique the use of internal standards is required. This is impractical for the number of compound observed in degraded amines so has not been carried out in this work.

3.3.1 Gas Chromatography

In chromatography the components are separated in a mobile phase which in GC is an inert gas, usually helium or nitrogen. The mobile phase carries the components to the stationary phase, contained within a column, which is a chemical that selectively attracts components within the mixture. Different components adsorb at different rates in the column and those which interact least are eluted first.[78] By altering the characteristics of the mobile and stationary phases, it is possible to separate different mixtures of chemicals. Further changes to the separation process are possible, such as changing the temperature of the stationary phase or the pressure of the mobile phase. The stationary phase column is housed within an oven which has a temperature gradient programmed into it. The gradual ramping of the temperature causes components with lower boiling points to be eluted before those with higher boiling points. Eluted compounds enter a detector which produces a signal on a chromatogram. The time taken from injection (time zero) to the elution is called the retention time. For a given set of conditions each compound within a mixture will always be eluted at a characteristic retention time so it is possible to make judgements about the identity of the compound.[78] However, similar compounds often have similar retention times so it is necessary to gather more information before a reasonable identification can be made. This is achieved by using mass spectroscopy.

3.3.2 Mass Spectroscopy

The individual components eluted by GC enter a mass spectroscopy detector where they are bombarded with a stream of electrons (electron ionisation, EI) causing them to fragment. The fragments produced are charged ions with a certain mass which depends on the natural scission point of a molecule, inherent to its structure. Since most fragments have a charge of +1, the mass to charge ratio (m/z) is representative of the molecular weight of the fragment.[79] In quadrupole mass spectroscopy a group of four electromagnets focuses each fragment through a slit and into a detector. The electromagnets focus on one m/z ratio at a time and perform several scans per second.[80] This produces the mass spectrum for a compound and is essentially a fingerprint for the molecule. Within the GC-MS system there is a library of known compounds to which the mass spectra may be compared in order to identify the compounds when EI is used.

3.3.3 GC-MS Standard Preparation

In order to prepare the standards for GC-MS analysis approximately 10 µL or 0.1 g each of HEEDA, OZD, HEA, HEIA, HEI, bicine, N-(2-hydroxyethyl) succinimide and succinic anhydride was added to a 1.5 mL GC glass vial and 1.3 mL methanol was added. A multi-component standard was also made by adding the same amount of each component named above to the same glass vial and diluting with methanol. These standards were used to identify the retention times of each component which was used for GC-FID analysis (see Section 3.4). The GC-MS chromatograms for the standards can be found in Appendix A.

3.3.4 GC-MS Sample Preparation

For each degraded amine sample to be analysed 30 µL of the sample was transferred to a 1.5 mL GC glass vial and 1.3 mL methanol was added.

3.3.5 GC-MS Operating Procedure

The analysis of degradation products was carried out using a Varian CP-3800 GC coupled to a Varian 1200 MS, with helium carrier gas. The GC was operated in EI mode with a 70 electron-volt (eV) setting and operated in full scan mode. The column used was a low-mid polarity ZB-1701 (60 m x 0.32 mm x 0.25 µm) which was packed with 14 % cyanopropylphenyl and 86 % dimethylpolysiloxane. It was found that this column gave the best peak separation.

The sample was injected at 70 °C and the temperature was ramped to 300 °C at a heating rate of 5 °C/ min. The final hold time was 14 minutes, giving a total run time of 60 minutes. The scan range was 20 - 450 m/z in order to detect the low molecular weight amine fragments as well as the higher molecular weight degradation products. An initial solvent delay of five minutes allowed for the solvent to elute without obscuring the spectrum. This scan method was named ‘SCAN 60m Splitless’. All samples were analysed in triplicate and an average result is reported, with error analysis being reported to one standard deviation.

3.4 Gas Chromatography Flame Ionisation Detection

Flame ionisation detection (FID) is used to measure the concentration of organic species in a gas stream. It is often used as a detector in GC. It is a mass sensitive detector as the response is proportional to the mass of carbon which passes through the detector, which is measured in picograms of carbon per second (pg C s^{-1}).[81]

In FID the samples and carrier gas are passed from the GC column through a hydrogen-air flame. Alone, the hydrogen-air flame only creates a few ions but when an organic compound is burned there is an increase in the number of ions produced. The ions are attracted to a collector near the flame by a polarizing voltage. The current produced is proportional to the amount of sample being burned.[81] Molecules which contain heteroatoms such as oxygen decrease the detectors response.[82] For example, the response of FID to methane (CH_4) is excellent but for formaldehyde (CH_2O) the response is quite poor. Therefore, highly oxygenated molecules or sulphides may be best detected using other methods.

The unit carbon response means that FID responds linearly to the mass of carbon flowing through it, regardless of carbon structure. The error in unit carbon response for most hydrocarbons is 1 – 2 % which allows the quantification of mixtures to be carried out without having calibration standards for every component.[81] Amounts of components in a sample relate to their relative peak area so a simple area per cent report will fairly closely reflect the mass per cent of each component in a mixture. The relative ratio of the area of one peak to another closely reflects its relative amount in the sample which is useful when estimating the concentration levels of components in a sample when identities are unknown or standards are not available for calibration.

3.4.1 GC-FID Standard Preparation

In order to prepare the standards for GC-FID analysis individual 1000 ppm solutions of each standard were made by adding 0.1 g each of HEEDA, OZD, HEA, HEIA, HEI, bicine, N-(2-hydroxyethyl) succinimide and succinic anhydride to separate 100 mL volumetric flasks and filling to the 100 mL mark with ultrapure water (18.2 MΩ.cm^{-1}).

To make a 100 ppm solution, 0.1 mL of the 1000 ppm solution was transferred to a clean 100 mL volumetric flask and filled to the line with ultrapure water.

To make a 10 ppm solution, 0.1 mL of the 100 ppm solution was transferred to a clean 100 mL volumetric flask and filled to the line with ultrapure water.

To make a 1 ppm solution, 0.1 mL of the 10 ppm solution was transferred to a clean 100 mL volumetric flask and filled to the line with ultrapure water.

Each standard was diluted in methanol (30 µL standard in 1.3 mL methanol) and analysed by GC in the Agilent 5977A MSD/ 7890B GC system using the same column and conditions as for GC-MS analysis (see Section 3.3.5). The 1000 ppm standard was used for identification of the individual components. However, only HEA, OZD, N-(2-hydroxyethyl) succinimide and bicine were identifiable. HEEDA, HEIA, HEI and succinic anhydride appear not to have been eluted from the column.

3.4.2 GC-FID Sample Preparation

The degraded amine samples for GC-FID analysis were prepared in the same way as for GC-MS analysis (Section 3.3.4).

3.4.3 GC-FID Operating Procedure

The GC-FID analysis was run on an Agilent Technologies 5977A MSD and 7890B GC system. The method used was the same as that which was used for the GC-MS analysis (Section 3.3.5). All samples were analysed in triplicate and an average result is reported, with error analysis being reported to one standard deviation.

3.5 Inductively Coupled Plasma Mass Spectroscopy

Inductively coupled plasma mass spectroscopy (ICPMS) is a powerful analytical technique used to determine the levels of trace metals in a sample. A wide range of elements can be detected and quantitatively measured using ICPMS.

3.5.1 Ionisation

Free electrons are introduced into a plasma gas, usually argon (Ar), by a spark. The electrons are accelerated by a magnetic field to reach the ionisation potential of the gas (15.76 eV for Ar). This causes an avalanche breakdown to form a steady state plasma (Equation 3.1 and Equation 3.2).[83]

$$Ar + e^- \rightarrow Ar^+ + 2e \qquad \textbf{Equation 3.1}$$

$$Ar + e^- \rightarrow Ar^* + e^* \rightarrow Ar^+ + 2e \qquad \textbf{Equation 3.2}$$

The sample is introduced into the ICP by either a nebuliser with a spray chamber or by laser ablation. Over 90 % of analyses use a nebuliser and spray chamber. Standard concentric or cross flow nebulisers with a spray chamber operate at 0.5 – 2.0 mL/min and achieve only ~2 % analyte transport efficiency.[83]

3.5.2 Collision-Reaction Cells

A collision-reaction cell is an additional multi-pole placed between the interface of the ICP and the analytical MS quadrupole. It can be pressurised with a collision or reaction gas to resolve problems of spectral interferences. Common multipoles used include: quadrupole, hexapole, octapole and flatapole.[83]

3.5.3 ICPMS Standard Preparation

Internal standards were used with the following concentrations in 2 % nitric acid (HNO_3): scandium = 50 parts per billion (ppb), germanium = 20 ppb, rhodium = 10 ppb and iridium = 5 ppb. External calibration standards were all in the range 0 – 100 ppb.

3.5.4 ICPMS Sample Preparation

To analyse samples by ICPMS serial dilutions were carried out. First, 100 µL of degraded amine sample was transferred to an ICPMS sample tube. To this, 9.9 mL 2 % HNO_3 was added to give a 1:100 dilution. Then 1000 µL of the 1:100 dilution was transferred to a clean ICPMS sample tube. To this, 9 mL 2 % HNO_3 was added. This gave a 1:1000 dilution which was used for analysis.

3.5.5 ICPMS Operating Procedure

Multi-element analysis was carried out using either a Thermo Fisher Scientific X-Series II with a 'hexapole collision cell' (typically charged with 7 % hydrogen in helium) upstream of the analytical quadrupole, or a Thermo Fisher Scientific iCAP-Q with a 'Flatopole collision cell' (typically charged with helium gas) upstream of the analytical quadrupole to reduce polyatomic interferences. Samples were introduced via a covered autosampler (Cetac ASX-520) through a concentric glass venturi nebuliser (Thermo-Fisher Scientific). For the X-Series II instrument, sample processing was undertaken using Plasmalab software (version 2.5.4; Thermo-Fisher Scientific). Sample processing for the iCAP-Q instrument was carried out using Qtegra software (Thermo Fisher Scientific). Each analysis was reported as the average of three runs of each sample. Standard multi element analysis included: B, Na, Mg, P, S, K, Ca, Ti, Li, Be, Al, V, Cr, Mn, Fe, Co, Ni, Cu, Zn, As, Se, Rb, Sr, Mo, Ag, Cd, Cs, Ba, Tl, Pb and U.

All analyses were carried out by Dr. Saul Vazquez-Reina in the School of Biosciences at the University of Nottingham. All samples were analysed in triplicate and an average of the results is reported, with error analysis being reported to one standard deviation.

3.6 Ion Chromatography

Ion Chromatography (IC) is a form of liquid chromatography which uses ion-exchange resins to separate atomic or molecular ions based on their interaction with the resin within the analytical column. Ionic species are separated by passing through a pressurised chromatographic column in which the constituents of the column absorb ions. As the eluent (mobile phase) runs through the column the ions absorbed by the stationary phase start to separate out according to the strength of the interaction with the stationary phase. Components which react weakly with the stationary phase will elute first and those which have a strong interaction with the stationary phase will elute last. After separation in the column, the ions arrive at a suppressor. Suppression is necessary to reduce the conductivity of the eluent. Since the eluent contains a relatively high amount of salt it has very high conductivity. In order to detect the much lower concentrations of sample ions the number of dissolved ions in the eluent must be decreased after the column separation. This is the role of the suppressor- to lower the background conductivity and to increase the sensitivity for the sample ions.[84]

3.6.1 Anion Chromatography

In anion exchange chromatography the negatively charged ions are attracted to a positively charged resin in the analytical column. Strong bases are chemical compounds which are able to deprotonate very weak acids and will remain ionised, to some extent, over the whole pH range. Ion exchange functional groups based on quaternary amines are known as strong anion exchangers.[85] Weak anion exchangers are usually primary, secondary or tertiary amino functional groups and are capable of being fully ion- suppressed at a sufficiently high pH.[85]

3.6.2 Cation Chromatography

In cation exchange chromatography the positively charged ions are attracted to a negatively charged resin in the analytical column. Strong acids ionise completely in an aqueous solution and therefore will always be ionised, to some extent, over the entire pH range.[85] Ion exchange functional groups based on strong acidic functional groups such as sulphonic groups are known as strong cation exchangers. Ion exchange functional groups based on weak acidic compounds such as carboxylic acids, are known as weak cation exchangers. These compounds do not fully ionise in an aqueous solution and as such can be fully ion suppressed below certain pH values.[85]

3.6.3 Anion Chromatography Standard Preparation

To make a 2000 ppm stock anion standard solution, approximately 200 mL of ultrapure water was added to an empty 1 L volumetric flask. To this, 2.00 g each of sodium nitrate, sodium nitrite and oxalic acid were added, followed by 2.0 mL acetic acid, 2.3 mL formic acid and 2.9 mL glycolic acid. The flask was filled to the 1 L mark with ultrapure water.

To make the 10 ppm stock anion standard, 0.5 mL of the 2000 ppm stock anion standard was transferred to an empty 100 mL volumetric flask. The flask was then filled to the 100 mL mark with ultrapure water.

To make the 20 ppm stock anion standard 1.0 mL of the 2000 ppm stock anion standard was transferred to an empty 100 mL volumetric flask. The flask was then filled to the 100 mL mark with ultrapure water.

To make the 30, 40 and 50 ppm stock anion standards, the process above was repeated with 1.5, 2.0 and 2.5 mL respectively of the 2000 ppm stock anion standard transferred into three separate 100 mL volumetric flasks and diluted with ultrapure water.

3.6.4 Anion Chromatography Sample Preparation

For each degraded amine sample to be analysed 0.1 mL of the sample was transferred to a 15 mL glass vial. Then 10.0 mL ultrapure water was added to the vial to dilute the sample by approximately 100 times.

Amide concentration analysis was carried out by adding 1 g of 5 M sodium hydroxide (NaOH) to 1 g degraded amine sample and allowing 24 hours for the reaction to go to completion. Dilution was carried out as above. The NaOH hydrolysed any amides which were present in the degraded amine solution and recovered the respective carboxylic acids and amines. Any increase in carboxylic acid concentration between the two samples was considered to be amide that had been recovered in the form of carboxylic acid. To prepare the 5 M NaOH solution, 30 mL ultrapure water was added to a 100 mL volumetric flask. Then 26.4 mL of NaOH (50 % in water) was added carefully to the flask. Finally, the volumetric flask was filled to the line with ultrapure water.

3.6.5 Anion Chromatography Operating Procedure

For the analysis of anionic species produced from the oxidative degradation of amines a Dionex ICS-5000+ Dual Reagent Free Ion Chromatography (RFIC) system was used. The system included a dual pump (DP) module, eluent generation (EG) module and a conductivity (DC) module. Experimental samples were introduced manually via a 1 mL plastic syringe through the injection port. A majority of the sample was flushed through a 25 µL injection loop to ensure that there was no cross-contamination from previous samples. The remainder of the sample was passed through the injection loop and carried by the mobile phase to the inlet of the column.

The mobile phase was an aqueous solution of potassium hydroxide (KOH). Ultrapure water, produced at 18.2 MΩ.cm^{-1}, was provided from a Sartorius arium$^{®}$ pro ultrapure water supply. The ultrapure water was transferred from the 2 L plastic reservoir located on top of the DC module using an isocratic pump located in the DP module. Eluent was produced by mixing the water with concentrated KOH from a KOH EluGen Cartridge (EGC). A specific ratio of KOH was dispensed and mixed with the water using the interface on Chromeleon software (version 7.20). The generated eluent then exited the EGC and passed through a Continuously Regenerated Anion Trap Column (CR-ATC) which is a selective ion exchange membrane to remove ionic contaminants. The eluent then passed through the eluent generation (EG) degas tubing and then to the injection valve. Eluent passed through the injection loop picking up the sample. The eluent/ sample mixture was pumped through the AG15 Guard column (2 x 50 mm) then the AS15 Analytical Column (2 x 250 mm). Both columns are packed with a cross-linked ethylvinylbenzene/ divinylbenzene resin affixed with quaternary ammonium groups. These columns were designed specifically for the separation of low molecular weight compounds. After the anionic species had been flushed from the columns the eluent carried them to the anion self-regenerating suppressor (ASRS) which separated the ionic species in solution. The anions were weakly ionized in the suppressor and once they had exited the suppressor they passed through a 2 mm carbonate removal device (CRD) which uses ion exchange to scrub out any carbonate in the eluent. Once the solution had been scrubbed for carbonate it travelled to a conductivity cell. As the solution passed through the cell any anionic species travelling through produced a response that is represented by a peak (measured in microSiemens, µS). The height and area of each peak is directly proportional to the concentration of each of the anionic species in solution. The solution exited the cell and entered the suppressor where it was used as the water source for the regenerant chamber. The flow was directed through the CRD again, through the EG degas tubing and the CR-ATC and then to waste.

The method used for anion analysis was taken from the thesis by Sexton and was as follows: 2 mM KOH from 0 – 17 minutes, linear gradient to 45 mM KOH from 17.1 –

25 minutes, hold at 45 mM KOH to 35 minutes, equilibration for 6 minutes to return to time zero conditions.[59] Flow rate was 0.50 mL/min. The upper and lower pressure limits were 200 and 5000 psi respectively.

3.6.6 Cation Chromatography Standard Preparation

To make the standards used for cation analysis, a multi-element standard containing barium, calcium, potassium, lithium, magnesium, manganese, sodium, ammonium and strontium was used. The cations of interest were calcium, potassium, lithium, magnesium, sodium and ammonium.

For the 10 ppm solution, 1 mL of the multi-element standard was added to a 10 mL volumetric flask and diluted with ultrapure water. For the 20, 30, 40 and 50 ppm standards 2, 3, 4, and 5 mL respectively of the multi-element standard was added to different 10 mL volumetric flasks which were then diluted with ultrapure water.

3.6.7 Cation Chromatography Sample Preparation

For each degraded amine sample to be analysed 0.1 mL of the sample was transferred to a 15 mL glass vial. Then 10.0 mL ultrapure water was added to the vial to dilute the sample by approximately 100 times. To achieve a 1:10,000 dilution, 0.1 mL of each 1:100 dilution was transferred to a clean 15 mL sample vial and to this 10.0 mL ultrapure water was added. The 1:10,000 dilution was used for analysis.

3.6.8 Cation Chromatography Operating Procedure

For the analysis of cationic species produced from the oxidative degradation of amines a Dionex ICS-5000+ Dual RFIC system was used. The system included a DP module, EG module and a DC module. Experimental samples were introduced manually via a 1 mL plastic syringe through the injection port. A majority of the sample was flushed through a 25 µL injection loop to ensure that there was no cross-contamination from previous samples. The remainder of the sample was passed through the injection loop and carried by the mobile phase to the inlet of the columns.

The mobile phase was an aqueous solution of methane sulphonic acid (MSA). Ultrapure water, produced at 18.2 MΩ.cm^{-1}, was provided from a Sartorius arium® pro ultrapure water supply. The deionized water was transferred from the 2 L plastic reservoir located on top of the DC module using an isocratic pump located in the DP-1 module. Eluent was produced by mixing the water with concentrated MSA from an EluGen MSA Cartridge. A specific ratio of MSA was dispensed and mixed with the water using the interface on Chromeleon software (version 7.20). The generated eluent then exited the EGC and passed through a Continuously Regenerated Cation Trap Column (CR-CTC) which is a selective ion exchange membrane to remove ionic contaminants. The eluent then passed through the EG degas tubing and then to the injection valve. Eluent passed through the injection loop picking up the sample. The eluent/ sample mixture was pumped through the CG17 Guard column (2 x 50 mm) then the CS17 Analytical Column (2 x 250 mm). Both columns are packed with a cross-linked ethylvinylbenzene/ divinylbenzene resin, functionalised with carboxylic acid groups which have a high selectivity for hydronium ions. These columns were designed specifically for the analysis of hydrophobic and/ or polyvalent amines as well as alkali metals, alkaline earth metals and ammonium ions. After the cationic species had been flushed from the columns the eluent carried them to the cation self-regenerating suppressor (CSRS) which separated the ionic species in solution. The cations were weakly ionized in the suppressor and once they had exited the suppressor they passed into a conductivity cell. As the solution passed through the cell any cationic species travelling through produced a response that is represented by a peak (measured in μS). The height and area of each peak is directly proportional to the concentration of each of the cationic species in solution. The solution exited the cell and entered the suppressor where it was used as the water source for the regenerant chamber. The flow was directed through the EG degas tubing and the CR-CTC and then to waste.

The method used for cation analysis was a gradient method: linear gradient from 0.5 mM MSA to 25 mM MSA from 0 to 25 minutes, step change to 10 mM MSA at 25.1 minutes, isocratic to 32 minutes, step change to 0.5 mM MSA at 32.1 minutes, isocratic to 35 minutes. Equilibration time was two minutes. The upper and lower pressure limits were 200 and 5000 psi respectively.

3.7 Nuclear Magnetic Resonance Spectroscopy

Nuclear magnetic resonance (NMR) spectroscopy is a non-destructive analytical technique which uses the magnetic properties of atomic nuclei to determine the physical and chemical properties of atoms or the molecules in which they are contained.

3.7.1 ^{13}C NMR Spectroscopy

NMR is a spectroscopic technique which uses the magnetic properties of atomic nuclei to determine the structure of molecules. When certain nuclei are immersed in a static magnetic field and exposed to a secondary oscillating magnetic field the nuclei resonate at a specific characteristic frequency which is dependent on the strength of the magnetic field and the magnetic properties of the nucleus. The property which determines whether a nucleus is susceptible to this phenomenon is known as spin.[86]

3.7.1.1 Spin

Magnetic nuclei possess an intrinsic angular momentum,P, known as spin. The angular momentum is quantised as shown in Equation 3.3 where $\hbar = {}^{h}/_{2\pi}$ where h is Planck's constant ($= 6.626\,x\,10^{-34}\,J\,s$), and I is the angular momentum quantum number, usually simply called nuclear spin.[87]

$$P = \sqrt{I(I+1)}\hbar \qquad \textbf{Equation 3.3}$$

The nuclear spin can have values of $I = 0, {}^{1}/_{2}, 1, {}^{3}/_{2}, 2$ ... up to 6. It is not possible to predict the values of either I or P.

There is a magnetic moment, μ, associated with angular momentum. These two vector quantities are proportional to each other, as seen in Equation 3.4.

$$\mu = \gamma P \qquad \textbf{Equation 3.4}$$

The proportionality factor, γ, is a constant for each nucleus and is called the gyromagnetic ratio. Those nuclei with a large value of γ are said to be sensitive to detection and are therefore easy to observe in the NMR experiment, whereas those nuclei with a small value of γ are said to be insensitive.[87] By combining Equation 3.3 and Equation 3.4, the equation for the magnetic moment, μ, is obtained (Equation 3.5):

$$\mu = \gamma\sqrt{I(I+1)}\hbar \qquad \textbf{Equation 3.5}$$

Therefore, nuclei with spin $I = 0$ have no nuclear magnetic moment and cannot be observed by NMR spectroscopy.

The spin angular momentum of a spin-I nucleus has $2I + 1$ possible directions on an arbitrarily chosen axis. For example, the z component of P, denoted as P_z, is quantised as in Equation 3.6, where m is magnetic quantum number.

$$P_z = m\hbar \qquad \textbf{Equation 3.6}$$

3.7.1.2 Effect of a magnetic field

When there is no magnetic field present all orientations of a spin-I nucleus have the same energy. When a magnetic field, B, is applied this degeneracy is removed. The energy of a magnetic moment in a magnetic field is given by Equation 3.7. The magnetic field is also a vector quantity.[86]

$$E = -\mu B \qquad \textbf{Equation 3.7}$$

When the magnetic field is strong the direction of quantisation coincides with the direction of the field. The energy of the nucleus is shifted by an amount proportional to the magnetic field strength, the gyromagnetic ratio and the directional component of the angular momentum (Equation 3.8).[86, 87] The $2I + 1$ states for the spin-I nucleus are equally spaced, with an energy gap of $\hbar\gamma B$.

$$E = -m\hbar\gamma B \qquad \textbf{Equation 3.8}$$

The selection rule for NMR is $\Delta m = \pm 1$, ie. the transitions are only allowed between adjacent energy levels. The resonance condition is $\Delta E = h\nu$ where $\upsilon = {}^{\gamma B}/_{2\pi}$, and ν is the electromagnetic radiation frequency. A nucleus in a molecule experiences a slightly different magnetic field to the external field, B_0, which gives the nucleus a characteristic resonance frequency specific to the environment of the nucleus. This is how the structure of a molecule is determined by NMR spectroscopy.

3.7.1.3 Relaxation

The time taken for a nucleus to return to its ground state after excitation in the magnetic field is the relaxation time. The relaxation time for a ^{13}C nucleus is very slow. Allowing plenty of time for all ^{13}C atoms to relax between pulses gives more proportionally sized peaks but at the expense of a very long NMR acquisition time. The delay between pulses can be reduced by using a smaller pulse angle. For example, a 90° angle will require a delay of five times the relaxation time, but a pulse angle of 30° (as used here) only required a delay of twice the relaxation time. For this reason, ^{13}C

NMR spectroscopy is not particularly quantitative unless acquired over a very long time. Peaks in a ^{13}C NMR spectrum do not accurately reflect the number of nuclei due to the Nuclear Overhauser Effect (NOE) caused by ^{1}H decoupling and the long relaxation times. To reduce the NOE, it is possible to used gated decoupling, in which the signal is decoupled during the relaxation of the ^{13}C nuclei. In the analyses carried out here, it is used to measure the extent of degradation. Some attempt to quantify the peaks has been made but, as noted, this is not accurate and should be treated with caution.

3.7.2 ^{13}C NMR Standard Preparation

Standards were prepared in $CDCl_3$ with 1,4-dioxane as an internal reference standard. A solution of $CDCl_3$/1,4-dioxane was prepared by adding 1 g dioxane to 52 g $CDCl_3$. To make the standards for analysis 0.5 g of each standard was added to 5 mL of the $CDCl_3$/ 1, 4-dioxane solution. Approximately 0.5 mL of each solution was transferred to an NMR tube. Standards analysed were: Amine1, Amine2, HEEDA, OZD, HEA, HEIA, HEI, bicine, N-(2-hydroxyethyl) succinimide and succinic anhydride.

3.7.3 ^{13}C NMR Sample Preparation

In order to analyse the degraded amines by ^{13}C NMR spectroscopy 3.5 g of degraded amine solvent was added to 0.5 g of $CDCl_3$/ 1, 4-dioxane solution which was prepared as described in Section 3.7.2. Approximately 0.5 mL of each solution was transferred to an NMR tube.

3.7.4 ^{13}C NMR Operating Procedure

A Bruker AV3500 spectrometer fitted with a cryoprobe system was used to carry out the ^{13}C NMR analysis of degraded amine solvents. ^{13}C NMR spectra were recorded with the following acquisition parameters: pulse width = 8 μs, acquisition time = 1.1 s, relaxation time = 1.5 s, number of scans = 2048 and excitation angle = 30°. ^{13}C NMR data was processed with an exponential multiplication window function that uses a line broadening factor of 1 Hz.

The peaks obtained from the standards were used to analyse the degraded amine solvents. For those peaks which did not result from degradation compounds, i.e. amine/ protonated amine, carbonate/ bicarbonate and carbamate, peak positions were taken from previous works in available literature.

Analyses were carried out by Mr. Shazad Aslam in the School of Chemistry at the University of Nottingham.

3.8 Electrochemical Corrosion Testing

Electrochemical corrosion testing can be used to determine the effects of the solvent on metals. Most metallic corrosion occurs via electrochemical reactions at the interface between the metal and an electrolytic solution.[88] The rate at which corrosion occurs is determined by an equilibrium between opposing electrochemical reactions. One reaction is the anodic reaction where the metal is oxidised, releasing electrons into the solution. The other is the cathodic reaction where a solution species (often O_2 or H^+) is reduced, removing electrons from the metal. When there is an equilibrium between these two reactions the electron flow is balanced so there is no net flow therefore no electrical current occurs. The two reactions can occur on one metal or on two dissimilar metals that are electrically connected.[88]

Figure 3.1 displays this process. The vertical axis is the electrical potential and the horizontal axis is the logarithm of the absolute current. The straight lines represent the theoretical current for the anodic and cathodic reactions, and the curved line is the total current (the sum of the anodic and cathodic currents). This is the current which is measured when a potential sweep is performed using a potentiostat. The point in the curve is the point at which the current reverses polarity as the reaction changes between anodic and cathodic. A wide range of current values must be recorded during a corrosion experiment as the phenomenon of passivity can cause the current to change by several orders of magnitude.

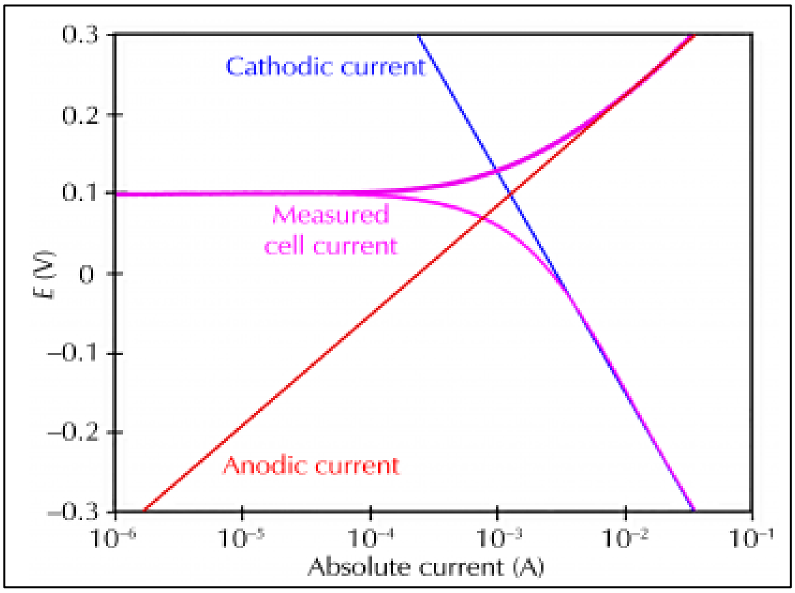

Figure 3.1: Corrosion process showing anodic and cathodic components of current[88]

The anodic and cathodic reactions are kept balanced by the potential of the metal. The equilibrium potential of the metal when there is no electrical connection to the metal is called the open-circuit potential, E_{oc}. This is the first measurement taken in electrochemical corrosion experiments. The value of either the anodic or cathodic current at E_{oc} is called the corrosion current, I_{corr}. This cannot be directly measured but can be estimated using electrochemical techniques.[88]

Many metals form an oxide layer on their surface as they corrode which can inhibit further corrosion. If this happens the metal is said to passivate. It is possible for localised areas of the passive film to break down, leading to significant metal corrosion in a small area. This is known as pitting.[88]

Electrochemical techniques are ideal for studying corrosion of metals as the corrosion occurs via electrochemical reactions. Forcing the potential away from the E_{oc} value is known as polarising the sample and the current which occurs as a result of this polarisation is measured. This provides information about the corrosion behaviour of the metal.

3.8.1 Potentiodynamic Polarisation Scans

In a potentiodynamic experiment the driving force (the potential) for anodic or cathodic reactions is controlled and the change in current is observed. The potentiostat measures the current which needs to be applied to the system to achieve the desired increase in driving force, known as the applied current. As a result, at the E_{oc} the applied current will be zero.[89]

3.8.1.1 The Anodic Scan

Figure 3.2 shows a schematic of an anodic polarisation curve. The potential is increased in a positive direction from point 1 until the set termination point at 2. The labelled points on the curve are described below:

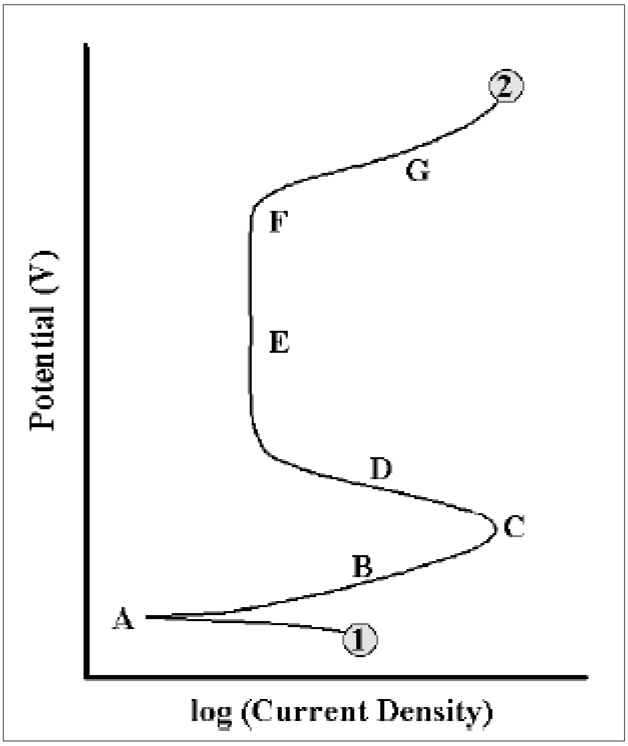

Figure 3.2: Theoretical anodic polarisation scan[89]

A) This is the E_{oc}, the potential at which the sum of the anodic and cathodic currents is zero.
B) The active region- oxidation of the metal is the dominant reaction taking place.
C) This point is the passivation potential, E_{pp}.
D) As the potential increases above the E_{pp} value the current density decreases until a low, passive current density is reached.
E) This is the passive region, where the low, passive current density is seen.
F) As the potential continues to become increasingly positive, a value is reached at which the applied current rapidly increases (region G). This is usually due to a localised breakdown of the passivity, known as pitting.

3.8.2 Electrochemical Corrosion Testing Sample Preparation

Samples of stainless steel to be tested were mounted in epoxy resin with an electrode connection. Samples were ground to a 600-grit finish using silicon carbide paper. Figure 3.3 shows a typical test sample.

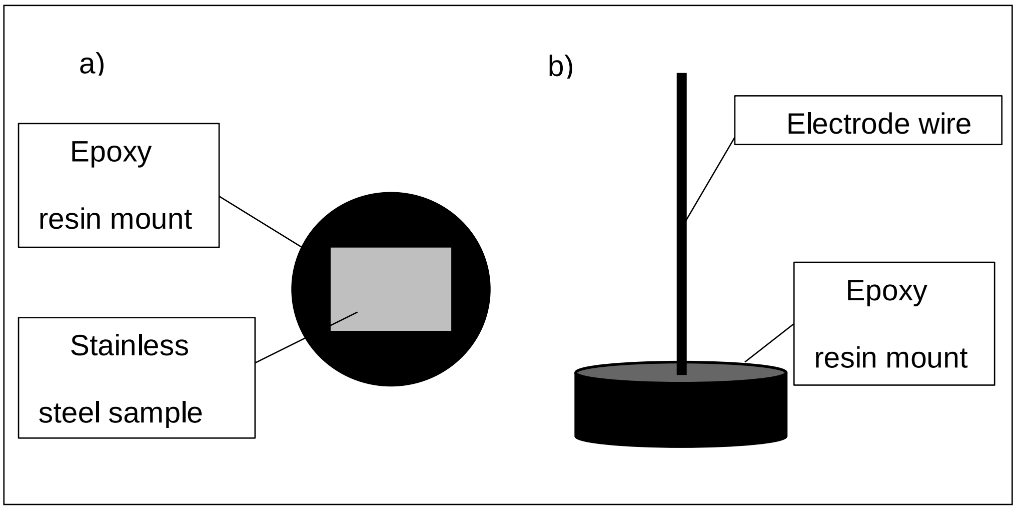

Figure 3.3: Stainless steel sample for electrochemical testing: a) view from below; b) view from side

3.8.3 Electrochemical Corrosion Testing Operating Procedure

Using a Gamry Ref600 Potentiostat the corrosive effect of the solvent on a sample of cast 316 stainless steel taken from the hot lean inlet to the heat exchanger in the pilot plant in North West Europe was investigated. A 600 mL glass vessel was filled with the test solvent and placed in a heated, stirred oil bath to maintain a constant set temperature. The temperature of the test solvent was measured using a mercury thermometer. A reflux condenser was fitted to the test vessel and a silver/silver chloride (Ag/AgCl) reference electrode, platinum counter electrode and the stainless steel working electrode were submerged in the solution. The reference electrode was housed in a Luggin probe to prevent reduction in potential. All of the electrodes were connected to a potentiostat which allowed the potential of the metal sample to be changed in a controlled manner, and also allowed the measurement of the current which flowed as a function of this applied potential. A gas inlet was attached to the test vessel to allow the introduction of CO_2 and/or air into the test solution. Figure 3.4 shows a diagram of the experimental set up. The potentiostat was used to run potentiodynamic scans under the following conditions: scan rate 5 mV/s, initial E -0.5 V, final E +1.0 V, vs. E_{ref}. If CO_2 or air was used in the experiment, flow rates were 0.2 L/ min and 0.05 L/ min respectively.

Electrochemical corrosion testing was carried out with the assistance of Mr. Colin Davis at Uniper Technologies, Ratcliffe-on-Soar.

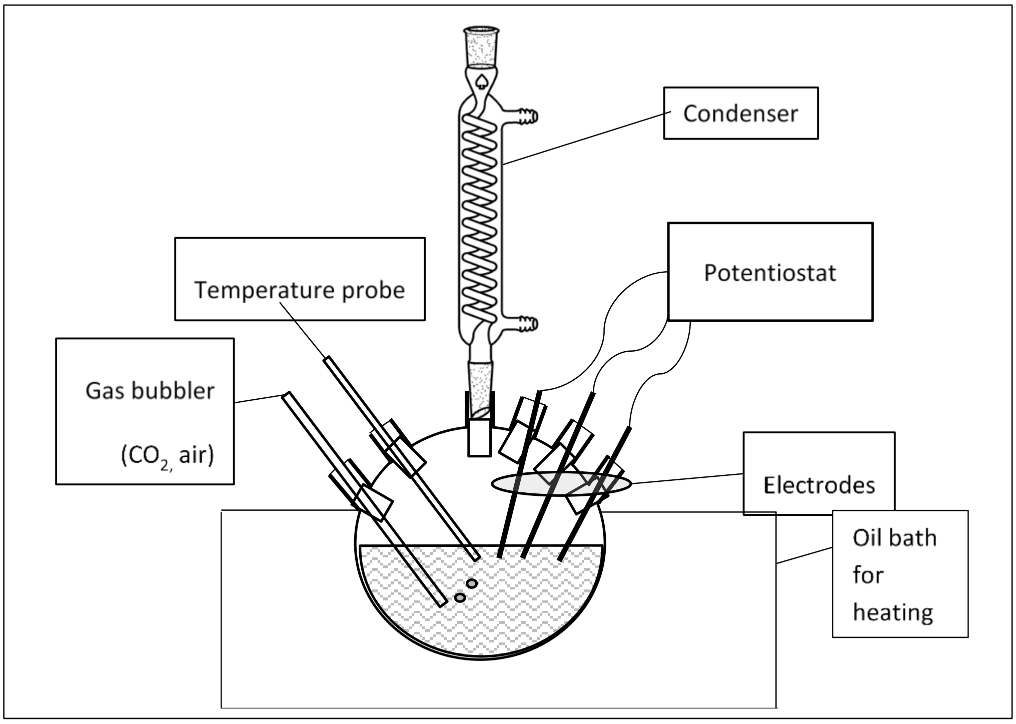

Figure 3.4: Electrochemical corrosion testing apparatus

3.9 Summary of Analytical Methods

The analytical methods described in this chapter provided a comprehensive analysis of degraded amine solvents. By using a variety of analytical techniques this allowed a confident interpretation of how solvents behave at pilot plant scale. The information gathered from each analysis enabled accurate determination of the processes involved at large scale, long-term operation. By identifying how the solvents behave it will be possible to optimise the operation of post-combustion carbon capture plants so that they run as efficiently as possible with minimal increase to the operating costs.

Chapter 4: Characterisation of Major Degradation Products in Blended Amine Solvents

4.1 Introduction

A coal-fired power plant in the UK was retro-fitted with an amine-based capture plant to process the combustion flue gas which contained impurities. The amine plant captured approximately 100 tonnes CO_2 per day and was operational for approximately 700 hours. The first testing campaign used a primary amine solvent to remove the CO_2 from the flue gases. One sample of the primary amine solvent was provided for analysis in this work but due to it being heavily degraded only GC-MS analysis was carried out in order to identify the major degradation products. The solvent was found to be ~45 % amine with the remaining ~55 % being made up of degradation products. The results are shown in Appendix B. A second campaign was run using a proprietary blended amine solvent, which was a binary blend of two amines termed Amine1 and Amine2. Further analysis of single amine solvents is presented in Chapter 5. This current chapter provides a detailed description of the information gained from the use of different analytical techniques in the analysis of the degraded blended amine solvent only. The techniques used were GC-MS, GC-FID, ICPMS, IC, and ^{13}C NMR spectroscopy. Although GC-MS has been widely used in degraded amine analysis this only provides semi-quantitative information.[15, 18, 32, 35, 63, 71] The aim of this chapter is to compare the GC-MS data to GC-FID results which provides a more quantitative estimate of the levels of degradation products. The correlation of results from ICPMS and IC allowed a thorough investigation of the trends in the levels of metals present in degraded amines as well as investigation into any heat stable salts which had formed. The use of ^{13}C NMR spectroscopy was investigated as a rapid method of monitoring the extent of oxidative/ thermal degradation and was carried out on selected samples only. The results of this are presented at the end of this chapter.

The solvents tested in this chapter were those from the UK pilot plant, as listed in Table 3-I. The analytical techniques applied to each solvent are listed below in Table 4-I (conditions and operating hours as in Table 3-I) and Figure 4.1. However, because this single batch of blended amine solvent was operated under different conditions during parametric testing on the plant it is difficult to determine which individual condition led to the greatest amount of degradation. The operation of the solvent was carried out non-continuously; that is to say that the capture plant was only operated during day-to-day working hours. In addition to this, while the capture plant was non-operational the hot lean solvent was repeatedly exposed to air which will have affected the condition of the solvent. There were also several solvent 'top-ups', where the amine solvent was replenished. These occurred at various times before samples B1-3 were taken and also at times before samples B3.3 and B4 were taken and can be seen in Figure 4.1. The solvents were significantly degraded as evidenced by the discolouration of the samples which can be seen in Figure 4.2.

The analysis of degraded solvents enables a better understanding of the processes involved in the amine scrubbing system. Understanding solvent behaviour can help in the optimisation of the capture process, both in terms of solvent selection and plant operation. If conditions can be controlled such that degradation and corrosion are minimised then the plant will be operational for longer and problems/ outages will be minimised. The efficient operation of the plant will also serve to minimise capital and operational costs.

Table 4-I: Blended amine solvent and analytical techniques

Sample ID	GC-MS	GC-FID	Anion IC	Cation IC	ICPMS	^{13}C NMR
B1	✓	✓	✓	✓	✓	×
B2	✓	✓	✓	✓	✓	×
B3	✓	✓	✓	✓	✓	×
B3.1	✓	✓	✓	✓	✓	×
B3.2	✓	✓	✓	✓	✓	✓
B3.3	✓	✓	✓	✓	✓	×
B3.4	✓	✓	✓	✓	✓	×
B3.5	✓	✓	✓	✓	✓	✓
B3.6	✓	✓	✓	✓	✓	×
B4	✓	✓	✓	✓	✓	×
B5	✓	✓	✓	✓	✓	✓

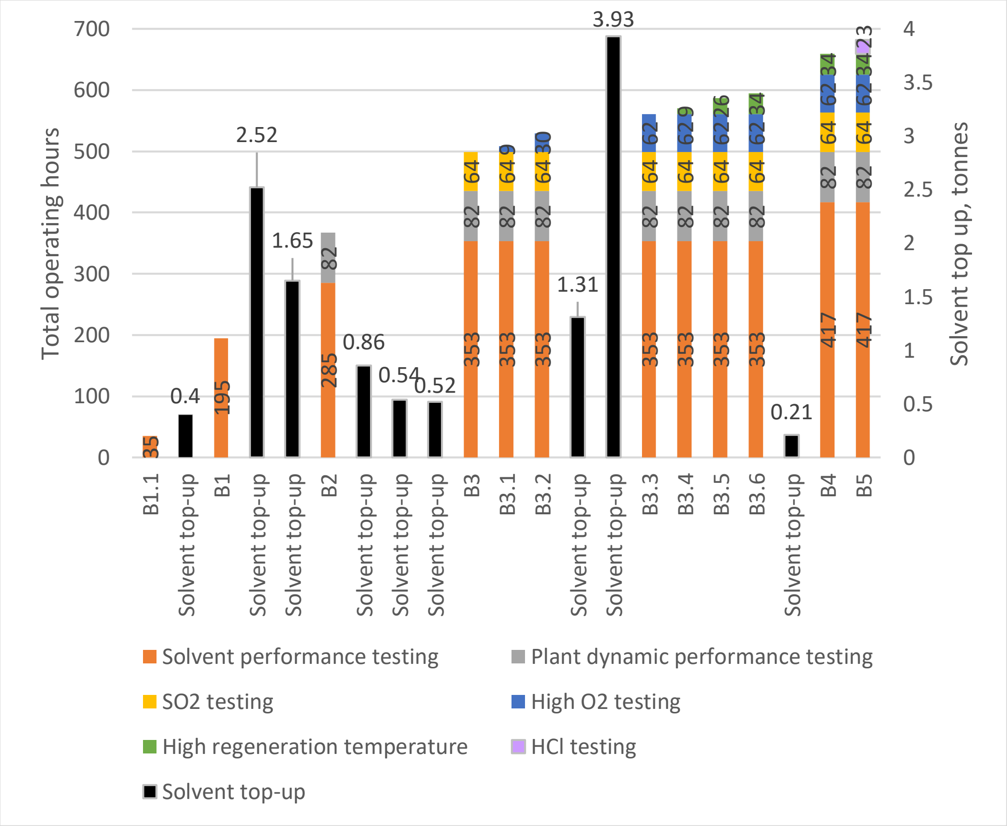

Figure 4.1: Blended amine solvent operating conditions

Figure 4.2: Discolouration of solvents, operation time increasing from left to right

4.2 GC-MS

As discussed in Section 3.3 GC-MS is used to separate and identify major degradation products. It is used as a semi-quantitative analytical technique. The samples were prepared for GC-MS analysis as described in Section 3.3.4, and the analysis was carried out as described in Section 3.3.5.

4.2.1 GC-MS Analysis of Blended Amine Solvent

The major degradation products which were identified by GC-MS are shown in Figure 4.3 and Table 4-II. There were also several peaks in the GC-MS chromatogram which were unidentifiable by library searches (peak groups A and B). Further examples of GC-MS analysis of the blended amine solvent can be found in Appendix C.

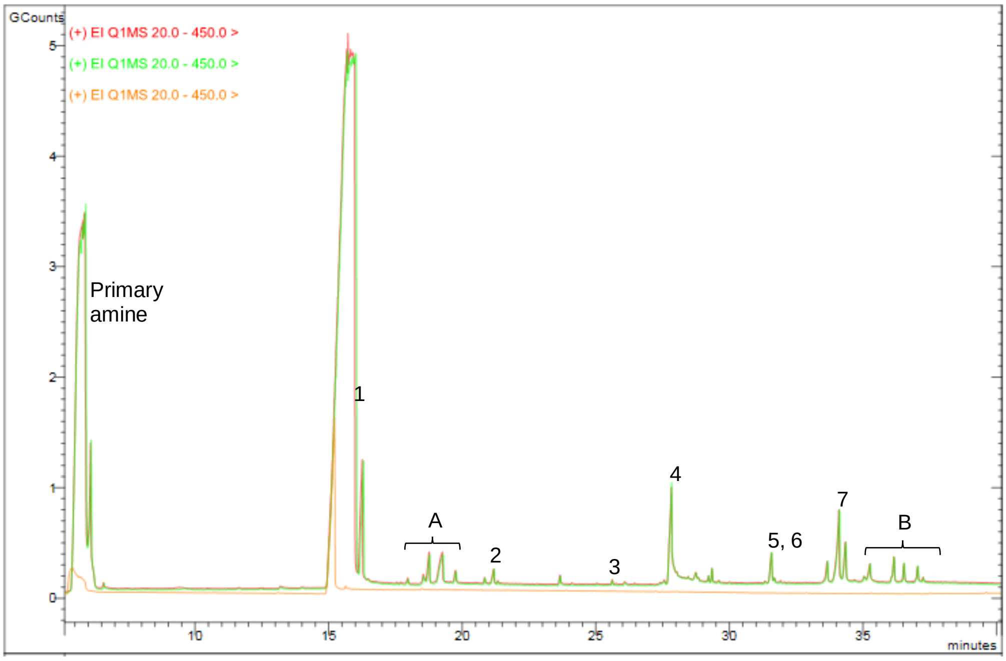

Figure 4.3: Typical GC-MS chromatogram for blended amine solvent degradation

Table 4-II: Degradation product identified in Figure 4.3

Peak	Product	Mw (nominal mass)	Structure
1	DEA	105.14	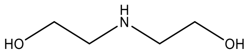
2	OZD	87.08	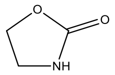
3	N-(2-hydroxyethyl) succinimide	143.14	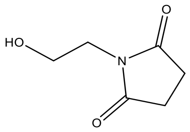
4	Bicine	163.17	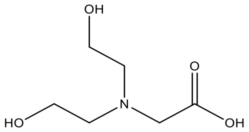
5	1-methyl-2,5-pyrrolidinedone	113.11	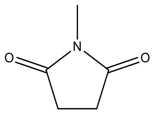
6	Piperidine-2,5-dione	113.12	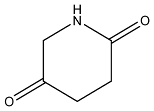
7	Aspartic acid	133.10	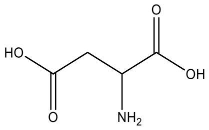

The trends in degradation product formation are shown in Figure 4.4 where the total ion current (TIC) is used as a semi-quantitative measure of concentration (error bars are to one standard deviation). Samples B1- B5 were subjected to increasingly severe operational conditions in order to test the limits of the solvent, described in Table 3-I. By analysing the solvent at different time points it is possible to monitor the formation of degradation products. However, as noted above, due to the purposefully harsh operating conditions which were all applied to the same batch of solvent, it is difficult to distinguish the effects that each individual condition had on the solvent.

DEA has previously been noted as a degradation product of the primary amine MEA and a mechanism of formation has been proposed, shown in Figure 4.5.[29] This mechanism proceeds via an unstable diazonium ion intermediate which can form a secondary amine. There are several competing pathways but the formation of DEA is favoured by high amine concentration. It was also proposed that the secondary amine can be nitrosated to form the stable nitrosamine, nitrosodiethanolamine (NDELA) although this was not identified in any of the solvents tested.

OZD has also previously been identified as both an oxidative and thermal degradation product, and a proposed mechanism for its formation is shown in Figure 4.6.[16]

The presence of bicine in all the samples analysed is significant as there is evidence that iron becomes more soluble when bicine is present in the system.[67] This would indicate an increased potential for corrosion. It has also been shown that iron carbonate is more soluble in lean solution than in rich solution so the presence of bicine may cause increased corrosion in the lean side of the amine system, with increased deposits of iron carbonate in the rich side of the system.[67]

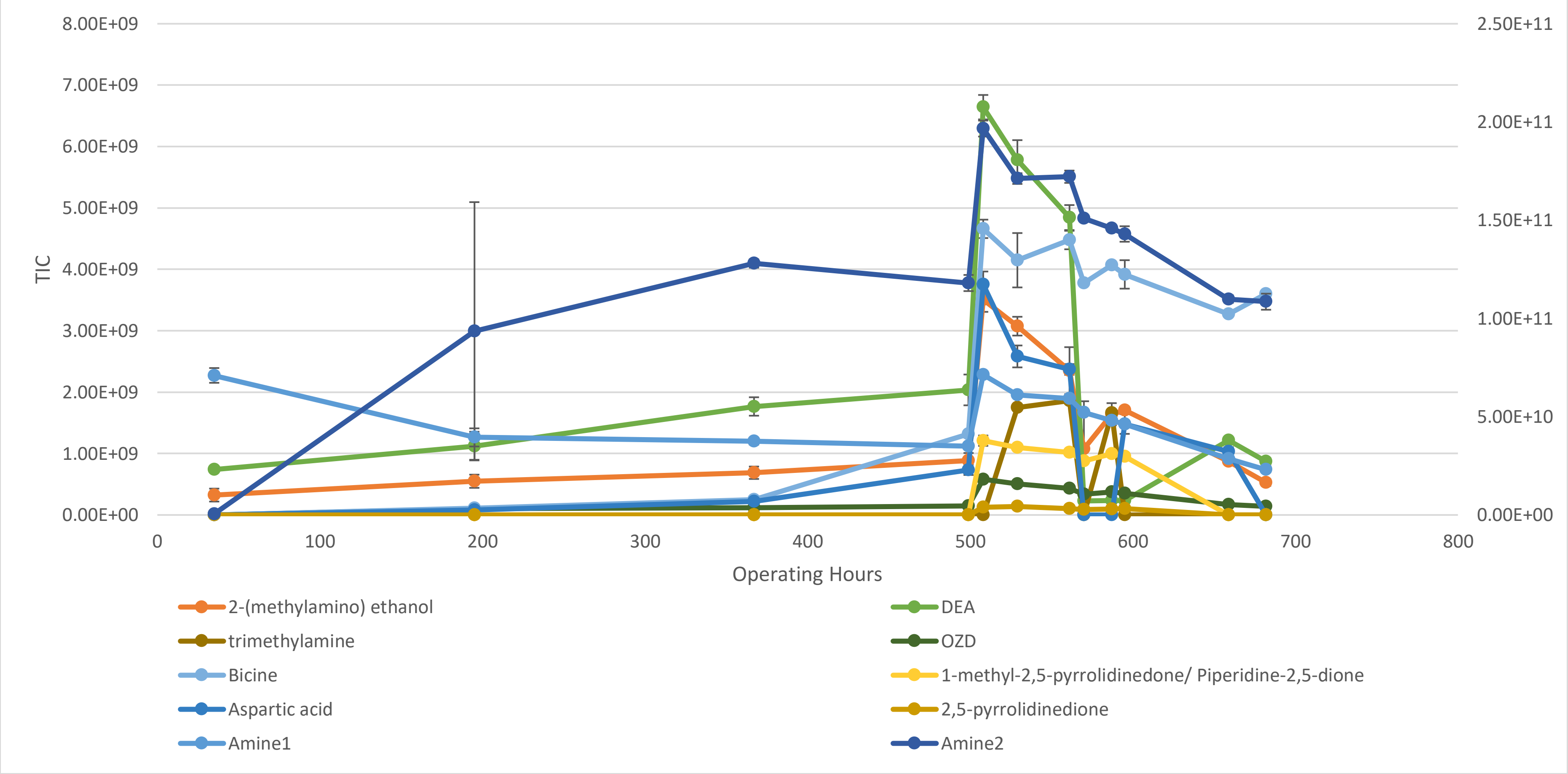

Figure 4.4: Blended amine solvent GC-MS

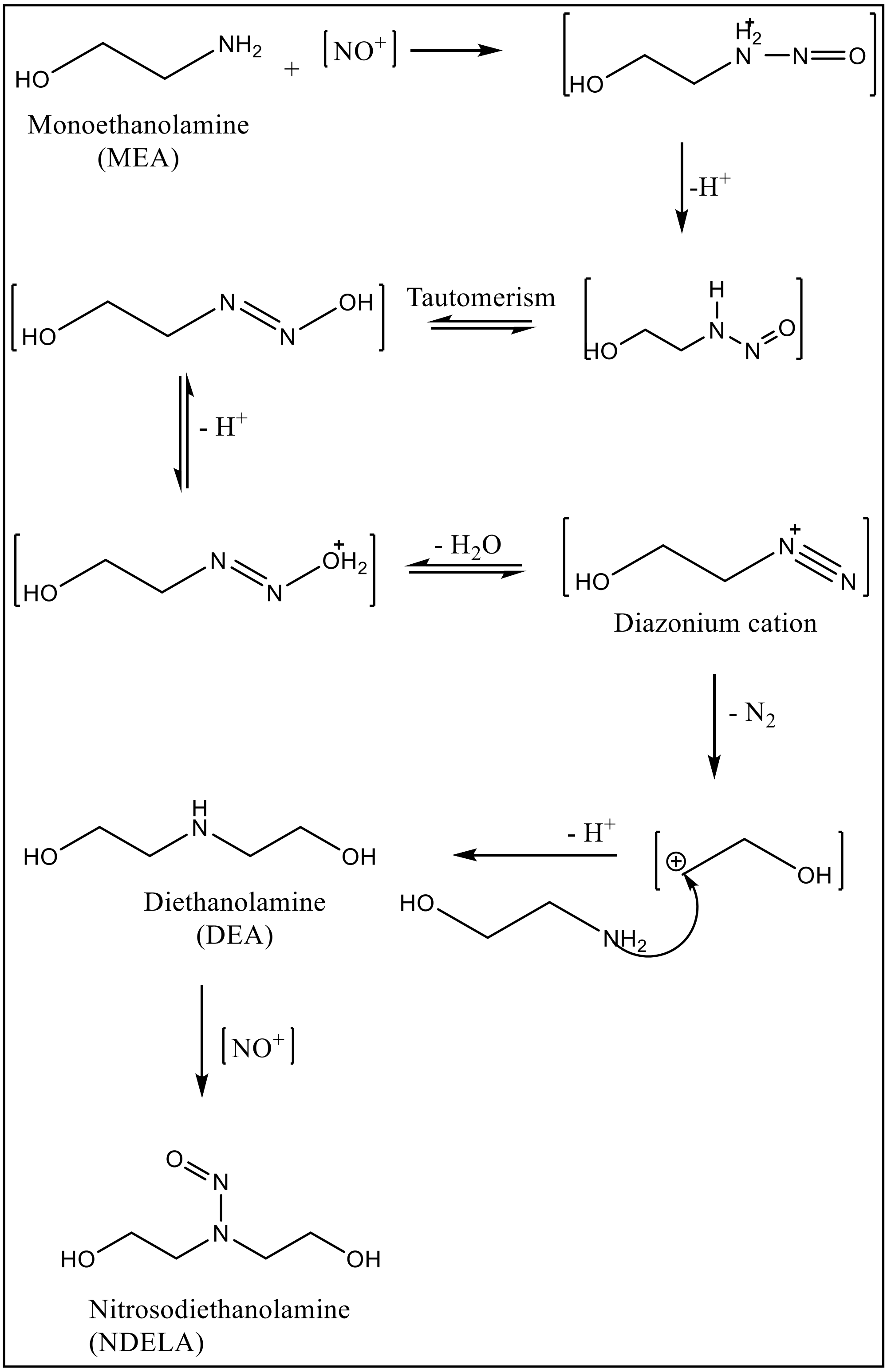

Figure 4.5: Proposed mechanism of formation of DEA and NDELA[29]

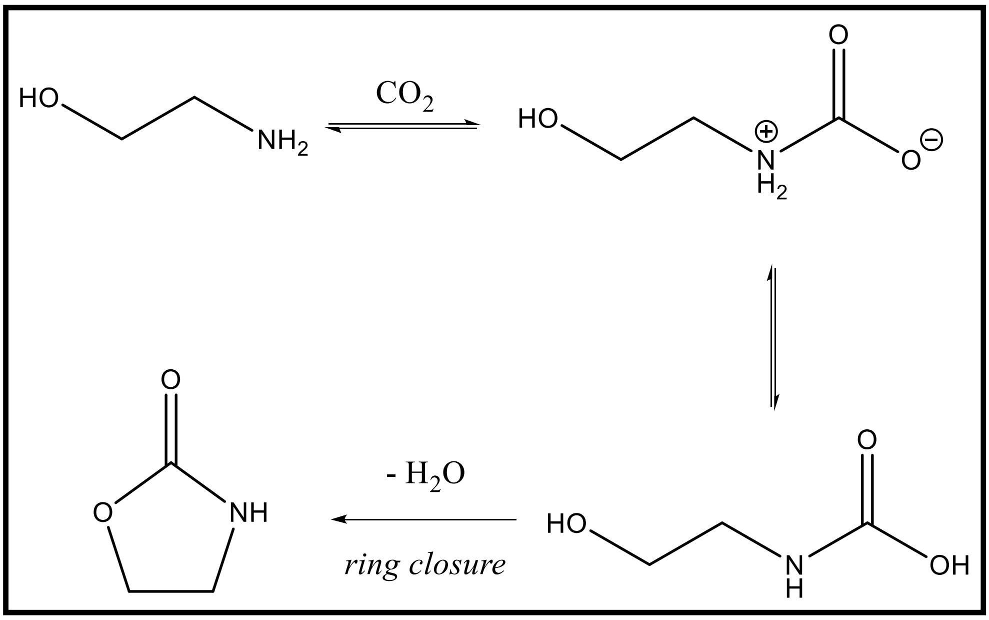

Figure 4.6: Proposed mechanism of formation of OZD[16]

By 499 hours of operation, the solvent had been operated for 64 hours with increased SO_2 levels. The effect of the increasing the SO_2 concentration to 70 ppm caused a slight increase in degradation products from the previous sample which had not experienced high levels of SO_2. Between these two samples (367 hours and 499 hours) the solvent was topped-up three times, so the degradation products were diluted by the fresh solvent.

The solvent was then exposed to high levels of oxygen for a total of 62 hours, ranging from 10 to 15 % O_2. At 508 hours, the solvent had experienced 9 hours of increased O_2 levels, which appears to have caused an increase in the levels of all degradation products displayed in Figure 4.4, with the largest increase being in DEA. By 30 hours of exposure to increased O_2 levels (529 total hours) these products reduced again, with the exception of trimethylamine. This could indicate that trimethylamine formation is favoured by increased O_2 levels, whereas all other degradation products are only intermediates which degrade further over time. By the time the solvent had been operational for 62 hours with high O_2 levels (561 total hours) there had been a small increase in the level of bicine present. The small change in degradation products is again likely to be due to the two additions of fresh solvent into the system between 30 and 62 operational hours at increased O_2 levels. After the end of the testing with increased O_2 the level of DEA decreased sharply. This could indicate that DEA formation is favoured when O_2 is present in the system. Aspartic acid also appears to follow the same trend.

The effect of increasing the regeneration temperature appears to have had little effect on the solvent in terms of degradation products. There is minimal change in all species, despite the solvent being operational at this condition for 34 hours. There were no further solvent top-ups during the high regeneration temperature testing. The solvent was then operated under normal conditions for 64 hours and was topped-up during this time, before being dosed with HCl and operating for a total of 23 hours at this condition. The sample at 682 hours had experienced the full 23 hours of HCl testing. It can be seen that the only degradation product to increase in this time was bicine.

4.3 GC-FID

As discussed in Section 3.4, GC-FID is a quantitative analytical technique due to the accuracy of the response from the detector. Four of the major degradation products were analysed by GC-FID. The peak response corresponds to the mass of carbon in the molecule, regardless of carbon structure. In order to identify the standards, each individual standard was first run on GC-MS, then compared to the GC-FID results which used the same column. The order in which the compounds eluted in the GC-MS analysis allowed interpretation of the GC-FID results. As discussed in Section 3.4.1 the four compounds quantitatively analysed using this method were HEA, OZD, N-(2-hydroxyethyl) succinimide and bicine. These were chosen as they have been identified as degradation products in previous studies and were easily identifiable in the GC-FID analysis.

4.3.1 GC-FID Analysis of Blended Amine Solvent

A typical GC-FID trace is shown in Figure 4.7 (further examples of GC-FID analysis of the blended amine solvent can be found in Appendix D). The results of GC-FID analysis of the blended amine solvent can be seen below in Figure 4.8. N-(2-hydroxyethyl) succinimide was more susceptible to detection with GC-FID than with GC-MS analysis, due to the low concentration of this trace component in the solvent. In the GC-FID analysis, it was detected from 367 operating hours, whereas in GC-MS it was only detected from 659 hours (for this reason it was not shown in Figure 4.4 above). Figure 4.8 shows that levels of N-(2-hydroxyethyl) succinimide remain low in all samples (530 ppm maximum), but bicine, OZD and HEA levels continuously increase throughout the solvent operation. HEA was not detected by GC-MS analysis, showing that GC-FID analysis is a more suitable method for detecting this species. GC-MS data for this solvent showed that bicine levels increase after 499 hours of operation, and the levels of N-(2-hydroxyethyl) succinimide remain low throughout, which is in agreement with the GC-FID data. However, there is a sharp increase in OZD observed in GC-MS after 499 hours operation followed by a steady decrease (Figure 4.4 above), whereas GC-FID analysis shows a steady increase in OZD levels throughout. Figure 4.9 and Figure 4.10 show the similarity in trends in the FID and MS data. All error bars are to one standard deviation.

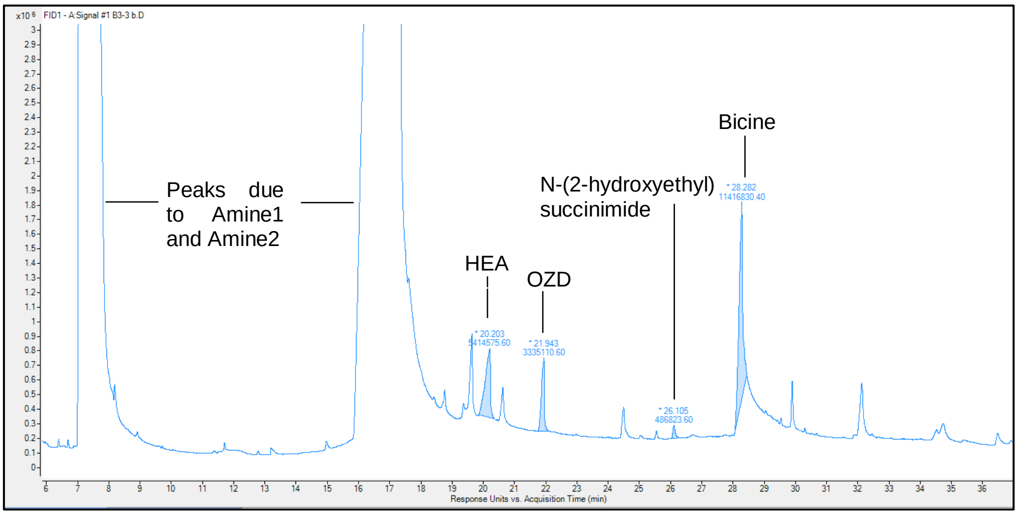

Figure 4.7: Typical GC-FID trace for blended amine solvent

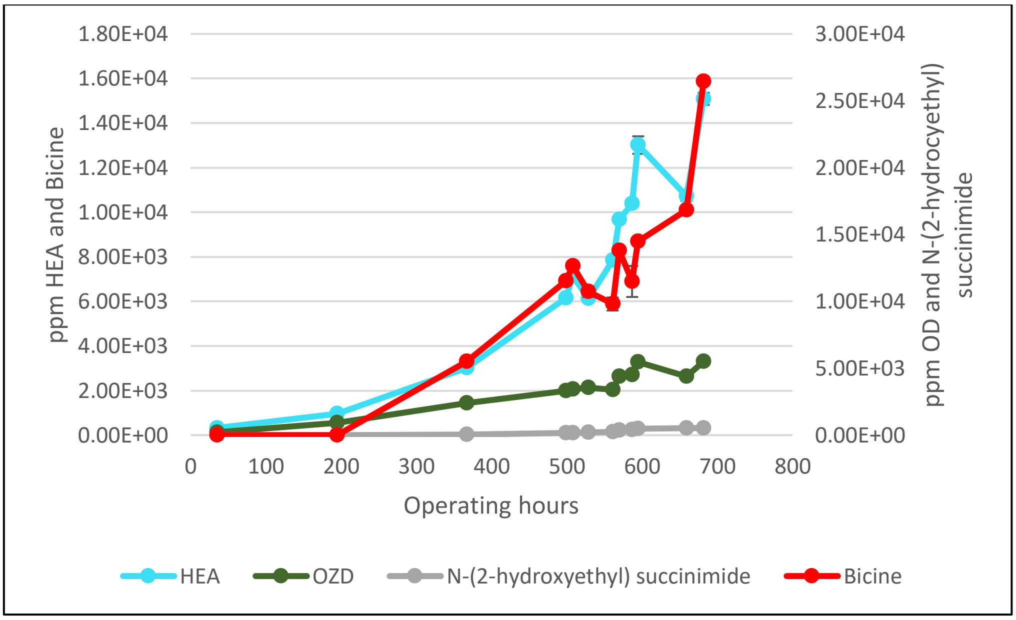

Figure 4.8: Blended amine solvent GC-FID analysis

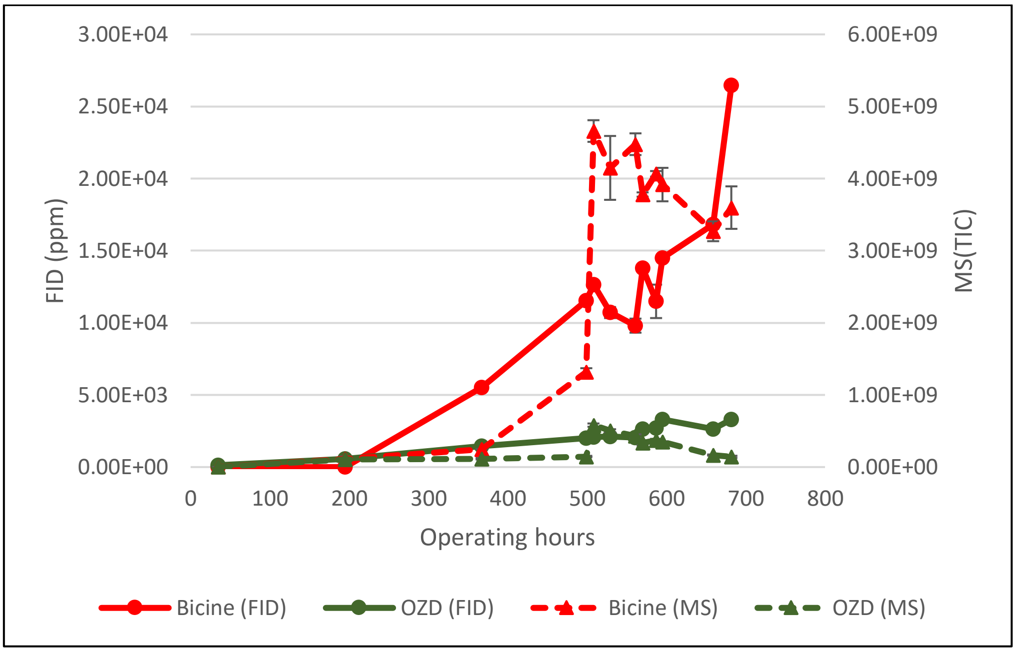

Figure 4.9: Correlation between MS and FID data for bicine and OZD

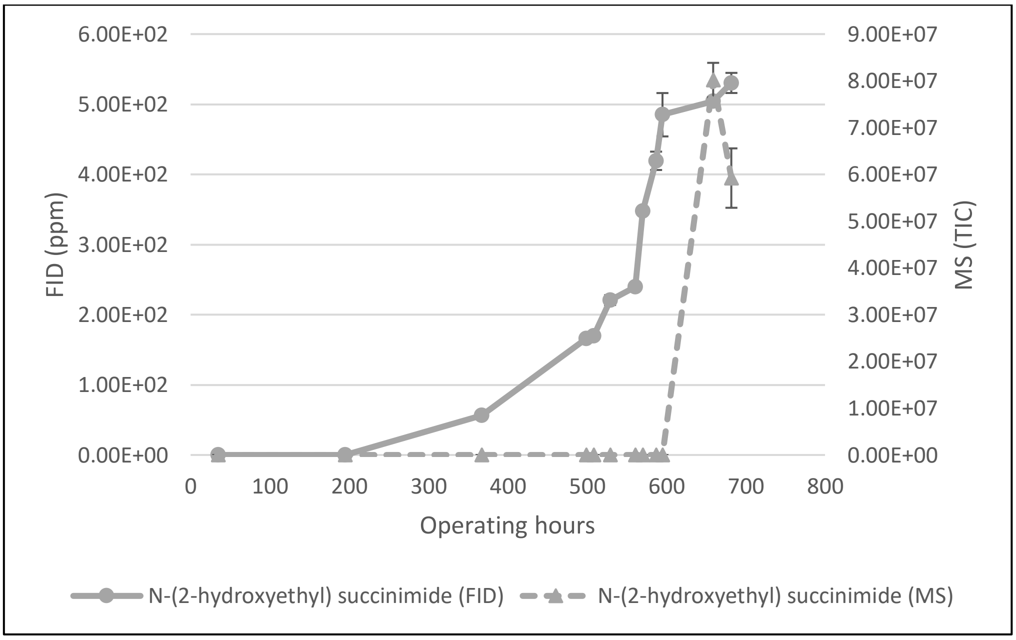

Figure 4.10: Correlation between MS and FID data for N-(2-hydroxyethyl) succinimide

4.4 ICPMS

As discussed in Section 3.5, ICPMS is a useful tool in the identification of metals present in the solvent. It can be used as a qualitative analytical technique. All standards and samples were prepared as described in Sections 3.5.3 and 3.5.4. Analysis was carried out as described in Section 3.5.5.

4.4.1 ICPMS Analysis of Blended Amine Solvent

Figure 4.11 shows the ICPMS analysis of the blended amine solvent throughout the test campaign (all error bars are one standard deviation). Iron is the predominant transition metal present reaching up to 300 ppm by the end of the testing. Chromium follows the same trend as iron but there is much less of it present (max. 70 ppm). Nickel also follows this trend but there is less of this present than the chromium (max. 45 ppm). Other metals of interest which are thought to have some impact on degradation and corrosion are copper and vanadium.[17, 40, 54-58] However, neither of these were detected in any measurable quantity (< 0.5 ppm) so have not been shown on the graph.

As discussed previously, the solubility of iron has been shown to increase when bicine is present in both CO_2-rich and CO_2-lean solvents.[67] This indicates a potential for increased corrosion due to increased iron solubility. Iron carbonate has also been shown to be much more soluble in lean solution than in rich solution so the presence of bicine causes solubility to increase in the lean side of the amine system. This is problematic as the iron carbonate will precipitate out in the rich-side of the system leaving the bicine free to chelate more iron in the lean side of the system. If this cycle repeats itself several times then severe corrosion could be observed on the lean side of the system.[67] The levels of iron present in the solvents are consistent with the results from both GC-MS and GC-FID where bicine appears to increase as the solvent continues operation. Figure 4.12 and Figure 4.13 show the correlations for clarity (all error bars are to one standard deviation). The other products identified by GC-FID (HEA, OZD and N-(2-hydroxyethyl) succinimide) also follow a similar trend with iron levels.

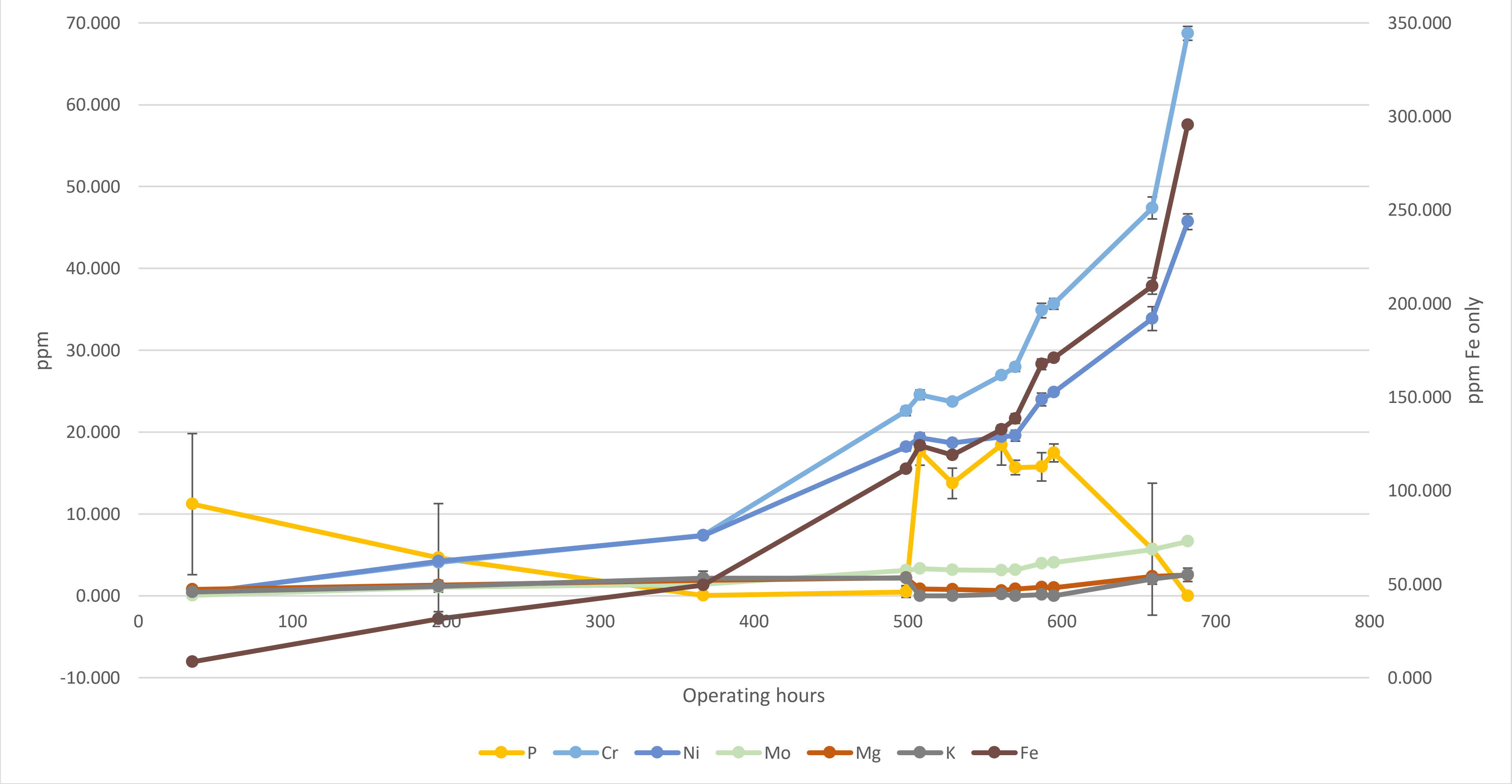

Figure 4.11: ICPMS analysis of blended amine solvent

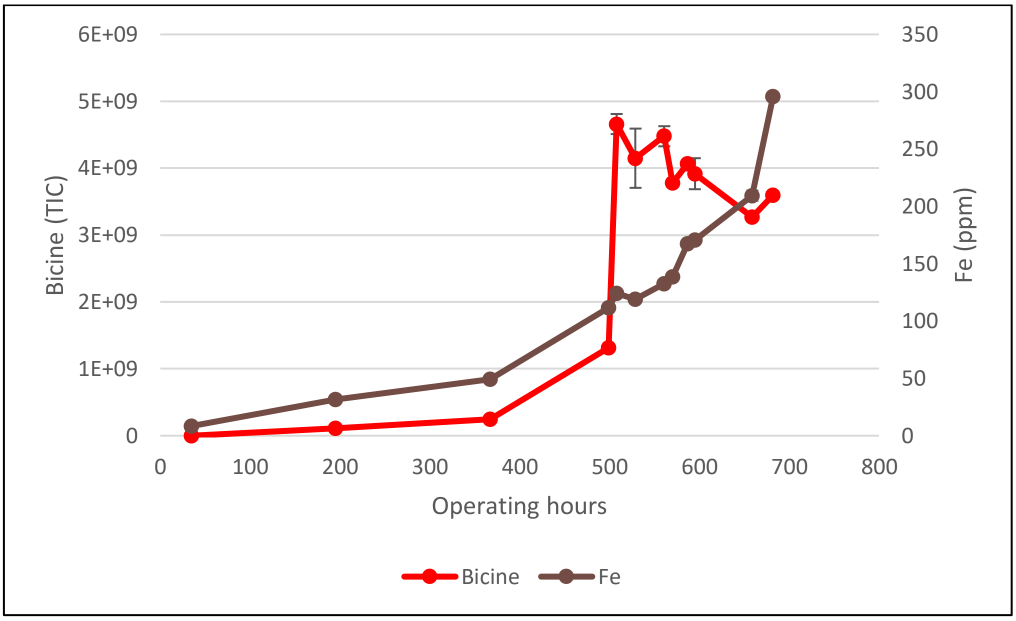

Figure 4.12: Correlation between iron and bicine by GC-MS analysis

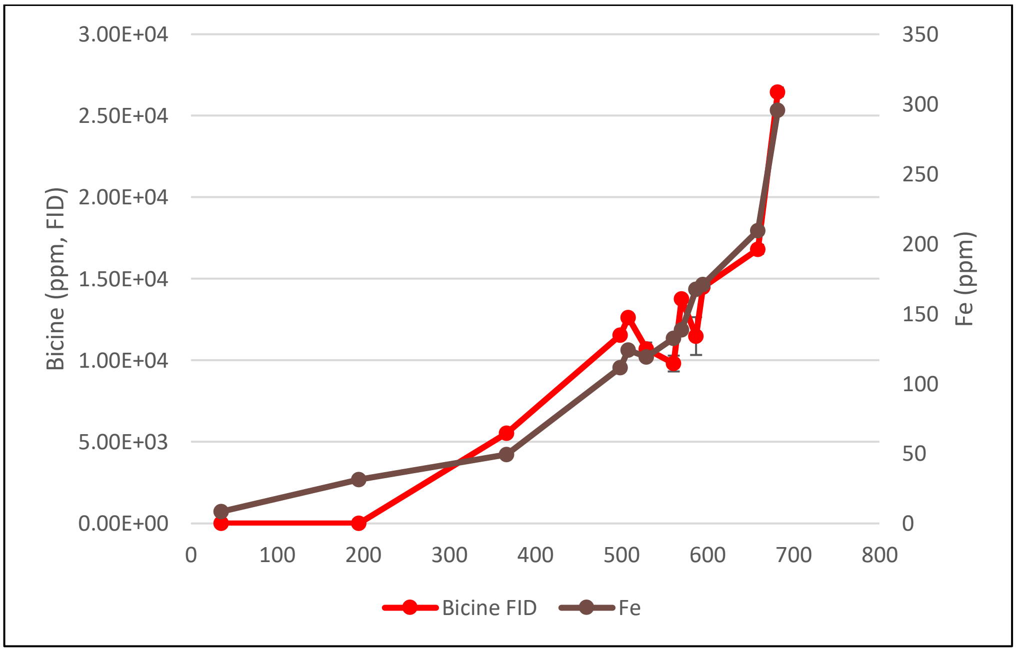

Figure 4.13: Correlation between iron and bicine by GC-FID analysis

4.5 IC

As discussed in Section 3.6 IC has been used primarily to identify heat stable salts. It is used as a qualitative analytical technique. Samples and standards were prepared for analysis as described in sections 3.6.3, 3.6.4, 3.6.6 and 3.6.7. Analysis was carried out as described in sections3.6.5 and 3.6.8.

4.5.1 Cation IC Analysis of Blended Amine Solvent

A typical cation chromatogram is shown in Figure 4.14 (further examples of cation analysis of the blended amine solvent can be found in Appendix E). From Figure 4.15 below it can be seen that cation chromatography is dominated by the detection of potassium. Comparing this result to the ICPMS data (Figure 4.16) it is clear that IC is more sensitive to potassium in the solvent. It is unclear what causes the drop in potassium after ~500 hours operation. For this reason, it is suggested that cation chromatography is ineffective in these circumstances and ICPMS is the preferred technique for cation analysis. Cation chromatography may be useful for monitoring the loss of amine in the solvent but this was not carried out in this work.

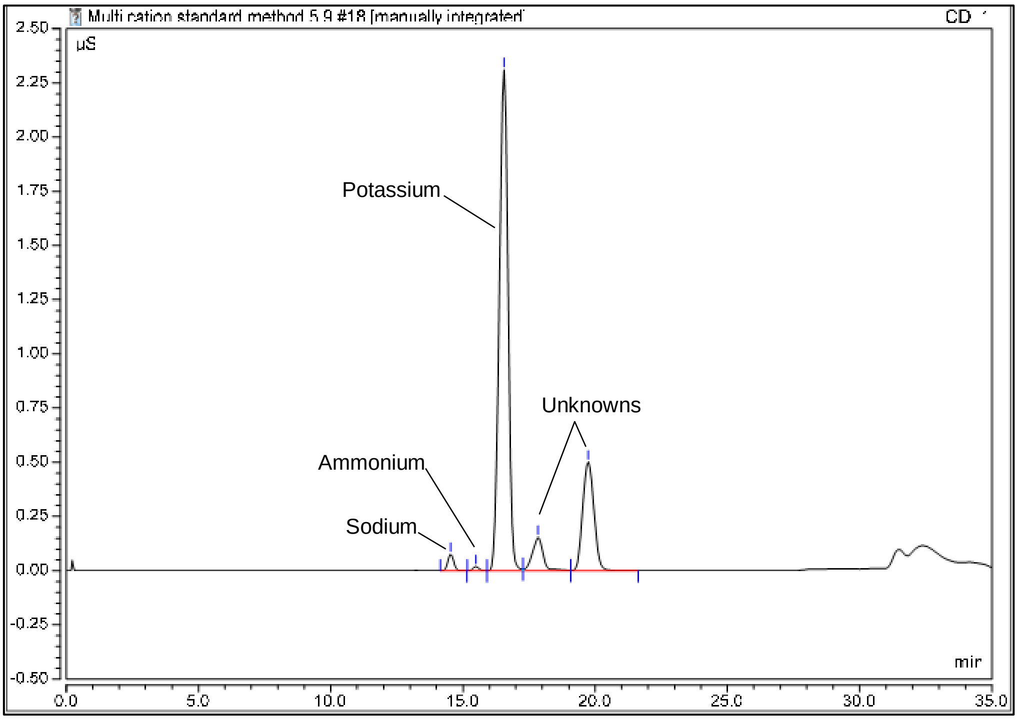

Figure 4.14: Typical cation chromatogram of blended amine solvent

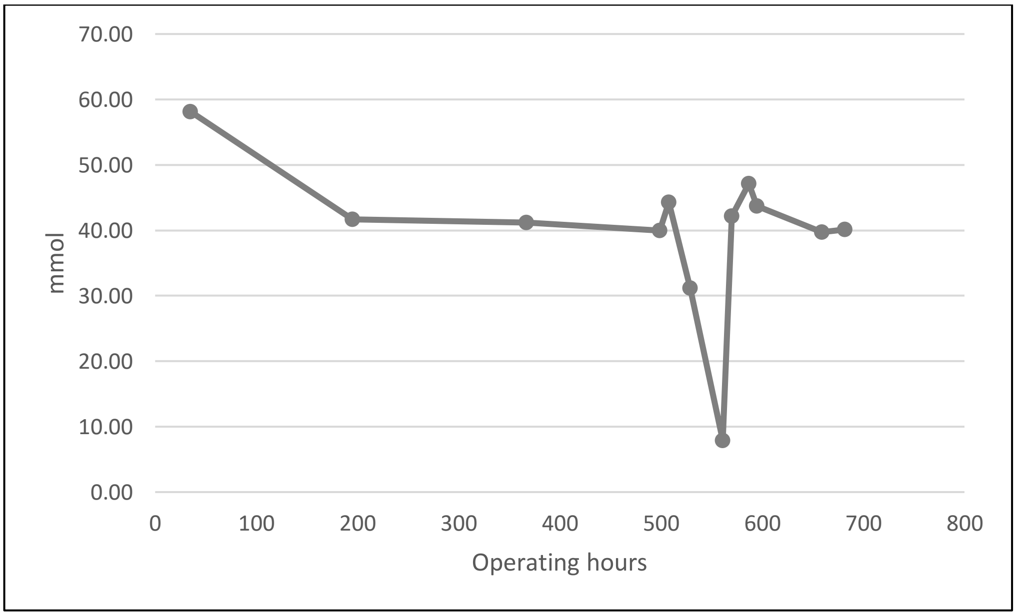

Figure 4.15: Cation chromatography analysis of potassium in blended amine solvent

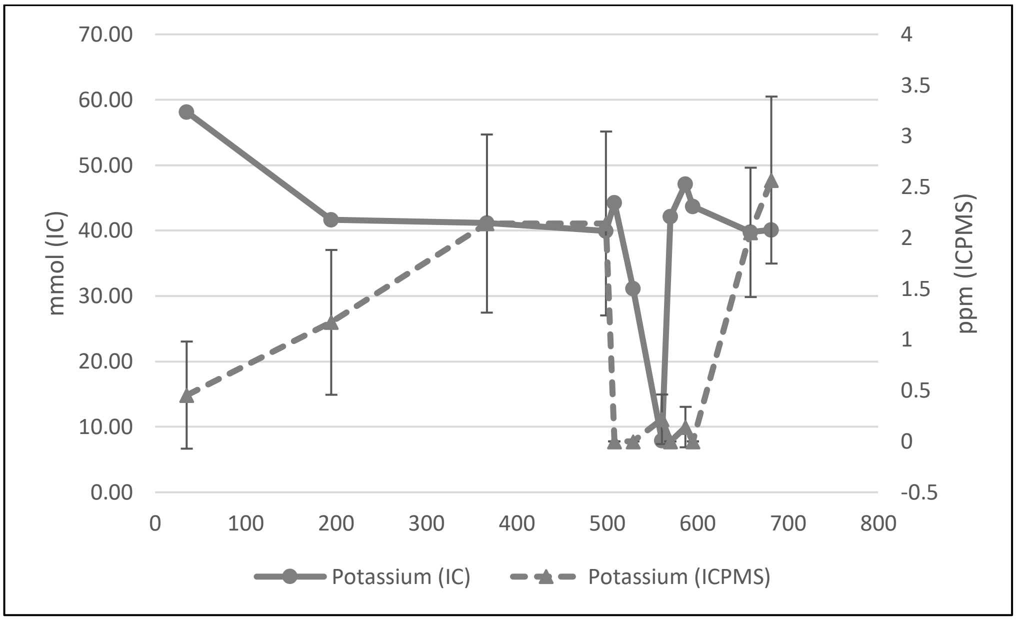

Figure 4.16: Correlation between IC and ICPMS data for potassium levels

4.5.2 Anion IC analysis of blended amine solvent

Formate, nitrate, nitrite, oxalate, acetate and glycolate were identified and quantified using external standards. An example chromatogram is shown in Figure 4.17 (further examples of anion analysis of the blended amine solvent can be found in Appendix E). Acetate and glycolate were not detected in the samples so are not shown in Figure 4.18.

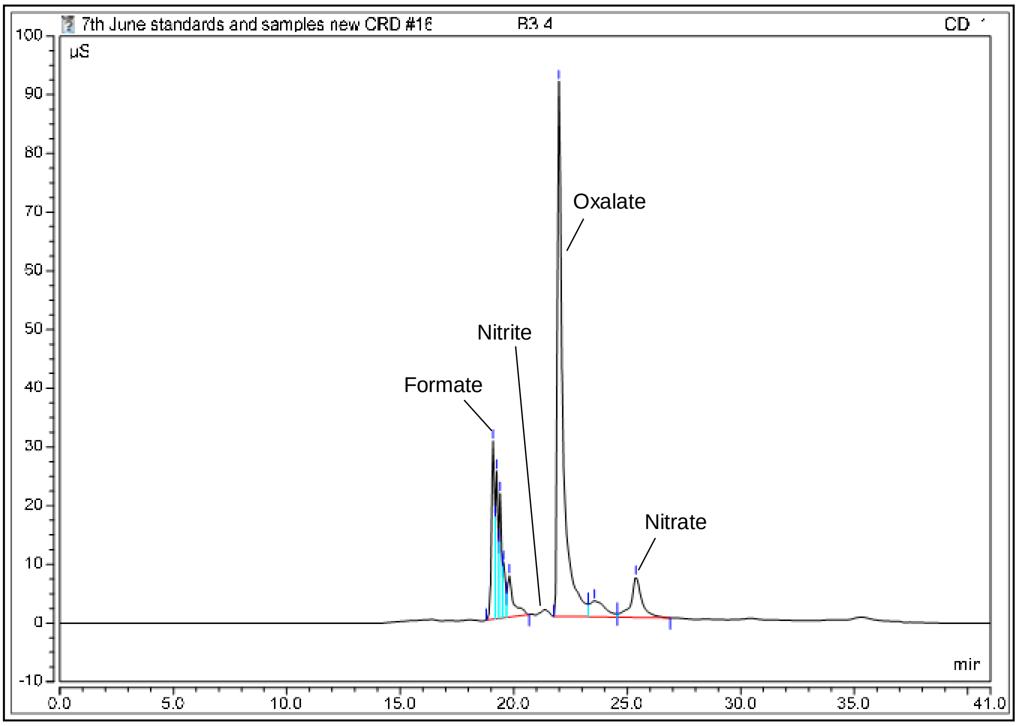

Figure 4.17: Typical anion chromatogram of blended amine solvent

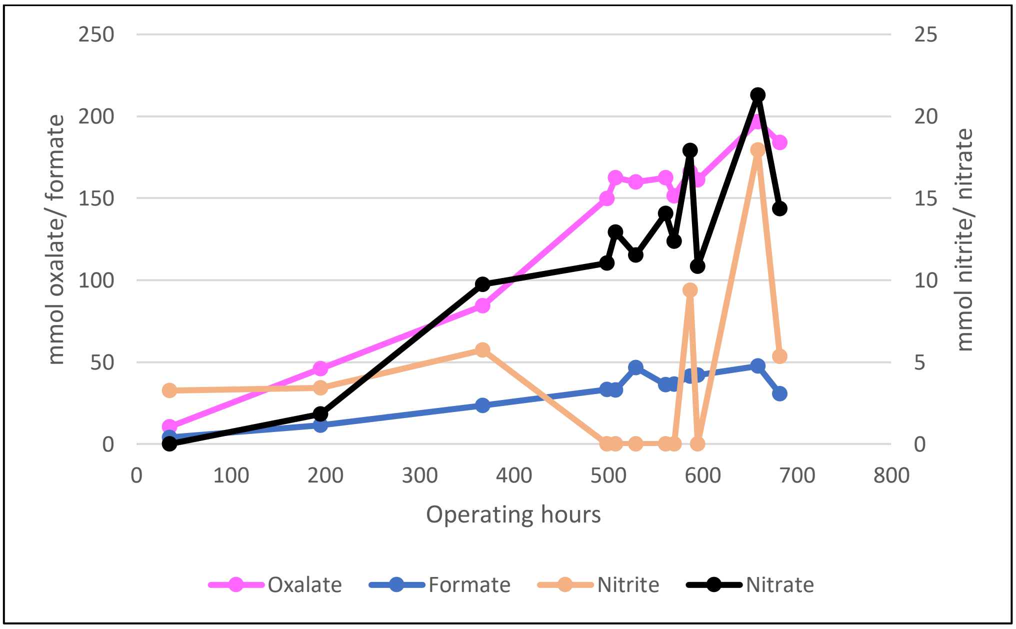

Figure 4.18: Anion chromatography analysis of blended amine solvent

As shown in Figure 4.18 the predominant HSS present in all samples is oxalate, with formate being the next most abundant. These two anions appear to react similarly to an increase in SO_2 concentration (367-499 hours, high SO_2 operation for 64 hours) and from this point the effect of increasing the oxygen concentration seems minimal, as does the subsequent increase in regeneration temperature (508-561 hours (operated for 62 hours) and 570-595 hours (operated for 34 hours) respectively). However, the ratio of formate to oxalate reduces at the higher temperatures, which could indicate that the formation of oxalate is favoured at higher temperatures.[48]

4.5.3 Amide Analysis of Blended Amine Solvent

In order to analyse for formamide, oxamide, acetamide and glycolamide, the reaction with NaOH was carried out as described in Section 3.6.4. Any increase in carboxylic acid concentration between the two samples was considered to be amide that had been recovered in the form of carboxylic acid. Neither acetamide nor glycolamide were detected so are not shown in Figure 4.19.

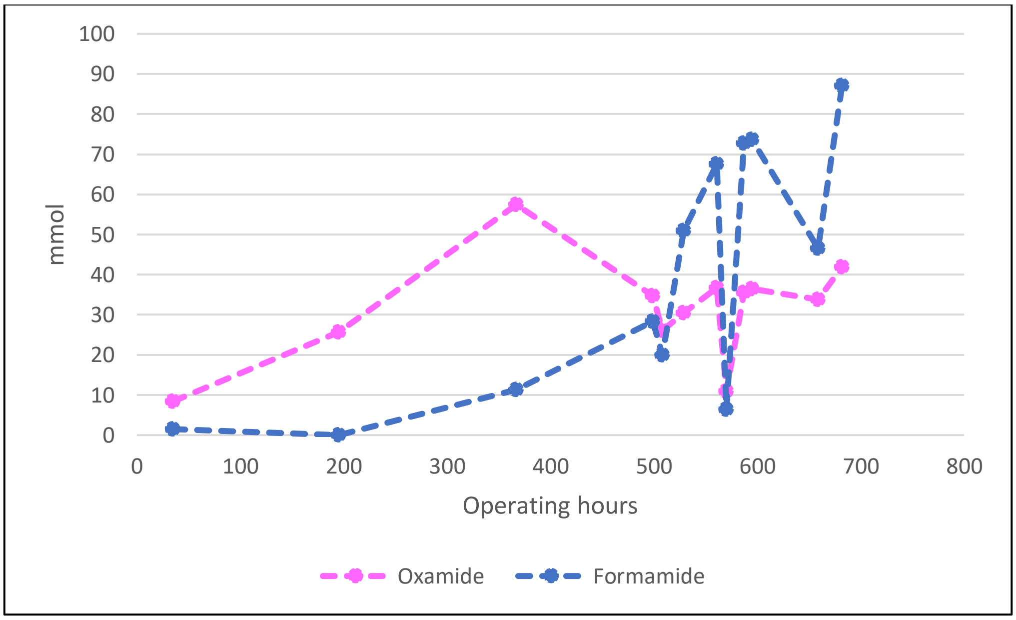

Figure 4.19: Amide analysis of blended amine solvent

The increase in the amount of formamide detected indicates that formate is the predominant HSS present in the solvent. The decrease in oxamide however could be due to oxalic acid being a reactive intermediate which decomposes to give formic acid, which then goes on to produce the stable compound HEF.[37] This would explain the increase in formamide on reaction with NaOH.

4.6 ^{13}C NMR Spectroscopy

As discussed in Section 3.7 ^{13}C NMR can be used to investigate the extent of degradation. It is a used here as a semi-quantitative analytical technique. Due to the slow relaxation of ^{13}C, long pulse relaxation times are required for accurate analysis. In the experiments carried out here, the acquisition time was 1.1 s and the pulse relaxation time was 1.5 s (pulse angle 30°). This enabled a basic analysis to be carried out, but the quantification is to be treated with caution. All standards and samples were prepared for analysis as described in Sections 3.7.2 and 3.7.3. Analysis was carried out and peaks were assigned as described in Section 3.7.4. The standards of the expected degradation products were analysed but when comparing these to the samples analysed it was not possible to identify individual degradation products for the reasons discussed above.

4.6.1 ^{13}C NMR Analysis of Blended Amine Solvent

^{13}C NMR analysis was carried out on a select few blended amine samples. The samples analysed by this technique had been operational for 529, 587 and 682 hours (Figure 4.20, Figure 4.21 and Figure 4.22 respectively). Peaks of interest are listed in Table 4-III, Table 4-IV and Table 4-V respectively.

When CO_2 is added to amine solutions, it can be expected that the following species will be observed in ^{13}C NMR spectra: protonated amine, molecular amine, amine carbamate, carbonate and bicarbonate. In systems which have fast exchanging protons, i.e. carbonate/ bicarbonate (CO_3^{2-}/ HCO_3^-) and molecular/ protonated amine (amine/ amineH$^+$), it is not possible to distinguish between the species, as the rate of proton transfer is faster than the NMR time scale.

From the spectra it is clear to see that the amine solvent is heavily degraded. Due to the relatively short experimental time of the NMR experiment, it was not possible to assign the peaks to individual degradation products. However, the number of peaks indicates there is significant degradation of the solvent. The cluster of peaks in the region 160-180 ppm are those of degradation products, and all others are of the amine/ amineH^+, amine carbamate or CO_3^{2-}/ HCO_3^- species, as labelled. Figure 4.23 shows the changes in each amine species as well as the carbamate and CO_3^{2-}/ HCO_3^- species over time. The small changes in concentrations of Amine1 and Amine2 are most likely to be due to the solvent top-ups which occurred throughout the testing campaign.

It has been shown that as CO_2 loading increases the concentration of amine carbamate observed also increases incrementally.[90] When the CO_2 loading reaches 0.5 mol CO_2/ mol amine then the concentration of protonated amine continues to increase at the expense of the carbamate concentration, and the released CO_2 reacts to form HCO_3^-.[91, 92] From Table 4-III, Table 4-IV and Table 4-V it can be seen that there is a trend in the signals corresponding to CO_3^{2-}/ HCO_3^- to move towards lower chemical shifts as the CO_2 loading increases (see Table 3-I). According to previous studies by Perinu *et al.* this is due to an increase in the HCO_3^- concentration.[90] This indicates that the protonated amine concentration is also increasing and the concentration of carbamate is decreasing. However, as Figure 4.23 shows the concentration of carbamate increases at the highest measured loading and the concentration of CO_3^{2-}/ HCO_3^- decreases, which is in conflict with the previous statement. This result could be due to the fast exchanging protons causing the line broadening of the NMR spectrum (see Figure 4.22) which would result in inaccuracies in the integration of the peaks.[86] The loading data for the solvents is not highly accurate as the equipment used to measure this on site was not always fully functional. Given the trends in the ^{13}C NMR data the values given for the solvent loading should be treated with caution.

Comparing the amount of carbonate/ bicarbonate to carbamate provides the ratio of the remaining two amines in the degraded solution. If the level of solvent regeneration was known then it would be possible to plot the ratio of the two loaded amines. The ratios of remaining loaded Amine1:Amine2 in the three analysed samples are 10:1, 1:1.75 and 5.4:1 respectively. This is due to the regeneration energy for Amine2 being lower than for Amine1, therefore there will be less residual Amine2 in the solvent (having been regenerated) and more carbamate from Amine1.[93] This information is useful when investigating the loading of the two amines in the solvent.

By converting the mg/ C to weight percent of amines and comparing this to the percent total amines in GC-MS for the same samples, it can be seen that the two analytical methods correlate fairly well for the sample at 529 hours only (Figure 4.24). As discussed, the relatively short relaxation time used means that the integration of the peaks will not be as accurate as the GC-MS analysis. This shows that ^{13}C NMR is suited to the rapid analysis of the extent of degradation, although longer experimental times would have allowed more accurate quantitative data to be collected.

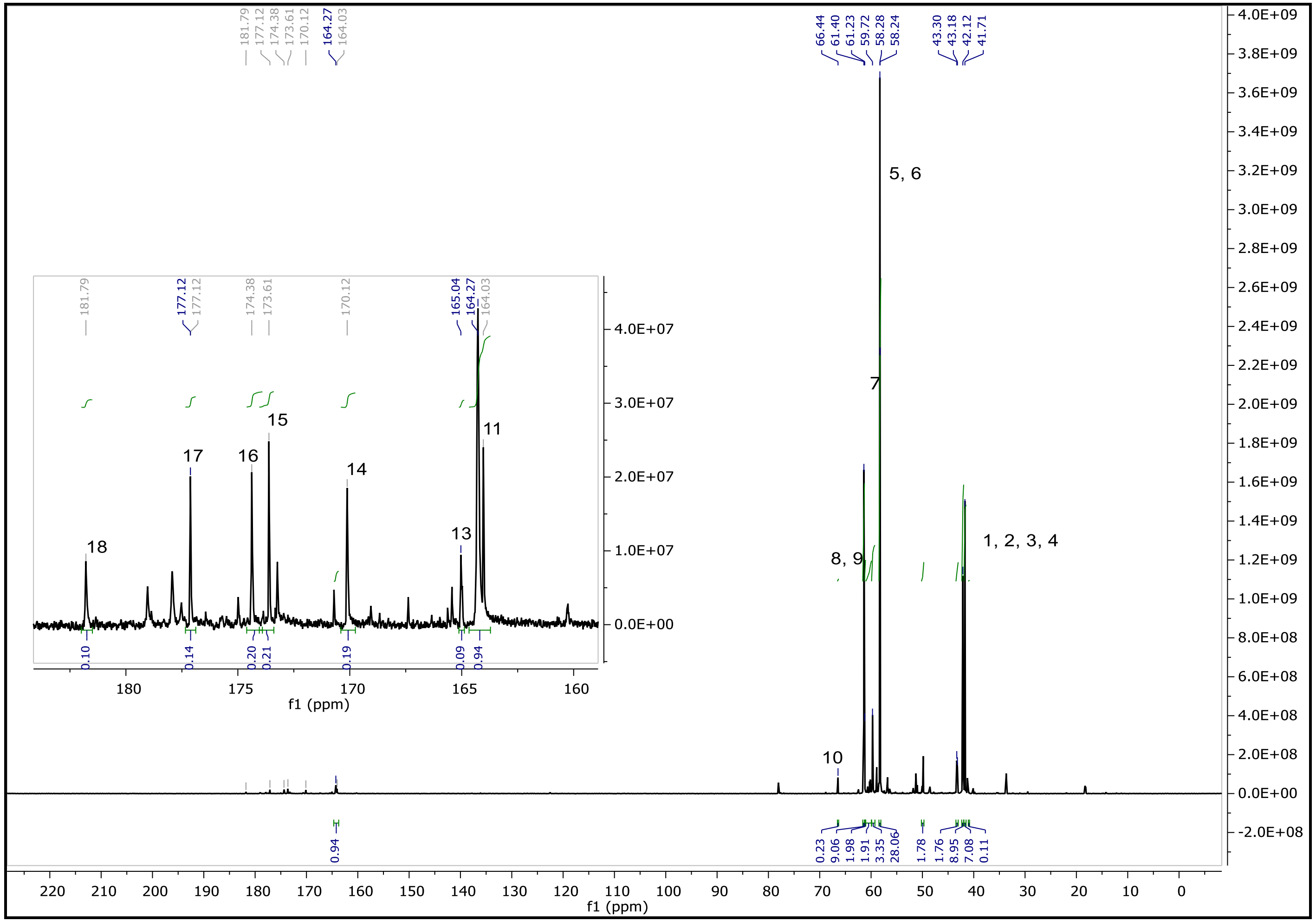

Figure 4.20: ^{13}C NMR spectrum, blended amine, 529 hours

Table 4-III: Peaks of interest in Figure 4.20

Peak	δ (ppm)	Integration area (arbitrary units)	mg/ C	Assignment
1	41.7	7.1	37.9	Amine2/Amine2H$^+$ (next to N)
2	42.1	9.0	47.9	Amine1/Amine1H$^+$ (next to N)
3	43.2	1.8	9.4	Amine1 carbamate (next to N)
4	43.3			
5	58.2	28.1	150.1	Amine2/Amine2H$^+$ (next to OH group)
6	58.3			
7	59.7	3.4	17.9	Amine2/Amine2H+ (next to N)
8	61.2	2.0	10.6	Amine1 carbamate (next to OH group)
9	61.4	9.1	48.5	Amine1/Amine1H+ (next to OH group)
10	66.4	0.2	1.2	1,4-dioxane (internal standard)
11	164.0	0.9	5.0	Amine1 carbamate (C=O)
12	164.3			
13	165.0	0.1	0.5	Carbonate/Bicarbonate (CO_3^{2-}/ HCO_3^-)
14	170.1	0.2	1.0	Unknown
15	173.6	0.2	1.1	Unknown
16	174.4	0.2	1.1	Unknown
17	177.1	0.1	0.7	Unknown
18	181.8	0.1	0.5	Unknown

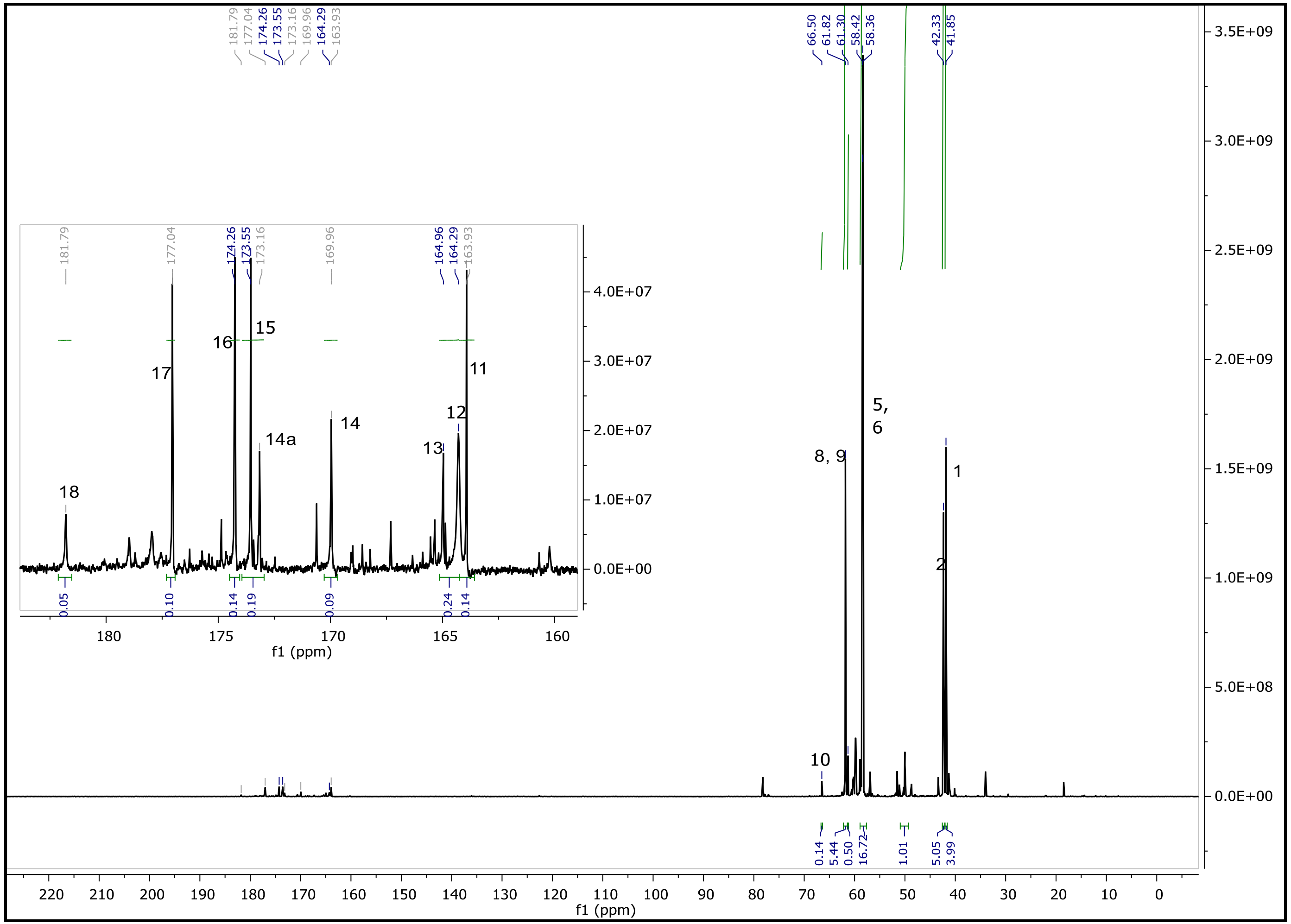

Figure 4.21: ^{13}C NMR spectrum, blended amine, 587 hours

Table 4-IV: Peaks of interest in Figure 4.21

Peak	δ (ppm)	Integration area (arbitrary units)	mg/ C	Assignment
1	41.9	4.0	35.1	Amine2/Amine2H$^+$ (next to N)
2	42.3	5.1	44.4	Amine1/Amine1H$^+$ (next to N)
5	58.4	16.7	146.9	Amine2/Amine2H$^+$ (next to OH group)
6	58.4			
8	61.3	0.5	4.4	Amine1 carbamate (next to OH group)
9	61.8	5.4	47.8	Amine1/Amine1H$^+$ (next to OH group)
10	66.5	0.1	1.2	1,4-dioxane (internal standard)
11	163.9	0.1	1.2	Amine1 carbamate (C=O)
12	164.3			
13	165.0	0.2	2.1	Carbonate/Bicarbonate (CO_3^{2-}/ HCO_3^-)
14	170.0	0.1	0.8	Unknown
14a	173.2	0.2	1.7	Unknown
15	173.6			Unknown
16	174.3	0.1	1.2	Unknown
17	177.0	0.1	0.9	Unknown
18	181.8	0.1	0.4	Unknown

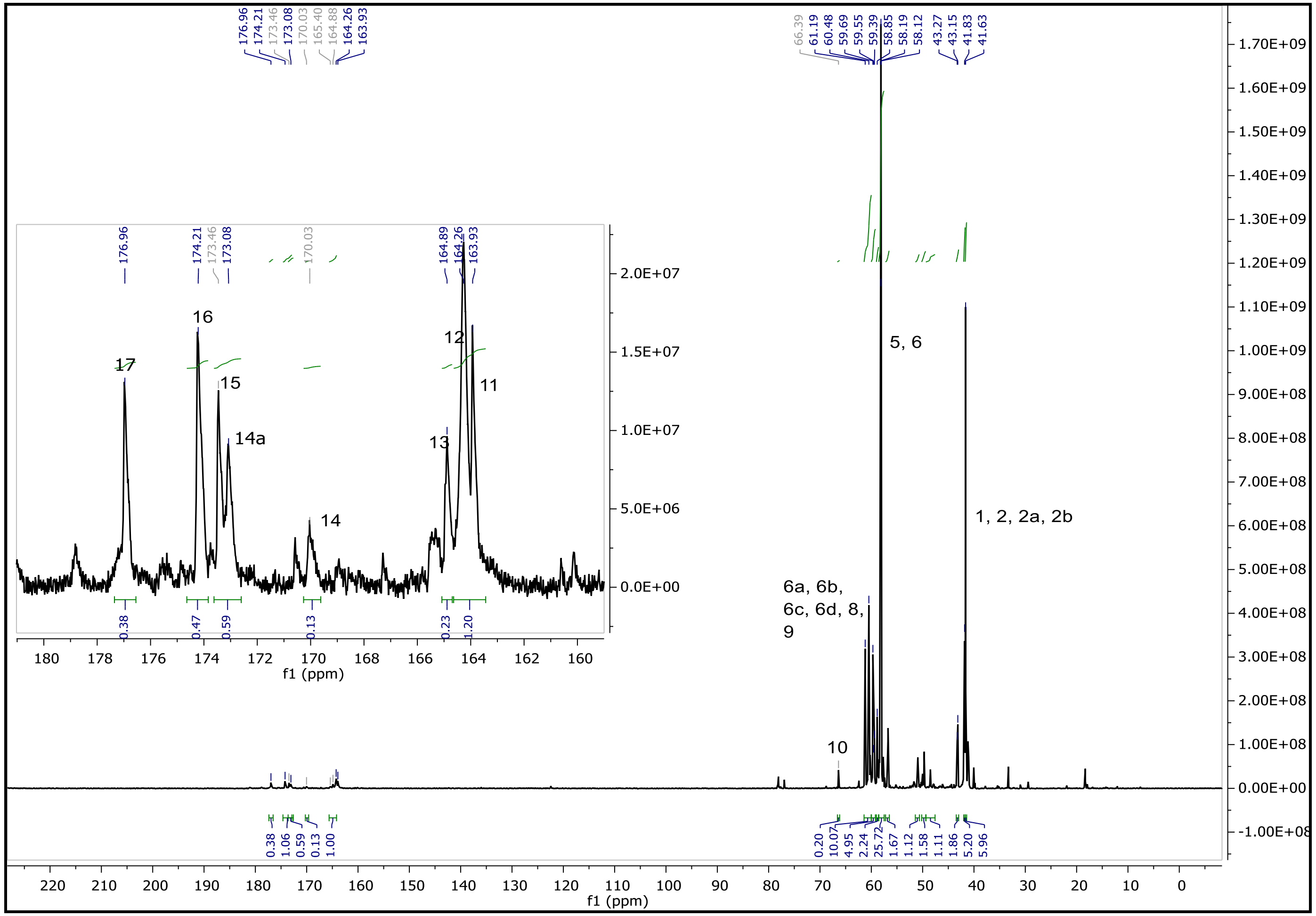

Figure 4.22: ^{13}C NMR spectrum, blended amine, 682 hours

Table 4-V: Peaks of interest in Figure 4.22

Peak	δ (ppm)	Integration area (arbitrary units)	mg/ C	Assignment
1	41.6	6.0	37.3	Amine2/Amine2H$^+$ (next to N)
2	41.8	5.2	32.5	Amine1/Amine1H$^+$ (next to N)
2a	43.2	1.9	11.6	Amine1/Amine1H$^+$ (next to N)
2b	43.3			
5	58.1	25.7	160.8	Amine2/Amine2H$^+$ (next to OH group)
6	58.2			
6a	58.9	7.2	44.9	Amine1/Amine1H$^+$ (next to OH group)
6b	59.4			
6c	59.6			
6d	59.7			
8	60.5	10.1	62.9	Amine1 carbamate (next to OH group)
9	61.2			
10	66.4	0.2	1.3	1,4-dioxane (internal standard)
11	163.9	1.2	7.5	Amine1 carbamate (C=O)
12	164.3			
13	164.9	0.2	1.4	Carbonate/Bicarbonate (CO_3^{2-}/ HCO_3^-)
14	170.0	0.1	0.8	Unknown
14a	173.1	0.6	3.7	Unknown
15	173.5			Unknown
16	174.2	0.5	2.9	Unknown
17	177.0	0.4	2.4	Unknown

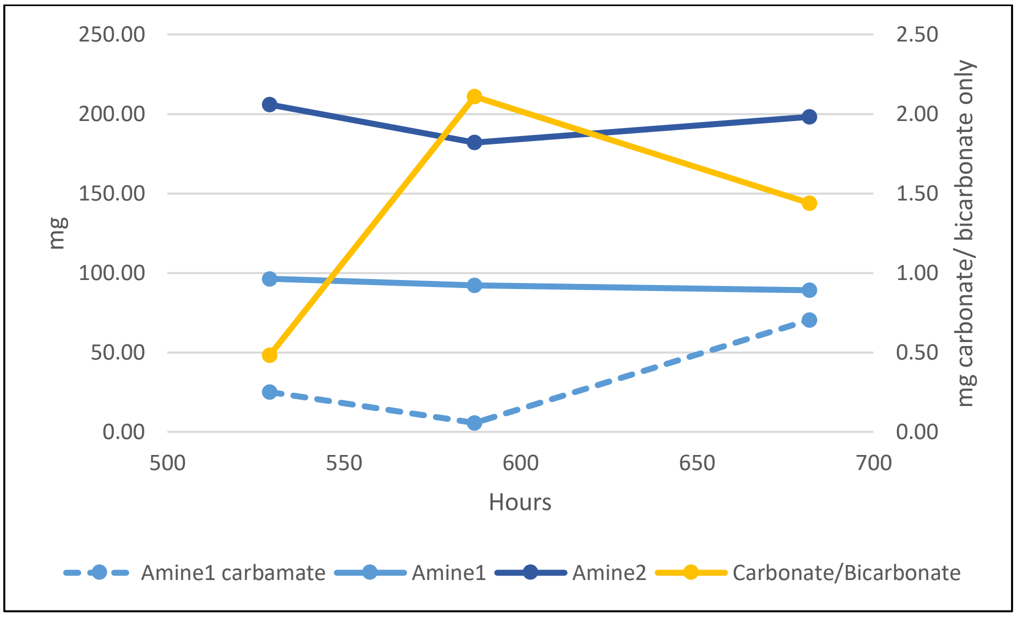

Figure 4.23: Speciation of amines by ^{13}C NMR analysis

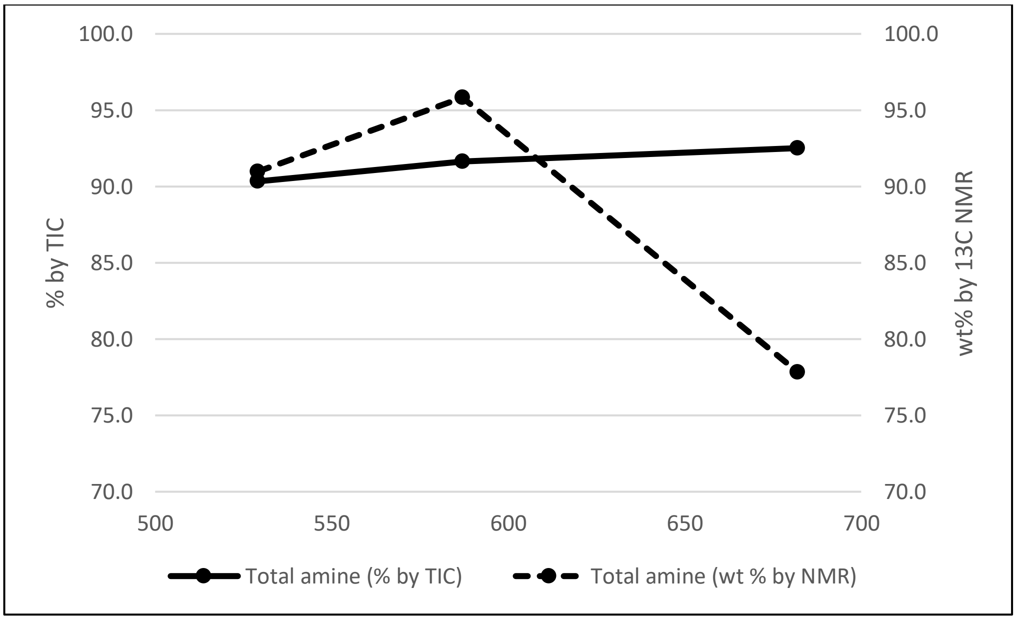

Figure 4.24: Correlation between GC-MS and ^{13}C NMR analysis for starting amines

4.7 Summary and Conclusions

Detailed analysis of the blended amine solvent has been carried out using GC-MS, GC-FID, ICPMS, IC and ^{13}C NMR Spectroscopy. The following outcomes were found:

- GC-MS was used to semi-quantitatively identify several major degradation products. The products identified were: 1-methyl-2,5-pyrrolidinedone, piperidine-2,5-dione, N-(2-hydroxyethyl) succinimide, DEA, bicine, OZD and aspartic acid, as well as the starting amines, Amine1 and Amine2.
- GC-FID was required to quantify some of the degradation products and to identify HEA. The main finding was that N-(2-hydroxyethyl) succinimide was the predominant species, and the levels of bicine present agreed with the GC-MS data. The correlation between GC-FID and GC-MS showed that bicine and iron levels are consistent with the theory that iron is more soluble in the presence of bicine.
- ICPMS was used to quantitatively analyse metals in the solution. Iron was the predominant transition metal in the solvents, which is to be expected given the levels of bicine identified using GC-MS and GC-FID. Iron is known to be more soluble in the presence of bicine, so these results are not unexpected.
- The only cation identified by cation chromatography was potassium. Correlating the levels of K found by cation IC with those found by ICPMS showed that neither analytical technique is particularly effective in monitoring potassium levels in the solvent. Overall, cation IC was not particularly useful in this work- more should be done to focus on the loss of amines rather that the identification of cationic species.
- Anion chromatography was used to analyse the levels of HSSs in the solvents. Oxalate and formate were the two most abundant HSSs identified,

with both reacting in a similar way to the increase in SO_2 levels, higher O_2 levels and high regeneration temperature. It is possible that the formation of oxalate is favoured over formate at higher temperatures, as the ratio of formate to oxalate decreases at higher temperatures.

- ^{13}C NMR proved useful as a rapid analytical technique to indicate the extent of degradation. There is a fairly good correlation between the levels of amine/ protonated amine found by ^{13}C NMR and those found by GC-MS analysis for the sample at 529 hours only. For the remaining two samples, there is not very good correlation between the techniques. The relatively short experimental time used means that the integration of the peaks will not be as accurate as the GC-MS analysis. This shows that ^{13}C NMR is suited to the rapid analysis of the extent of degradation, but not for quantitative analysis. Due to inaccuracies in the loading data from the plant, the trends observed are to be treated with caution. This does not detract from the usefulness of ^{13}C NMR as an analytical technique but is a reflection of the importance of accurate monitoring of the solvent while it is operation in the plant.

Chapter 5: Suppressing Degradation by Ion Exchange

5.1 Introduction

This chapter discusses the effects of suppressing degradation in primary amine solvents by using imine based cation exchange resins to remove metals. All samples were supplied from the pilot plant in North West Europe and were of a single primary amine solvent. Two sets of ion exchange (IX) have been carried out. The first occurred on cold solvent which had been running in the plant for 4425 hours and was significantly degraded. This solvent was passed through the IX resin once, when cold and without further processing in the plant. For this solvent samples have been analysed before and after the IX process, in order to assess how effective a single IX treatment was on the solvent. The discolouration of the solvent is shown in Figure 5.1.

A new batch of the same primary amine solvent was then used in the plant which was operated with IX continually occurring. Samples were taken at the operating hours specified in Table 3-II and analysed in this work (W1- 17). Within this continuous IX testing phase there were three periods of reclaiming, details of which are given in Table 3-II. The purpose of the analysis was to track the development of certain degradation products and the solvent quality as a function of time with continuous IX. Results from the continuous IX process were compared to those of the single IX process to assess the effectiveness of the two approaches to mitigating degradation.

As in Chapter 4 a variety of analytical techniques were used to study the degraded solvents and results were compared. Table 5-I lists the analytical techniques applied to each solvent tested (conditions and operation hours as in Table 3-II). Where repeat analysis was carried out (GC-MS, GC-FID and ICPMS) the results for the 'Before IX' samples are reported as the mean of all six analyses as the two samples were the same. All other results are the mean of three analyses. All errors are reported to one standard deviation.

The solvents were not significantly degraded as evidenced by the small amount of discolouration of the samples which can be seen in Figure 5.2.

Table 5-I: Single amine solvent and analytical techniques

Sample ID	GC-MS	GC-FID	Anion IC	Cation IC	ICPMS	^{13}C NMR
Before IX 1	✓	✓	✓	✓	✓	×
Before IX 2	✓	✓	✓	✓	✓	×
After IX	✓	✓	✓	✓	✓	×
W1	✓	✓	✓	✓	✓	×
W2	✓	✓	✓	✓	✓	✓
W3	✓	✓	✓	✓	✓	×
W4	✓	✓	✓	✓	✓	✓
W5	✓	✓	✓	✓	✓	×
W6	✓	✓	✓	✓	✓	✓
W7	✓	✓	✓	✓	✓	×
W8	✓	✓	✓	✓	✓	✓
W9	✓	✓	✓	✓	✓	×
W10	✓	✓	✓	✓	✓	×
W11	✓	✓	✓	✓	✓	✓
W12	✓	✓	✓	✓	✓	×
W13	✓	✓	✓	✓	✓	✓
W14	✓	✓	✓	✓	✓	×
W15	✓	✓	✓	✓	✓	×
W16	✓	✓	✓	✓	✓	✓
W17	✓	✓	✓	✓	✓	×

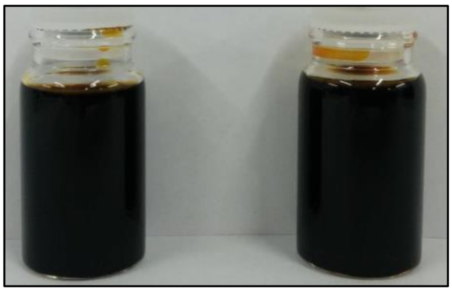

Figure 5.1: Discolouration of solvent, before (left) and after (right) IX

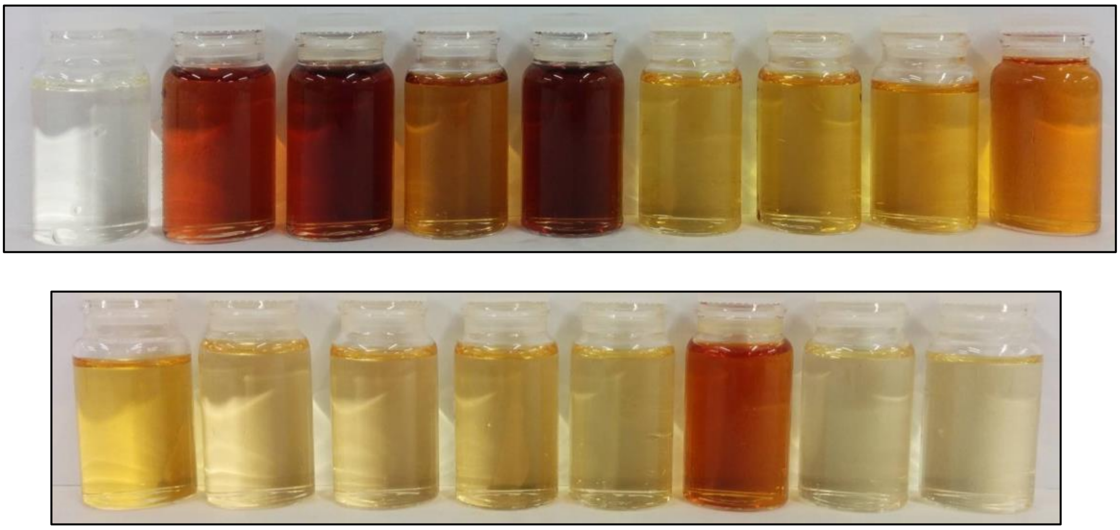

Figure 5.2: Discoloration of continually ion exchanged solvents
Top image: W1-9 (left to right); Bottom image: W10-17 (left to right)

As described in Section 3.6 concerning chromatography, ion exchange is the process of using resins to separate atomic or molecular ions based on their interaction with the resin in an analytical column. The purpose of using ion exchange resins in the pilot plant was to remove metals from the solvent system as metals are thought to catalyse the formation of some degradation products (see Section 2.3.4). By removing the metals it is thought that degradation can be managed and minimised. Some degradation products are also thought to enhance corrosion, for example the previously discussed increase in iron solubility in the presence of bicine. By removing all possible contributing factors to corrosion and degradation it may be possible to improve solvent management.

5.2 GC-MS of Single Ion Exchange Process

As discussed in Section 3.3, GC-MS is used to separate and identify major degradation products. It is used as a semi-quantitative analytical technique. The samples were prepared for GC-MS analysis as described in Section 3.3.4, and the analysis was carried out as described in Section 3.3.5.

5.2.1 GC-MS Analysis

Figure 5.3 shows a typical GC-MS chromatogram for the amine solvent taken before the ion exchange process, with identified peaks in Table 5-II. The extent of degradation in the sample is approximately 38 % (taking into account all degradation products, both identified and unidentified). Peak groups A, B and C were not identified by GC-MS.

The sample had been operational for 4425 hours and it is clear that the solvent is significantly degraded at this point. In order to see what effect IX had on degraded solvent, the sample was then passed once through an imine based cation exchange resin. As discussed above, this was carried out on cold solvent without further capture in the plant occurring.

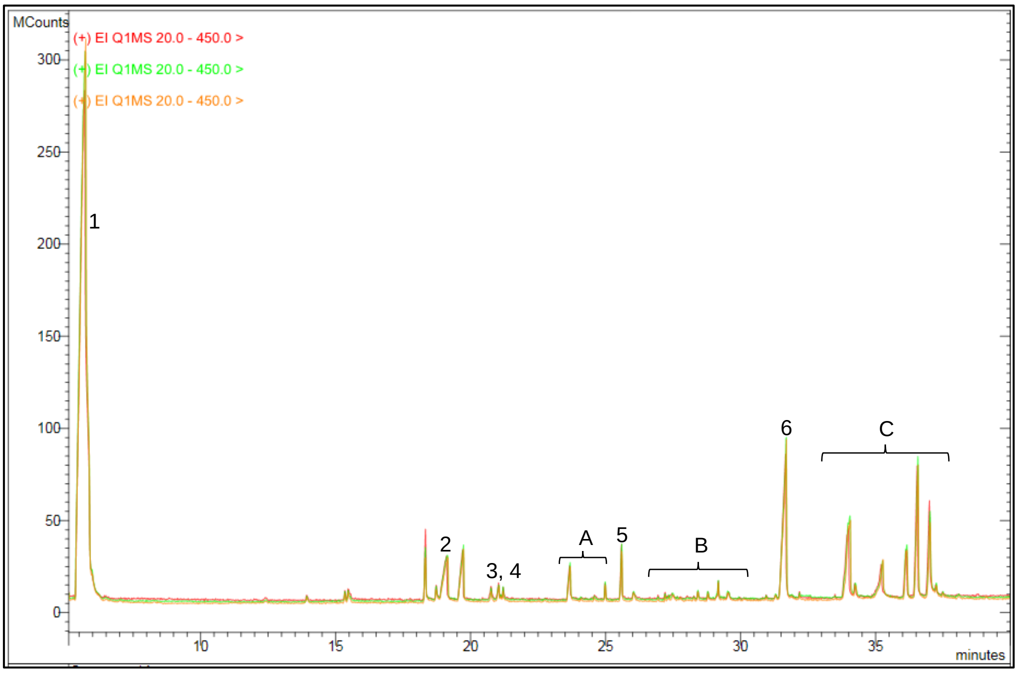

Figure 5.3: GC-MS before ion exchange

Table 5-II: Products identified by GC-MS

Peak	Product	Mw (nominal mass)	Structure
1	MEA	61.08	
2	N-(2-hydroxyethy) acetamide	103.12	See Table 2-I
3	OZD	87.08	See Table 2-III
4	Piperidine-2,5-dione	113.12	See Table 4-II
5	N-(2-hydroxyethyl) succinimide	143.14	See Table 2-II
6	Piperidine-2,5-dione/ 1-methyl-2,5-pyrrolidinedione	113.12/ 113.11	See Table 4-II

Figure 5.4 shows the GC-MS chromatogram for the sample after it had undergone ion exchange, with identified products also listed in Table 5-II. Peak groups A, B and C were not identified by GC-MS. The IX process had little effect on the number of degradation products observed in the solvent as the products identified by GC-MS are not cationic so would not have been affected by IX. The concentration of each degradation product has reduced slightly, suggesting that carrying out IX on already degraded solvent is of a small benefit in terms of solvent quality.

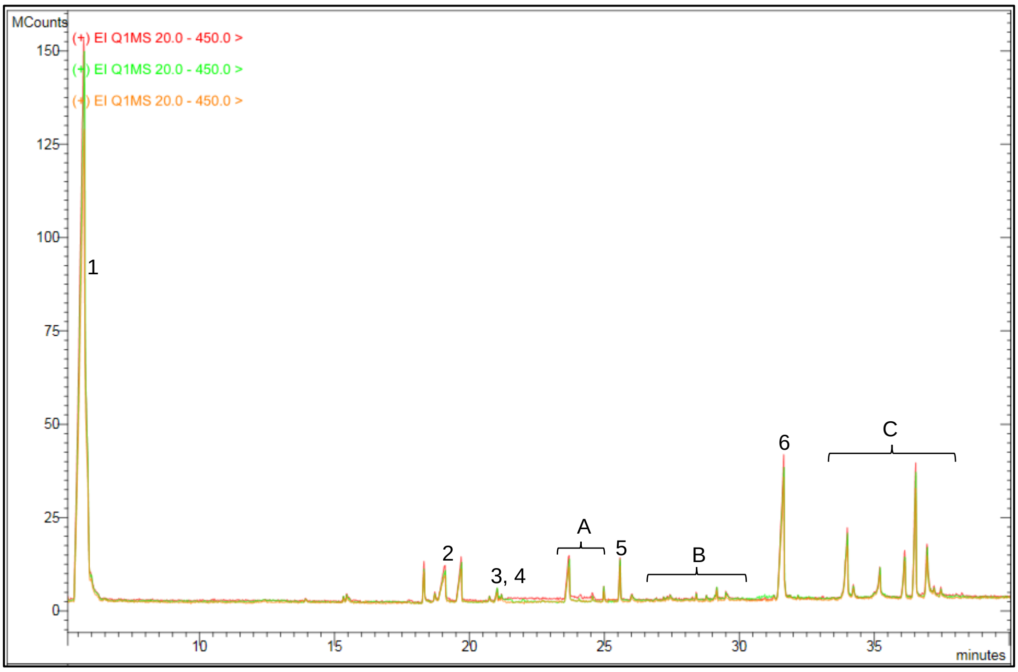

Figure 5.4: Sample after ion exchange

The major degradation products identified by GC-MS both before and after IX are shown in Figure 5.5 (all error bars are to one standard deviation). The decrease in concentration after IX indicates that the process has reduced the concentration of identifiable degradation products in the solvent, as well as the concentration of primary amine. This indicates that amine is being absorbed by the IX column in its protonated form. As shown in Figure 5.6 the level of primary amine almost halves after IX whereas the level of degradation products significantly increases. The percent degradation products presented in Figure 5.6 represents all degradation products in the solvent, not just the major ones which were identified in Table 5-II.

The increase in total percent of degradation products after IX could be due to the protonated amine being absorbed by the IX column. This would mean that a greater proportion of the solvent is now made up of degradation products. Also, the removal of metals by IX may initiate the formation of secondary degradation products. This is due to metals, particularly iron, being able to chelate with some primary degradation products and which can further degrade once the metals are removed in the IX process. For example, it has been shown that iron carbonate chelates with bicine and this explains the increased solubility of iron in the lean side of the amine scrubbing system.[67] However, bicine was not one of the degradation products identified in these samples.

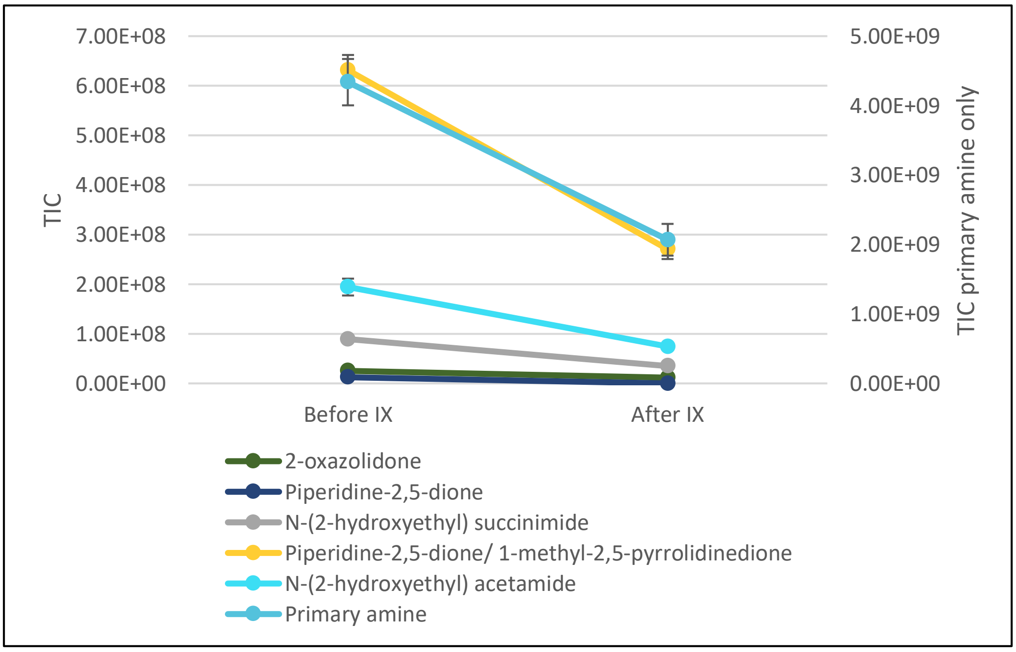

Figure 5.5: GC-MS trends in degradation products

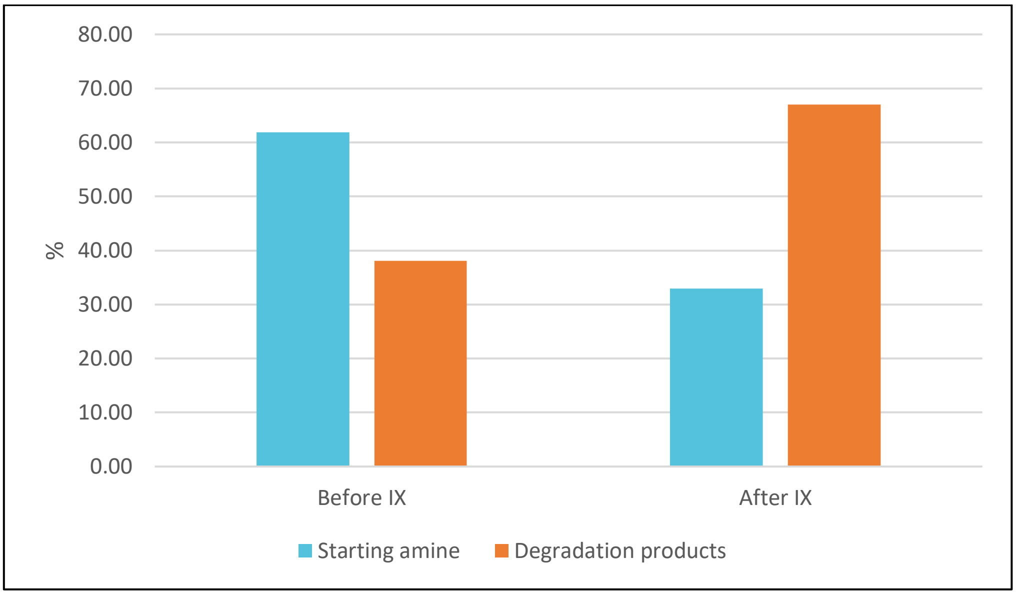

Figure 5.6: Effect of single ion exchange (IX) on starting materials and degradation products

5.3 GC-FID of Single Ion Exchange Process

GC-FID analysis was carried out with the aim of using it as a quantitative measure of the degradation of the solvent. All standards and samples were prepared for analysis as described in Sections 3.4.1 and 3.4.2, and the analysis was carried out as described in Section 3.4.3.

As discussed in Section 3.4, GC-FID can be used as a quantitative analytical technique due to the accuracy of the response from the detector. Four of the major degradation products were analysed by GC-FID. The peak response corresponds to the mass of carbon in the molecule, regardless of carbon structure. In order to identify the standards, each individual standard was first run on GC-MS, then compared to the GC-FID results which used the same column. The order in which the compounds eluted in the GC-MS analysis allowed interpretation of the GC-FID results. As discussed in Section 3.4.1 the four compounds quantitatively analysed using this method were HEA, OZD, N-(2-hydroxyethyl) succinimide and bicine. These were chosen as they are known degradation products and were easily identifiable in the GC-FID analysis.

5.3.1 GC-FID Analysis

Typical GC-FID traces for before and after the single ion exchange process are shown in Figure 5.7. Peaks which are unlabelled were unidentified. The GC-FID analyses of the solvent before and after IX are shown below in Figure 5.8 (all error bars are to one standard deviation). This shows that the levels of HEA and bicine decreased after the IX process, but OZD and N-(2-hydroxyethyl) succinimide were not really affected by the process. This could indicate that these products are not affected by the level of metals in the system. The reduction in levels of bicine after iron has been removed by IX could indicate that bicine is being absorbed by the IX column. The GC-FID results suggest that IX is an effective technique for reducing the levels of HEA and bicine.

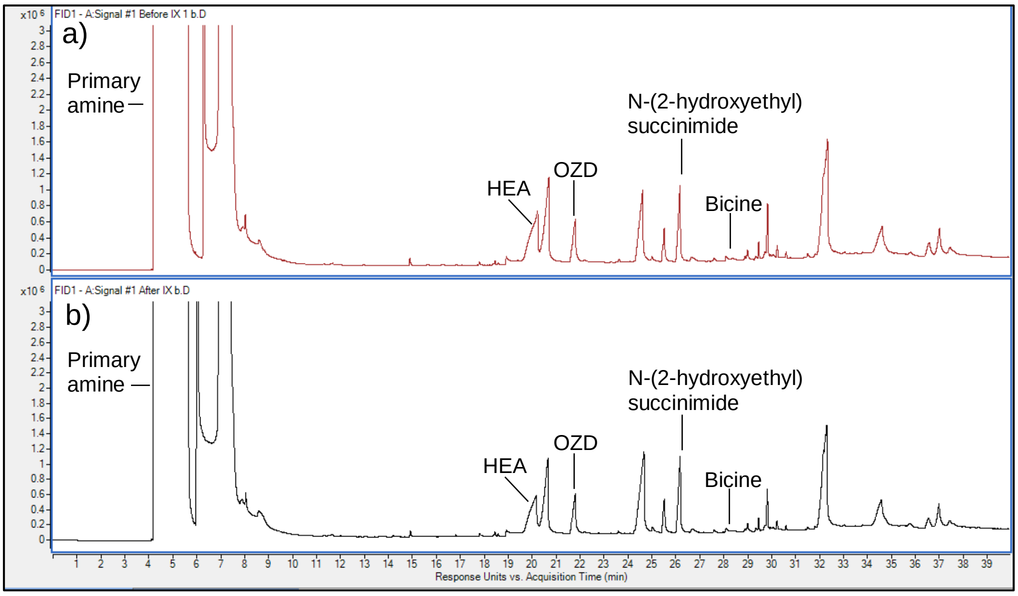

Figure 5.7: Typical GC-FID traces for solvent a) before; and b) after the single ion exchange process

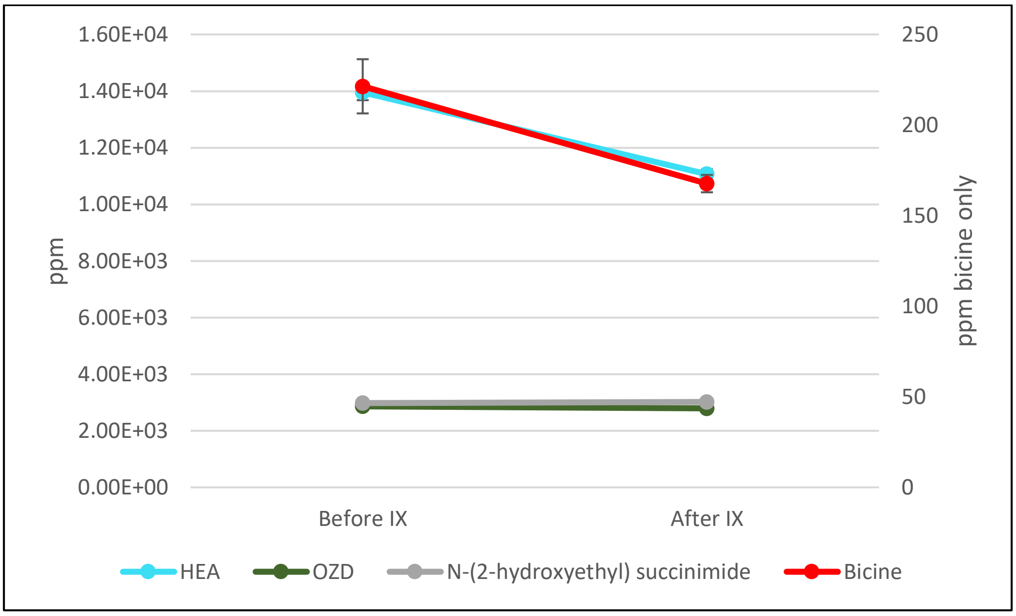

Figure 5.8: GC-FID analysis of solvent before and after ion exchange

Comparing the GC-MS and GC-FID analyses of the solvent before and after IX shows that FID is better suited to detecting bicine than MS is, as bicine was not found when MS analysis was carried out. This could indicate that the levels of bicine are low enough to avoid detection by GC-MS, but the more sensitive GC-FID was able to detect it. The trends from the two analytical techniques are shown in Figure 5.9 (error bars are to one standard deviation). Analysis of N-(2-hydroxyethyl) succinimide by FID shows minimal changes before and after IX, whereas the analysis by MS suggests a much larger decrease in concentration after IX. This suggests that the GC-MS analysis may not be as accurate as the GC-FID analysis. However, GC-MS did not detect any bicine in the samples whereas GC-FID was able to detect this compound. Both OZD and HEA display similar trends in both analytical techniques. Figure 5.10 shows the correlation between MS and FID analysis of remaining primary amine (error bars to one standard deviation). FID results show a very small increase in primary amine after IX whereas MS shows a marked decrease. These results show that in order to identify all degradation products in the solvents it is necessary to use more than one analytical technique.

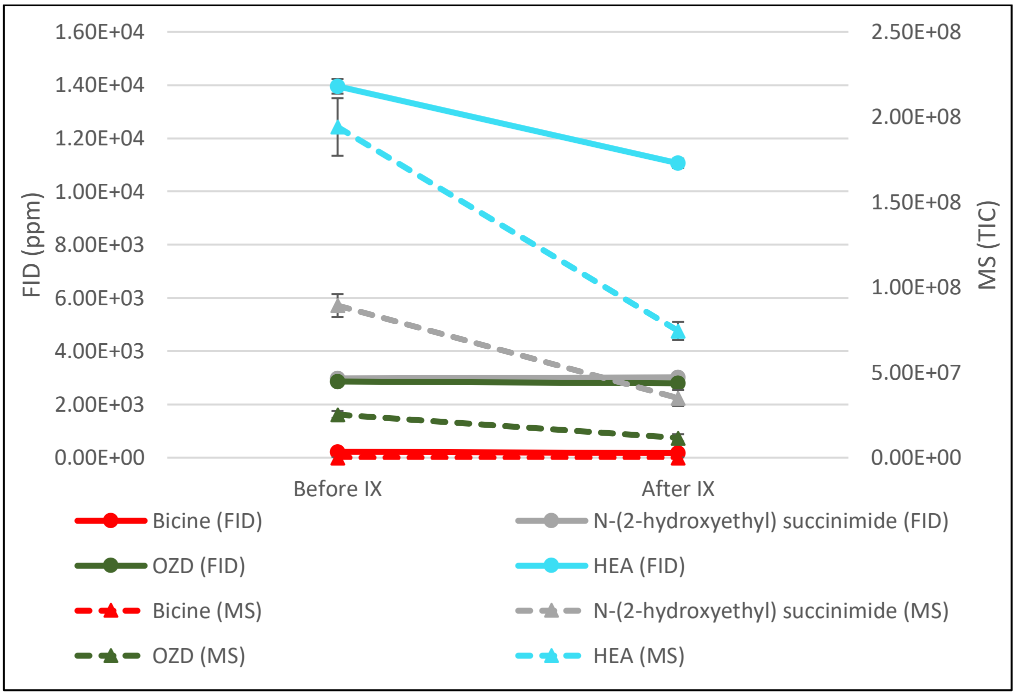

Figure 5.9: Correlation between MS and FID data for bicine and N-(2-hydroxyethyl) succinimide

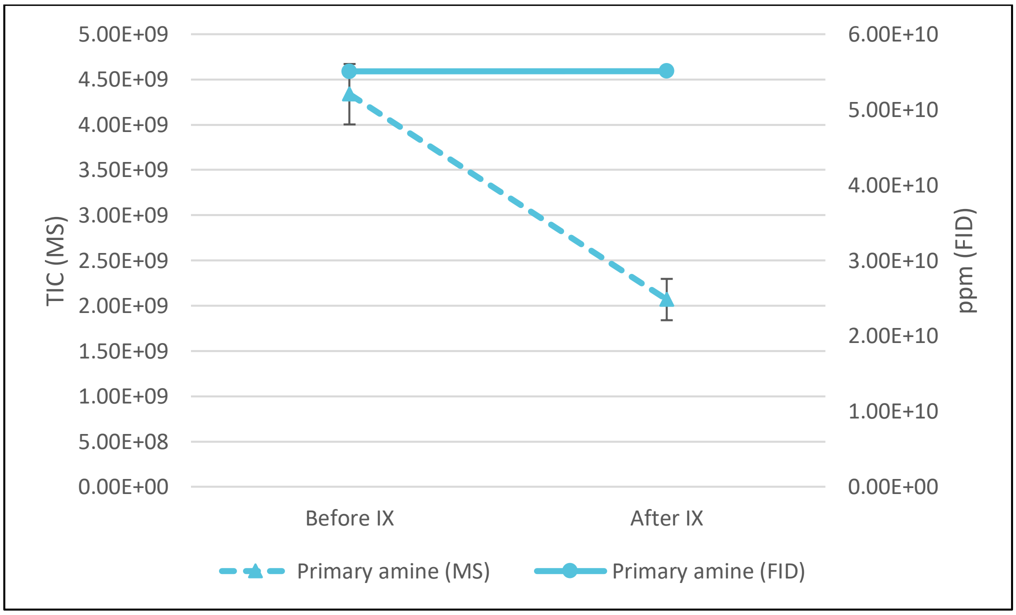

Figure 5.10: Correlation between MS and FID for primary amine

5.4 ICPMS of Single Ion Exchange Process

As discussed in Section 3.5, ICPMS is used to identify and quantify any metals present in the solvent. All standards and samples were prepared as described in Sections 3.5.3 and 3.5.4. Analysis was carried out as described in Section 3.5.5.

5.4.1 ICPMS Analysis

Figure 5.11 shows the ICPMS analysis for the solvent before and after IX (all error bars are to one standard deviation). The metal which has been effected the most by this process is iron as this has the largest decrease after IX treatment being reduced from 537 ppm to 9 ppm. The results show that the IX process is very effective in its removal of metals. Metals of interest which are thought to have some impact on degradation and corrosion are nickel, chromium, copper and vanadium, but neither of the latter two were detected in any measurable amount (< 1 ppm) so have not been shown on the graph.[17, 40, 54-58] Nickel and chromium levels both decrease after IX. The decrease in iron compared to the decrease in levels of bicine observed by GC-FID is approximately 10:1 (Figure 5.12). This implies that bicine is also complexed with other ions in the system.[94] HEA also follows a similar trend with iron levels.

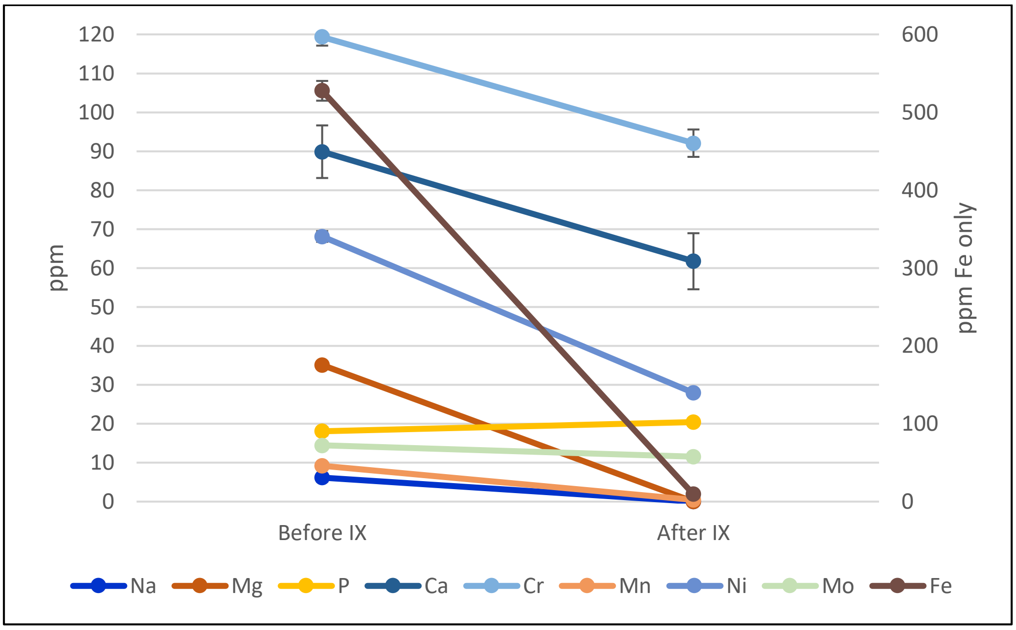

Figure 5.11: ICPMS of single ion exchange process samples

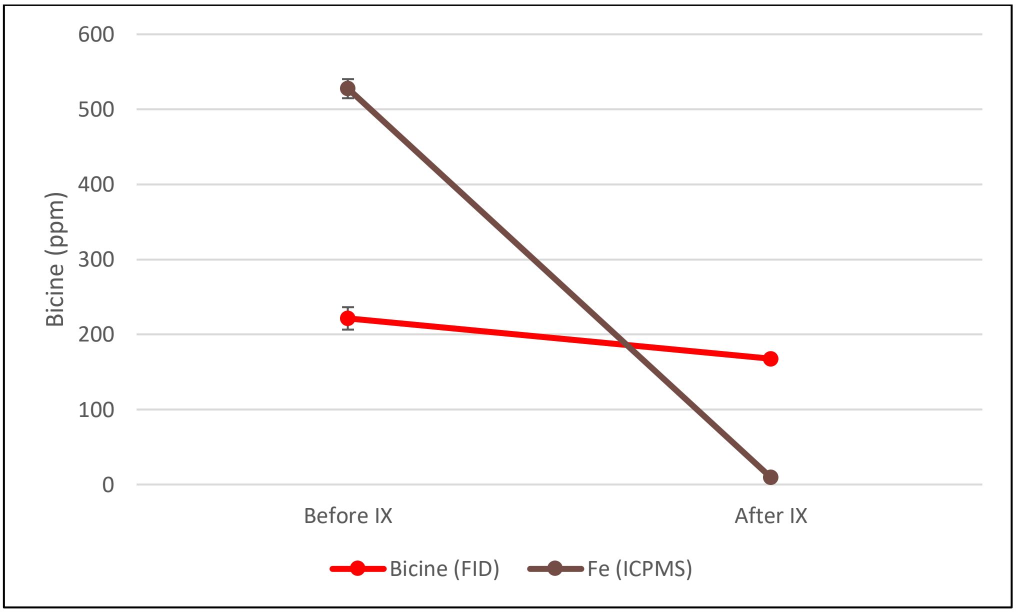

Figure 5.12: Correlation in bicine and iron levels, single ion exchange process

5.5 IC of Single Ion Exchange Process

As discussed in Section 3.6 IC is used for the identification of heat stable salts. It is a qualitative analytical technique. Samples and standards were prepared for analysis as described in Sections 3.6.3, 3.6.4, 3.6.6 and 3.6.7. Analysis was carried out as described in Sections 3.6.5 and 3.6.8.

5.5.1 IC Analysis

5.5.1.1 Cation Analysis

Typical cation chromatograms for the amine before and after the single IX process are shown in Figure 5.13 and Figure 5.14. Cation chromatography was found to be useful in the detection of calcium and potassium only (Figure 5.15), with all other cations below the limit of quantification of the instrument. There was very little reduction in calcium after ion exchange and only a small (~ 10 mmol) reduction in potassium. This suggests that cation chromatography is ineffective in these circumstances and ICPMS is the preferred technique for cation analysis. Cation chromatography may be useful for monitoring the loss of amine in the solvent but this was not carried out in this work.

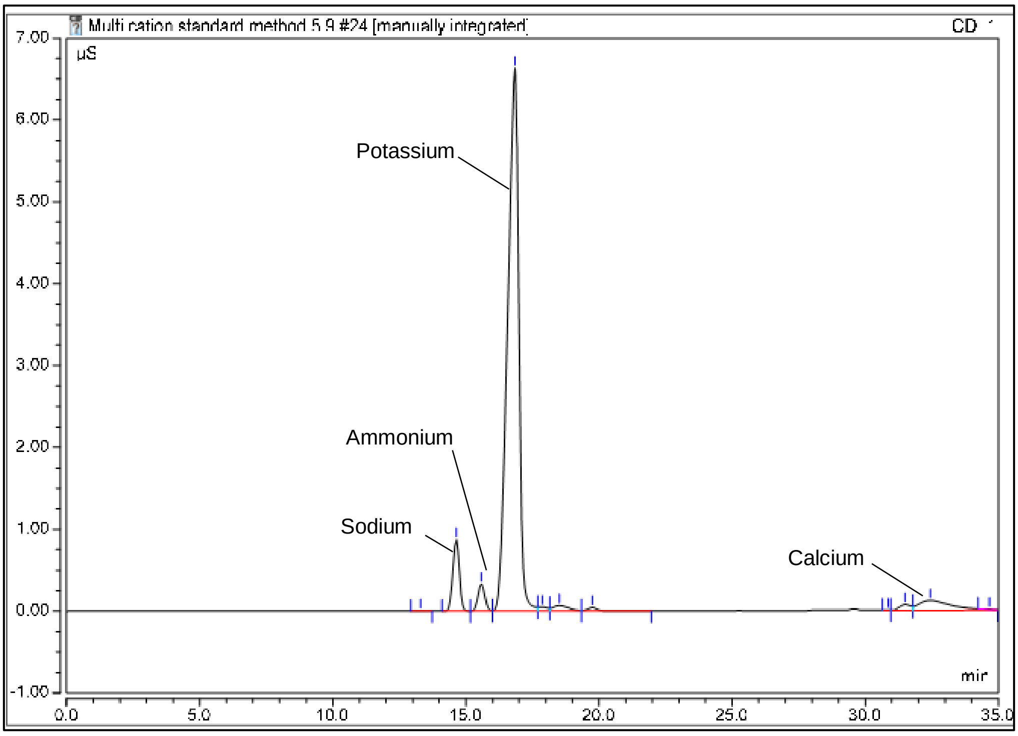

Figure 5.13: Cation chromatogram of solvent before single ion exchange process

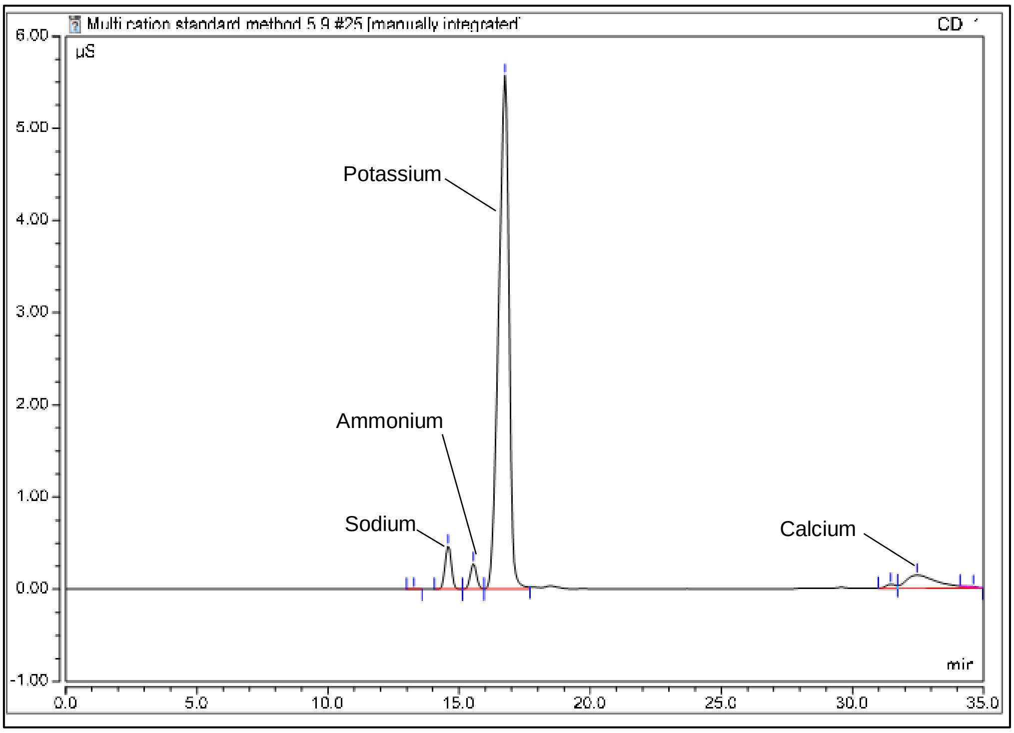

Figure 5.14: Cation chromatogram of solvent after single ion exchange process

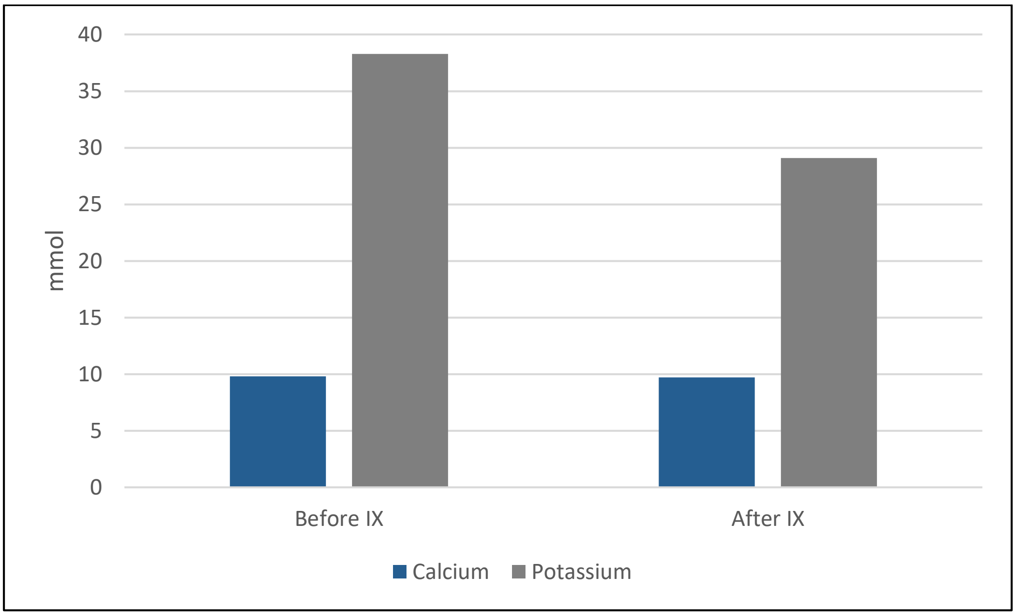

Figure 5.15: Cation analysis of non-continuous ion exchange

Correlating the data from ICPMS and IC for calcium and potassium (Figure 5.16) shows that IC is more sensitive to potassium levels and ICPMS is more sensitive to calcium levels. This is further evidence that in order to fully understand solvent degradation it is necessary to use more than one analytical technique.

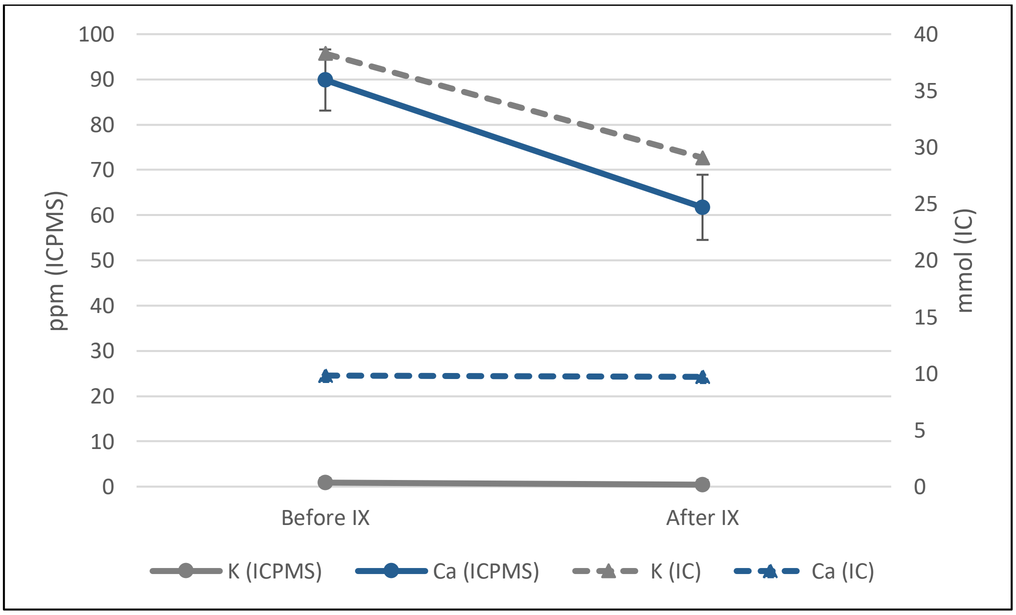

Figure 5.16: Correlation between ICPMS and IC for calcium and potassium

5.5.1.2 Anion Analysis

Formate, nitrate, nitrite, oxalate, acetate and glycolate were identified and quantified using external standards. Typical anion chromatograms for the amine before and after the single IX process are shown in Figure 5.17 and Figure 5.18. Figure 5.19 shows the anion analysis for before and after IX to remove metals.

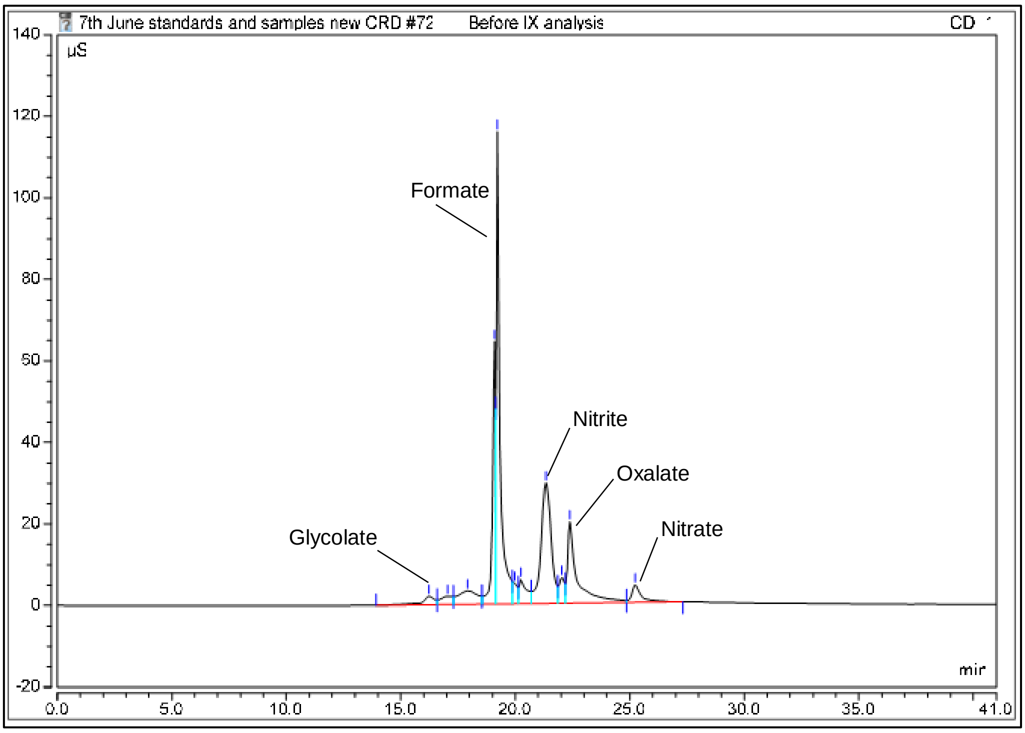

Figure 5.17: Anion chromatogram of before single ion exchange process

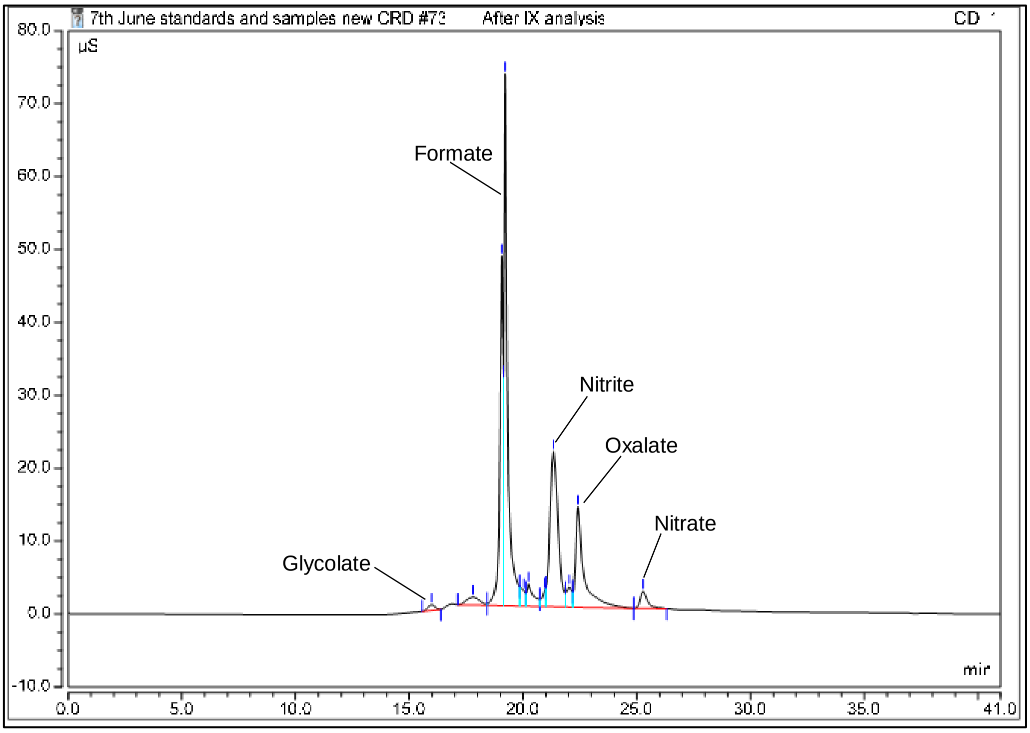

Figure 5.18: Anion chromatogram of after single ion exchange process

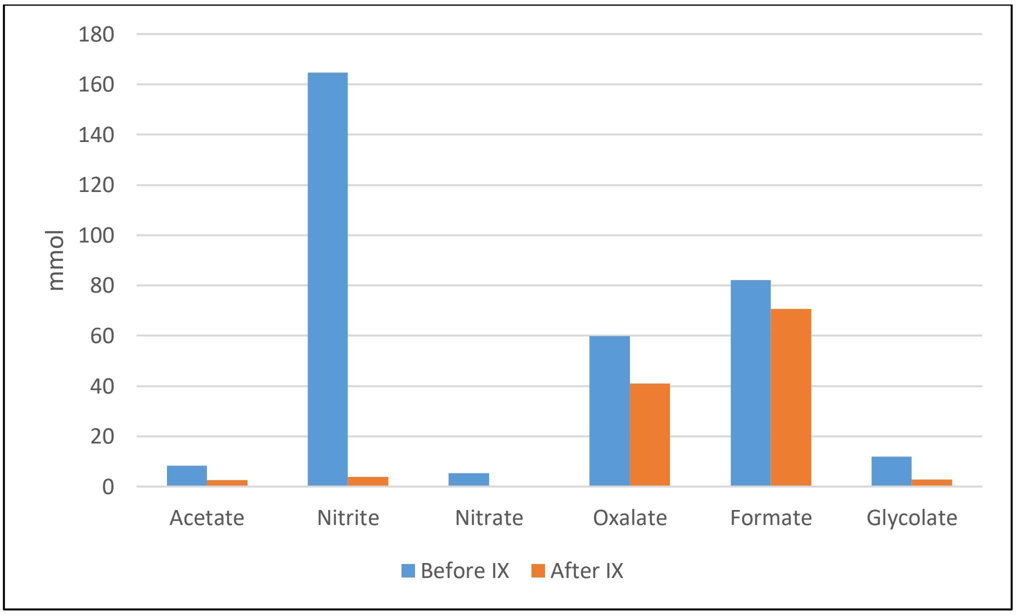

Figure 5.19: Anions for single ion exchange process

As can be seen, nitrite was the predominant HSS present in the sample before IX and had been significantly reduced after undergoing the process. Levels of all HSSs were reduced by the IX process proving that this is an effective technique for the removal of anionic species.

5.5.1.3 Amide Analysis

In order to analyse for formamide, oxamide, acetamide and glycolamide, the reaction with NaOH was carried out as described in Section 3.6.4. Any increase in carboxylic acid concentration between the two samples was considered to be amide that had been recovered in the form of carboxylic acid. Neither acetamide nor glycolamide were detected so are not shown in Figure 5.20. The increase in both oxamide and formamide after IX could indicate that oxalic acid is acting as a reactive intermediate which then decomposes to give formic acid, eventually producing the stable compound HEF.[37]

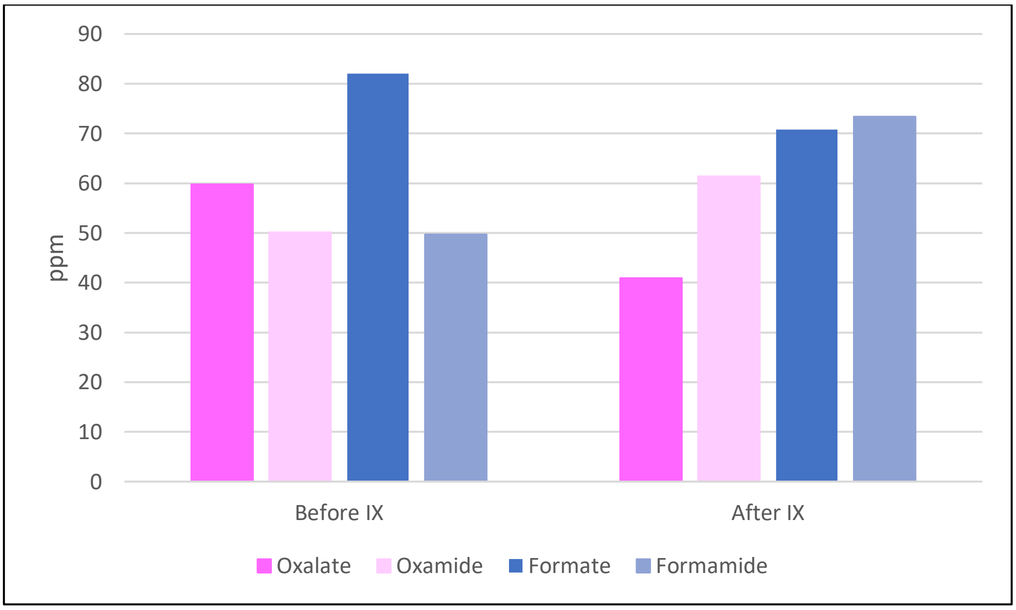

Figure 5.20: Amide analysis of non-continuous ion exchange

5.6 GC-MS of Continuous Ion Exchange Process

As discussed in Section 3.3, GC-MS is used to separate and identify major degradation products. It is used as a semi-quantitative analytical technique. The samples were prepared for GC-MS analysis as described in Section 3.3.4 and the analysis was carried out as described in Section 3.3.5.

5.6.1 GC-MS Analysis

Continuous IX to remove metals was carried out on samples W1-17 with the samples being taken at the times specified in Table 3-II. A typical GC-MS trace for the continuous ion exchanged samples is shown in Figure 5.21, with an expansion shown in Figure 5.22 (further examples of GC-MS analysis of the continually IX solvent can be found in Appendix F). The GC-MS results show that this minimised the degradation within the process (Figure 5.23, error bars to one standard deviation). After 2179 hours of operation GC-MS analysis showed that only approximately 4.5 % of the sample was made up of degradation products (Figure 5.24).

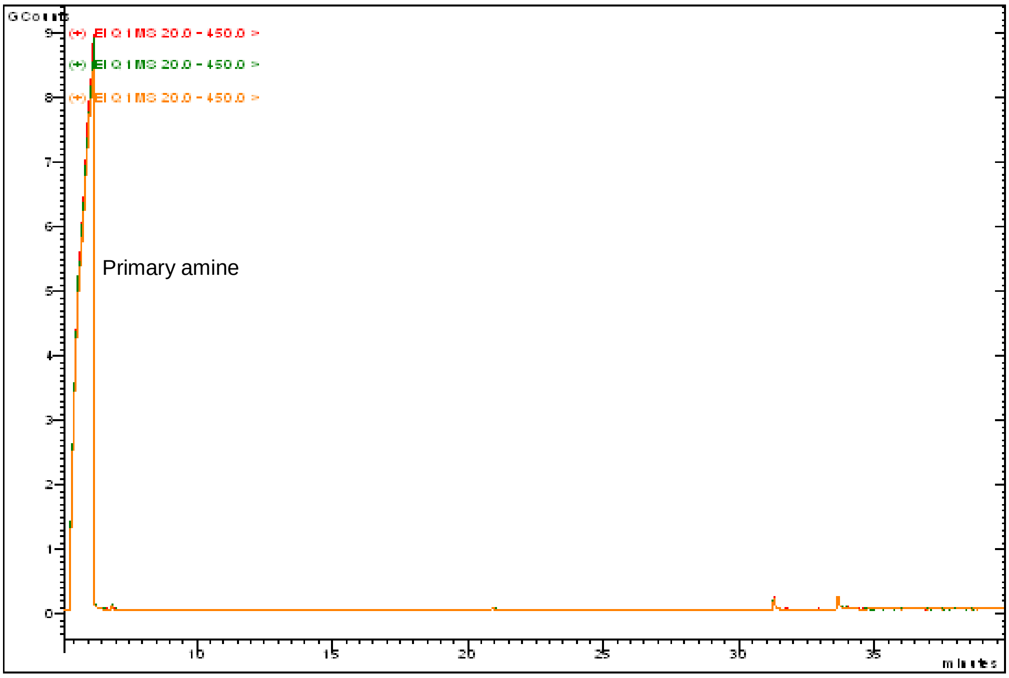

Figure 5.21: Typical GC-MS chromatogram for continuous ion exchange process

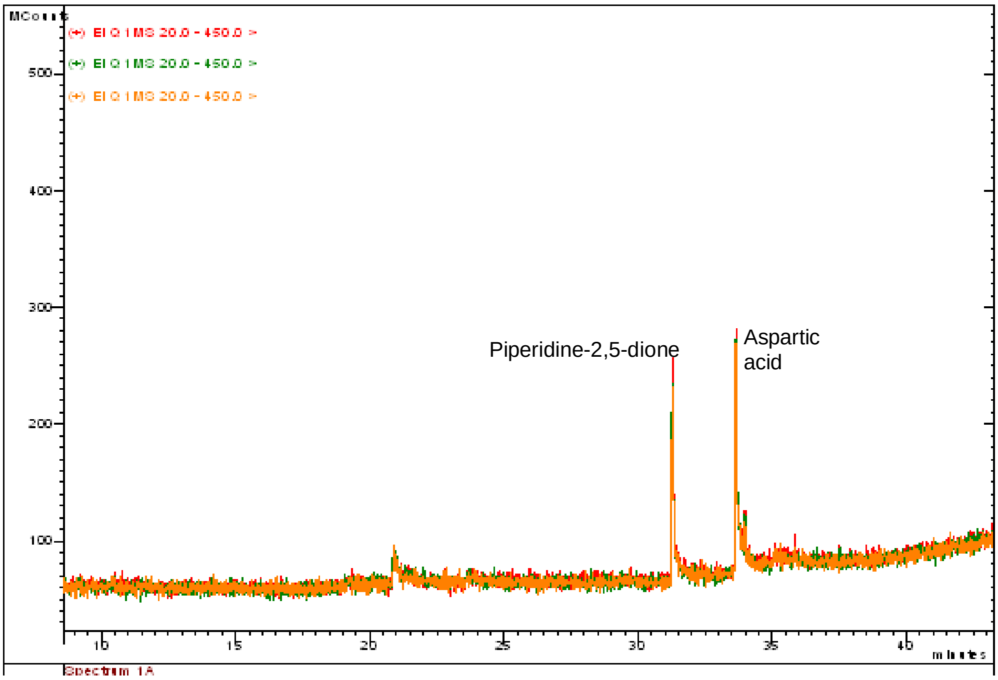

Figure 5.22: Expansion of Figure 5.21

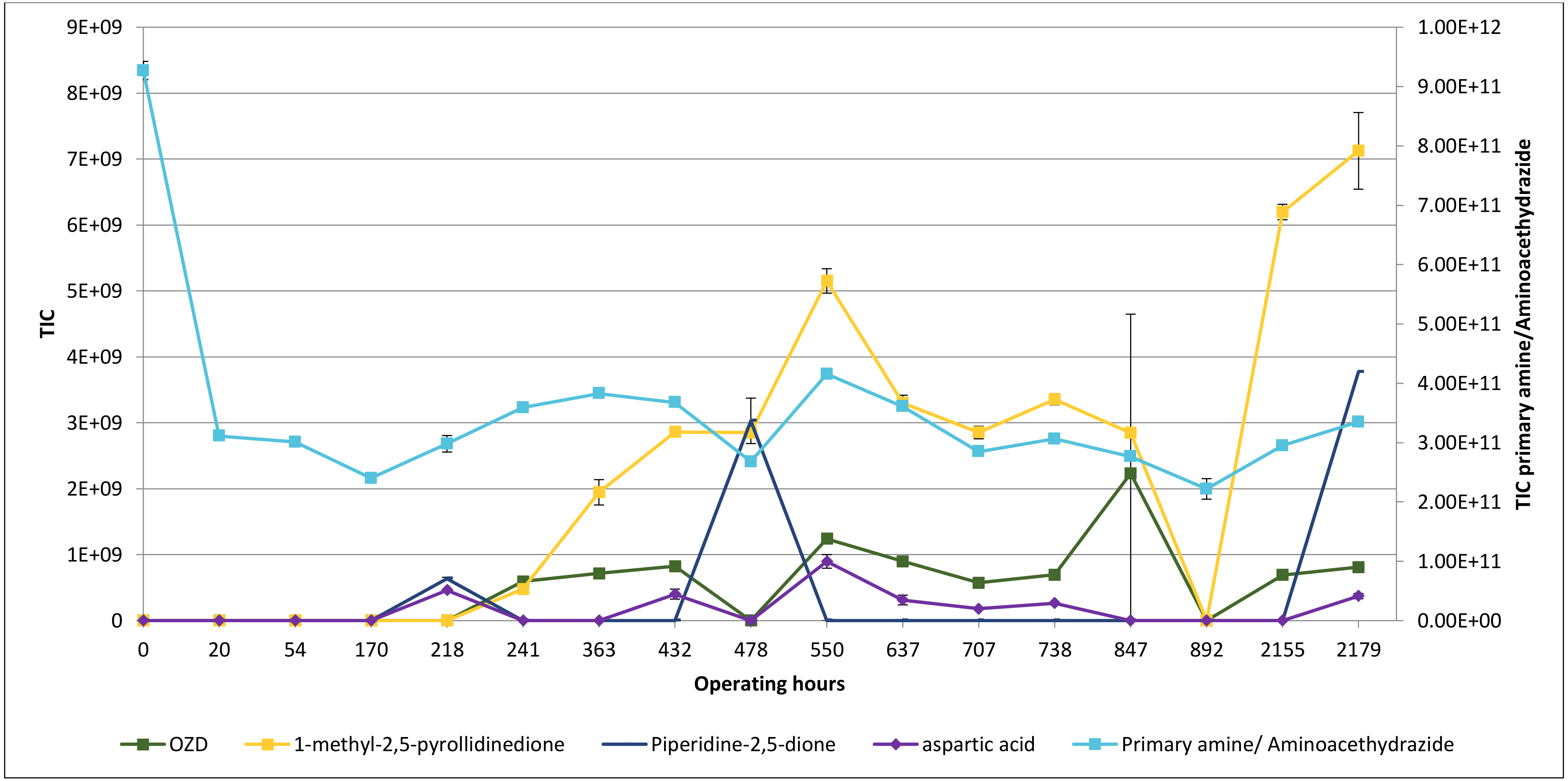

Figure 5.23: Continuous ion exchange samples GC-MS analysis

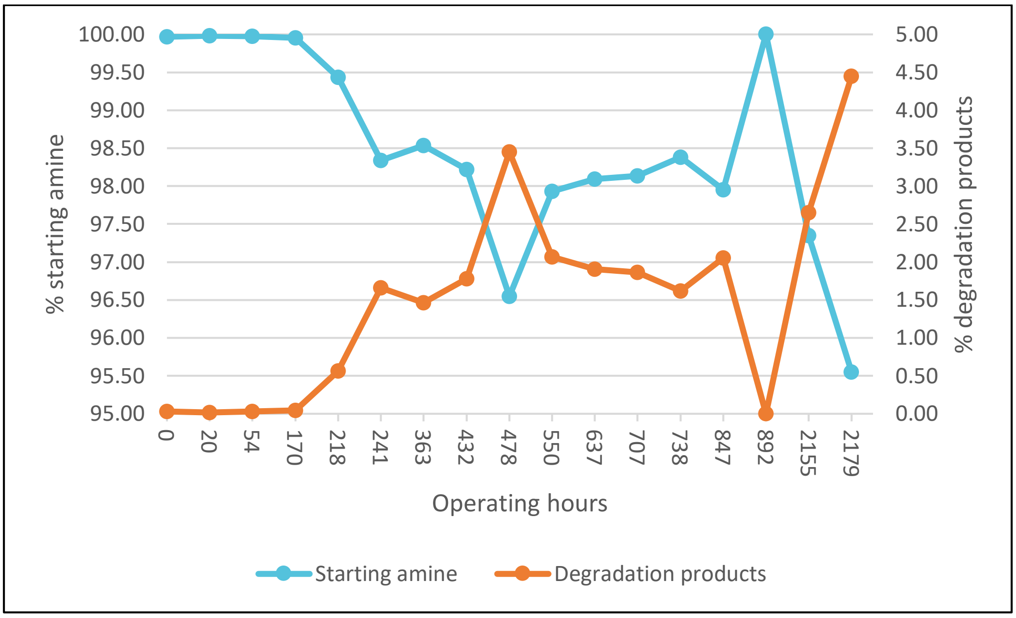

Figure 5.24: Per cent starting amine and degradation products remaining

Despite there being a number of solvent top-ups throughout the testing period in the pilot plant, this appears to have had little effect in terms of maintaining solvent levels as a number of dips are observed shortly after some of these top-ups occurred. However, the overall solvent loss is minimal.

Comparing these results to the single IX processed solvents, it is clear that maintaining low levels of metals in the solvent by using cationic IX resins from the start of operation is a highly effective way of minimising degradation and prolonging the lifetime of the solvent.

5.7 GC-FID of Continuous Ion Exchange Process

GC-FID analysis was carried out with the aim of using it as a quantitative measure of the degradation of the solvent. All standards and samples were prepared for analysis as described in Sections 3.4.1 and 3.4.2 and the analysis was carried out as described in Section 3.4.3.

5.7.1 GC-FID Analysis

As for the GC-MS analysis, the solvent which had been subjected to continuous IX was analysed by GC-FID. A typical GC-FID trace is shown in Figure 5.25 (further examples of GC-FID analysis of the continually IX solvent can be found in Appendix G). The only identifiable degradation products by GC-FID were HEA and OZD (peaks 1 and 2 respectively). The trends in their formation are shown in Figure 5.26 (error bars are shown to one standard deviation).

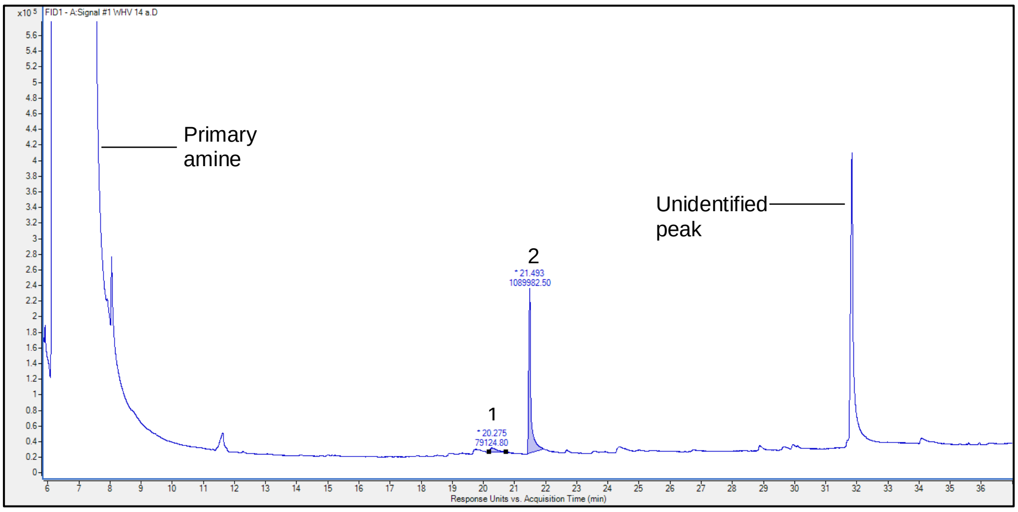

Figure 5.25: Typical GC-FID trace for continuous ion exchange sample

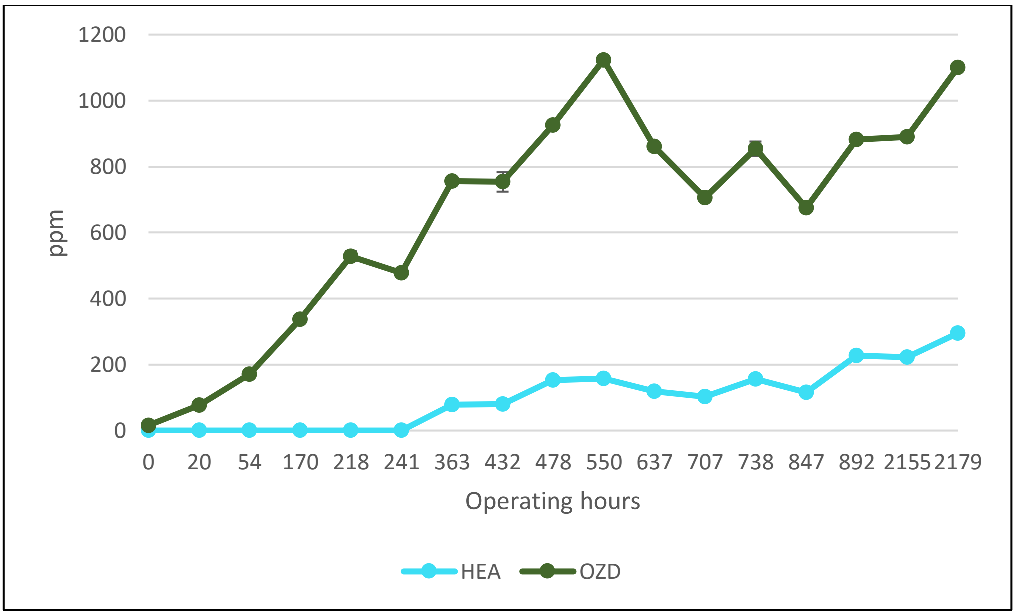

Figure 5.26: Continuous ion exchange GC-FID analysis

For both of the identified species the concentrations steadily increase throughout the 2179 hours of operation, although remain much lower than in the solvent which had not undergone IX. However, as the continually ion exchanged solvent was only operational for approximately half the time of the previous batch it is possible that this is the reason for the low levels of HEA and OZD. The level of OZD at 2179 hours is approximately 38 % that of the solvent before ion exchange. If the concentration continued to follow the same trend as observed in Figure 5.26 it would be a reasonable prediction that it would reach approximately the same levels by 4425 hours, therefore suggesting that the IX process has little effect on preventing the formation of OZD. In contrast to this, the level of HEA at 2179 hours is approximately 2.0 % that of the solvent before IX. This indicates that even if the concentration continues to increase if the solvent was operated for a longer time period, by 4425 hours the levels would be significantly lower than the batch which did not undergo IX at all. This suggests the removal of metals contributes to maintaining low levels of HEA.

Comparing the FID data to MS data (Figure 5.27, errors shown to one standard deviation) shows that MS is poor at detecting both HEA and OZD. This is further evidence that in order to identify all degradation products in the solvent it is necessary to use more than one analytical technique.

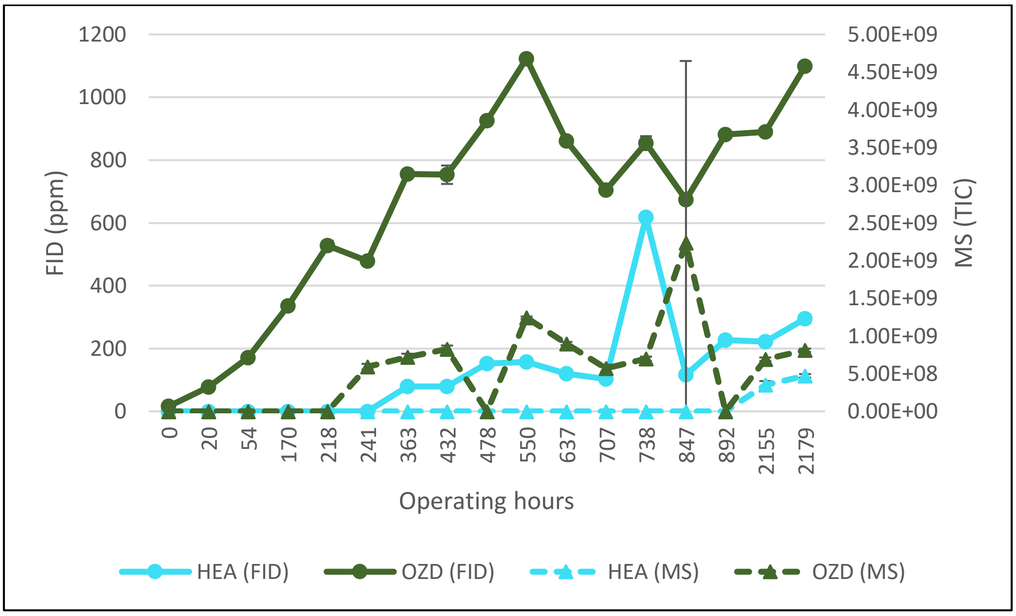

Figure 5.27: Correlation between FID and MS for continuous ion exchange

5.8 ICPMS of Continuous Ion Exchange Process

As discussed in Section 3.5 ICPMS is used to identify and quantify any metals present in the solvent. All standards and samples were prepared as described in Sections 3.5.3 and 3.5.4. Analysis was carried out as described in Section 3.5.5.

5.8.1 ICPMS Analysis

Figure 5.28 shows the ICPMS analysis of the primary amine solvent (all error bars are to one standard deviation) with Table 5-III detailing the values. It can be seen that the levels of all metals remain much lower than in the solvent which had not undergone IX, indicating that this process is a very effective method of proactively preventing corrosion. The low levels of iron observed are consistent with the lack of bicine identified by GC-MS or GC-FID.

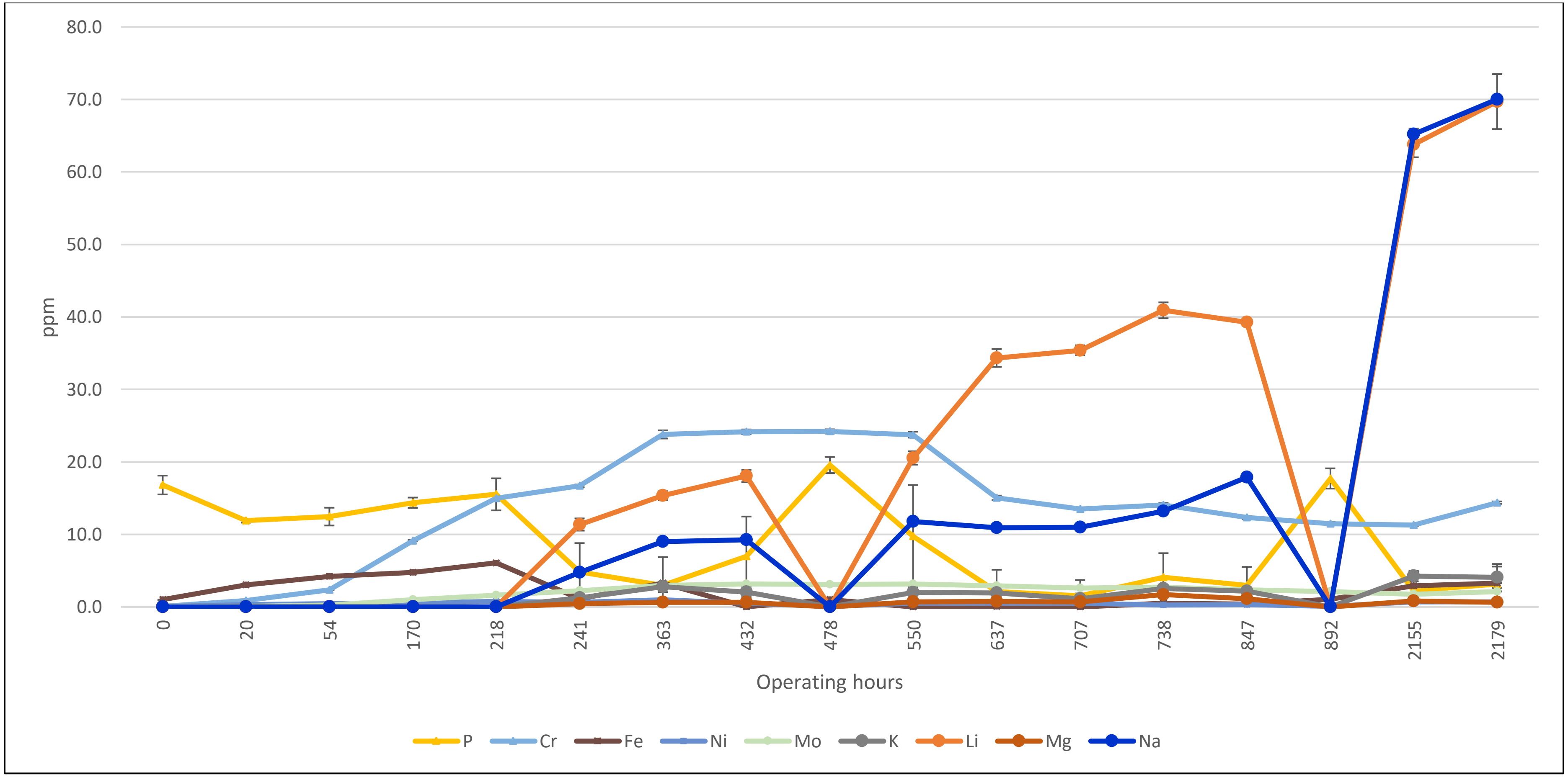

Figure 5.28: ICPMS of single amine, continuous ion exchange

Table 5-III: ICPMS of single amine, continuous ion exchange

Operating hours	P	Cr	Mn	Fe	Ni	Mo	K	Li	Mg	Na
0	16.8	0.1	0.0	1.0	0.0	0.0	0.0	0.0	0.0	0.0
20	11.9	0.9	0.1	3.0	0.3	0.1	0.0	0.0	0.0	0.0
54	12.5	2.4	0.1	4.2	0.4	0.3	0.0	0.0	0.0	0.0
170	14.4	9.1	0.1	4.8	0.5	1.0	0.0	0.0	0.0	0.0
218	15.5	15.0	0.1	6.1	0.7	1.6	0.0	0.0	0.0	0.0
241	4.9	16.7	0.0	1.1	0.6	2.3	1.3	11.4	0.5	4.8
363	3.0	23.8	0.1	3.3	1.0	3.0	2.8	15.3	0.6	9.0
432	7.0	24.2	0.0	0.1	0.5	3.2	2.1	18.1	0.6	9.2
478	19.6	24.2	0.0	1.0	0.1	3.1	0.0	0.0	0.0	0.0
550	9.8	23.8	0.0	0.0	0.5	3.1	2.0	20.5	0.7	11.8
637	2.1	15.1	0.0	0.1	0.5	2.9	1.9	34.3	0.7	10.9
707	1.5	13.5	0.0	0.0	0.5	2.6	1.1	35.4	0.7	11.0
738	4.1	14.0	0.0	0.5	0.3	2.7	2.6	40.9	1.7	13.2
847	3.0	12.3	0.0	0.4	0.3	2.3	2.2	39.3	1.2	17.9
892	17.7	11.5	0.0	1.0	0.1	2.1	0.0	0.0	0.0	0.0
2155	2.3	11.3	0.1	2.9	0.7	1.8	4.2	63.8	0.8	65.2
2179	3.2	14.4	0.1	3.3	0.7	2.1	4.1	69.7	0.6	70.0

5.9 IC of Continuous Ion Exchange Process

As discussed in Section 3.6 IC is used for the identification of heat stable salts. It is a qualitative analytical technique. Samples and standards were prepared for analysis as described in Sections 3.6.3, 3.6.4, 3.6.6 and 3.6.7. Analysis was carried out as described in Sections 3.6.5 and 3.6.8.

5.9.1 IC Analysis

5.9.1.1 Cation Analysis

A typical cation chromatogram for continuous IX process is shown in Figure 5.29 (further examples of cation analysis of the continually IX solvent can be found in Appendix H). Cation chromatography was found to be useful in the detection of calcium and potassium only (Figure 5.30), with all other cationic species below the limit of quantification of the instrument. Calcium was not observed in all samples, and in those in which it was detected the level remains low. Potassium appears to decrease once solvent operation began and appears to become almost steady, with a few anomalous results at 363 and 478 hours. The correlation in trends between the IC results and ICPMS results for potassium (Figure 5.31) is poor until approximately 432 hours operation. The IC results give much higher concentrations of potassium in all samples, suggesting that IC is more sensitive than ICPMS for this cation. This is further evidence that in order to fully understand solvent degradation it is necessary to use more than one analytical technique.

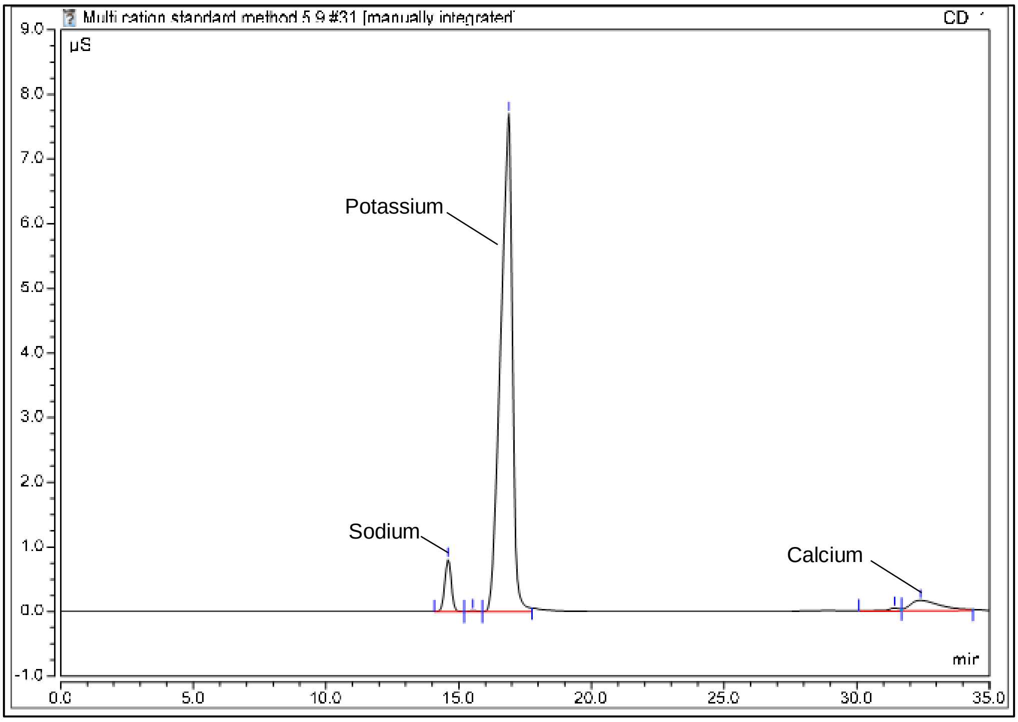

Figure 5.29: Typical cation chromatogram for continuous ion exchange process

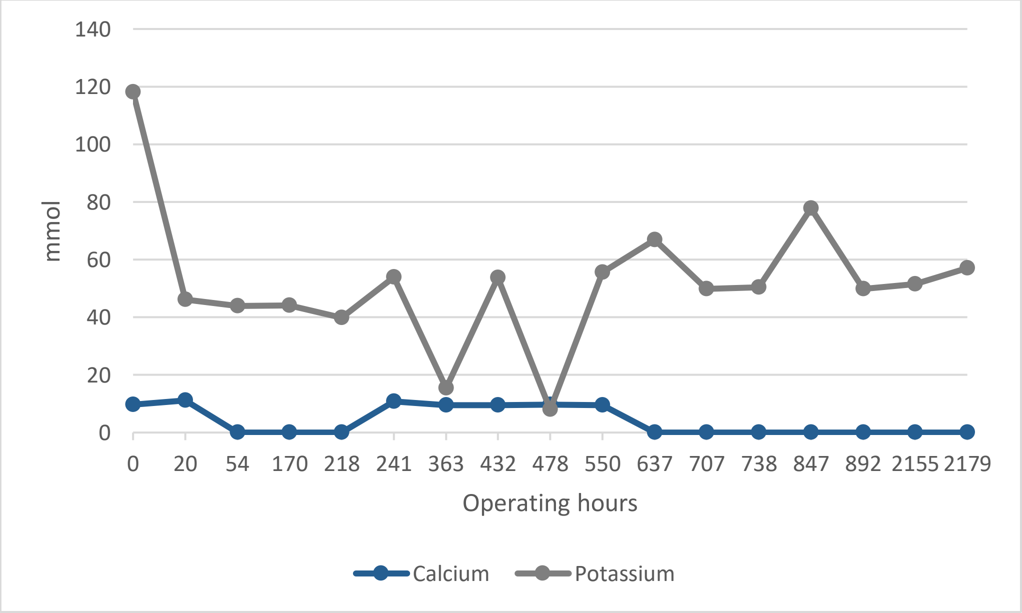

Figure 5.30: Cation analysis of continuous ion exchange

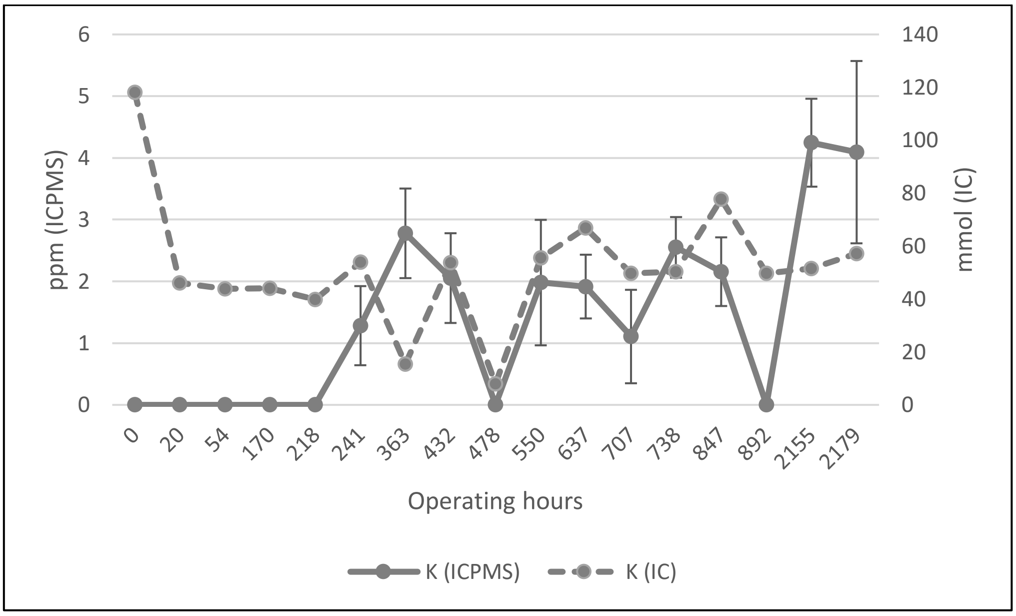

Figure 5.31: Correlation between ICPMS and IC for potassium

5.9.1.2 Anion Analysis

As for the single ion exchanged process samples, the solvent which continuously underwent this process was analysed by anion IC. A typical anion chromatogram is shown in Figure 5.32 (further examples of anion analysis of the continually IX solvent can be found in Appendix H). Figure 5.33 shows the effect this had on the HSSs. Acetate was not detected so is not shown on the graph.

From the graph it is clear that oxalate is the predominant HSS, although levels of all those detected are below 15 mmol, significantly lower than for the solvents before the IX process. Despite the continuous IX process only lasting for approximately half the time that the previous batch was operated for, the levels are still low. Oxalate has only reached approximately 20 % of the level before IX at roughly half as many hours, which suggests that if this continually ion exchanged batch was allowed to reach 4425 operating hours the level of oxalate would be less than half that of the solvent which had not experienced any ion exchange. This indicates that continuous IX is successful in minimising HSS formation.

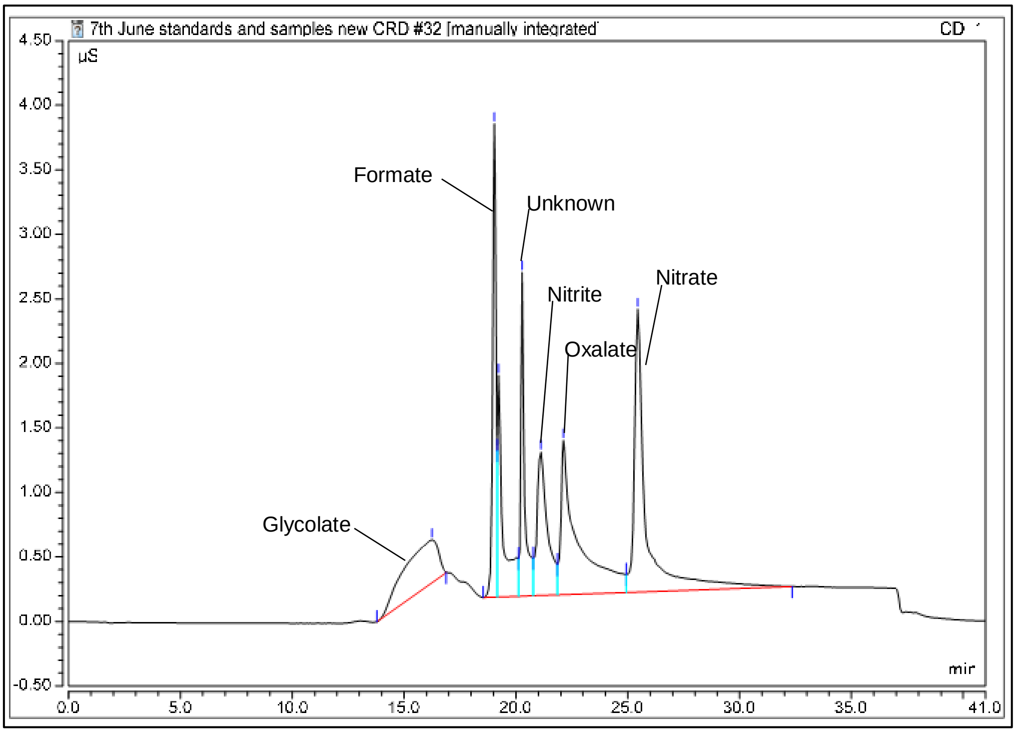

Figure 5.32: Typical anion chromatogram for continuous ion exchange process

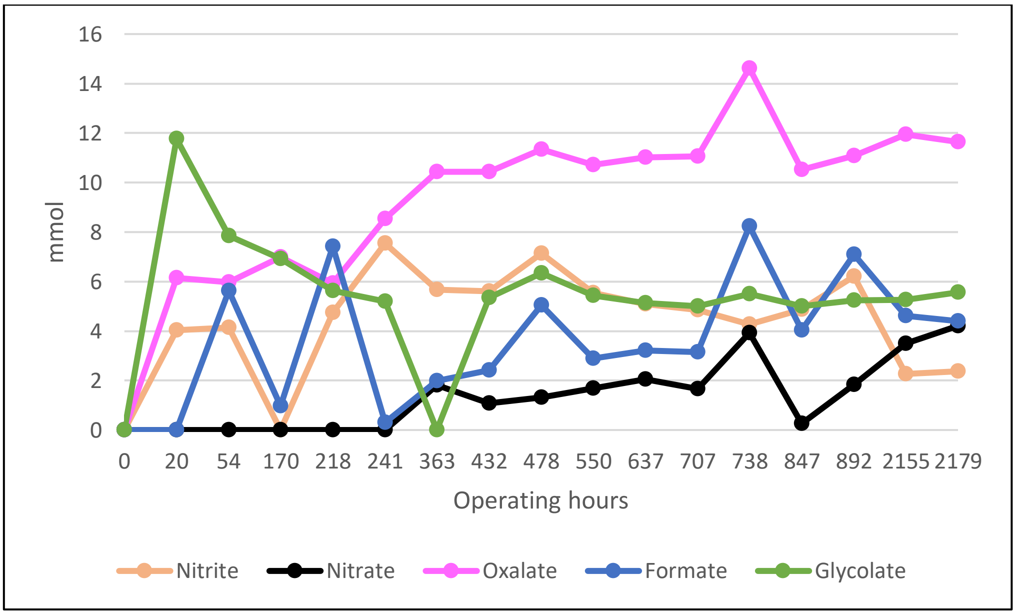

Figure 5.33: Anion analysis of continuous ion exchange

5.9.1.3 Amide Analysis

In order to analyse for formamide, oxamide, acetamide and glycolamide, the reaction with NaOH was carried out as described in Section 3.6.4. Any increase in carboxylic acid concentration between the two samples was considered to be amide that had been recovered in the form of carboxylic acid. Figure 5.34 shows the amide analysis for the continuous IX samples. Acetamide and glycolamide were not detected after treatment with NaOH so are not shown in the graph. As seen in the graph there was no increase in oxamide until 432 hours and there is only a small amount of formamide after 847 hours. This indicates that continuous IX is preventing the formation of these species.

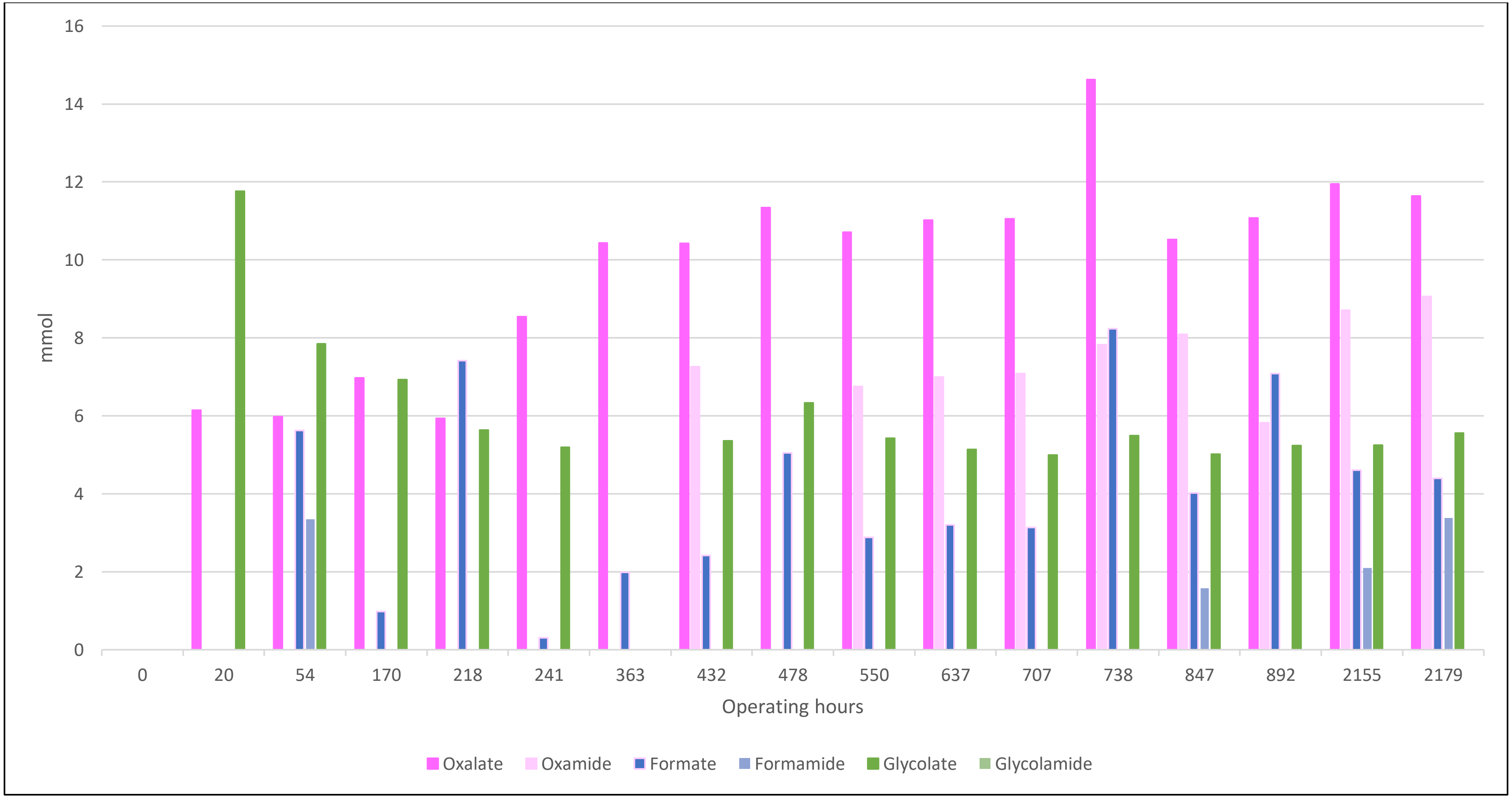

Figure 5.34: Amide analysis of continuous ion exchange

5.10 ^{13}C NMR

5.10.1 ^{13}C NMR Analysis of Primary Amine Solvent

^{13}C NMR analysis was carried out on a select few solvent samples, as detailed in Table 5-I. The ^{13}C NMR spectra are shown in Figure 5.35 to Figure 5.41 with peaks of interest listed in Table 5-IV to Table 5-X.

As previously discussed, the species observable by ^{13}C NMR spectroscopy are protonated amine, molecular amine, amine carbamate, carbonate and bicarbonate. The fast exchanging protons of the carbonate/ bicarbonate and molecular/ protonated amine make it impossible to distinguish between these species, resulting in their concentrations being reported together.

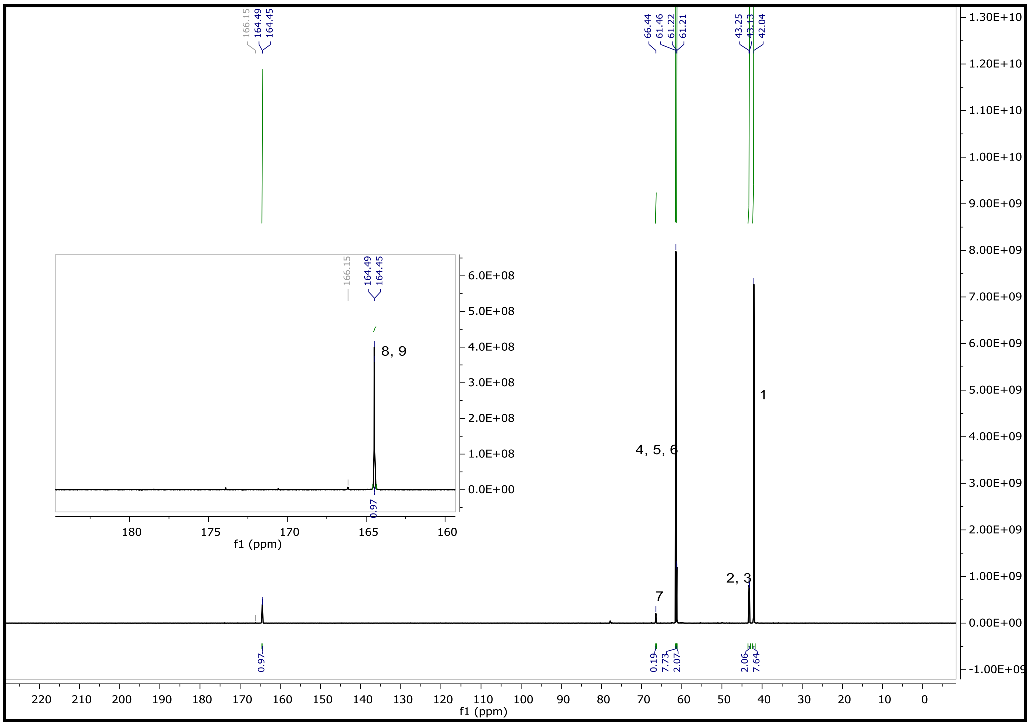

Figure 5.35: ^{13}C NMR spectrum, primary amine, 20 hours

Table 5-IV: Peaks of interest in Figure 5.35, single amine, 20 hours

Peak	δ (ppm)	Integration area (arbitrary units)	mg/ C	Assignment
1	42.04	7.64	48.25	Amine/AmineH$^+$ (next to NH_2)
2	43.13	2.06	13.01	Amine-carbamate (next to NH)
3	43.25			
4	61.21	2.07	13.07	Amine carbamate (next to OH)
5	61.22			
6	61.46	7.73	48.82	Amine/AmineH$^+$ (next to OH)
7	66.44	0.19	1.20	1,4-dioxane
8	164.45	0.97	6.13	Amine-carbamate (C=O)
9	164.49			

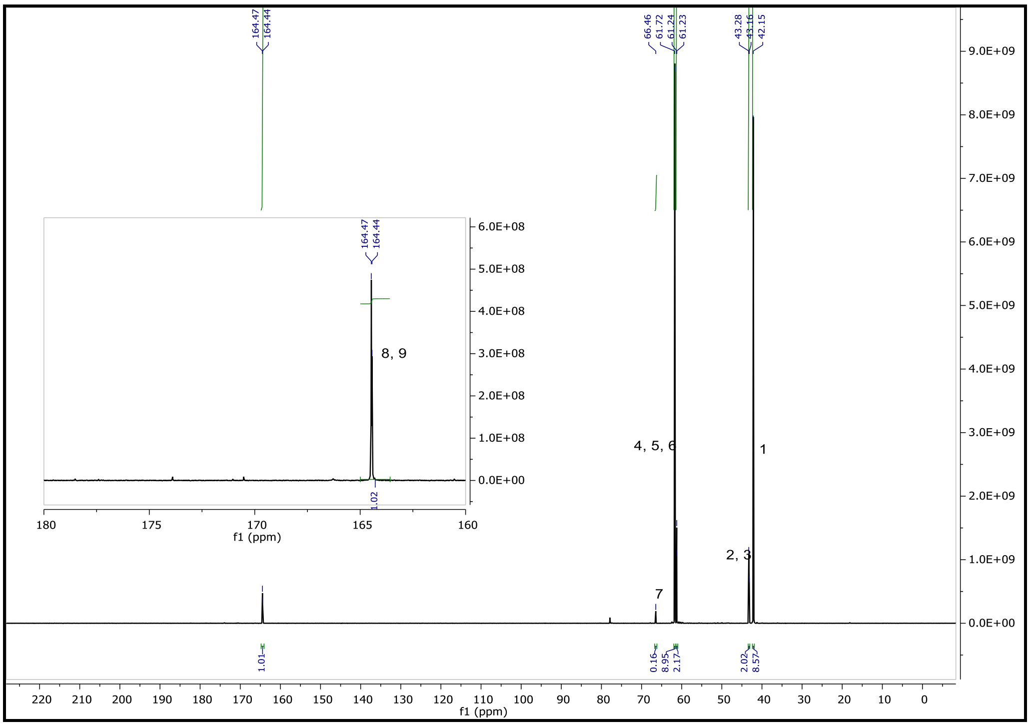

Figure 5.36: ^{13}C NMR spectrum, primary amine, 170 hours

Table 5-V: Peaks of interest in Figure 5.36, single amine, 170 hours

Peak	δ (ppm)	Integration area (arbitrary units)	mg/ C	Assignment
1	42.15	8.57	64.28	Amine/AmineH$^+$ (next to NH$_2$)
2	43.16	2.02	15.15	Amine carbamate (next to NH)
3	43.28			
4	61.23	2.17	16.28	Amine carbamate (next to OH)
5	61.24			
6	61.72	8.95	67.13	Amine/AmineH$^+$ (next to OH)
7	66.46	0.16	1.20	1,4-dioxane
8	164.44	1.02	7.65	Amine carbamate (C=O)
9	164.47			

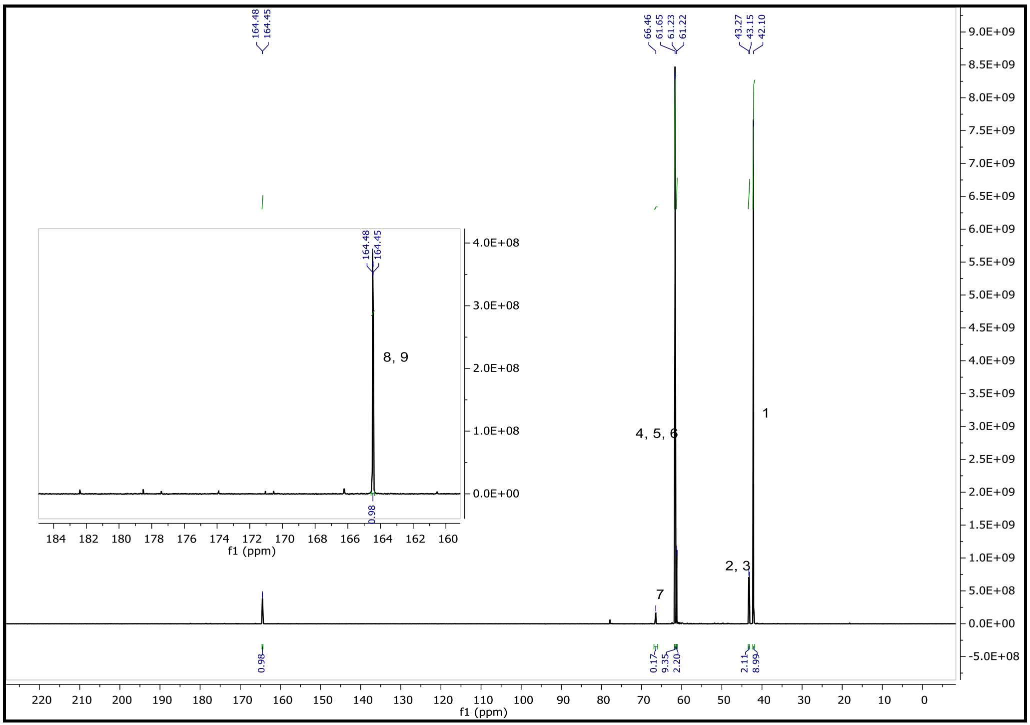

Figure 5.37: ^{13}C NMR spectrum, primary amine, 241 hours

Table 5-VI: Peaks of interest in Figure 5.37, single amine, 241 hours

Peak	δ (ppm)	Integration area (arbitrary units)	mg/ C	Assignment
1	42.1	8.99	63.46	Amine/AmineH$^+$ (next to NH$_2$)
2	43.15	2.11	14.89	Amine carbamate (next to NH)
3	43.27			
4	61.22	2.20	15.53	Amine carbamate (next to OH)
5	61.23			
6	61.65	9.35	66.00	Amine/AmineH$^+$ (next to OH)
7	66.46	0.17	1.20	1,4-dioxane
8	164.45	0.98	6.92	Amine carbamate (C=O)
9	164.48			

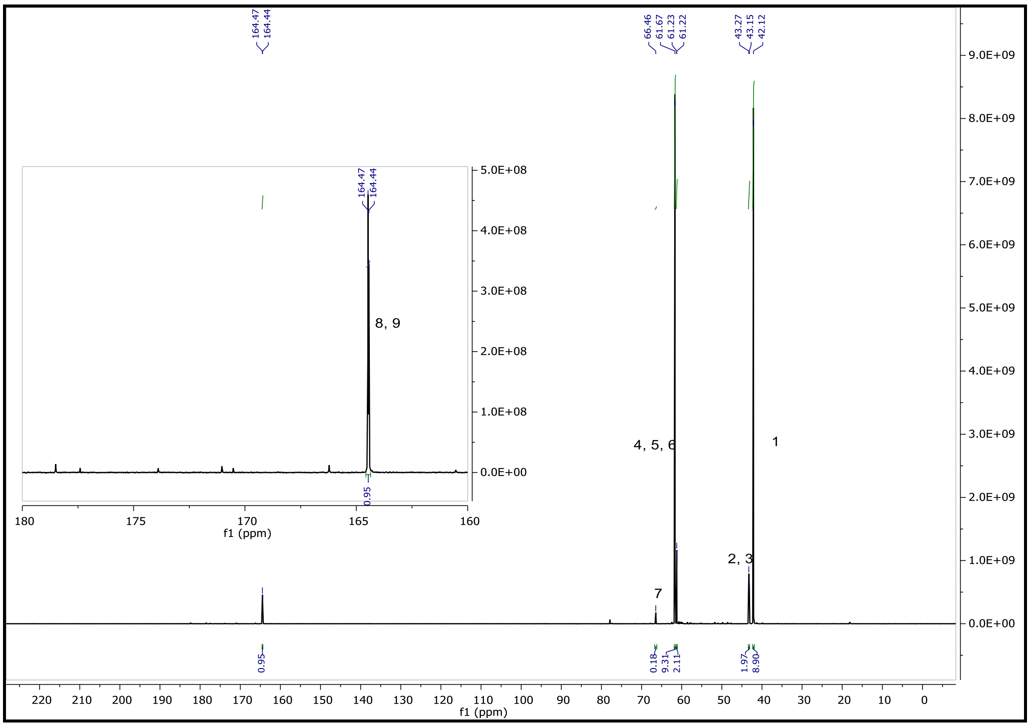

Figure 5.38: ^{13}C NMR spectrum, primary amine, 432 hours

Table 5-VII: Peaks of interest in Figure 5.38, single amine, 432 hours

Peak	δ(ppm)	Integration area (arbitrary units)	mg/ C	Assignment
1	42.12	8.9	59.33	Amine/AmineH$^+$ (next to NH$_2$)
2	43.15	1.97	13.13	Amine carbamate (next to NH)
3	43.27			
4	61.22	2.11	14.07	Amine carbamate (next to OH)
5	61.23			
6	61.67	9.31	62.07	Amine/AmineH$^+$ (next to OH)
7	66.46	0.18	1.20	1,4-dioxane
8	164.44	0.95	6.33	Amine carbamate (C=O)
9	164.47			

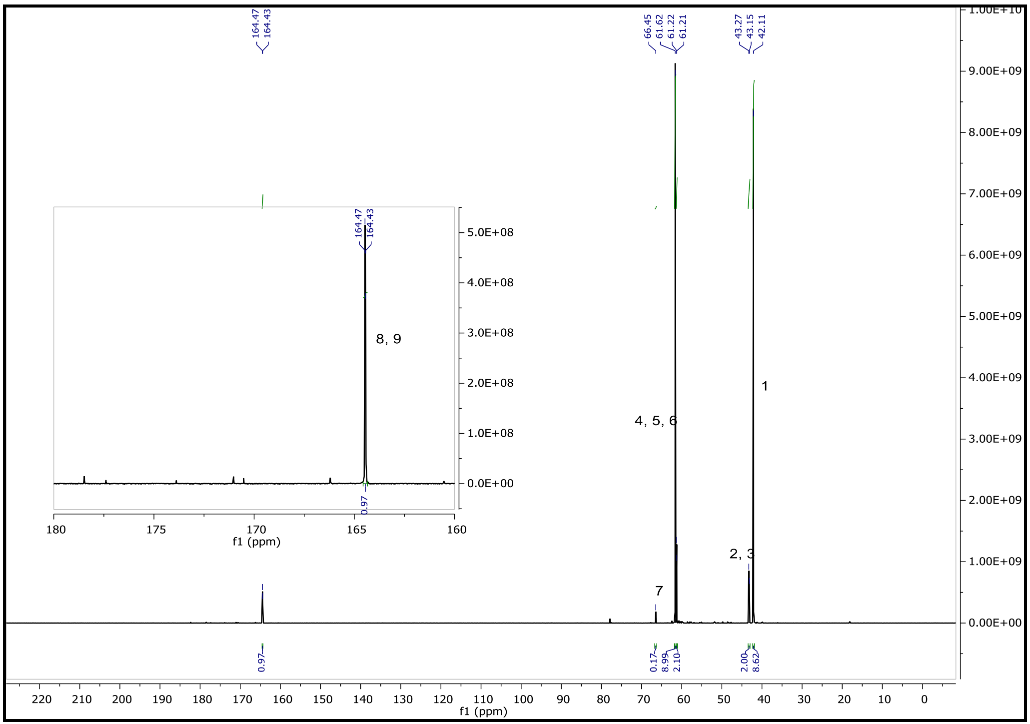

Figure 5.39: ^{13}C NMR spectrum, primary amine, 637 hours

Table 5-VIII: Peaks of interest in Figure 5.39, single amine, 637 hours

Peak	δ (ppm)	Integration area (arbitrary units)	mg/ C	Assignment
1	42.11	8.62	60.85	Amine/AmineH$^+$ (next to NH_2)
2	43.15	2.00	14.12	Amine carbamate (next to NH)
3	43.27			
4	61.21	2.10	14.82	Amine carbamate (next to OH group)
5	61.22			
6	61.62	8.99	63.46	Amine/AmineH$^+$ (next to OH group)
7	66.45	0.17	1.20	1,4-dioxane
8	164.43	0.97	6.85	Amine carbamate (C=O)
9	164.47			

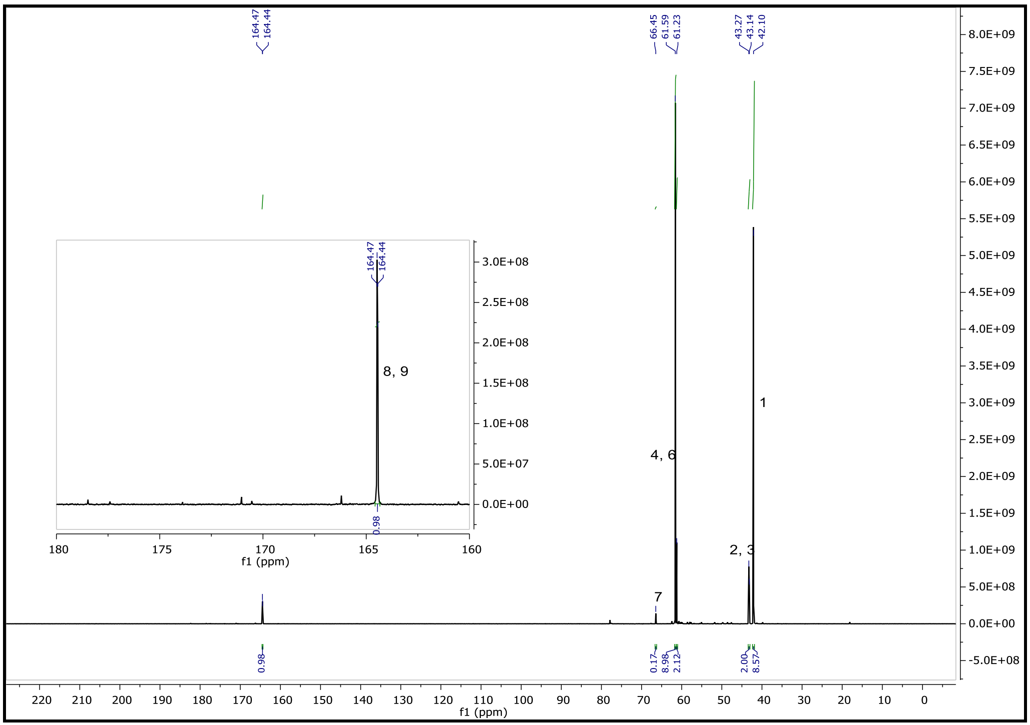

Figure 5.40: ^{13}C NMR spectrum, primary amine, 738 hours

Table 5-IX: Peaks of interest in Figure 5.40, single amine, 738 hours

Peak	δ (ppm)	Integration area (arbitrary units)	mg/ C	Assignment
1	42.1	8.57	60.49	Amine/AmineH$^+$ (next to NH_2)
2	43.14	2.00	14.12	Amine carbamate (next to NH)
3	43.27			
4	61.12	2.12	14.96	Amine carbamate (next to OH group)
6	61.59	8.98	63.39	Amine/AmineH$^+$ (next to OH group)
7	66.45	0.17	1.20	1,4-dioxane
8	164.44	0.98	6.92	Amine carbamate (C=O)
9	164.47			

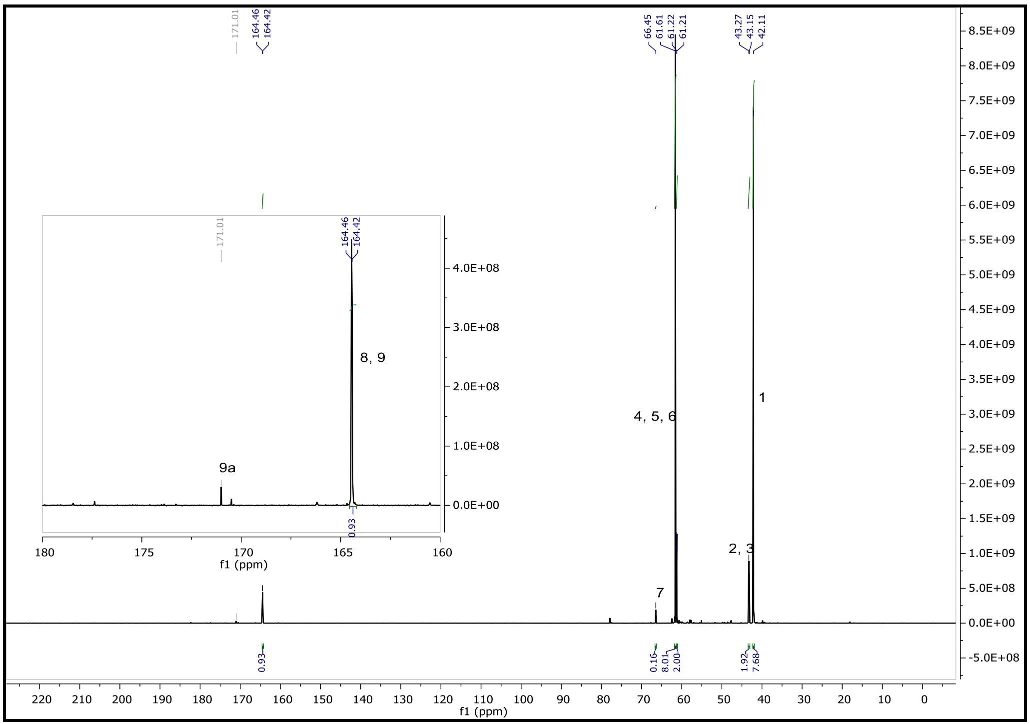

Figure 5.41: ^{13}C NMR spectrum, primary amine, 2155 hours

Table 5-X: Peaks of interest in Figure 5.41, single amine, 2155 hours

Peak	δ (ppm)	Integration area (arbitrary units)	mg/ C	Assignment
1	42.11	7.68	57.60	Amine/AmineH$^+$ (next to NH$_2$)
2	43.15	1.92	14.40	Amine carbamate (next to NH)
3	43.27			
4	61.21	2.00	15.00	Amine carbamate (next to OH group)
5	61.22			
6	61.61	8.01	60.08	Amine/AmineH$^+$ (next to OH group)
7	66.45	0.16	1.20	1,4-dioxane
8	164.42	0.93	6.98	Amine carbamate (C=O)
9	164.46			
9a	171.01	-		unknown

From the spectra above it is clear that the solvent is not heavily degraded. The majority of peaks correspond to amine/ amineH$^+$ as shown in Figure 5.42 below. The loading for all samples did not vary much (refer to Table 3-II), so the trends in levels of amine carbamate are expected to remain steady.[90] Similarly there is not much variation in the peak positions for the amine/ amineH$^+$ signals which indicates that the concentration of protonated amine remains steady at the given loadings.[90]

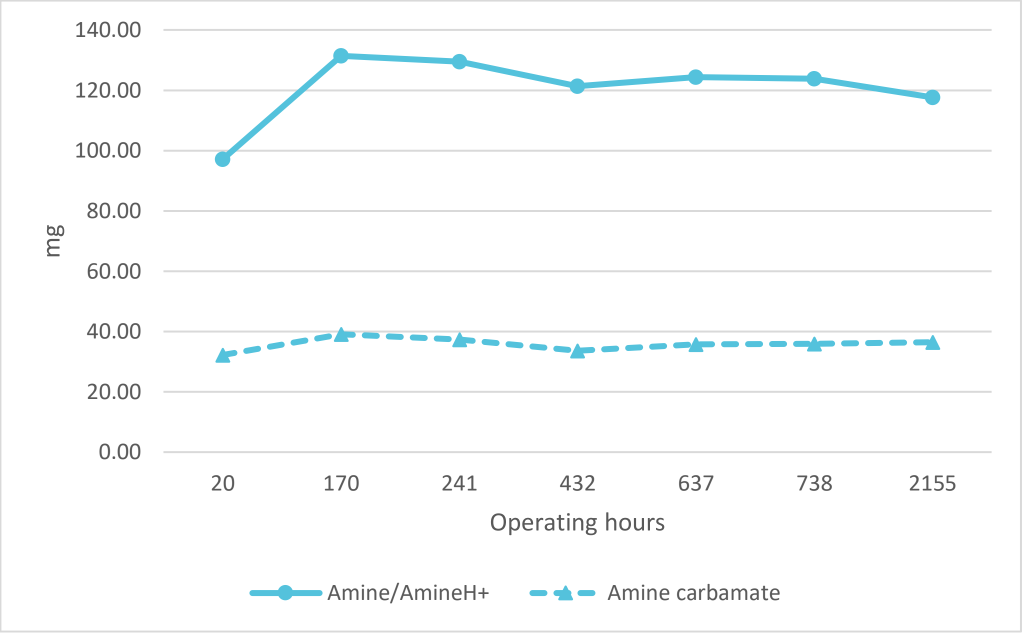

Figure 5.42: Speciation of amine in primary amine solvent

By converting the mg/ C to weight percent of amines and comparing this to the percent total amines in GC-MS analysis for the same samples it can be seen that the two analytical methods correlate fairly well in terms of amine remaining (Figure 5.43). It is also possible to study the loading of the solvent given the trend in carbamate levels- comparing these to the loadings given in Table 3-II there is a fairly good correlation between the values. This shows that ^{13}C NMR is suited to the rapid analysis of the extent of amine degradation.

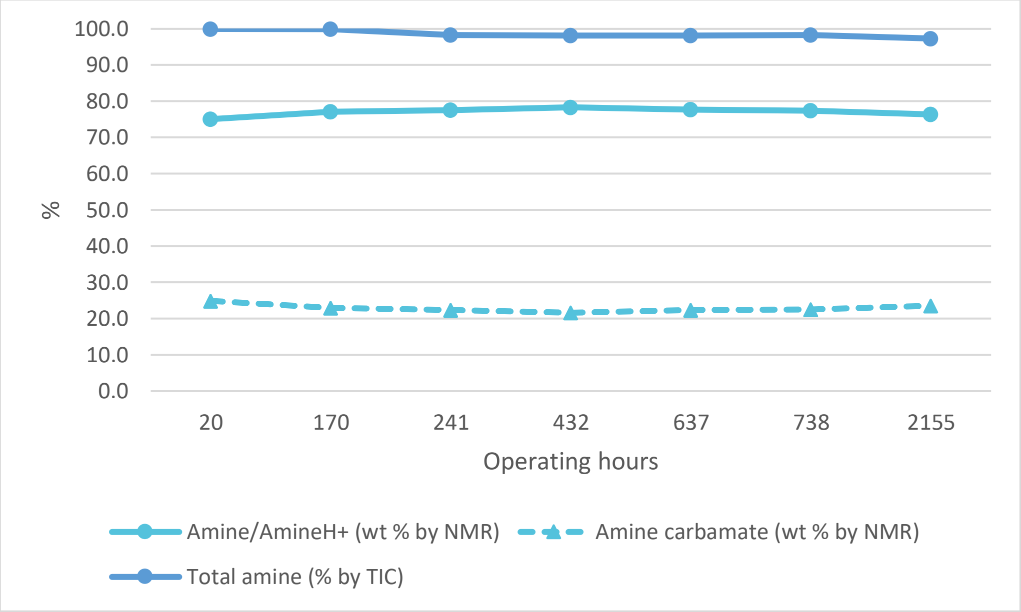

Figure 5.43: Correlation between GC-MS and ^{13}C NMR

5.11 Summary and Conclusions

The analysis of two batches of the same primary amine solvent, one subjected to once-through ion exchange and one which underwent continuous ion exchange, has been carried out. The following outcomes were found:

- GC-MS was used to semi-quantitatively identify several major degradation products. In the single ion exchanged samples, the major degradation products identified by GC-MS were OZD, piperidine-2,5-dione, N-(2-hydroxyethyl) succinimide, HEA, 1-methyl-2,5-pyrrolidinedione and remaining primary amine. In the continuously ion exchanged solvents the major degradation products identified were OZD, 1-methyl-2,5-pyrrolidinedione, piperidein-2,5-dione, aspartic acid and primary amine/ aminoacethydrazide which co-eluted from the column.
- GC-FID was required to detect bicine in the single ion exchanged samples, as this was not detected by GC-MS analysis. The general trend for OZD seen

in GC-MS is confirmed by GC-FID analysis, as levels increase in both analytical techniques.

- ICPMS was used to quantitatively analyse metals in solution. The predominant transition metal present was iron. There was good correlation between the levels of iron and bicine detected by ICPMS and GC-FID.
- Cation chromatography was only useful for the detection of calcium and potassium. Correlating the levels of potassium found by cation IC with those found by ICPMS showed that IC is more sensitive to detecting potassium. Overall, cation IC was not particularly effective in this work and ICPMS is more suited to the accurate determination of dissolved metals.
- Anion chromatography was used to qualitatively analyse the levels of HSSs in the solvents. Oxalate was the predominant HSS, although levels were significantly lower than for the solvents before the ion exchange process. Despite the continuous ion exchange process only lasting for approximately half the time that the previous batch was operated for, the levels were still low. Oxalate only reached approximately 20 % of the level before ion exchange at roughly half as many hours, which suggests that if this continually ion exchanged batch was allowed to reach 4425 operating hours the level of oxalate would be less than half that of the solvent which had not experienced any ion exchange. This indicates that continuous ion exchange is successful in minimising HSS formation.
- ^{13}C NMR has been proved to be a rapid analytical technique to indicate the extent of degradation in the solvents. Comparing the data from GC-MS analysis with ^{13}C NMR analysis shows there is fairly good correlation between levels of starting amine and amine/ amineH^{+} identified by ^{13}C NMR. However, this is to be treated cautiously as the relatively short experimental time means that the integration of the peaks will not be as accurate as the GC-MS analysis.

- Continuous ion exchange has been shown to be an effective way of proactively preventing degradation of the solvent and corrosion in the plant.

Chapter 6: Corrosion

6.1 Introduction

This chapter describes the electrochemical corrosion testing which was carried out on a sample of cast 316 stainless steel (SS) from the pilot plant in North West Europe in order to investigate the link between corrosion and solvent degradation. The component from which the steel sample was removed had been shown to be vulnerable to corrosion in the pilot plant.

The effect of metals in amine solutions has been discussed previously in Section 2.3.4. In order to investigate how the level of solvent degradation and other process parameters effects corrosion of stainless steel, a sample of steel from the hot lean pipe after the stripper and before the lean/ rich heat exchanger in the pilot plant was tested in both clean and degraded solvent, both with and without CO_2/ air being purged into the solutions.

All electrochemical testing was carried out as detailed in Section 3.8.3 unless otherwise stated herein. For interpretation of the graphs, Figure 3.2 is reproduced here.

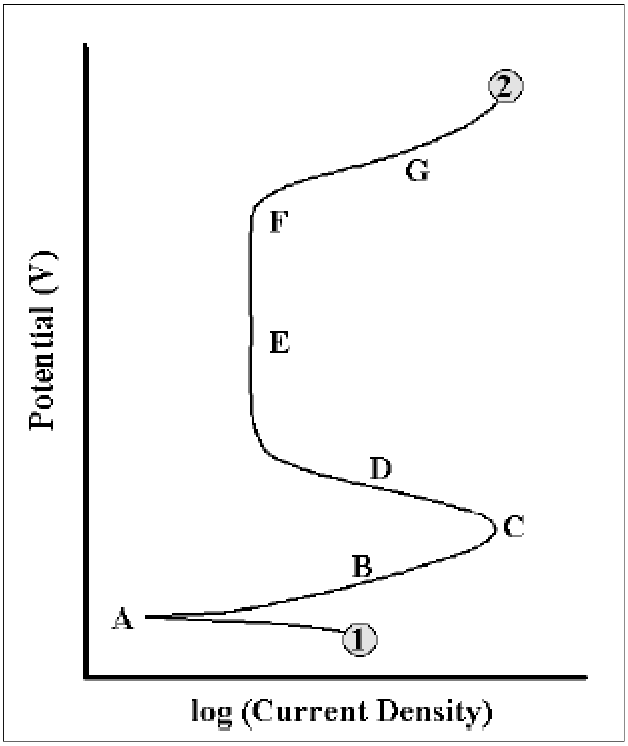

Figure 3.2: Theoretical anodic polarisation scan[89]

A) This is the E_{oc}, the potential at which the sum of the anodic and cathodic currents is zero.

B) The active region- oxidation of the metal is the dominant reaction taking place.

C) This point is the passivation potential, E_{pp}.

D) As the potential increases above the E_{pp} value the current density decreases until a low, passive current density is reached.

E) This is the passive region, where the low, passive current density is seen.

F) As the potential continues to become increasingly positive, a value is reached at which the applied current rapidly increases (region G). This is usually due to a localised breakdown of the passivity, known as pitting.

6.2 Stainless Steel in Clean Amine Solvent

The first analysis was carried out in clean amine solvent at 40 °C for a total of 672 hours. The steel was then re-polished (as described in Section 3.8.2) and the temperature was increased to 80 °C for a further 672 hours. Figure 6.1 shows the effect of increasing the temperature on the polarization behaviour of the SS 316. Although the current density is higher at 80 °C than at 40 °C (which indicates a higher dissolution rate of the metal into the solution) there was little difference in the corrosion of the steel at each temperature.[95]

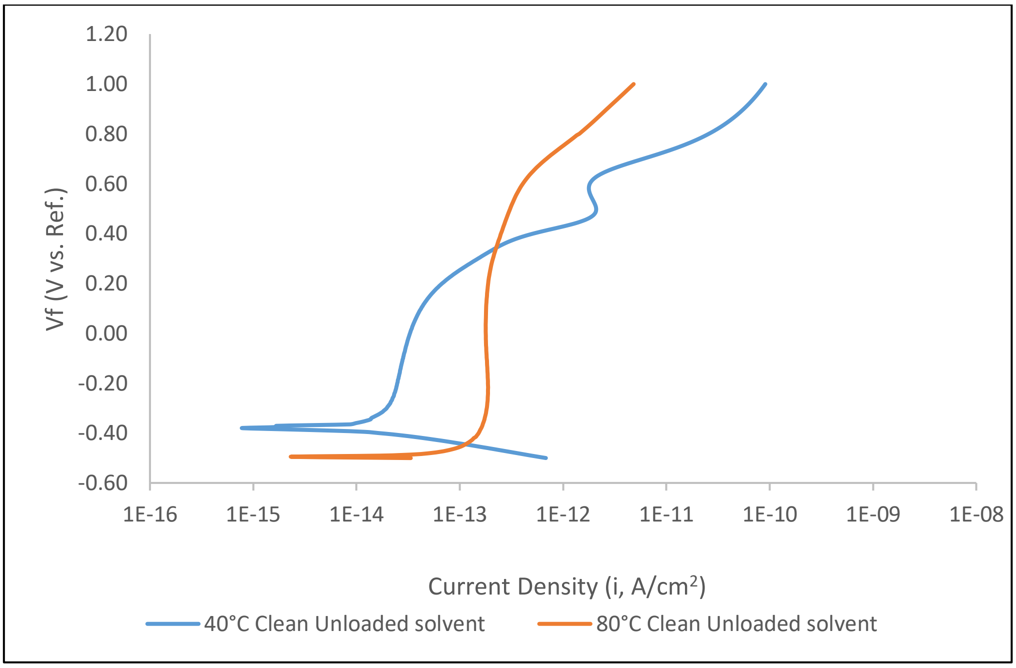

Figure 6.1: Potentiodynamic curves of SS 316 in clean unloaded amine solvent at different temperatures

6.2.1 Effect of Loading

The steel was then re-polished and a new batch of clean solvent was tested for 672 hours at 40 °C with the addition of CO_2 loading (0.17 mol CO_2/ mol amine). Loading was achieved by sparging CO_2 into the solvent at a rate of 0.20 L/ min for 24 hours. After this time, CO_2 was purged over the top of the solution to maintain loading. Titration against 1 M HCl was carried out in order to calculate the amine concentration and the loading of the solvent. By titrating to an end point of pH 7.0 and then to a second end point of pH 4.0 it is possible to calculate these values using Equation 6.1 and Equation 6.2, where M_w is the molecular weight of the amine.

$$\frac{(Eq./kg\ @\ pH\ 4.0)x\ M_w}{100} = wt\ \%\ amine$$

Equation 6.1

$$\frac{(Eq./kg\ \ @\ pH\ 4.0) - (Eq./kg\ @\ pH\ 7.0)}{(Eq./kg\ \ @\ pH\ 4.0)} = mol\ CO_2/mol\ amine$$

Equation 6.2

The steel was then re-polished and the temperature was increased to 100 °C for 480 hours. At this temperature the Ag/ AgCl reference electrode was moved to be external to the reaction vessel and connection was maintained via a salt bridge. This was done because the higher temperature is not compatible with the reference electrode.

The effect of loading the solvent with CO_2 was minimal. Figure 6.2 and Figure 6.3 show the effect of CO_2 loading on SS 316 corrosion behaviour in clean amine solution. Figure 6.2 shows the potentiodynamic curves at 40 °C and those for 80-100 °C are shown in Figure 6.3. Increasing the carbon loading did not change the characteristics of the curves for either temperature. The curve at 40 °C shifted to a higher current density indicating a higher metal dissolution rate, and the point at which the curve begins to passivate (passivation potential, E_{pp}) is at a lower potential for the unloaded solution which indicates that the cathodic protection was easier in lean solutions.[95] At 100 °C the curve not only moved to a higher current density but also to a slightly higher E_{OC} when loaded (-325 mV compared to -486 mV). The difference indicates that CO_2 loading at 40 °C has less impact on the corrosion of SS 316 than at 80-100 °C.[95] Even at the higher temperature the effect of carbon loading is rather insignificant.

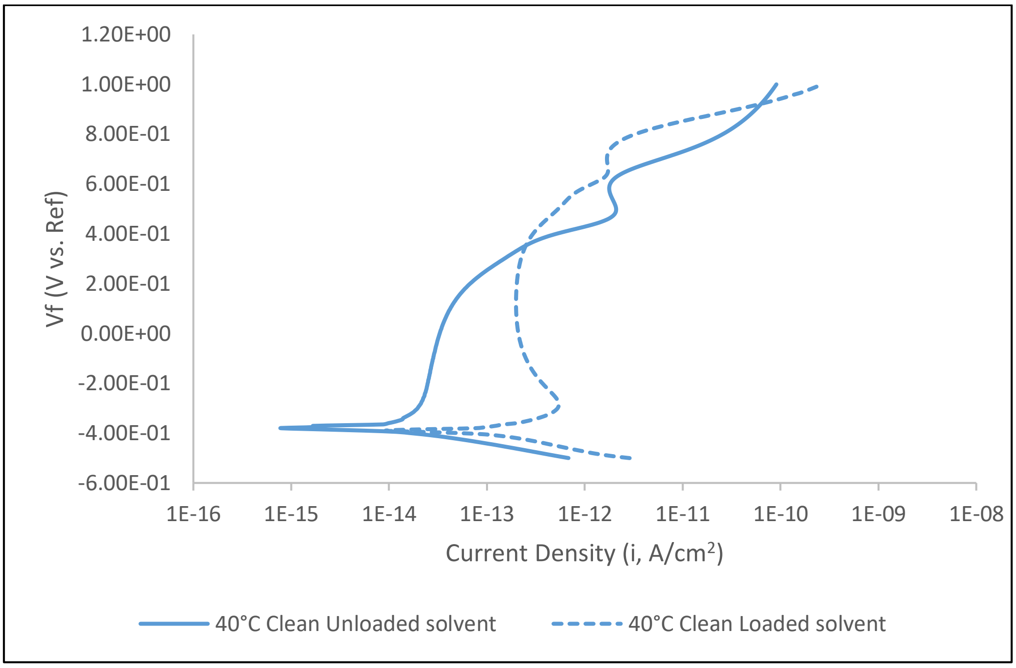

Figure 6.2: Potentiodynamic curves of SS 316 in clean unloaded and loaded amine solvent at 40 °C

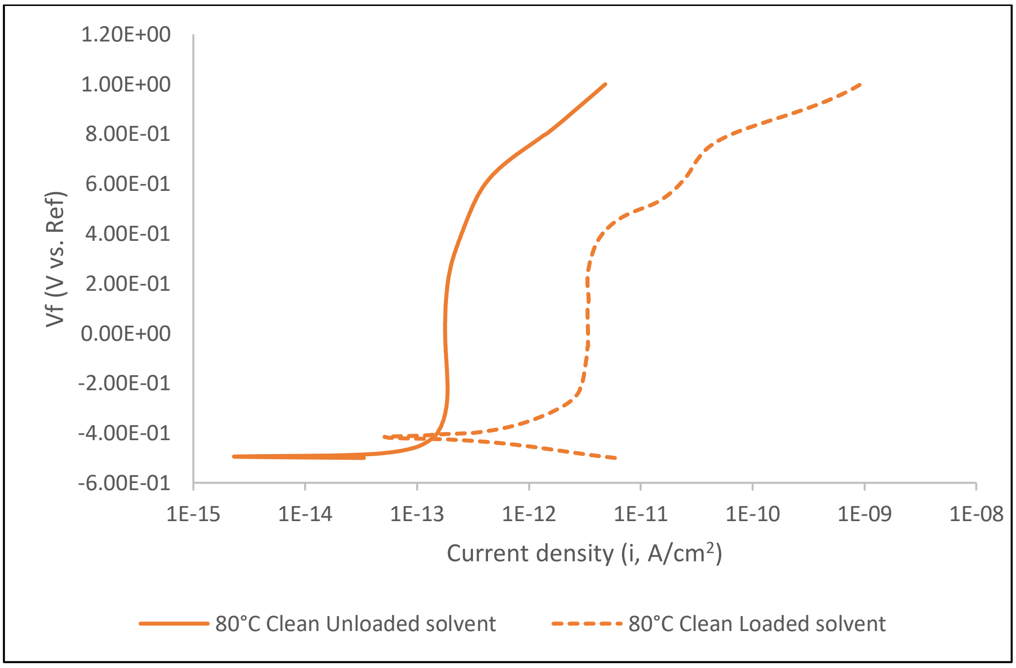

Figure 6.3: Potentiodynamic curves of SS 316 in clean unloaded and loaded amine solvent at 80-100 °C

6.2.2 Effect of Loading and Air

The same sample of SS 316 was re-polished and then tested in a new batch of clean amine, while loaded with CO_2 and with air purging into the system in order to study the effects of oxygen on corrosion. This was done at both 40 °C and 100 °C, ramping the temperature between these two values and carrying out a potentiodynamic scan at every 10 °C increase in temperature. Figure 6.4 shows the potentiodynamic curves for the two temperature limits. As the temperature was increased, the E_{OC} decreased and the current density increased. This indicates more corrosion at higher temperatures than at lower ones. The presence of air in the system appears to have increased the corrosion compared to when the solvent was only loaded with CO_2.

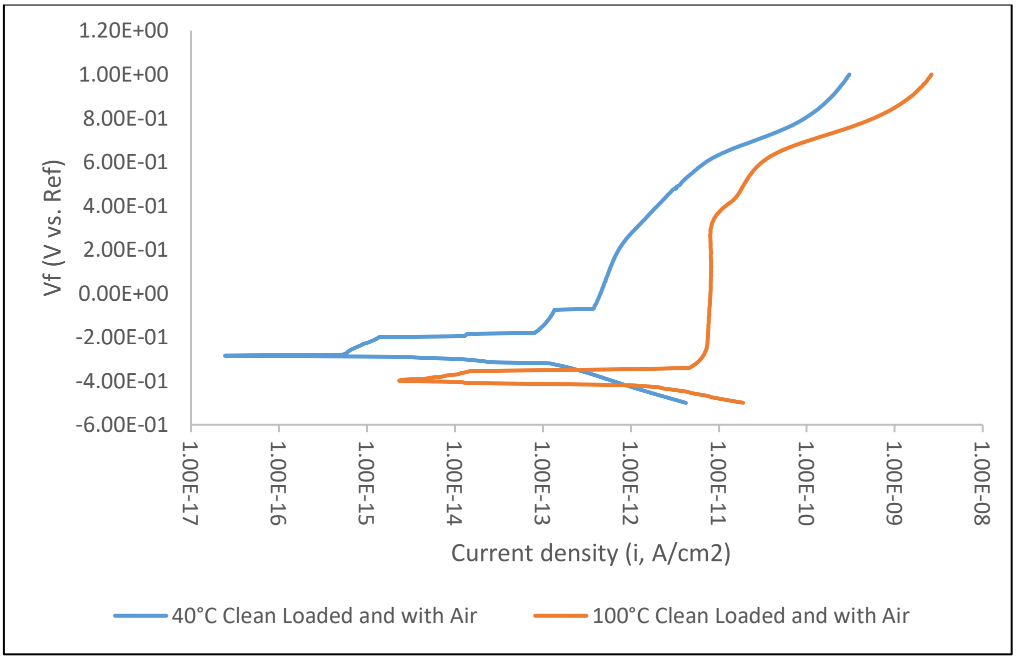

Figure 6.4: Potentiodynamic curves of SS 316 in clean, loaded solvent with air at 40 °C and 100 °C

6.3 Stainless Steel in Degraded Amine Solvent

In order to investigate the effect of degraded solvent on SS 316, the same analysis as above (Section 6.2.2) was carried out, ramping the temperature from 40 °C to 100 °C and returning to 40 °C. Potentiodynamic scans were performed every 10 °C change of temperature. The SS 316 was re-polished and then was tested in the amine solvent which had not undergone ion exchange (see Chapter 5), both at 40 °C and 100 °C. As there had been little change in the steel with the clean amine solvent, for this investigation the tests were carried out over 168 hours.

Figure 6.5 shows the effect of CO_2 and air at 40 °C and 100 °C. The current density at each temperature is similar in both cases, but the E_{oc} at 100 °C is lower than at 40 °C. Similar to the tests run in clean solvent, as the temperature is increased, the E_{OC} decreased and current density increased. This indicates more passivation at the lower temperature.[95] When the system returned to 40 °C, re-passivation of the steel was observed as can be seen from the reduction in current density at the second 40 °C scan.

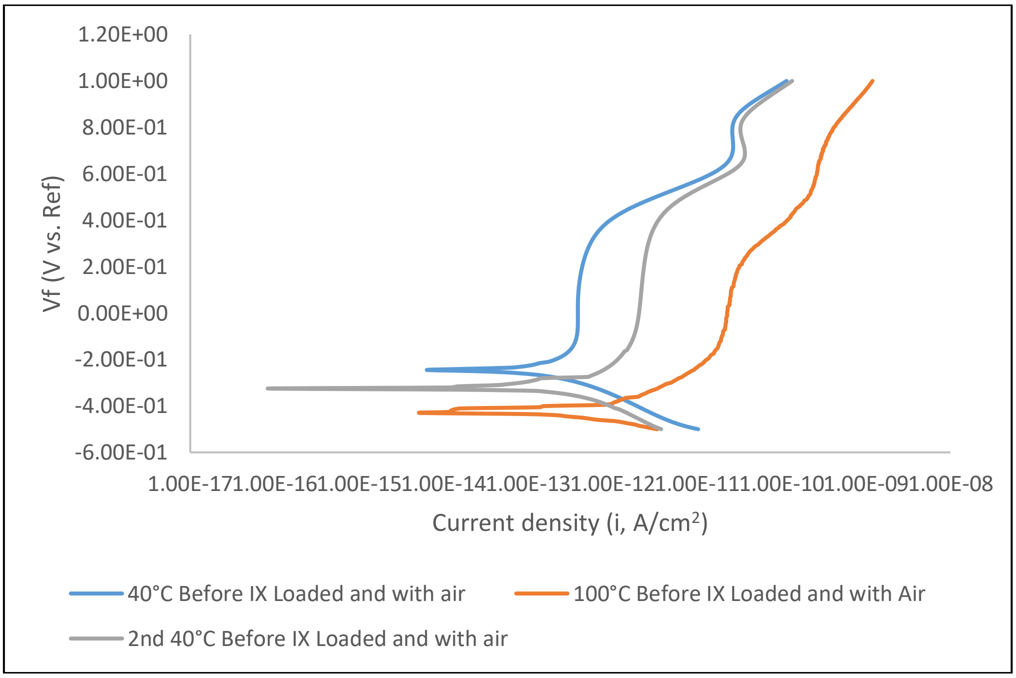

Figure 6.5: Potentiodynamic curves of SS 316 in degraded amine, loaded and with air, at 40 °C and 100 °C

6.4 Stainless Steel in De-ionised Water

In order to test whether the properties observed in the above analyses were specific to the amine solvent, the previous test was repeated in de-ionised (DI) water. There was no passivation at either temperature, as shown in Figure 6.6. This suggests that the corrosion effects observed in previous tests are due to the amine rather than the water in the solvent.

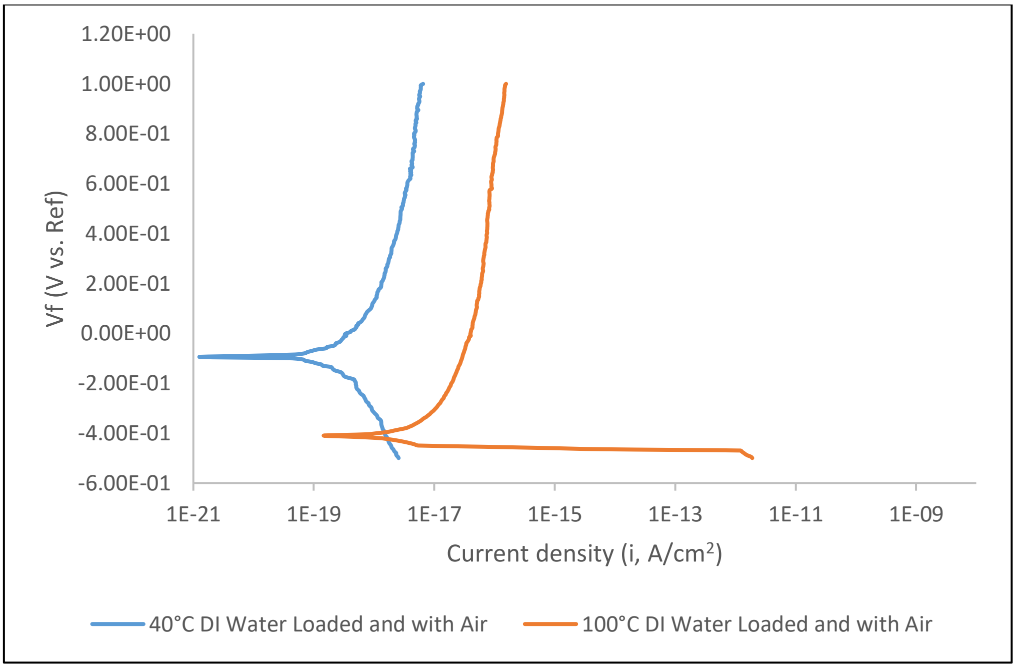

Figure 6.6: Potentiodynamic curves of SS 316 in DI water, loaded and with air at 40 °C and 100 °C

6.5 Summary and Conclusions

Electrochemical testing was used to investigate the corrosion behaviour of both clean and degraded amine solvents at different temperatures both loaded and unloaded, and with and without air. The results show that corrosion only increases when there is air (therefore oxygen) present in the system, but is still negligible at lower temperatures. The trend was the same in both clean and degraded solvent. This work was carried out at atmospheric pressures similar to those found in the absorber column, but the higher pressure found in the stripper column may have an impact on corrosion behaviour. In the pilot plant there was evidence that this cast steel corroded at higher pressures and temperatures, therefore there is much more scope for the use of electrochemical testing to investigate solvent corrosion than was covered in this work.

Chapter 7: Conclusions and Recommendations for Future Work

7.1 Summary of Conclusions and Novelty of Research

Whilst there have been a number of studies into lab scale amine degradation, few have investigated this phenomenon at pilot plant scale. Previous studies used individual analytical techniques to investigate amine degradation. While these offered some insight into the behaviour of amine solvents when used for post-combustion carbon capture, the work presented here has investigated the use of multiple analytical techniques and correlated the data in order to build a more comprehensive overview of how amine solvents behave at pilot scale.

In this work both single and blended amine solvents were investigated. The use of both GC-MS and GC-FID allowed identification and quantification of both major and trace degradation products such as OZD, bicine and N-(2-hydroxyethyl) succinimide.

Both ICPMS and cation chromatography were used to study the metals present in degraded solvents. Comparing the data from these techniques showed that while ICPMS was able to quantify the level of metals, cation chromatography was found to be ineffective. Therefore, ICPMS is the preferred technique for cation analysis. Anion chromatography was used to successfully identify and quantify heat stable salts.

^{13}C NMR spectroscopy was used to investigate the extent of amine degradation. It was shown that this can be used to give a rapid measure of the proportion of remaining amine in the solvent compared to the level of degradation products. This data was correlated with the results from GC-MS which showed ^{13}C NMR to be a valuable technique in the study of amine degradation.

This work has also shown that continuous cation exchange to remove metals was an effective technique to mitigate amine degradation and corrosion in the plant.

Solvents which were subject to continuous ion exchange had significantly lower levels of degradation products than those which were not ion exchanged. This suggests that a simple way of prolonging solvent lifetime is to run the solvent through cationic ion exchange resins throughout its operation.

Electrochemical testing was used to investigate the corrosion behaviour of both clean and degraded amine solvents at different temperatures, similar to those which would be observed in a pilot plant. The results showed that corrosion only increases when there is air (therefore oxygen) present in the system, but it is still negligible at low temperatures. This was shown to be true for both clean and degraded solvent.

To the best of the authors knowledge this work presents for the first time a study using multiple analytical techniques to characterise degraded amine solvents from pilot plants. The work shows that in order to gain a comprehensive understanding of amine degradation at pilot scale it is necessary to use several analytical techniques in combination with one another. ^{13}C NMR spectroscopy has proven a rapid analytical technique which provides an overview of solvent degradation. This work demonstrates that the applied analytical methods have the potential (with further study) to offer a reliable and rapid method to accurately monitor solvent degradation both at pilot and commercial scale.

7.2 Recommendations for Future Work

While this work has shown the potential for using several analytical techniques to characterise degraded amine solvents there is the potential for more work to be done.

- There are several degradation products which were not identified in this work. It would be interesting to investigate these further, perhaps with other analytical methods such as Liquid Chromatography Mass Spectroscopy (LC-

MS), and to further establish any possible links between these products and corrosion within the system.

- The amine solvents analysed in this work were all unloaded, therefore it would be of interest to analyse loaded amine solvents for degradation products. This would provide insight into the solvent behaviour in the stripper side of the amine scrubbing system which may again lead to links with corrosive solvent behaviour.
- It would be interesting to calculate rates of oxidative and thermal degradation for both loaded and unloaded solvents. It would be necessary for more accurate measurement to be carried out in order to quantify the degradation products so that the calculated rates can be accurately reported. This could be achieved by on-line monitoring of the solvent, for example, on-line ^{13}C NMR measurements.
- It was shown that electrochemical testing was useful for investigating the corrosive effects of the solvents. It would be of interest to use this technique for further analysis, for example increasing the pressure and temperature to mimic those conditions found in the stripper column. It would also be of interest to apply the corrosion testing to the pilot plant while operational so that real-time analysis can occur. This would provide more detailed information on how the solvent is effecting the plant equipment on a day-to-day basis, and vice- versa.
- To further understand the corrosion behaviour of steel in amine systems, it may be of benefit to use scanning electron microscopy (SEM) to study the surface of the steel when passivation is seen. This would allow a better understanding of the nature of the passive films which form and breakdown leading to localised pitting.
- The link between metals and degradation products is still not fully understood, despite the continuous ion exchange process proving to be

effective at minimising degradation by removing metals in solution. By investigating the effect of certain metals ions in solution it would contribute greatly to the understanding of corrosion and solvent degradation. This could also be extended to doping the solvent with known amounts of degradation products to investigate which, if any, have the greatest effect on corrosion.

Appendices

Appendix A. Standards for GC-FID Analysis

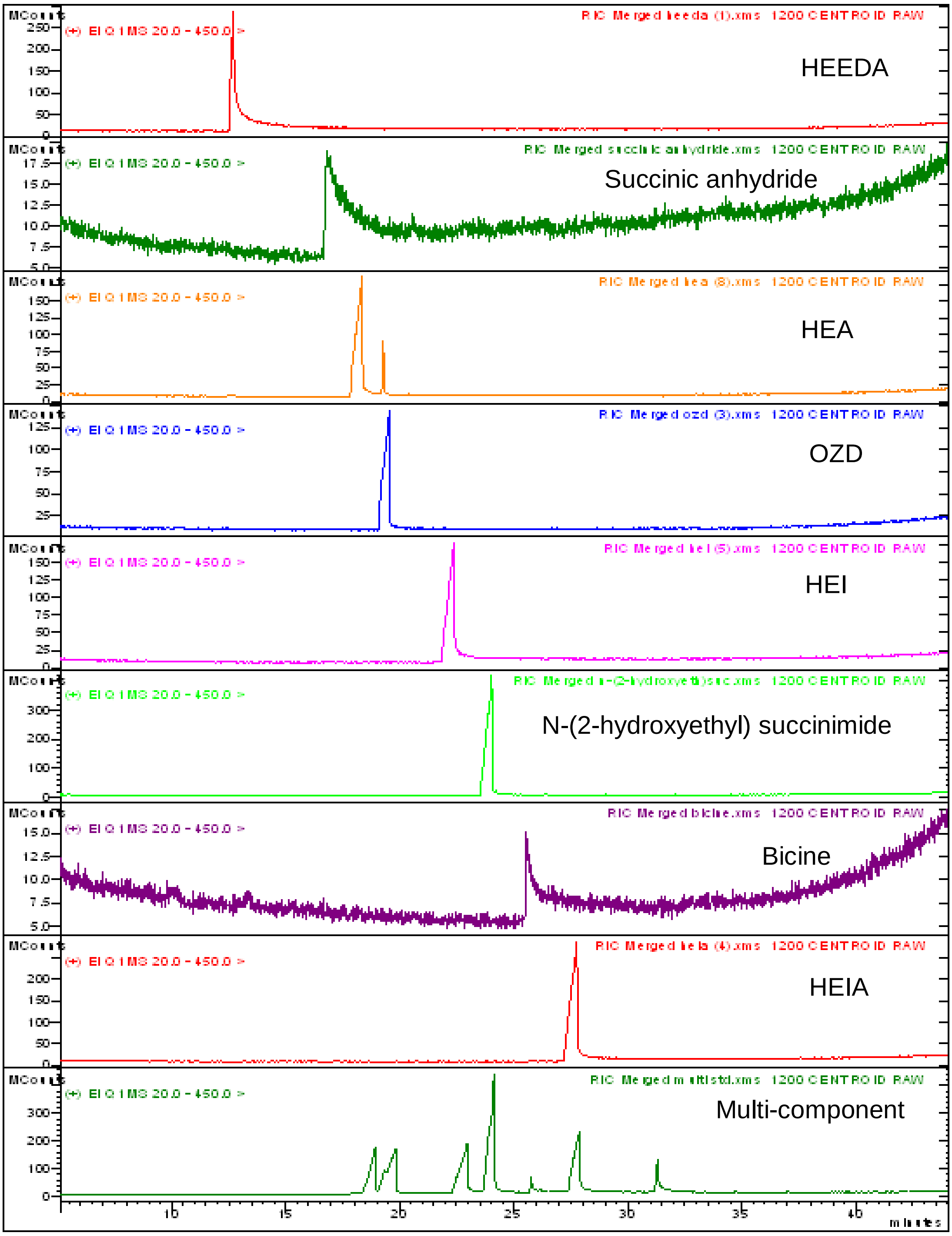

Figure A. 1: GC-MS chromatograms of standards used in identification of GC-FID species

From top to bottom: HEEDA; succinic anhydride; HEA; OZD; HEI; N-(2-hydroxyethyl) succinimide; bicine; HEIA; multi-compound standard

Appendix B. GC-MS Analysis of Degraded Primary Amine from UK Pilot Plant

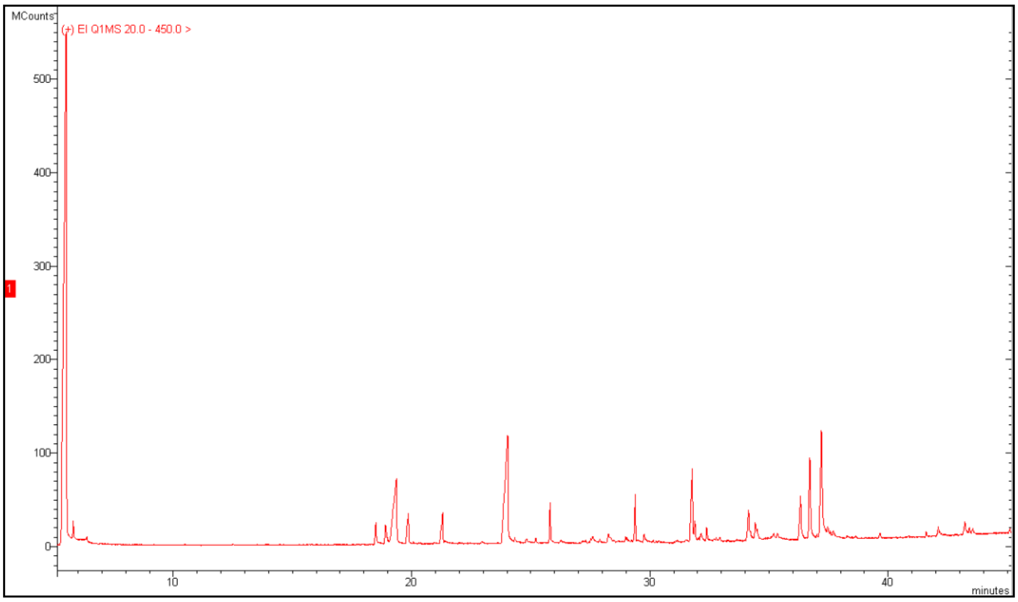

Figure B. 1: Heavily degraded primary amine solvent from UK pilot plant

Appendix C. GC-MS Chromatograms of Blended Amine Solvent

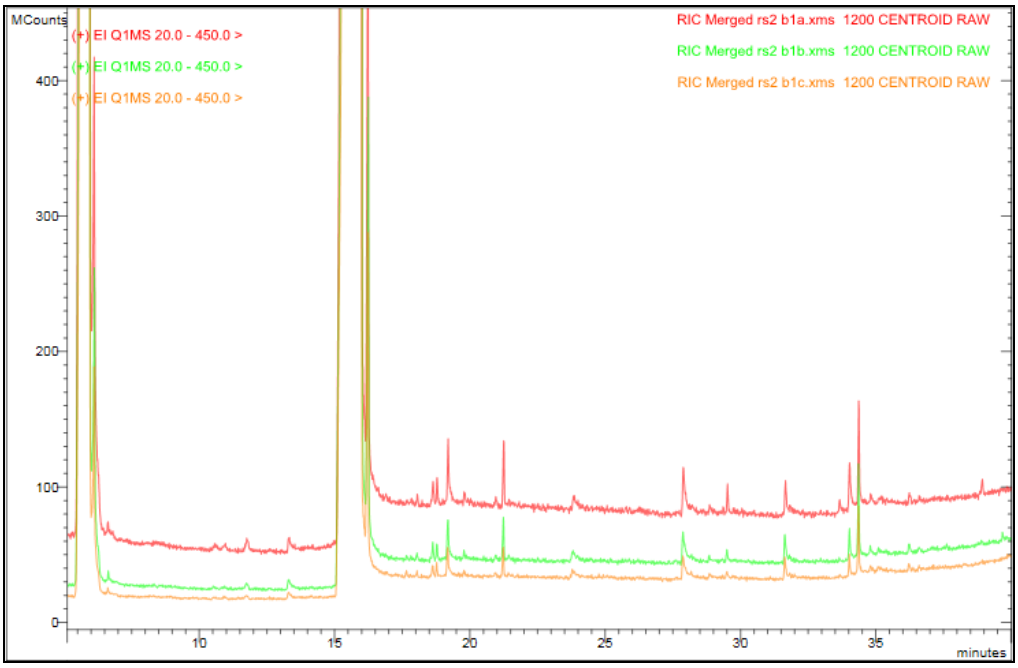

Figure C. 1: GC-MS of blended amine after 195 hours operation

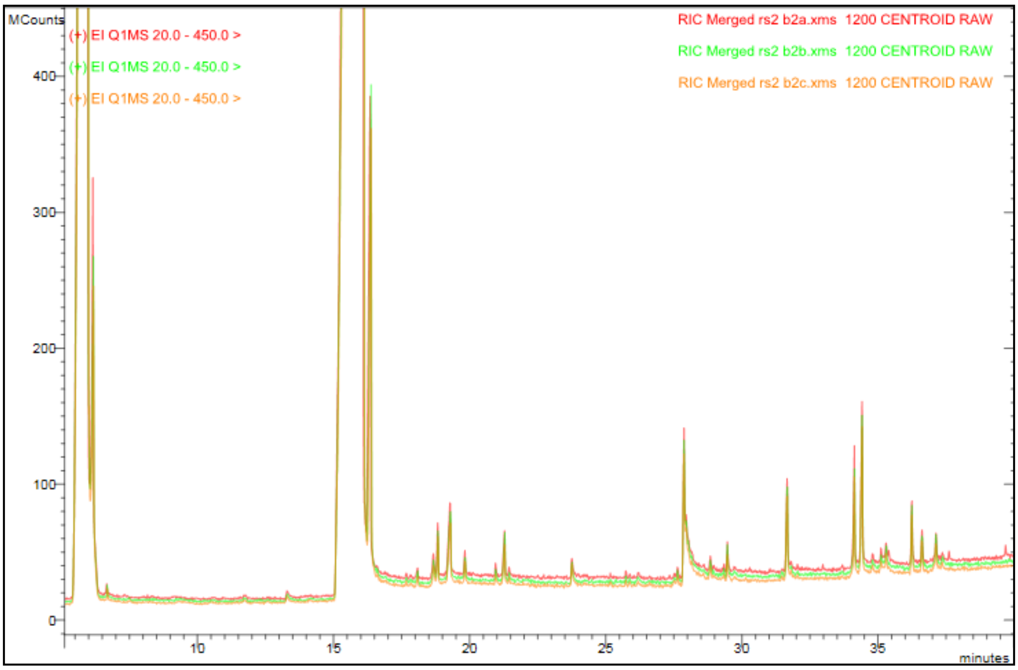

Figure C. 2: GC-MS of blended amine after 367 hours operation

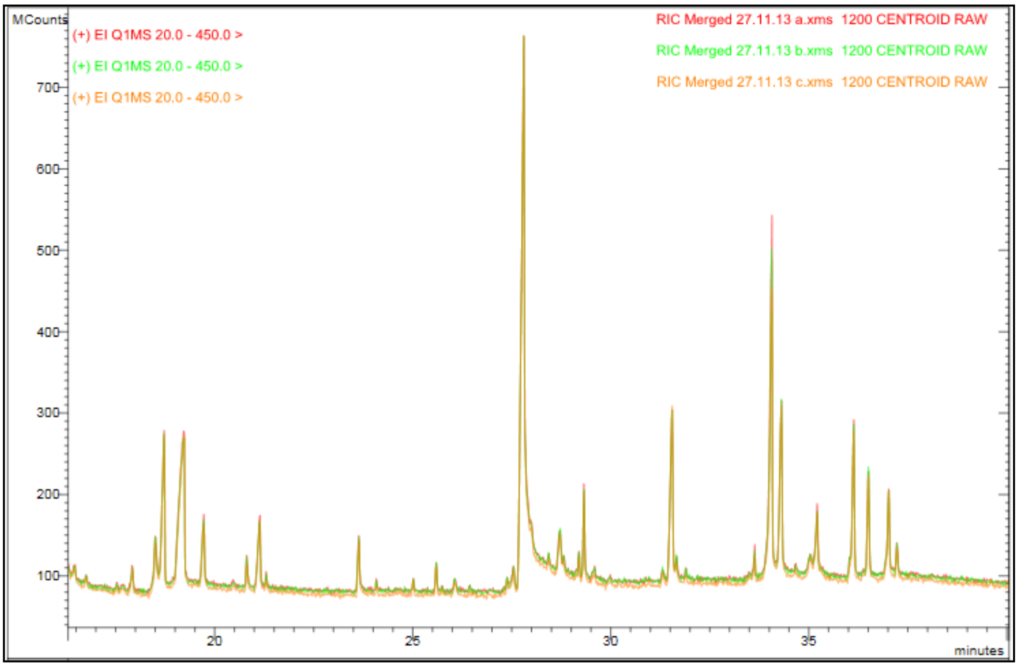

Figure C. 3: GC-MS of blended amine after 570 hours operation

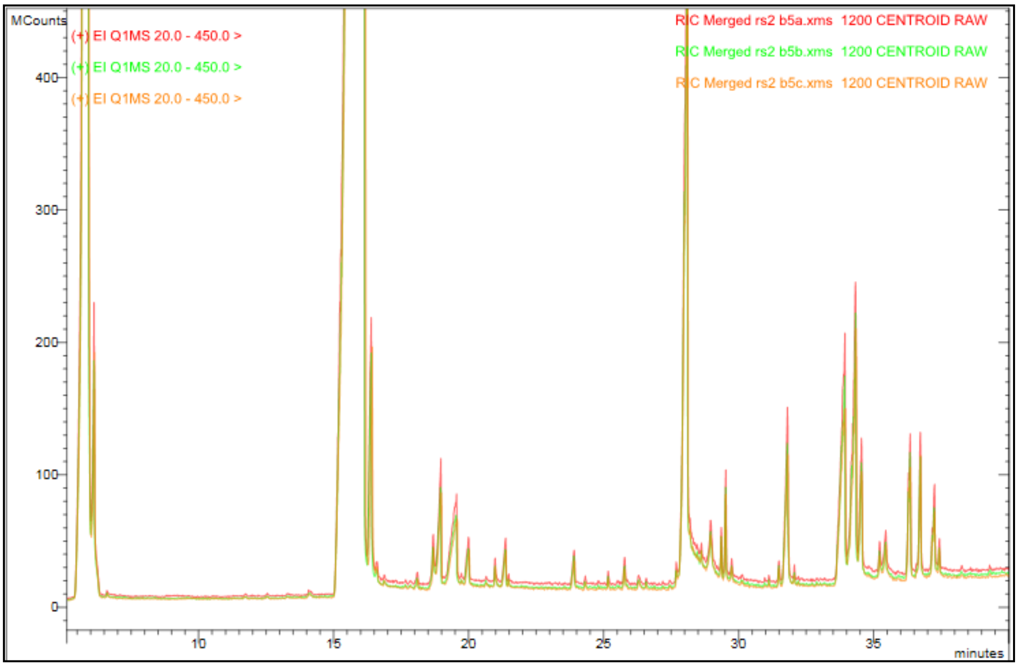

Figure C. 4: GC-MS of blended amine after 682 hours operation

Appendix D. GC-FID Chromatograms of Blended Amine Solvent

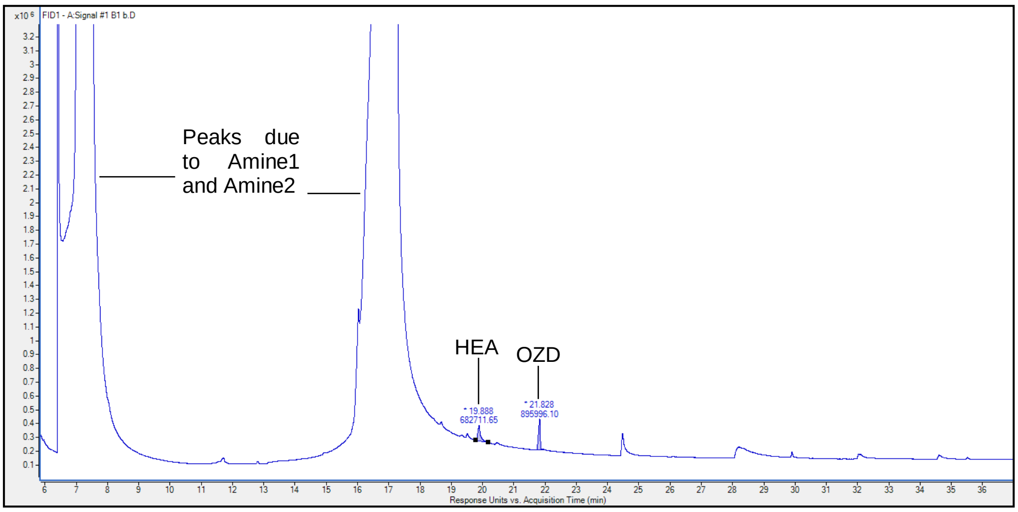

Figure D. 1: GC-FID of blended amine after 195 hours operation

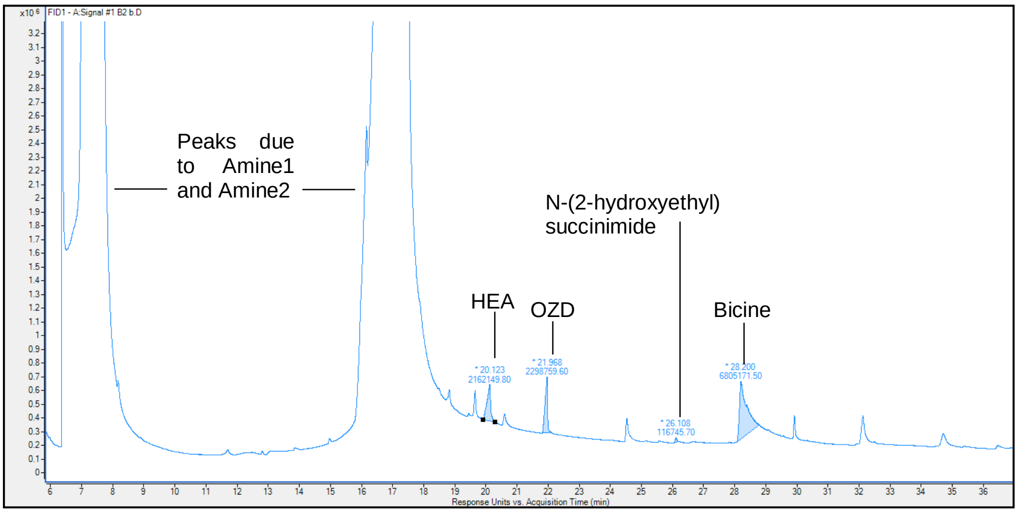

Figure D. 2: GC-FID of blended amine after 367 hours operation

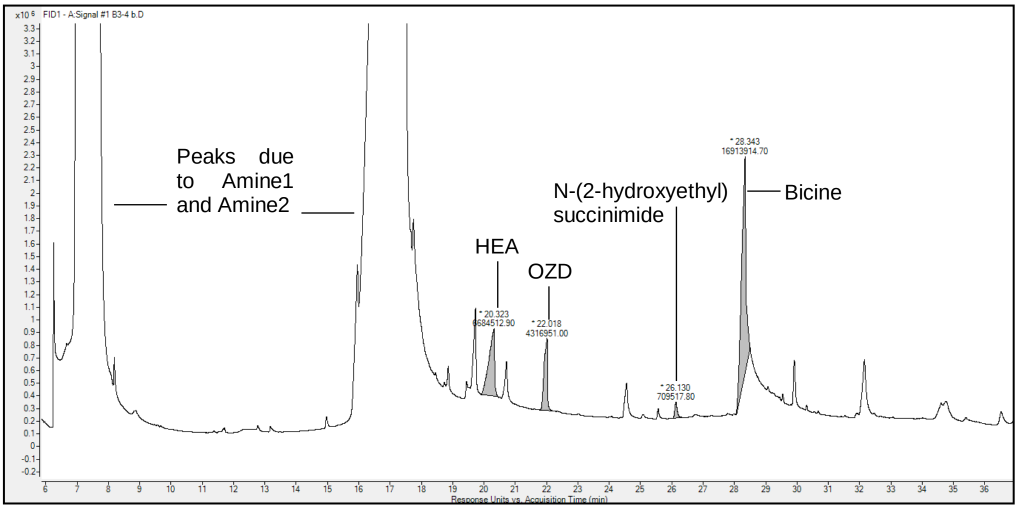

Figure D. 3: GC-FID of blended amine after 570 hours operation

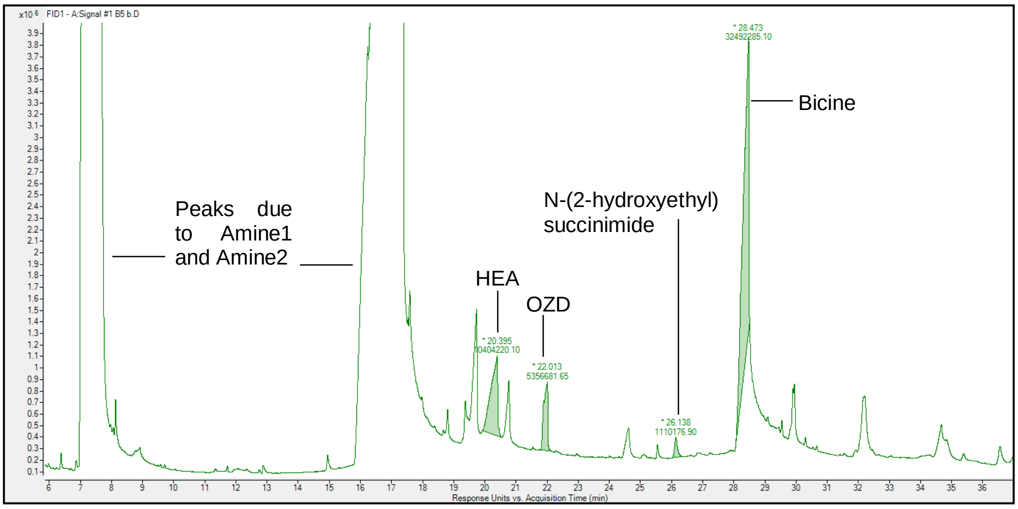

Figure D. 4: GC-FID of blended amine after 682 hours operation

Appendix E. Ion Chromatograms of Blended Amine Solvent

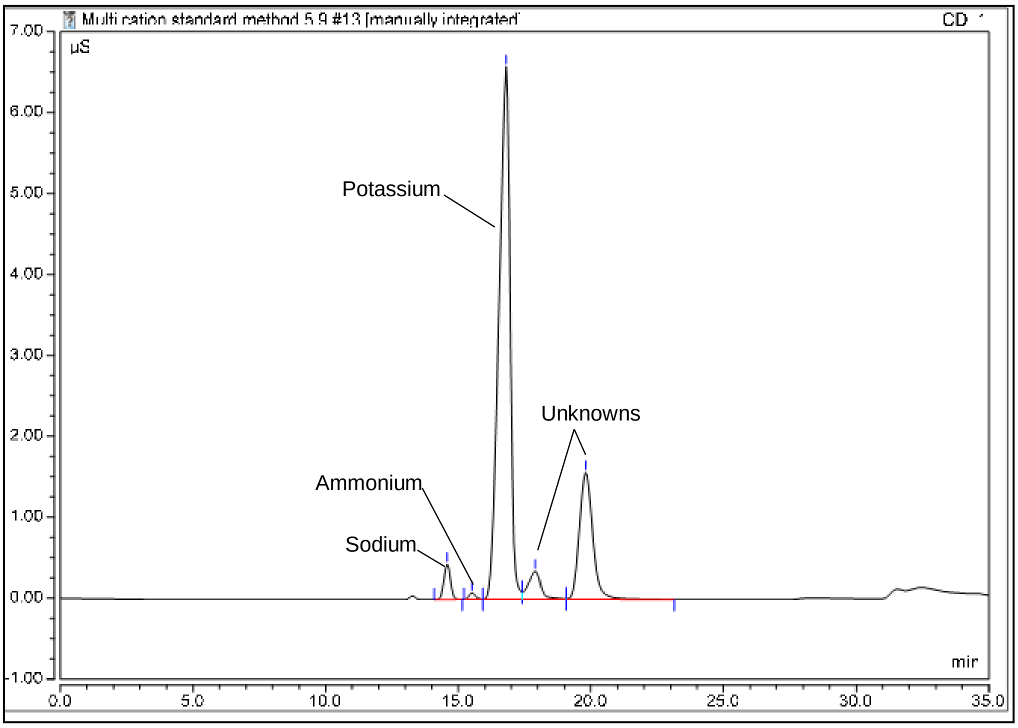

Figure E. 1: Cation chromatogram of blended amine after 195 hours operation

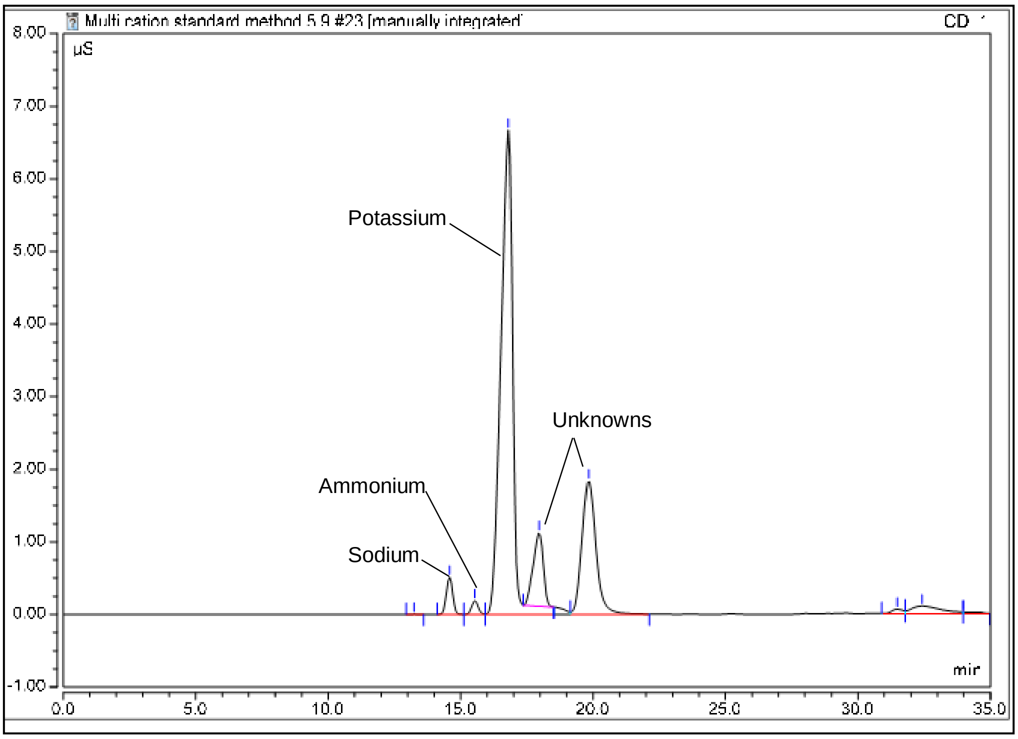

Figure E. 2: Cation chromatogram of blended amine after 682 hours operation

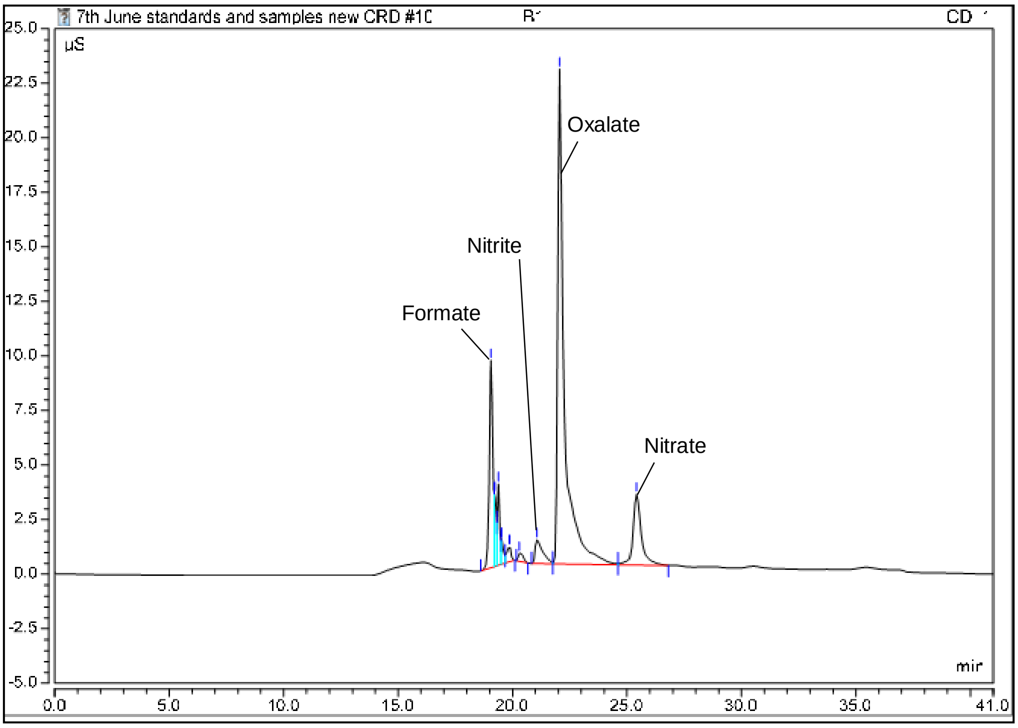

Figure E. 3: Anion chromatogram of blended amine after 195 hours operation

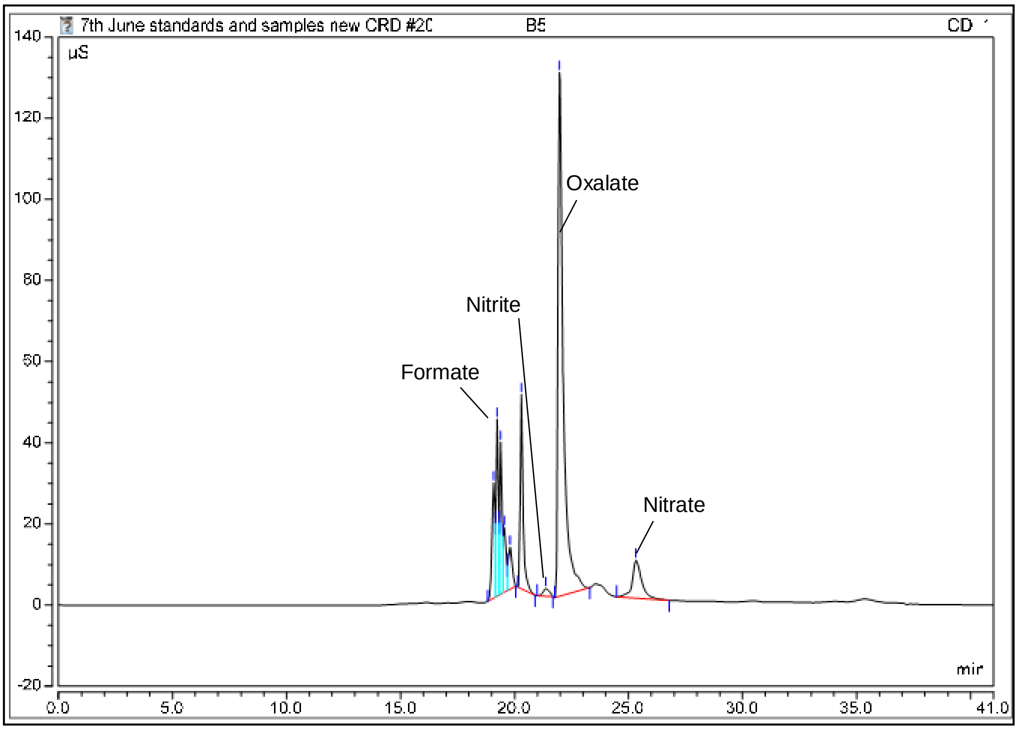

Figure E. 4: Anion chromatogram of blended amine after 682 hours operation

Appendix F. GC-MS Chromatograms of Continuously Ion Exchanged Primary Amine Solvent

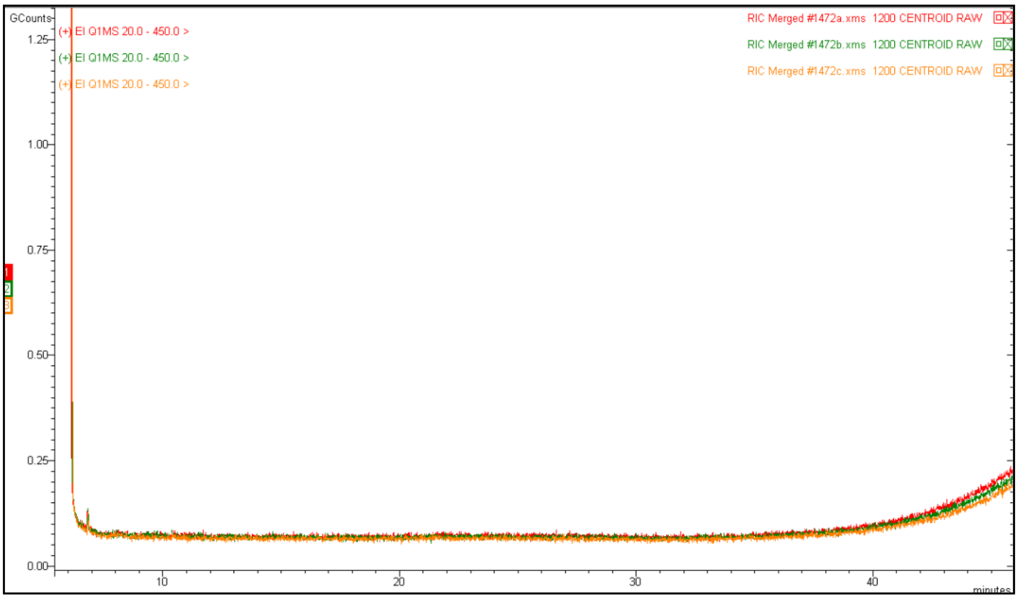

Figure F. 1: GC-MS of continually exchanged primary amine solvent after 20 hours operation

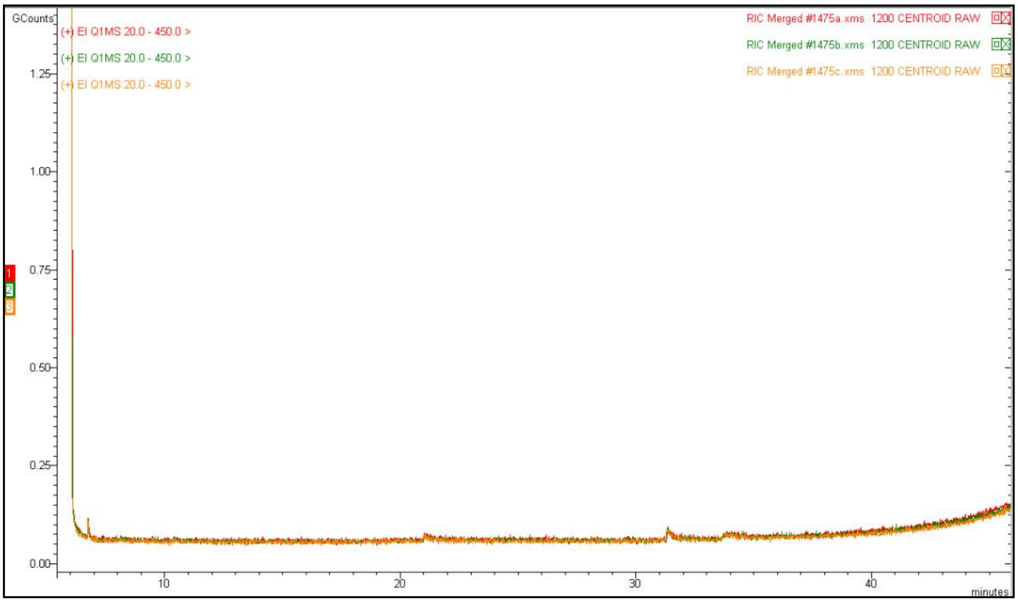

Figure F. 2: GC-MS of continually ion exchanged primary amine solvent after 170 hours operation

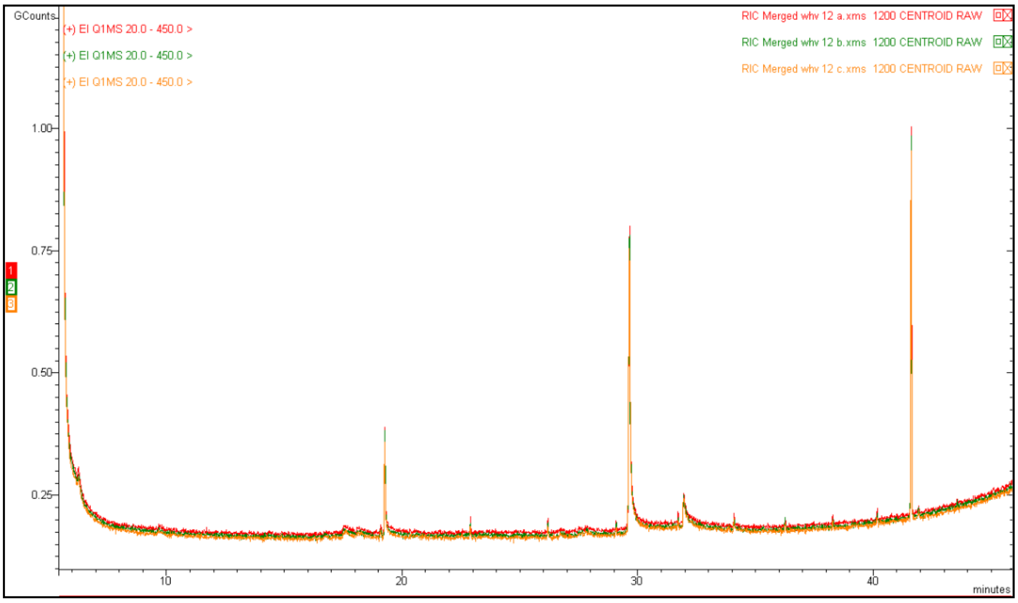

Figure F. 3: GC-MS of continually ion exchanged primary amine solvent after 707 hours operation

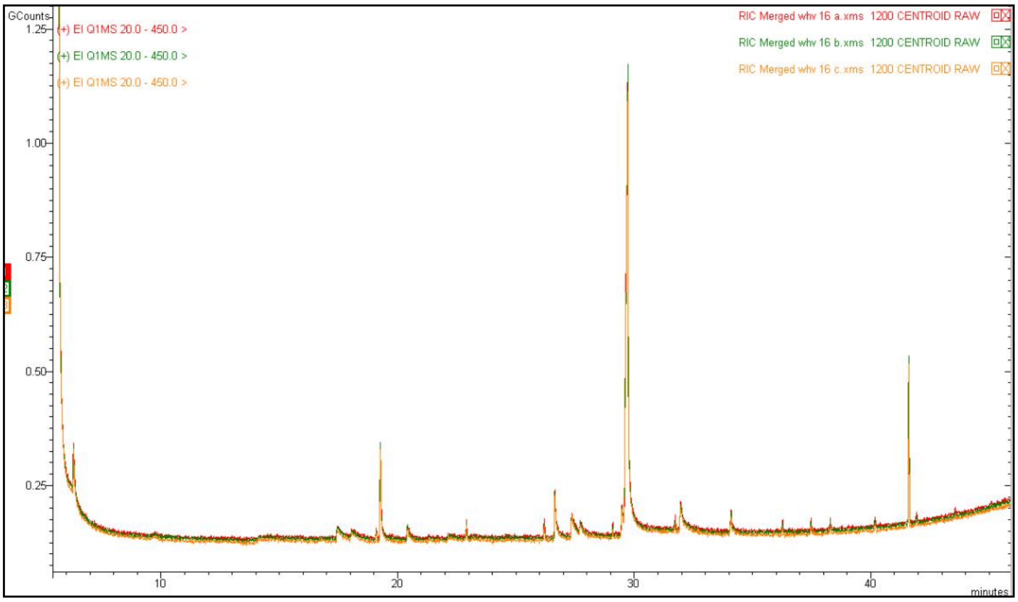

Figure F. 4: GC-MS of continually ion exchanged primary amine solvent after 2155 hours operation

Appendix G. GC-FID Chromatograms of Continuously Ion Exchanged Primary Amine Solvent

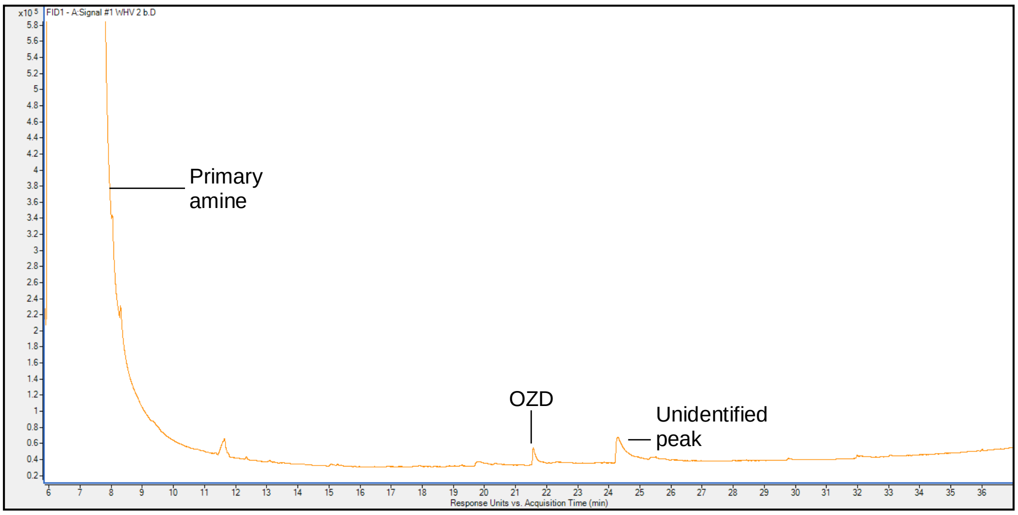

Figure G. 1: GC-FID of continually ion exchanged primary amine solvent after 20 hours operation

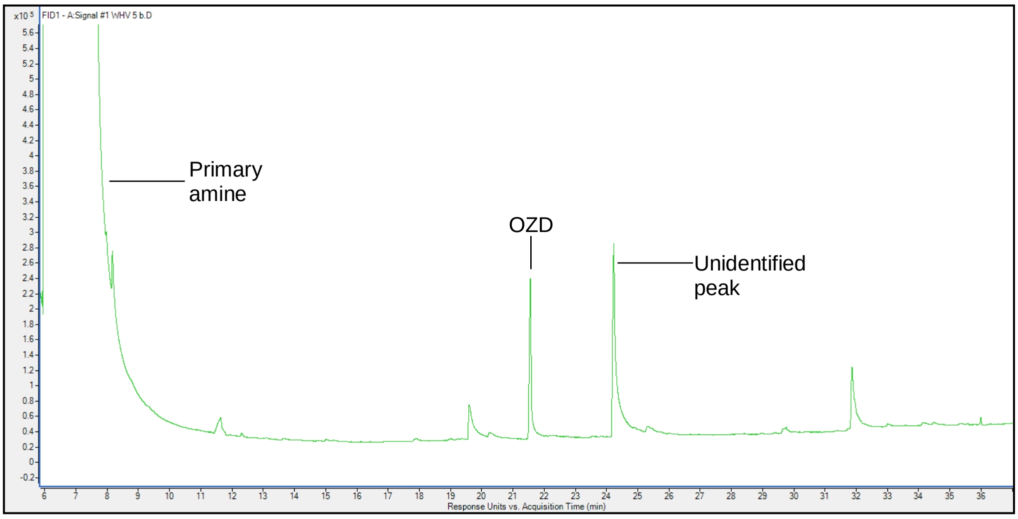

Figure G. 2: GC-FID of continually ion exchanged primary amine solvent after 218 hours operation

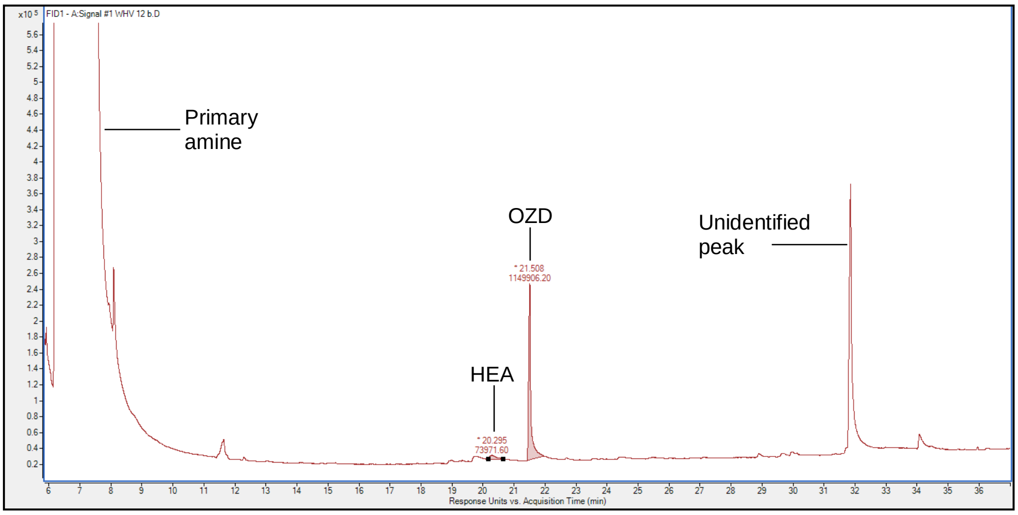

Figure G. 3: GC-FID of continually ion exchanged primary amine solvent after 707 hours operation

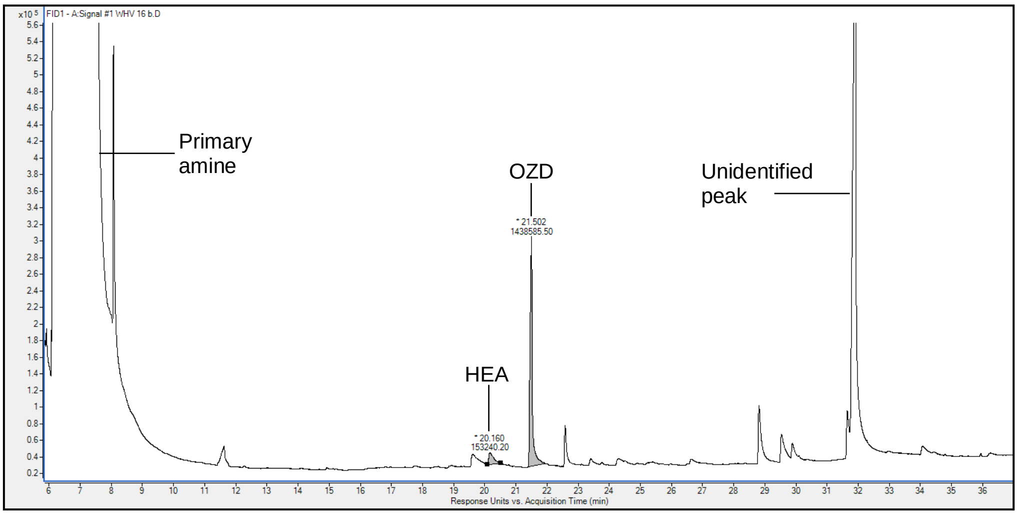

Figure G. 4: GC-FID of continually ion exchanged primary amine solvent after 2155 hours operation

Appendix H. Ion Chromatograms of Continuously Ion Exchanged Primary Amine Solvent

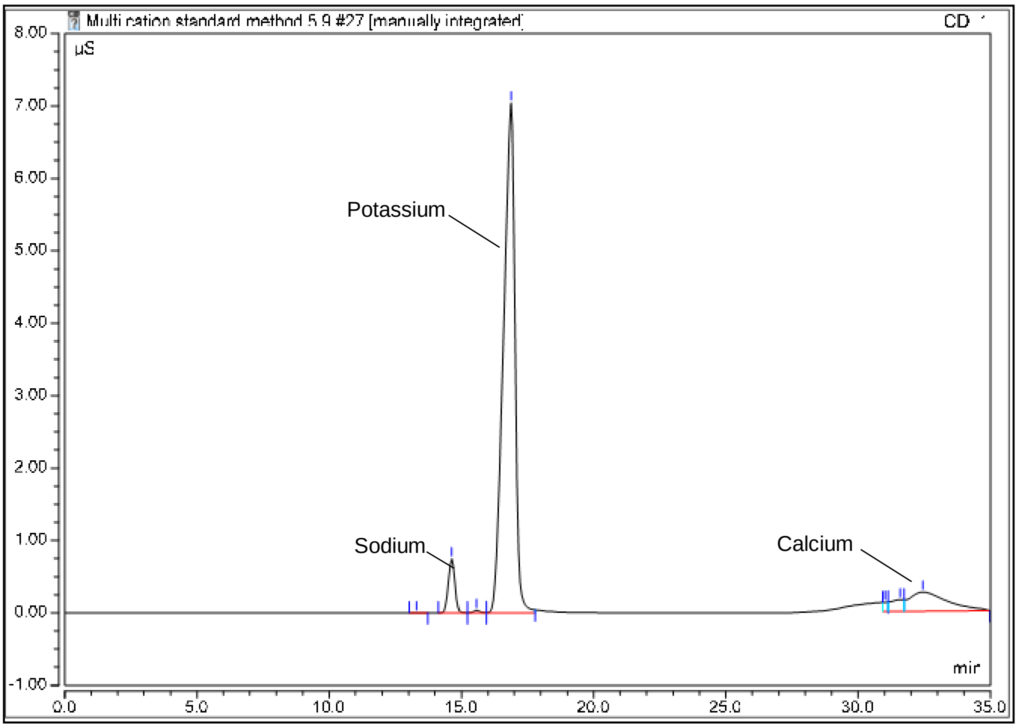

Figure H. 1: Cation chromatogram of continually ion exchanged primary amine solvent after 20 hours operation

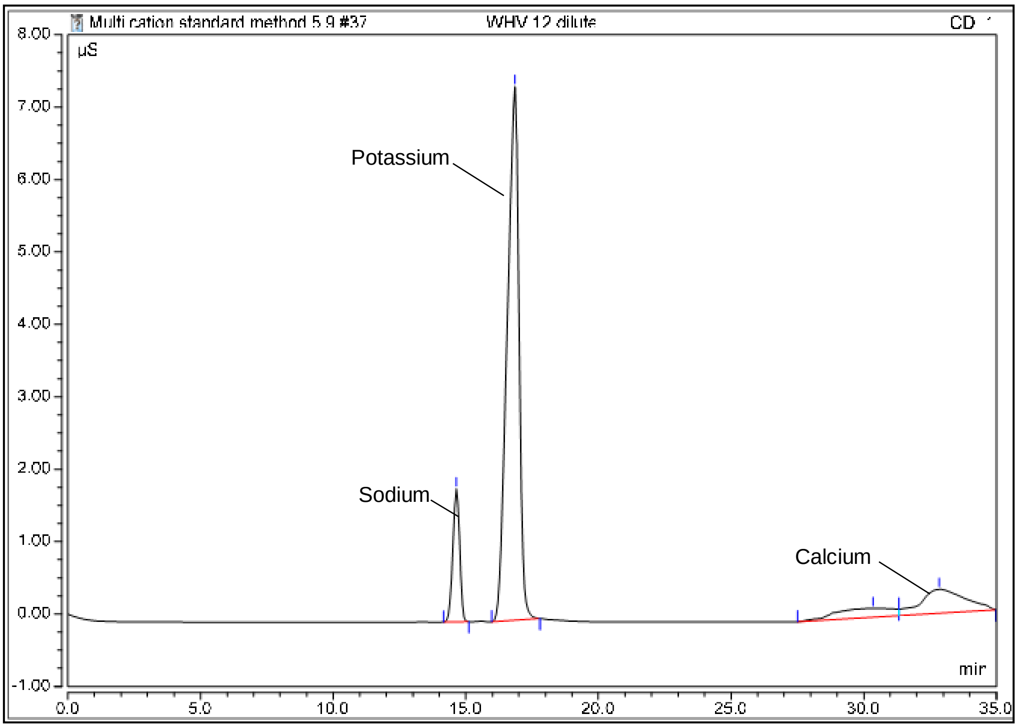

Figure H. 2: Cation chromatogram of continually ion exchanged primary amine solvent after 707 hours operation

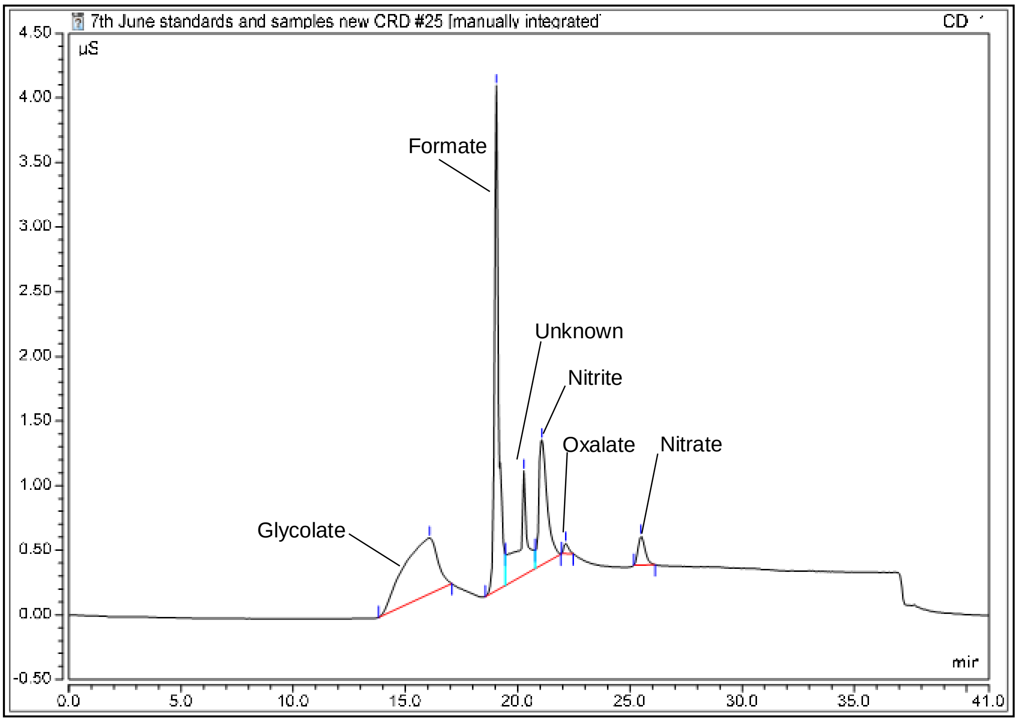

Figure H. 3: Anion chromatogram of continually ion exchanged primary amine solvent after 54 hours operation

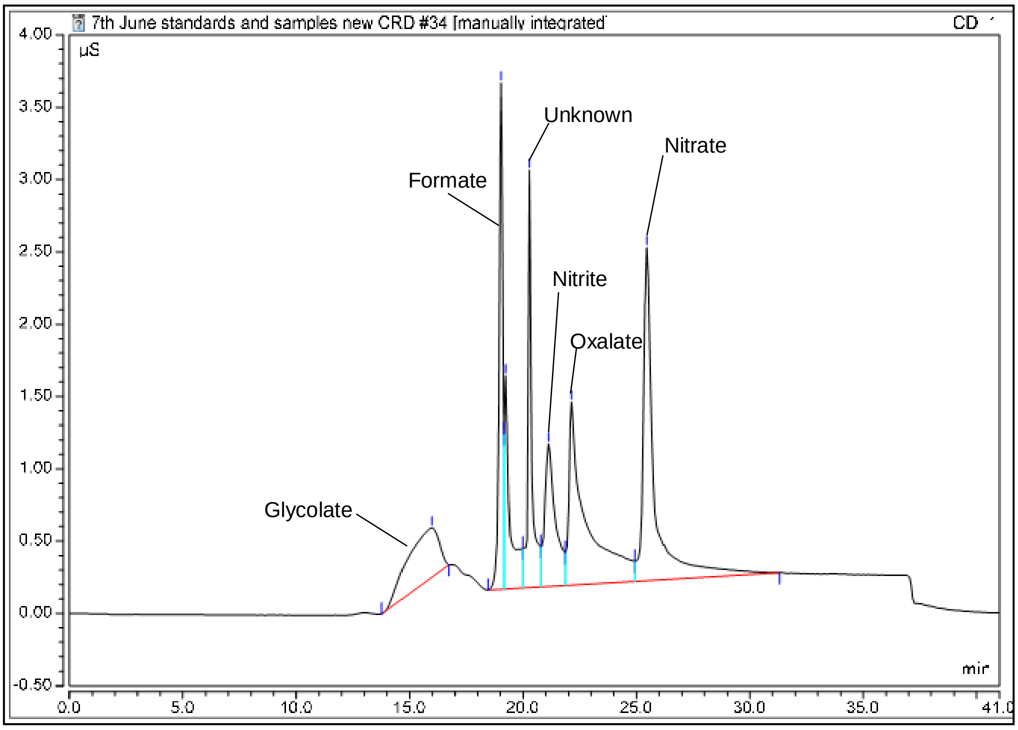

Figure H. 4: Anion chromatogram of continually ion exchanged primary amine solvent after 707 hours operation

References

1. S. Rackley, *Carbon Capture and Storage*, Elsevier Science, 2009.
2. M. Maroto-Valer, *Developments and Innovation in Carbon Dioxide (Co2) Capture and Storage Technology: Volume 1: Carbon Dioxide (Co2) Capture, Transport and Industrial Applications*, Woodhead Pub, 2010.
3. E. Wilson and D. Gerard, *Carbon Capture and Sequestration: Integrating Technology, Monitoring, Regulation*, John Wiley & Sons, 2007.
4. P. Tans, Trends in Atmospheric Carbon Dioxide, http://www.esrl.noaa.gov/gmd/ccgg/trends/global.html, (accessed 22nd September, 2016).
5. IPCC, *Fourth Assessment Report of the IPCC*, 2007.
6. R. Keeling, Scripps CO_2 Program, scrippsco2.ucsd.edu/, (accessed 19th May, 2016).
7. COP21, Paris Agreement, http://ec.europa.eu/clima/policies/international/negotiations/paris/index_en.htm, (accessed 19th May, 2016).
8. C. o. C. Change, Low-carbon fuels, https://www.theccc.org.uk/tackling-climate-change/reducing-carbon-emissions/what-can-be-done/low-carbon-fuels/, (accessed 01 September, 2016).
9. E.ON SE, Oxyfuel Combustion, http://www.eon.com/en/business-areas/power-generation/coal/carbon-capture-and-storage/oxyfuel-combustion.html, (accessed 14th August, 2013).
10. E.ON SE, Turning Coal into Clean Hydrogen: Pre-Combustion Capture, http://www.eon.com/en/business-areas/power-generation/coal/carbon-capture-and-storage/pre-combustion-capture.html, (accessed 21st July, 2013).
11. SaskPower, Boundary Dam Carbon Capture Project, http://saskpowerccs.com/ccs-projects/boundary-dam-carbon-capture-project/, (accessed 20th May, 2015).
12. Statoil, Sleipner West, http://www.statoil.com/en/TechnologyInnovation/NewEnergy/Co2CaptureStorage/Pages/SleipnerVest.aspx, (accessed 23rd May, 2016).
13. *United States Pat.,* 1930.
14. A. Bello and R. O. Idem, *Industrial & Engineering Chemistry Research*, 2006, **45**, 2569-2579.
15. E. F. da Silva, H. Lepaumier, A. Grimstvedt, S. J. Vevelstad, A. Einbu, K. Vernstad, H. F. Svendsen and K. Zahlsen, *Industrial & Engineering Chemistry Research*, 2012, **51**, 13329-13338.
16. J. Davis and G. Rochelle, *Greenhouse Gas Control Technologies 9*, 2009, **1**, 327-333.
17. G. S. Goff and G. T. Rochelle, *Industrial & Engineering Chemistry Research*, 2004, **43**, 6400-6408.
18. H. Lepaumier, E. F. da Silva, A. Einbu, A. Grimstvedt, J. N. Knudsen, K. Zahlsen and H. F. Svendsen, *10th International Conference on Greenhouse Gas Control Technologies*, 2011, **4**, 1652-1659.
19. B. R. Strazisar, R. R. Anderson and C. M. White, *Energy & Fuels*, 2003, **17**, 1034-1039.
20. D. A. Jones, T. F. McVey and S. J. Friedmann, *Technoeconomic Evaluation of MEA versus Mixed Amines for* CO_2 *Removal at Near-Commercial Scale at Duke Energy Gibson 3 Plant*, Lawrence Livermore National Laboratory, 2012.
21. K. A. Mumford, Y. Wu, K. H. Smith and G. W. Stevens, *Frontiers of Chemical Science and Engineering*, 2015, **9**, 125-141.

22. CSIRO, *Environmental Impacts of Amine-based CO_2 Post Combustion Capture (PCC) Process*, 2012.
23. C. Gouedard, D. Picq, F. Launay and P. L. Carrette, *International Journal of Greenhouse Gas Control*, 2012, **10**, 244-270.
24. P. T. Nielsen, L. Li and G. T. Rochelle, *Energy Procedia*, 2013, **37**, 1912-1923.
25. F. B. Closmann, Doctor of Philosophy, The University of Texas at Austin, 2011.
26. S. A. Freeman, Doctor of Philosophy, University of Texas at Austin, 2011.
27. A. O. Lawal and R. O. Idem, *Industrial & Engineering Chemistry Research*, 2005, **44**, 986-1003.
28. O. Lawal, A. Bello and R. Idem, *Industrial & Engineering Chemistry Research*, 2005, **44**, 1874-1896.
29. B. I. Fostås, A. Gangstad, B. Nenseter, S. Pedersen, M. Sjovoll and A. L. Sorensen, in *10th International Conference on Greenhouse Gas Control Technologies*, eds. J. Gale, C. Hendriks and W. Turkenberg, 2011, vol. 4, pp. 1566-1573.
30. T. Wang and K.-J. Jens, *International Journal of Greenhouse Gas Control*, 2014, **24**, 98-105.
31. P. Jackson and M. Attalla, *Energy Procedia*, 2011, **4**, 2277-2284.
32. H. Lepaumier, D. Picq and P. L. Carrette, *Industrial & Engineering Chemistry Research*, 2009, **48**, 9068-9075.
33. G. S. Goff, Ph.D. Thesis, The University of Texas at Austin, 2005.
34. A. J. Sexton and G. T. Rochelle, *Industrial & Engineering Chemistry Research*, 2011, **50**, 667-673.
35. T. Supap, R. Idem, P. Tontiwachwuthikul and C. Saiwan, *Industrial & Engineering Chemistry Research*, 2006, **45**, 2437-2451.
36. S. A. Bedell, *International Journal of Greenhouse Gas Control*, 2011, **5**, 1-6.
37. T. Supap, R. Idem and P. Tontiwachwuthikul, *Energy Procedia*, 2011, **4**, 591-598.
38. J. D. Davis, Ph.D Thesis, The University of Texas at Austin, 2009.
39. B. R. Strazisar, R. R. Anderson and C. M. White, *Abstracts of Papers of the American Chemical Society*, 2001, **223**, U569-U569.
40. S. Chi and G. T. Rochelle, *Industrial & Engineering Chemistry Research*, 2002, **41**, 4178-4186.
41. J. R. Lindsay-Smith and L. A. V. Mead, *J. Chem. Soc., Perkin Trans.*, 1973, **2**, 206-210.
42. W. H. Dennis, L. A. Hull and D. H. Rosenblatt, *Journal of Organic Chemistry*, 1967, **32**, 3783-3787.
43. L. A. Hull, G. T. Davis, D. H. Rosenblatt, H. K. Williams and R. C. Weglein, *Journal of the American Chemical Society*, 1967, **89**, 1163-1170.
44. L. A. Hull, G. T. Davis, D. H. Rosenblatt and C. K. Mann, *Journal of Physical Chemistry*, 1969, **73**, 2142-2146.
45. D. H. Rosenblatt, L. A. Hull, D. C. Deluca, G. T. Davis, R. C. Weglein and H. K. Williams, *Journal of the American Chemical Society*, 1967, **89**, 1158-1163.
46. S. A. Bedell, in *Greenhouse Gas Control Technologies 9*, eds. J. Gale, H. Herzog and J. Braitsch, 2009, vol. 1, pp. 771-778.
47. P. C. Rooney, M. S. DuPart and T. R. Bacon, *Hydrocarbon Processing*, 1998, **77**, 109-113.
48. S. J. Vevelstad, Ph.D., Norwegian University of Science and Technology (NTNU), 2013.
49. R. C. Kindrick, K. Atwood and M. R. Arnold, *Journal*, 1950, 1C-21C.
50. M. A. Scheiman, *Journal*, 1962, **Report No. 5746**.
51. P. C. Rooney and D. D. Daniels, *Petroleum Technology Quarterly*, 1998, 97-101.

52. W. Tanthapanichakoon, A. Veawab and B. McGarvey, *Industrial & Engineering Chemistry Research*, 2006, **45**, 2586-2593.
53. R. Veldman, *CORROSION 2000*, 2000.
54. Girdler Corporation, *Gas Process Division, Louisville, KY.*, 1950, **Contract No NObs-50023 for the Navy Department, Bureau of Ships, Washington DC**.
55. C. H. Blachly and H. Ravner, *Naval Research Laboratory Washington DC*, 1964, **AD609888, NRL-FR-6189**.
56. G. S. Goff and G. T. Rochelle, *Industrial & Engineering Chemistry Research*, 2006, **45**, 2513-2521.
57. A. J. Sexton and G. T. Rochelle, *Greenhouse Gas Control Technologies 9*, 2009, **1**, 1179-1185.
58. A. J. Sexton and G. T. Rochelle, *International Journal of Greenhouse Gas Control*, 2009, **3**, 704-711.
59. A. J. Sexton, Ph.D. Dissertation, The University of Texas at Austin, 2008.
60. Z. Wang and W. A. Mitch, *Environmental Science & Technology*, 2015, **49**, 11974-11981.
61. S. A. Mazari, B. Si Ali, B. M. Jan, I. M. Saeed and S. Nizamuddin, *International Journal of Greenhouse Gas Control*, 2015, **34**, 129-140.
62. C. J. Nielsen, B. D'Anna, C. Dye, C. George, M. Graus, A. Hansel, M. Karl, S. King, M. Musabila, M. Müller, N. Schmidbauer, Y. Stenstrøm and A. Wisthaler, *Norwegian Institute of Air Research*, 2010.
63. H. Lepaumier, D. Picq and P. L. Carrette, *Industrial & Engineering Chemistry Research*, 2009, **48**, 9061-9067.
64. M. J. Fazio, *Journal of Organic Chemistry*, 1984, **49**, 4889-4893.
65. A. Krzemień, A. Więckol-Ryk, A. Smoliński, A. Koteras and L. Więcław-Solny, *Journal of Loss Prevention in the Process Industries*, 2016, **43**, 189-197.
66. A. L. Cummings, F. C. Veatch and A. E. Keller, Houston, Texas, 1997.
67. A. L. Cummings, S. W. Waite and D. K. Nelsen, Banff, Alberta, 2005.
68. H. L. Craig and B. D. McLaughlin, Houston, Texas, 1996.
69. J. G. McCullough and R. B. Nielsen, Houston, Texas, 1996.
70. S. Bosen and S. A. Bedell, Houston, Texas, 2004.
71. H. Lepaumier, A. Grimstvedt, K. Vernstad, K. Zahlsen and H. F. Svendsen, *Chemical Engineering Science*, 2011, **66**, 3491-3498.
72. S. Zhou, S. J. Wang and C. H. Chen, *Industrial & Engineering Chemistry Research*, 2012, **51**, 2539-2547.
73. C. Perinu, B. Arstad and K. J. Jens, *Energy Procedia*, 2013, **37**, 7310-7317.
74. J. P. Jakobsen, E. F. da Silva, J. Krane and H. F. Svendsen, *Journal of Magnetic Resonance*, 2008, **191**, 304-314.
75. A. Hartono, E. F. da Silva, H. Grasdalen and H. F. Svendsen, *Industrial & Engineering Chemistry Research*, 2007, **46**, 249-254.
76. A. Hartono, U. E. Aronu and H. F. Svendsen, *10th International Conference on Greenhouse Gas Control Technologies*, 2011, **4**, 209-215.
77. W. Bottinger, M. Maiwald and H. Hasse, *Fluid Phase Equilibria*, 2008, **263**, 131-143.
78. S. Bouchonnet, in *Introduction to GC-MS Coupling*, CRC Press, 2013, ch. 1.
79. C. Creaser, *Journal*, 2013.
80. K. Downard, in *Mass Spectrometry: A Foundation Course*, Royal Society of Chemistry, Cambridge, UK, 2004, ch. 3.
81. M. Klee, GC Solutions #11: The Flame Ionization Detector, https://www.sepscience.com/Techniques/GC/Articles/208-/GC-Solutions-11-The-Flame-Ionization-Detector).
82. M. Klee, GC Solutions #12: The Flame Ionization Detector – Part 2, https://www.sepscience.com/Techniques/GC/Articles/210-/GC-Solutions-12-The-Flame-Ionization-Detector--Part-2).
83. H. J. Reid, unpublished work.

84. SeQuant, *Journal*, 2007.
85. CHROMacademy, *Journal*, 2016
86. P. J. Hore, *Nuclear Magnetic Resonance*, Oxford University Press, Oxford, 1995.
87. H. Friebolin, *Basic One- and Two-Dimensional NMR Spectroscopy*, Wiley-VCH, Germany, 4th edn., 2005.
88. GamryInstruments, Getting Started with Electrochemical Corrosion Measurement, http://www.gamry.com/application-notes/corrosion-coatings/basics-of-electrochemical-corrosion-measurements/).
89. D. G. Enos and L. L. Scribner, *The Potentiodynamic Polarization Scane*, Solartron, 1997.
90. C. Perinu, B. Arstad and K. J. Jens, *International Journal of Greenhouse Gas Control*, 2014, **20**, 230-243.
91. W. Bottinger, M. Maiwald and H. Hasse, *Industrial & Engineering Chemistry Research*, 2008, **47**, 7917-7926.
92. J. P. Jakobsen, J. Krane and H. F. Svendsen, *Industrial & Engineering Chemistry Research*, 2005, **44**, 9894-9903.
93. B. Dutcher, M. Fan and A. G. Russell, *ACS Applied Materials & Interfaces*, 2015, **7**, 2137-2148.
94. A. L. Cummings, G. D. Smith and D. K. Nelsen, Norman, Oklahoma, USA, 2007.
95. Y. Sun, J. E. Remias, J. K. Neathery and K. Liu, *Corrosion Engineering, Science and Technology*, 2011, **46**, 724-731.